Hyperglycaemia–induced mitochondrial DNA changes and mitochondrial dysfunction in diabetic nephropathy

Czajka, Anna Natalia

Awarding institution:
King's College London

Hyperglycaemia–induced mitochondrial DNA changes and mitochondrial dysfunction in diabetic nephropathy

A thesis submitted by

Anna Czajka

For the degree of Doctor of Philosophy from

King's College London

Diabetes Research Group

Division of Diabetes & Nutritional Sciences

Faculty of Life Sciences & Medicine

King's College London

2015

Abstract

Background: The mechanisms involved in the development of diabetic nephropathy (DN), which affects more than 30% of patients with diabetes worldwide, are not fully understood. DN is believed to result from hyperglycaemia-induced pathways in the kidney.

Hypothesis: Hyperglycaemia/high glucose causes early changes in mitochondrial DNA (MtDNA), possibly contributing to mitochondrial dysfunction.

Methods: Human renal immortalised and primary cultured mesangial cells (HMCL, HMCs) and transformed tubular epithelial cells (HK-2) were cultured in 5mM (NG) and 25mM (HG) glucose and in 5mM glucose plus 20mM mannitol. Organs and whole blood samples were collected from streptozotocin-induced (STZ), prohibitin 2 knockout (β-PhB2$^{-/-}$) and leptin deficient (Lep$^{ob/ob}$) diabetic mice. MtDNA content was measured in cultured renal cells, mouse organs and circulating cells using qPCR. The cellular bioenergetics of HMCs and HK-2 cells was measured using XF^{e}96 Seahorse analyser. Genes involved in mitochondrial life cycle and in the TLR-9 pathway in HMCs were measured using real-time qPCR. Reactive oxygen species (ROS) production and cell viability were assessed in HMCs using fluorescence and luminescent assays and hyperglycaemia-induced MtDNA damage using elongase PCR. Mitochondrial morphology and protein content were assessed by MitoTracker staining and Western blot respectively.

Results: Increased MtDNA levels in circulation in STZ-induced and β-PhB2$^{-/-}$ diabetic mice ($P<0.05$) was observed. In the STZ-induced mouse kidneys, MtDNA was reduced after 4 weeks diabetes ($P<0.05$); a similar trend was observed in the kidneys of the ob/ob mice ($P=0.08$). Growth of HMCs in HG resulted in 3-fold higher MtDNA and 2-fold higher *TFAM* ($P<0.05$), no significant changes were observed in HK-2 cells. The expression of two mitochondrial genome encoded mRNAs were reduced ($P<0.05$) in parallel with increased MtDNA damage, cellular ROS and apoptosis ($P<0.05$) in HMCs exposed to HG. Mitochondrial length and degree of branching were reduced in HMCs cultured in HG ($P<0.01$, $P<0.001$). *NF-κB* and *MYD88* expression were up-regulated in HMCs exposed to HG ($P<0.05$). Hyperglycaemia caused a decrease in basal, maximal and ATP-linked respiration ($P<0.001$) in the HMCs. Although no alteration in the MtDNA content was observed in HK-2 cells exposed to HG, bioenergetic profile of HK-2 cells was affected by hyperglycaemia with reduced basal, ATP-linked and maximal respiration ($P<0.01$).

Conclusion: These data show that hyperglycaemia can directly increase MtDNA in cultured renal and circulating cells in mouse models of diabetes. Hyperglycaemia-induced damage to MtDNA caused a dysregulation between MtDNA levels and mitochondrial transcription, suggesting the increased MtDNA may not be functional. Induction of the TLR-9 pathway suggests a potential inflammatory role of the damaged MtDNA.

Therefore, the *in-vitro* and *in-vivo* data suggest altered MtDNA content may be a biomarker of an adaptive mechanism of failing mitochondrial function under stress conditions. Such changes may be the foundation of the damage seen in patients with DN and needs further investigation.

Table of Contents

List of Figures

List of Tables

Abbreviations

ACE	Angiotensin-converting enzyme
ACR	Albumin Creatinine ratio
AD	Aldose reductase
AGEs	Advanced glycation end products
Ang	Angiotensinogen
ATP	Adenosine triphosphate
B2M	Beta 2 microglobulin
BHI	Bioenergetic health index
BSA	Bovine serum albumin
C57BL/6	C57 black 6
CDKs	Candidate diabetes associated kidney clones
cDNA	Complementary DNA
CKD	Chronic kidney disease
COX	Cytochrome C oxidase
COX3	Cytochrome c oxidase subunit 3
C_T	Threshold cycle
Cu/Zn SOD	Copper/zinc superoxide dismutase
D31	Diabetic mouse (duration of diabetes: 4 weeks)
D7	Diabetic mouse (duration of diabetes: 1 week)
DAG	Diacylglycerol
DCCT	Diabetes Control and Complications Trial
DMEM	Dulbecco's Modified Eagle's Medium
DMSO	Dimethyl Sulfoxide
DN	Diabetic nephropathy
DNA	Deoxyribonucleic acid
Drp1	Dynamin-1-like protein
dsDNA	Double stranded DNA
ECAR	Extracellular acidification rate
ECM	Extracellular matrix
EDIC	Epidemiology of Diabetes Interventions and Complications Study Research Group
EDTA	Ethylenediaminetetra-acetate
eGFR	Estimated glomerular filtration rate
eNOS	Endothelial nitric oxide synthase
ER	Endoplasmic reticulum
ESRD	End stage renal disease
ETC	Electron transport chain
FBS	Fetal bovine serum
FCCP	Carbonyl cyanide-*4*-(trifluoromethoxy)phenylhydrazone
FITC	Fluorescein isothiocyanate
FN	Fibronectin
G-6-P	Glucose 6-phosphate
GAPDH	Glyceraldehyde-3 phosphate dehydrogenase
GBM	Glomerular basement membrane

GFAT	Glutamine:fructose-6 phosphate amidotransferase
GFR	Glomerular filtration rate
GK	Goto Kakizaki
GLUT	Glucose transporter
HbA1C	Glycated hemoglobin
hB2M1	Human beta 2 microglobulin primers 1
HG	25mM (High) glucose
HG/NG	reversed cell culture conditions (25mM/5mM glucose)
HK-2	Human proximal tubule epithelialcell line
HMCL	Human mesangial cell line
HMCs	Human mesangial cells (primary cultured)
hMito3	human mitochondrial primers 3
HRP	Horseradish peroxidase
IGF	Insulin-like growth factor
ITS	Insulin-transferrin-selenium
LC	Light cycler
LDL	Low-density lipoprotein
mB2M	Mouse beta 2 microglobulin primer
MC	Mesangial cells
MNF1	Mitofusin 1
MFN2	Mitofusin 2
mMito	Mouse mitochondrial primer
MnSOD	Manganese superoxide dismutase
mRNA	Messanger RNA
Mt/N	mitochondrial/nuclear genome
MtDNA	Mitochondrial DNA
MYD88	Myeloid differentiation primary response gene (88)
NADP	Nicotinamide adenine dinucleotide phosphate
NADPH	Nicotinamide adenine dinucleotide phosphate
ND1	NADH oxidase subunit I
ND6	NADH oxidase subunit VI
nDNA	Nuclear DNA
NF-κB	Nuclear factor kappa B
NG	5mM (Normal) glucose
NGM	5mM glucose plus 20mM mannitol
NO	Nitric oxide
NOS	Nitric oxide synthase
NRF1,1	nuclear respiratory factor 1 and 2
OCR	Oxygen consumption rate
OD	Optical density
O-GlcNAc	O-linked N-acetylglucosamine
OPA1	Optic atrophy 1
OXPHOS	Oxidative phosphorylation
PAGE	Polyacrylamide gel electrophoresis
PARK2	Parkin RBR E3 ubiquitin protein ligase

PBMCs	Peripheral blood mononuclear cells
PBS	Phosphate buffer saline
PCR	Polymerase chain reaction
PGC-1α	Peroxisome proliferator-activated receptor gamma coactivator 1 alpha
PHB2	Prohibitin 2
PINK1	PTEN-induced putative kinase 1
PKC	Protein kinase C
POLG	mitochondrial DNA polymerase
qPCR	Quantitative PCR
RAGE	Receptor for advanced glycation end products
RAS	Renin-angiotensin system
RNA	Ribonucleic acid
RNS	Reactive nitrogen species
ROS	Reactive oxygen species
rRNA	Ribosomal RNA
RT-PCR	Reverse transcriptase polymerase chain reaction
SD	Standard deviation
SDS	Sodium dodecyl sulphate
SOD	Superoxide dismutase
SOD	Superoxide dismutase
STZ	Streptozotocin
T1D	Type 1 diabetes mellitus
T2D	Type 2 diabetes mellitus
T31	Treated diabetic mouse (cured for 4 weeks)
T7	Treated diabetic mouse (cured for 1 week)
TCA	Tricarboxylic acid cycle
TFAM	Mitochondrial transcription factor A
TGF-β1	Transforming growth factor beta 1
TLR4,9	Toll like receptor 4 and 9
TNF-α	Tumor necrosis factor-alpha
tRNA	Transfer ribonuclease
UCP1	Uncoupling protein 1
β-Phb2-/- mice	Beta prohibitin 2 knockout mice

Acknowledgements

I would like to express my gratitude to all those people who have contributed to this work in various different aspects and who have inspired me throughout my studies. Especially I would like to thank Dr Afshan Malik, who is probably the most enthusiastic supervisor a young scientist could wish for and who took the risk of taking me into her group. A special thanks to Prof Peter Jones for his encouragement and constructive comments all the way throughout my PhD.

I would also like to thank everyone in diabetes research group (especially PhD office) for a stimulating and fun environment and for providing help in experiments, samples collection (Dr Chloe Rackham) and lab safety (Jai). I cannot express my gratitude to my work colleagues (Saima, Saman, Liz and Kiran) for all the help and encouragement they gave me. It's a privilege to work among friends and I was extremely lucky to meet you girls :).

I also would like to thank Hiten for dedicating more than enough time to help me with my PhD and my writing phase and for being such a great inspiring scientist.

Special thanks to my friends; Rima, Yosef, Funso, Veronica, Ximo, Aitor, Laura, Evonne, Anabela, Pam, Alina, Ula and Gosia for keeping me 'sane' and providing help and fun in last four years.

I would like to especially thank my family, especially my mum for all the support she gave me throughout my studies and my sister and mum in law for the all the encouragement.

Finally, I would like to dedicate this thesis to my beloved husband Maciej, his love and positive attitude help me a lot during this PhD.

Declaration

Unless specifically stated in the text, all work described in this thesis is my own, completed under the supervision of Dr Afshan Malik and Prof Peter Jones.

The following work was carried out in our laboratory:

• Mitochondrial DNA damage using the PCR based elongase method was carried out by Ms Chandani Kiran Parsade.

No part of this thesis has been previously accepted for, or is currently being submitted for another degree.

Anna Czajka

October 2014

Chapter 1

Introduction

Chapter 1

1.1 Diabetes

Diabetes mellitus belongs to a group of metabolic syndrome diseases and has been characterised as persistently occurring high blood glucose (hyperglycaemia), caused by insulin deficiency or insulin resistance. Diabetes mellitus was first described as a disease linked to the urinary tract and kidney dysfunction. In 1674, the English physician, Thomas Willis (1621-1675), was the first to distinguish diabetes from other cases of polyuria and described the 'sweetness' of the urine and blood of affected patients. Matthew Dobson (1735-1784) reported that diabetic blood and urine contain sugar. A major breakthrough came in 1921, when Fredrick Banting (1891-1941) and Charles Best (1899-1978) in Toronto discovered insulin in the islets of the pancreas (Williams and Pickup, 1988, Eknoyan, 2006).

To the date more than 382 million people in the world have been diagnosed with diabetes and it has been predicted that by the year 2030, it will reach the pandemic levels, with 553 million diabetes patients (Wild et al., 2004, Whiting et al., 2011, WHO, 2013) (Fig.1.1.). It has also been projected that diabetes will be the 5th leading cause of death in 2030 with reduced life expectancy, approximately 20 years for T1D and up to 10 years in T2D (WHO, 2013). Currently more than 10% of the National Health Service (NHS) budget is spend on diabetes, which accounts for £173 million per week (DIABETES UK, 2014). In the United States, there are currently 24 million patients diagnosed with diabetes (IDF, 2014) and the predicted number is stated to be 29 million by 2050 (Boyle et al., 2001, IDF, 2013). In the United Kingdom, there were more than 3 million adults diagnosed with diabetes in 2013, which was an increase, when compared to year 2012 and accounts for more than 6% of population (DIABETES UK, 2014).

There are several pathogenic processes contributing to the onset of diabetes. The pancreatic β-cells and secretory insulin are known to be central to the pathophysiology of diabetes (Ferrannini, 2010).

Two main distinguished types of diabetes are known (Zimmet et al., 2001) :

Type 1 diabetes (T1D) or insulin dependent diabetes occurs in only 10-15% of patients and is characterised by a deficiency in insulin secretion with the presence of autoimmune destruction of pancreatic β-cells responsible for production of insulin. Although T1D can appear at any age, it is usually diagnosed under the age of 40 years and very often during childhood.

Type 2 diabetes (T2D) or adult - onset diabetes was previously known as non-insulin dependent diabetes and is observed in 85-90% of diabetic patients. T2D is characterised by a resistance to insulin, combined with a failure to produce sufficient insulin.

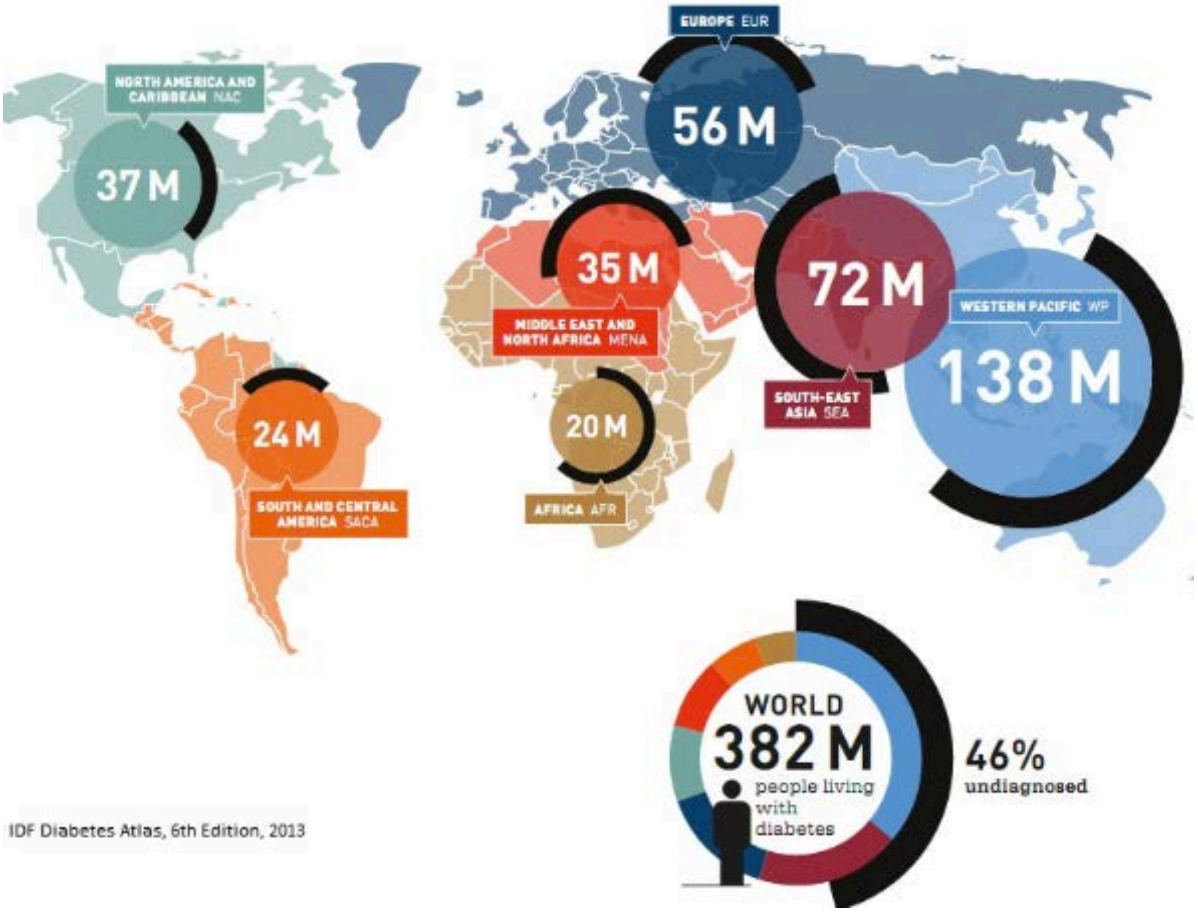

Fig.1.1. Global diabetes epidemic. There are approximately 382 million people with diabetes in the world. Taken from IDF diabetes Atlas 6th edition, 2013 (IDF, 2013).

A third main type of diabetes called gestational diabetes mellitus (GDM), previously known as a level of glucose intolerance at onset or first recognition in

pregnancy (Nolan, 2011). GDM is a common disorder in pregnancy and is associated with adverse pregnancy outcomes, including fetal macrosomia, stillbirth, neonatal metabolic disturbances and related problems. GDM, defined as a deficient insulin supply relative to increased demands that are characteristic of pregnancy is an increasing problem with an incidence of 7.6%. The causes are not known but are closely related to a constitutional risk of type 2 diabetes in later life and strongly associated with obesity (Mistry et al., 2012, Williams and Mistry, 2013).

Some other, less common forms of diabetes are directly inherited by the specific genes mutations. Mutation in the A3243G mitochondrial encoded tRNA (*Leu, UUR*) gene leads to mitochondrial diabetes, which is maternally transmitted and associated with hearing loss (maternally inherited diabetes and deafness, MIDD). The A3243G form of mitochondrial diabetes impairs metabolic pathways in beta cell function (de Andrade et al., 2006). Between 1-2% of all cases of diabetes is diagnosed with maturity onset diabetes of the young (MODY), caused by the mutation in the glucokinase or liver transcription genes, which lead to mild beta cell dysfunction and insulinopenia (Winter, 2000). Diabetes is also recognised as a first symptom of the autosomal recessive Wolfram syndrome (Zmyslowska et al., 2014) also called DIDMOAD syndrome after its four most common features (diabetes insipidus, diabetes mellitus, optic atrophy and deafness) and in Alport syndrome associated with T2D, kidney failure and obesity (Kruegel et al., 2013).

1.1.1 Diagnosis and risk factors

It is currently recognised that T2D and GDM are caused by different aetiological factors including: genetic (family history, genetic markers), demographic (sex, age and ethnicity), metabolic (impaired glucose tolerance, insulin resistance, pregnancy) and life-style dependent. T1D is postulated to be caused by genetic and environmental factors; however in some cases, the reasons behind the development of this type of diabetes are unknown (Zimmet et al., 2001). T2D has the strongest association with obesity as the 20th century's radical changes in lifestyle and food abundance have made a major contribution to the increased body mass index (BMI) in population (American Diabetes Association, 2014).

Hypertension, coronary heart disease, obesity and insulin resistance form the basis of the metabolic syndrome. The exact mechanism of development of metabolic syndrome is not known, but low physical activity, diet (Dunn et al., 2014) and genetic factors, especially maternal obesity (Armitage et al., 2008) are listed as major contributors to obesity and insulin resistance.

Well established criteria for diabetes recognition are: high levels of impaired fasting plasma glucose (IFG) ≥5.6mM, impaired glucose tolerance (IGT) ≥11mM and high levels of glycated haemoglobin (HbA_{1c}) ≥6,5% (Perry et al., 2001).

1.1.2 Diabetic complications

Sustained exposure to hyperglycaemia is a well-known cause of diabetic complications, including cardiovascular, renal and retinal disease (Table 1.1.). Patients with diabetes are at risk of stroke, kidney failure, retinopathy, myocardial complications and limb amputations (Vlassara and Striker, 2011, Brownlee, 2001).

Table.1.1. Diabetic complications. [Modified from (Williams et al., 2002)]

Organ affected	Disease complications
Eyes	Retinopathy, Glaucoma Blindness
Blood vessels	Coronary artery disease, Cerebral vascular disease Peripheral vascular disease Hypertension
Kidneys	Renal insufficiency Kidney failure
Skin, Muscle, Bone	Advanced infections Gangrene, Amputation

The pathophysiological effect of high glucose concentration on cells, tissues and organs involves induction of many factors, including, but not limited to oxidative stress, activation of pro-inflammatory gene expression and hypertension (Brownlee, 2005). Based on numerous studies, it is widely accepted that hyperglycaemia leads to increased cytosolic glucose concentrations in cells, with

consequent biochemical dysfunction, resulting in the activation of various signalling pathways (e.g. the polyol pathway, accumulation of advanced glycation end products (AGEs), activation of the hexosamine pathway; Fig. 1.2.) [reviewed in (Brownlee, 2005, Brownlee, 2001)]. Michael Brownlee suggested a unifying hypothesis linking all of hyperglycaemia-activated pathways, raised mitochondrial oxygen production, contributing to increased oxidative stress (Brownlee, 2005).

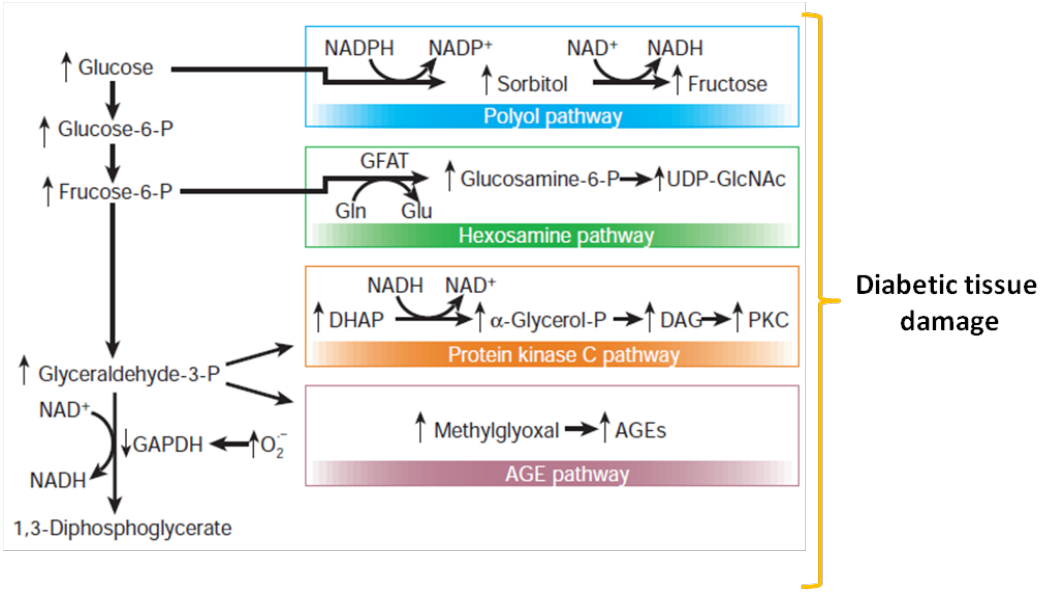

Fig.1.2. Hyperglycaemia induced tissue damage. Potential mechanism by which hyperglycaemia-induced mitochondrial superoxide ($O_2^{\cdot-}$) overproduction activates four pathways of hyperglycaemic damage. Excess $O_2^{\cdot-}$partially inhibits the glycolytic enzyme Glyceraldehyde 3-phosphate dehydrogenase (GAPDH), thereby diverting upstream metabolites from glycolysis into pathways of glucose overutilization. This results in increased flux of dihydroxyacetone phosphate (DHAP) to diacyl-glycerol (DAG), an activator of proteinase kinase C (PKC), and of triose phosphates to methylglyoxal, the main intracellular advanced glycation end products (AGE) precursor. Increased flux of fructose-6-phosphate to UDP-N-acetylglucosamine increases modification of proteins by O-linked N-acetylglucosamine (GlcNAc) and increased glucose flux through the polyol pathway consumes nicotinamide adenine dinucleotide phosphate (NADPH) and depletes glutathione (GSH). Adapted from (Brownlee, 2005). ↑increase

1.2 Diabetic nephropathy

Diabetic nephropathy (DN) is one of the microvascular complications associated with diabetes and is the main cause of end stage renal disease (ESRD) (Wada and

Makino, 2013). Between 30-40% of patients with both types of diabetes will develop DN and it has been estimated that ESRD will affect up to 60% of diabetic patients with recognised proteinuria (Singh et al., 2008).

The basic mechanisms behind the pathology of the disease are similar in both types of diabetes and the main cause of progressing fibrosis in the kidney, is hyperglycaemia. Results from the Diabetes Control and Complications Trial (DCCT, 1982-93) and the Epidemiology of Diabetes Interventions and Complications (EDIC, 1994-2006) follow-up study reported that insulin therapy with effective glycaemic control reduces the development of microalbuminuria by 39%, in patient with T1D. The DCCT was a randomized trial comparing different treatments used in diabetes while the EDIC examined longer-term effects of interventions used in DCCT, particularly focusing on diabetic complications. Data from both trials suggested that hyperglycaemia was a major mediator for progression of kidney disease (DCCT, 1993, de Boer and Group, 2014) and results from the DCCT trial indicated that strict glucose control reduces complications in patients with T1DM. Another multicentre trial, UK Prospective Diabetes Study (UKPDS) demonstrated that the risk of diabetic complications can be decreased significantly in patients with T2D under strict glycaemic control. UKPDS trial recruited 5,102 newly diagnosed patients monitored for up to 10 years. Results from this study showed, that patients with complications such as nephropathy, retinopathy and neuropathy can benefit from optimizing blood glucose control combined with pharmacological therapy in T2DM and their overall progression rate was decreased by 25%. Results from UKPDS also demonstrated that hyperglycaemia is the major contributor to these complications, but lowering blood glucose levels had no effect on macrovascular complications unlike control of blood pressure in all patients (King et al., 1999).

Results from DCCT, EDIC and UKPDS suggested that early metabolic control has beneficial effect on management of both types of diabetes. Furthermore, in the EDIC study, the phenomenon of 'metabolic memory' was proposed, as data showed that strict glycaemic control reduces development and progression of overall diabetes complication, by as much as 76% and between 60-84% of incidents of micro-and macroalbuminuria, respectively (Pop-Busui et al., 2010, de

Boer and Group, 2014). The molecular basis of this putative 'metabolic memory' remains unknown but strict glycaemic control should start as early as possible in a course of diabetes (Ceriello, 2009, Ihnat et al., 2007).

1.2.1 Pathology and development of diabetic nephropathy

The development of DN is complex and is proposed to involve at least three different mechanisms:

The first mechanism involves haemodynamic and structural abnormalities. Hyperfiltration/hypertension has been characterised in DN patients as an increased blood pressure in glomeruli which may cause cell damage and contribute to the development of glomerulosclerosis. Structural changes in the kidney involve thickening of the glomerulal basement membrane and expansion of extracellular matrix, with deposition of collagen type IV and VI, fibronectin and laminin (Fig.1.3.) (Wolf, 2004). Changes in the kidney glomeruli also correlate with reduced glomerular filtration rate (GFR). Tervaert et al., proposed an approved classification of structural changes in DN to assess the disease development; starting from mild glomerular basement thickening in stage one and advanced glomerulosclerosis in the last stage four (Tervaert et al., 2010).

The second mechanism involves the non-enzymatic reaction of glucose, where the carbonyl group reacts with proteins leading to accumulation of advanced glycation end products (AGEs) which have a long life time and cause renal tissue damage (Brosius et al., 2010). Accumulation of AGEs triggers the activation of transcription factors, like nuclear factor kappa-light-chain-enhancer of activated B cells (NF-κB) involved in the inflammatory response and production of cytokines and growth factors (Lehmann and Schleicher, 2000).

Following the inflammation, fibrosis and lesions in kidney structure lead to leakage of proteins into the urine, mostly albumin and this stage is called microalbuminuria with urinary albumin secretion from 30-300 mg/24h. Without proper glycemic control, microalbuminuria progresses to proteinuria, which manifests as a severe leakage of protein (>300mg/24h) and low GFR (Dabla, 2010). Patient with ESRD require kidney transplants as they cannot filtrate metabolites from their blood effectively.

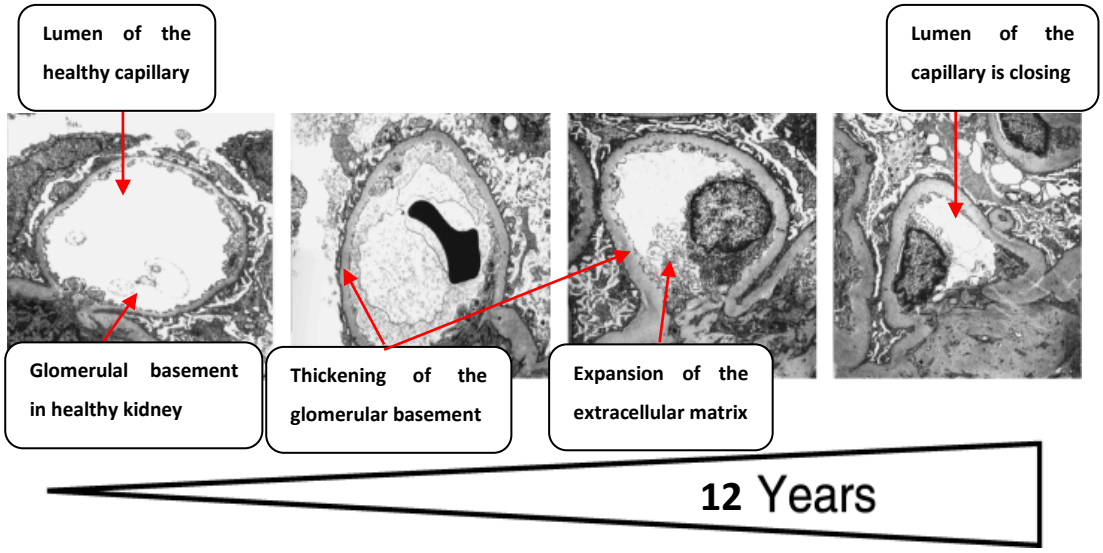

Fig.1.3.Progression of diabetic nephropathy. Renal biopsies (electron microscopy) taken from different patients, suffering fromT1D for various periods (3months to 12 years). There is a progressive increase in the thickness of the glomerular basement membrane from the normal kidney biopsy (left panel) to the narrowing capillary loops and expansion of extracellular matrix in nephropathy kidney biopsy (right panel). Adapted from (Wolf, 2004).

A third proposed mechanism involved in the development of DN and other diabetic complications involves enzymatic reactions of glucose, which leads to increased oxidative stress. It is now well established, through animal models and human studies, that imbalanced free radical production and failed antioxidant defence are major contributors in the development of diabetic complications, including DN (Jennings et al., 1987, Zhai et al., 2011, Asaba et al., 2005, Lee et al., 2003).

1.2.2 Definition of diabetic nephropathy

There are various tests used for detection of the renal disease, however the most commonly used are measurements of urine albumin and serum creatinine, as microalbuminuria and proteinuria are the major indications of occurrence of DN. To date DN is detected by monitoring kidney function through measuring urine albumin to creatinine ratio (ACR) and estimated GFR (eGFR; Table 1.2) (Mogensen, 2003, Mogensen et al., 1995). Most of the patients are diagnosed when the albuminuria is present and filtration rate affected (Fassett et al., 2011),

therefore there is a need for the discovery of new precursors of kidney damage. Current methods for detection of the DN are limited to the recognition of the albumin protein in diabetic patients' urine samples, combined with glomerular filtration rate (GFR) and albumin/creatinine ratio (ACR) (Tonelli et al., 2011). Albuminuria is a sign of the kidney damage; kidneys cannot properly filtrate substrates of metabolism and become 'leaky'.

Table 1.2. Definition of diabetic nephropathy. Adapted from (Mogensen, 2003, Mogensen et al., 1995)

Criteria	Range in DN	Normal range
Albumin/creatinine ratio	30-300mg/g USA 2.5-25mg/mmol Europe (men) 3.5 -25mg/mmol Europe (women)	<30mg/g <2.5mg/mmol (men) <3.5 mg/mmol (women)
Albumin concentration (mg/L)	30-300	<20
Creatine (mg/dL)	0.8-1.4 (men) 0.6-1.2 (women)	<0.8 (men) <0.6 (women)
Excretion rate	20-200µg/min or 30-300mg/24h	<20 µg/min
eGFR (mL/min/1.73m^2)	>60 (mild) 30-69 (moderate) <15 (kidney failure)	>90

Currently, that there are no markers available, which either predict the development of the disease, or indicate early stages of kidney failure before the occurrence of the structural changes that are irreversible.

Over the last decades a definition of five different stages of the development of DN have been characterised (Ritz, 2013, Pugliese, 2014):

a) Stage 1 is defined as an early kidney hypertrophy and early hyperfiltration rate (increased GFR) and can be partly reversible by glycaemic control.

b) Stage 2 is a clinically silent phase, which takes years to develop and it is characterised by morphologic lesion of the kidneys with increased GFR but without any clinical symptoms. Increased albumin excretion can be present during exercise (microalbuminuria with albumin loss >30mg/day). In parallel to albuminuria there is an increase in blood pressure

c) Stage 3, called microalbuminuria or incipient DN is defined by the presence of the albumin in the urine (albuminuria with albumin loss 30-300mg/day) and increased GFR, some of the patients at this stage will receive hypertensive treatment. At this stage kidneys are not able to filtrate blood properly and therefore urea and creatinine levels are raised in the blood.

d) Stage 4 is identified by the persistent proteinuria and by this stage GFR declines (<60ml/min). This stage is also known as advanced clinical nephropathy or chronic kidney failure (CKF).

e) Stage 5 is end-stage renal failure with extensive proteinuria and very low GFR (less than 15ml/min). At this stage patients require dialysis or transplantation to survive.

The average time for the progression from first stages of kidney dysfunction to stage 4 is 17 years per person and to stage 5, ESRD is 23 years. Therefore, there is a need for identification of new markers of kidney dysfunction in patients with DN in the clinically silent stage, which would help early detection of the disease and prevention of the organ damage.

1.3 Oxidative stress

Brownlee at al., (2001) suggested that one of the causes of the pathophysiological pathways activated in diabetes and its complications is hyperglycaemia-induced oxidative stress, produced by dysfunctional

mitochondria (Brownlee, 2001). Oxidative stress occurs when the balance between endogenous antioxidants and intracellular reactive oxygen species (ROS) is disturbed; with the body's natural antioxidant defence capacity becoming defective, thus creating an pro-oxidative environment (Halliwell, 2007). Postulated to play an important role in many mammalian diseases, oxidative stress contributes to cell damage and cell death through pathological reactions of free radicals (Coughlan et al., 2009, Halliwell and Gutteridge, 2007).

1.3.1 Free radicals

Free radicals are the molecules with an extra electron and are called either ROS or reactive nitrogen species (RNS) (Posada et al.) due to their spontaneous ability to bind to other molecules and compounds (Halliwell, 2011). Most of ROS are oxygen derivates (e.g. superoxide ion ($O_2^{\bullet -}$), peroxyl radical ($HO^{\bullet}$), hydrogen peroxide (H_2O_2). Oxygen derivates contribute to oxidative stress, while RNS, such as nitric oxide (NO) and peroxynitrate ($HNOO^-$) cause nitrative stress (Bashan et al., 2009). Proteins, lipids and nucleic acids serve as targets for oxidative reactions, which lead to creation of reactive intermediates (Hensley et al., 2000).

The main source of ROS/RNS in the cell are (a) the mitochondrial respiratory complexes, where accidental leakage of the electrons can occur (Halliwell and Gutteridge, 2007) and (b) the nicotinamide adenine dinucleotide phosphate-oxidase (NADPH oxidase) located in the cellular membrane and nitric oxide synthase (NOS) (Halliwell, 2011). The production of free radicals is also triggered by hormones and growth factors, endoplasmic reticulum (ER) stress, inflammation and nutrients (Bashan et al., 2009). Under normal conditions, oxidants are scavenged by endogenous antioxidant enzymes such as manganese superoxide dismutase (MnSOD, SOD2), catalase (Catherwood et al.), and glutathione peroxidase (GSH), which are abundantly present in cells. However, in the case of chronic over production of free radicals, antioxidant defences become overwhelmed and there is a resultant imbalance in the redox state of cells. Interestingly, free radical production is not always a bad thing and it is important to mention there is always a certain level of ROS molecules within the

cell, required for cell signalling. It has been shown that ROS molecules are very important in the immune and cardiovascular system, gene stimulation and protein production (Halliwell, 2011, Stanton, 2011).

1.4 The Mitochondrion

A commonly accepted 'endosymbiotic theory' proposes that mitochondria developed from a symbiosis between eukaryotic cell and α-proteobacterium more than 1.45 billion year ago (Gray et al., 1999). Mitochondrial ribosomes and transfer RNA molecules are similar to those of bacteria, as are components of their membrane. Mitochondria are key cellular organelles involved in energy metabolism and are often called the 'powerhouses' of the cells. The main role of mitochondria is production of adenosine triphosphate (ATP), an energy molecule required for cell biological processes. ATP is synthesised in the mitochondrial matrix through the Krebs cycle (also known as a tricarboxylic acid cycle, TCA), during oxidative phosphorylation (OXPHOS). Mitochondria also play a part in cellular division and sustaining the redox state of cells (Shadel, 2005) as well as many other important processes like apoptosis, calcium homeostatis, cellular differentiation and growth (Green and Reed, 1998, Chan, 2006). The main compartments of mitochondrial structure are the: outer membrane, intermembrane span, inner membrane, matrix and cristae (membrane compartments) (Fig.1.4).

Electron transport chain (ETC) proteins are located in the inner mitochondrial membrane. There are five main complexes distinguished (Gray et al., 1999, Sivitz and Yorek, 2010) (Fig.1.5.):

* complex I (NADH- ubiquinone oxidoreductase)

* complex II (sdh -succinate dehydrogenase)

*complex III (bc_1, ubiquinol-cytochrome c oxidoreductase)

*complex IV (cytochrome c oxidase, COX)

*complex V (ATP synthase)

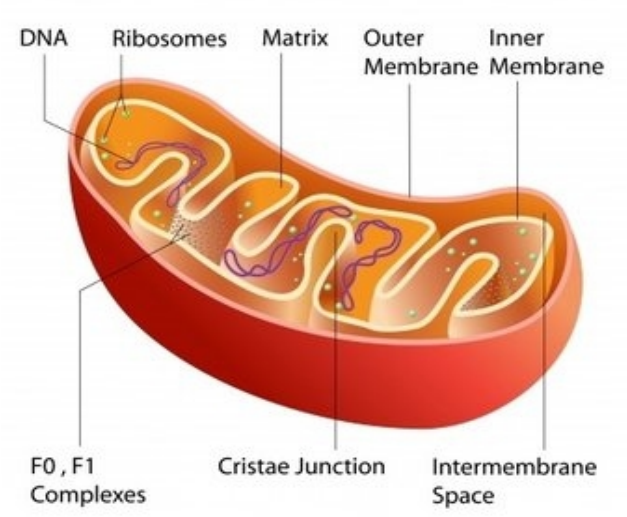

Fig.1.4. Structure of the mitochondria. Mitochondria are built from outer and inner membrane and mitochondrial matrix and cristae. The outer membrane is permeable for molecules such as ATP/ADP, the inner membrane is more complex in structure and folded into cristae. The inner membrane is permeable only to oxygen, ATP and it also helps in regulating transfer of metabolites across the membrane. Matrix contains proteins, mitochondrial ribosomes, tRNAs and circular mitochondrial DNA. Taken from (Tutorvista, 2014).

90% of the oxygen is channelled into mitochondria and energy derived from OXPHOS accounts for approximately 88% of total cellular energy produced (about 28/32 total ATP molecules). The rest of cellular energy is produced about equally from substrate level phosphorylation through glycolysis in the cytoplasm and through the TCA cycle in the mitochondrial matrix (2 ATP molecules each) (Seyfried and Shelton, 2010).

The ATP is synthesised through the redox potential created by nicotinamide adenine dinucleotide (NADH) and flavin adenine dinucleotide ($FADH_2$), reduced coenzymes, generated by the acceptance of electrons derived from the breakdown of organic substances in the TCA cycle. Four protein complexes in the inner membrane make up the ETC, which converts the redox energy, stored as NADH and $FADH_2$ into chemical energy in the form of ATP. Complexes I and II receive electrons, donated from NADH and $FADH_2$, respectively, followed by their shuttling to complexes III and IV and their final donation onto an oxygen molecule, creates H_2O.

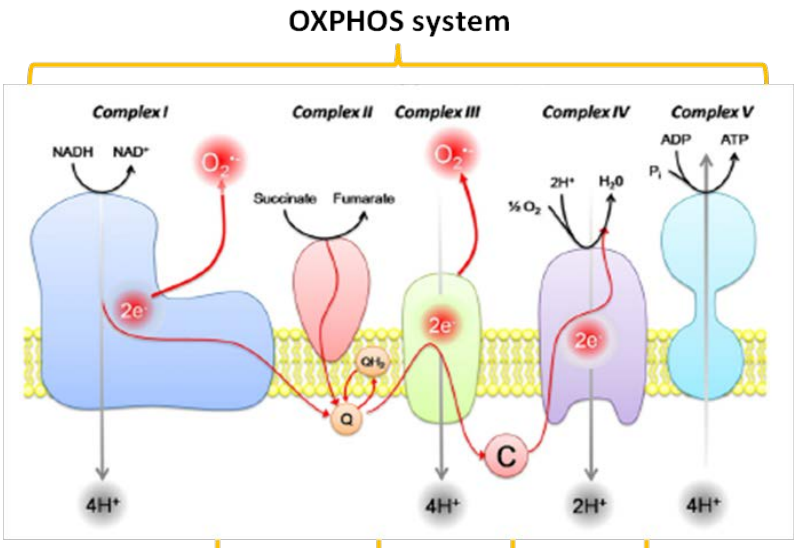

MtDNA	7	0	1	3	2
nDNA	36	4	10	10	14

Fig.1.5. Mitochondrial electron transport chain and oxygen radical production by respiratory chain complex, located in the inner mitochondrial membrane. Electrons donated by NADH enter mitochondria at complex I. Electrons generation in complex II have many ways: through conversion of succinate to fumarate, electron transfer flavoprotein and mitochondrial type of GAPDH. Reduction of ubiquinone (coenzyme Q_{10}) in complex III produces protons and electrons which are transferred to cytochrome C and cytochrome c oxidase in complex IV. Complex IV reduces oxygen to water and this is the end stage of respiration. Generation of protons by complexes I, II and III contributes to the synthesis of ATP by the ATP synthase. Mitochondrial DNA (MtDNA) codes for 13 OXPHOS polypeptides while nuclear DNA (nDNA) codes for 74 OXPHOS proteins. Adapted from (Blake and Trounce, 2014).

1.4.1 Mitochondrial biogenesis

Mitochondria are present in the cytoplasm in hundreds to thousands per cell and each mitochondrion can contain 2-10 copies of 5-µm circular MtDNA (Fig.1.6.). The number of mitochondria in cells is dependent on energy requirements and can vary from more than hundred thousands of mitochondria in oocytes (Piko and Matsumoto, 1976), to thousands in the brain (Uranova et al., 2001) and less than a hundred in the white blood cells (Selak et al., 2011).

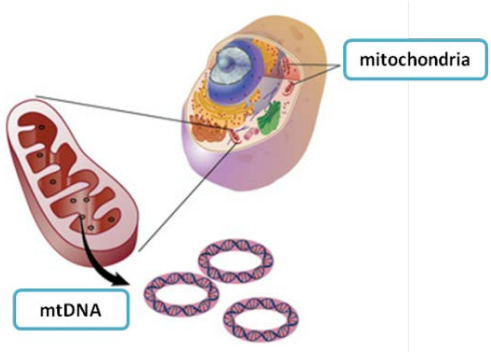

Fig.1.6. Mitochondria contain their own circular genome. Each mitochondrion contains between 2-10 copies of circular, double-stranded MtDNA. Adapted from National Human Genome Research Institute (NIH, accessed on 1st Sep, 2014).

The organisation of MtDNA is strongly conserved between organisms, in humans, MtDNA is present as a 16,569 bp double-stranded, circular structure, which encodes 37 genes; 13 mRNAs, 2 rRNAs and 22 tRNAs (Falkenberg et al., 2007). MtDNA is present in cells as a super coiled structure and unlike nDNA, is not protected by proteins, MtDNA is doubled stranded and built form heavy (H, on the outside) and light (L, on the inside) strands (Fig.1.7). Large number of MtDNA molecules in the cells are present as triple stranded structures, which contain D-loop regions for mitochondrial transcription and translation (Shadel and Clayton, 1997).

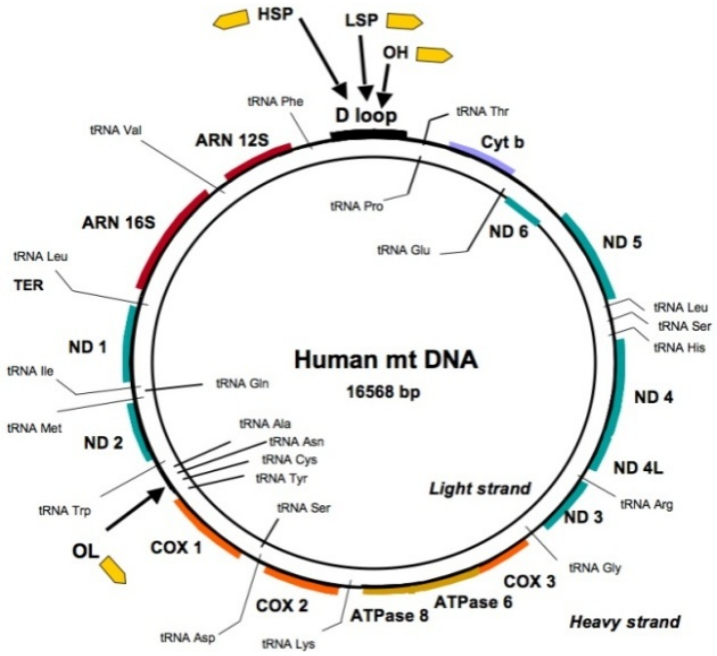

Fig.1.7. Human mitochondrial DNA. MtDNA encodes 22 tRNA, the 12 S and the 16 S rRNA and 13 genes of OXPHOS system subunits. Taken from (Bellance et al., 2009).

Most of the genes from the symbiont were transferred to the nuclear chromosomes, therefore despite essential mitochondrial coding, mitochondrial transcription and replication involves nuclear engagement as the majority of 1,500 mitochondrial proteins are encoded in nuclei, then synthesised as precursors in the cytosol and transported to mitochondria for further processing.

Mitochondrial DNA (MtDNA) codes for 13 OXPHOS polypeptides while nuclear DNA (nDNA) codes for 74 OXPHOS proteins (Blake and Trounce, 2014). Genes coding for all 13 proteins that are subunits for OXPHOS complexes are asymmetrically distributed in MtDNA and localised on both strands, the H-strand contains coding information for 12 OXPHOS polypeptides, while L-strand has only coding information for one of the complex I subunit, ND6 (Fernandez-Silva et al., 2003).

MtDNA is transcribed and translated within mitochondrion, however cells can control its transcriptional activity and MtDNA do not replicate like phase-restricted nDNA and can be continuously multiplied (Maechler and Wollheim, 2001, Falkenberg et al., 2007). Unlike nDNA, which is biparental, MtDNA is of uniparental inheritance and also have a higher mutation rate (Fernandez-Silva et al., 2003). MtDNA do not contain introns and only have two non-coding regions, a 1000 bp long D-loop region (which contains the origin of replication for H-strand) and the origin of replication for L-strand, which is approximately 30 bp long (Fernandez-Silva et al., 2003).

MtDNA replication is regulated by heterotrimeric MtDNA polymerase (POLG), the hexameric DNA helicase TWINKLE and the tetrameric single-stranded DNA-binding protein (mtSSB)(Milenkovic et al., 2013). MtDNA transcription requires mitochondrial RNA polymerase (POLRMT) and also transcription factors, which help POLRMT recognise MtDNA promoters. These three transcription factors include, mitochondrial transcription factor A (TFAM); mitochondrial transcription factor B 1 and 2 (TFB1M, TFB2M); nuclear respiratory factor 1 and 2 (NRF1 and NRF2) and Peroxisome proliferator-activated receptor gamma coactivator 1-alpha (PGC-1α) (Leigh-Brown et al., 2010, Fernandez-Silva et al., 2003).

MtDNA is organised in cells in the form of nucleoids, which contain molecules of MtDNA and several proteins involved in mitochondrial replication e.g. TFAM, which seem to be a major regulatory element of MtDNA copy number and also play a protective role against oxidative stress (Falkenberg et al., 2007). However, it has been shown using a transient over-expression of TFAM in cultured human embryonic kidney (HEK) cells, that only small increase of TFAM protein can have stimulatory effects on mitochondrial transcription, and high levels of TFAM have an inhibitory effect on the transcription rate (Maniura-Weber et al., 2004). Choi at al., (2001) have suggested a link between increased TFAM levels and MtDNA damage, caused by oxidative stress (Choi et al., 2001).

Although several proteins can bind to MtDNA, it is not protected against oxidative damage or repaired like nDNA. One has to remember that MtDNA are exclusively responsible for coding only 13 subunits of OXPHOS proteins, which are detrimental to the 'well-being' and proper function of the cells. Accidental leakage of electrons in the electron chain stimulates ROS production and oxidative damage to MtDNA, which causes accumulation of mutations. Increased numbers of mutations in MtDNA are the main cause of mitochondrial dysfunction and also results in increased free radical production by the overworked mitochondria, damaging MtDNA even more through a vicious cycle. Moreover, mitochondrial lipids are very sensitive to ROS-induced lipid peroxidation as they contain great amounts of unsaturated fatty acids, when oxidised, their derivates can further damage mitochondrial proteins and DNA (Ma et al., 2009). It has been shown in isolated rat cardiomyocytes exposed to H_2O_2, that the amount of intact MtDNA decreased by half as quickly as within 15 minutes after treatment (Suematsu et al., 2003).

Therefore, any mutation in the MtDNA sequence may have a detrimental effect on mitochondrial function and contribution to the increase of the ROS though the vicious cycle caused by malfunctioning mitochondria. When the number of mutated mitochondria is greater than the wild type, there are disturbances in energy production and this may contribute to the development of several diseases such as cancer, diabetes, HIV as detailed in section 1.4.3 (Wallace and Fan, 2010).

1.4.2 Mitochondrial dynamics

Mitochondria are not static organelle and they are constantly undergoing a process of fusion and fission. Fusion is maintained by mitofusin1, 2 (MFN1 and MFN2) and optic atrophy gene 1 (OPA1) (Fig.1.8). The way mitochondria select their 'partners' to fuse is not known. One possibility is a membrane potential, as by the fusion process some mitochondria can rescue their falling membrane potential (Twig and Shirihai, 2011). Fission which leads to mitochondrial fragmentation ismediated by three proteins, mitochondrial fission protein 1 (FIS1), mitochondrial fission factor (MFF) and dynamin-related protein 1 (DRP1). Fission can precede mitochondrial removal, process called mitophagy which is mediated by PTEN-induced putative kinase 1 (PINK1), parkin (PARK2).

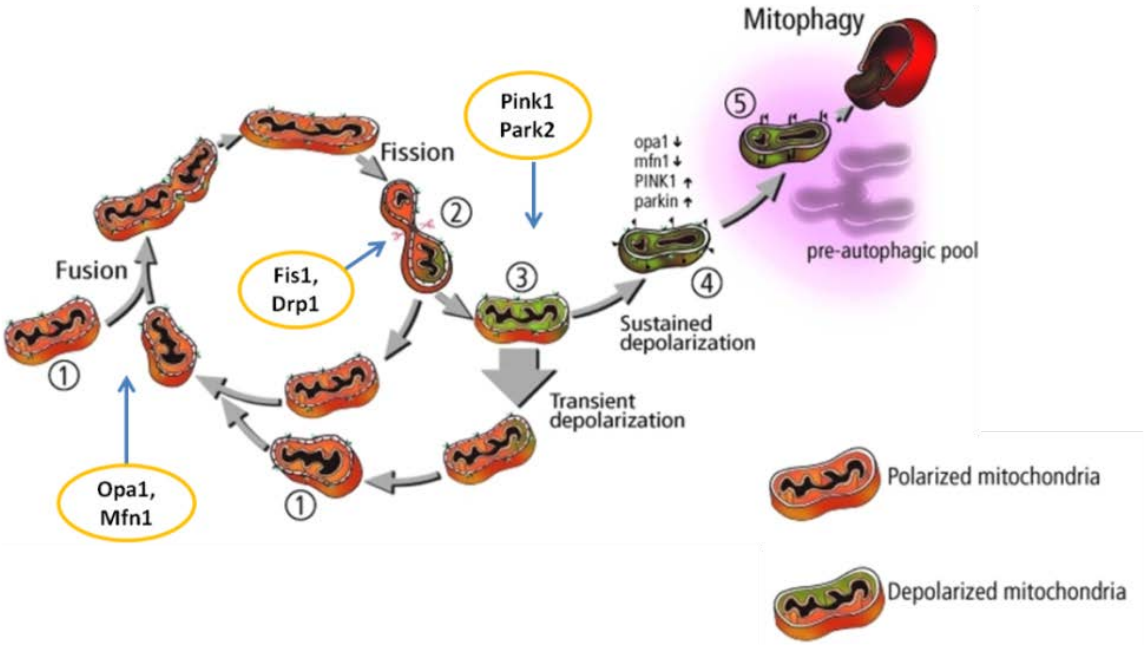

Fig.1.8. A schematic illustration of mitochondrion's life cycle. Mitochondria cyclically shifts between a post fusion state (networked) that lasts tens of seconds and a post fission state (solitary) that can last tens of minutes. Following a fission event, the mitochondrion can depolarize and restore an intact potential (*thick arrow*) or remain in a depolarized level. Removal of dysfunctional mitochondria by autophagy is based on drop in mitochondrial membrane potential which triggers cleavage of OPA1, accumulation of PINK1/PARK2, and reduction in mitofusin capacity. The mitochondrion may spend several hours in this pre-autophagic state before targeted by the autophagy machinery. Adapted from (Twig and Shirihai, 2011).

All of the listed proteins are located in the mitochondrial outer and inner membranes, but DRP1 is restricted cytosolic protein and has to translocate to the mitochondria during the fission process. OPA1 has also been shown to take part in the apoptosis process, when it is released from the mitochondria into cytosol. Both fission and fusion take place due to the hydrolytic activities of the mediating proteins (Ashrafi and Schwarz, 2013). It has been reported that by the addition of mitochondrial membrane potential couplers and uncouplers, the process of fusion and fission can be modulated, another important factor is nutrient availability or excess, which can affect mitochondrial network structure (Liesa and Shirihai, 2013).

1.4.3 Diseases linked to mitochondrial dysfunction and altered levels of mitochondrial DNA

In healthy conditions, the amount of MtDNA is proportionally correlated with mitochondrial function, as well as the number of mitochondria. They are flexibly regulated, due to the energy metabolism demand and redox state of the tissues (Hock and Kralli, 2009, Williams, 1986) . However, this does not seem to be the case in disease states. To date there have been many diseases attributed to mitochondrial dysfunction [reviewed in (Malik and Czajka, 2013)]. Altered mitochondrial genome, impairment of respiratory chain function and changes in mitochondrial copy number have an impact on development of variety of diseases such as Alzheimer's (Coskun et al., 2010), several types of cancers (Harbottle and Birch-Machin, 2006, Hosgood et al., 2010, Radpour et al., 2009, Lee et al., 2005, Shen et al., 2010), cardiovascular complications (Makazan et al., 2007, Tsutsui, 2006), myopathy (Durham et al., 2005) and maternally inherited mitochondrial diabetes (Alcolado et al., 2002). As shown in the tables 1.3 and 1.4, MtDNA content has been assessed in different tissues and body fluids in various diseases. The onset of clinical symptoms, caused by mitochondrial dysfunction/MtDNA mutations are caused by a number of factors, including the threshold effect, mitotic segregation, and a genetic bottleneck (Tuppen et al., 2010).

Table.1.3. Mitochondrial DNA content in human tissues and cells. Taken from (Malik and Czajka, 2013).

Body tissue/ cells, cell lines	Disease	MtDNA content	Reference
Tissue	Ovarian tumour	↑	(Wang et al., 2006)
	Breast cancer	↓	(Yu et al., 2007)
		↓	(Fan et al., 2009)
		↓	(Bai et al., 2011)
		↑	(Hsu et al., 2010)
	Hepatocellular carcinoma	↓	(Yamada et al., 2006)
	Biliary artresia and non-alcoholic fatty liver disease	↓	(Tiao et al., 2007)
	Pancreatic islets-aging	↓	(Cree et al., 2008)
	Adipose tissue in metabolic syndrome	↑	(Lindinger et al., 2010)
		↑	(Kaaman et al., 2007)
		↓	(Bogacka et al., 2005)
	Renal carcinoma	↓	(Meierhofer et al., 2004)
	Brain- aging	↑	(Barrientos et al., 1997)
	Multiple sclerosis	↑	(Blokhin et al., 2008)
	Nasal polyps	↑	(Park et al., 2009)
Cells/ Cell lines	Prostate cancer cells	↑	(Mizumachi et al., 2008)
	Adipocytes in HIV therapy	↓	(Hammond et al., 2004)
	Nerve cells in HIV	↓	(Dalakas et al., 2001)
	Lymphoblast cells In HIV therapy	↑	(Bjerke et al., 2008)
	Oocytes –fertilisation and its complications	↓	(Zeng et al., 2009)
		↓	(May-Panloup et al., 2005)
		↓	(Santos et al., 2006)
	Pimary culture neurons after radio frequencies exposure	↓	(Xu et al., 2010)
	Endometrial adenocarcinoma	↑	(Wang et al., 2005)

↑, increased; ↓, decreased

Table.1.4. MtDNA content in body fluids. Taken from (Malik and Czajka, 2013).

Body fluid	Disease	MtDNA	Reference
Whole Blood	Breast cancer	↑	(Shen et al., 2010)
	Breast cancer	↓	(Xia et al., 2009)
	Lymphoblastic lymphoma	↑	(Kwok et al., 2011)
	Type 2 diabetes	↓	(Lee et al., 1998)
	Type 2 diabetes	↑	(Wong et al., 2009)
	Type 2 diabetes	↓	(Xu et al., 2011)
	Type 2 diabetes	↓	(Song et al., 2001)
	Type 2 diabetes	↑	(Weng et al., 2009a)
	Type 2 diabetes	↑	(Cormio et al., 2009)
	Diabetic nephropathy	↑	Malik et al., 2009
	Intrauterine growth restriction	↑	(Colleoni et al., 2010)
	Benzene exposure	↑	(Carugno et al., 2012)
PBMCs	Sepis	↑	(Pyle et al., 2010)
	HIV -treatment	↓	(Chene et al., 2007)
PBMCs Leukocytes	Non-Hodgkin lymphoma	↑	(Lan et al., 2008)
	Hepatitis B virus related carcinoma	↓	(Zhao et al., 2011)
	Colorectal cancer	↑	(Qu et al., 2010)
	Type 2 diabetes	↓	(Gianotti et al., 2008a)
	Renal failure	↑	(Chen et al., 2008)
	Autosomal dominant optic atrophy	↓	(Kim et al., 2005)
PBMCs Lymphocytes	HIV complications	↑	(Cossarizza et al., 2003)
	HIV- treatment interruption	↑	(Mussini et al., 2005)
	Type 2 diabetes	↓	(Khan et al., 2011)
Lymphoblasts	HIV	↑	(Bjerke et al., 2008)
Blood Serum	Testicular cancer	↑	(Ellinger et al., 2009)
Blood plasma	Hemodialysis	↑	(Wang et al., 2011)
	Sepsis	↑	(Garrabou et al., 2012)
Urine pellets	Urothelial cell carcinoma	↑	(Dasgupta et al., 2012)
Saliva	Head and neck cancer	↑	(Jiang et al., 2005)
	Smoking	↑	(Masayesva et al., 2006)
Sperm	Infertility	↓	(Kao et al., 2004)
	Fertility	↑	(Amaral et al., 2007)
Cerebrospinal fluid	Lymphoblastic leukemia	↑	(Egan et al., 2010)

↑, increased; ↓, decreased

1.4.4 Mitochondrial dysfunction in diabetes

It has been proposed that ROS/RNS play an important role in insulin action and resistance, as they are produced in response to insulin and they are also necessary for its action (Bashan et al., 2009). Insulin secretion in response to glucose can be divided into two phases, the first involves activation of ATP – sensitive K^+ channels (K_{ATP}) and the second phase is K_{ATP} channel independent, with calcium signalling and ROS formation (from both mitochondria and cellular NADPH) as the main factors (Szabadkai and Duchen, 2009). Goldstein at al., (2005) discussed in great detail the involvement of insulin in ROS production. They reported stimulation of ROS production, mostly H_2O_2 in adipocytes treated with insulin. When cells were then treated with NADPH oxidase blocker, reduced insulin-stimulated H_2O_2 production was observed, followed by reduction in IRS-1/2 tyrosine phosphorylation, through inhibition of protein-tyrosine phosphatases (PTPases). PTPases are key negative regulatory enzymes in insulin action, therefore when ROS blocks their enzymatic activity, an increase in activation of phosphorylation of insulin receptor substrates is observed. The generation of ROS by insulin may be enhanced by high glucose conditions, which increases mitochondrial superoxide production (Figure 1.9.)(Mahadev et al., 2001, Goldstein et al., 2005).

Mitochondrial ROS production may also be important in development of T2D through mediating tumor necrosis factor-alpha (TNF-α) signalling pathway. TNF-α inhibits insulin action by regulating apoptosis signal-regulating kinase 1 (ASK1), followed by the activation of proteins involved in serine phosphorylation of insulin receptor substrates (IRS-1 and IRS-2) and decrease in insulin-stimulated tyrosine phosphorylation of IRS-1 (Nishikawa et al., 2007).

Imoto at al., (2006) conducted experiments on hepatocarcinoma cells and reported stimulatory effect of TNF-α on mitochondrial ROS production and ASK1 activation. All of the stimulatory actions of TNF-α were reverted by over expressing the mitochondrial antioxidant defence enzyme MnSOD and uncoupling protein 1 (UCP1), which take part in reducing the proton gradient in

oxidative phosphorylation. These data suggest a key involvement of mitochondrial ROS in the regulation of insulin signalling (Imoto et al., 2006).

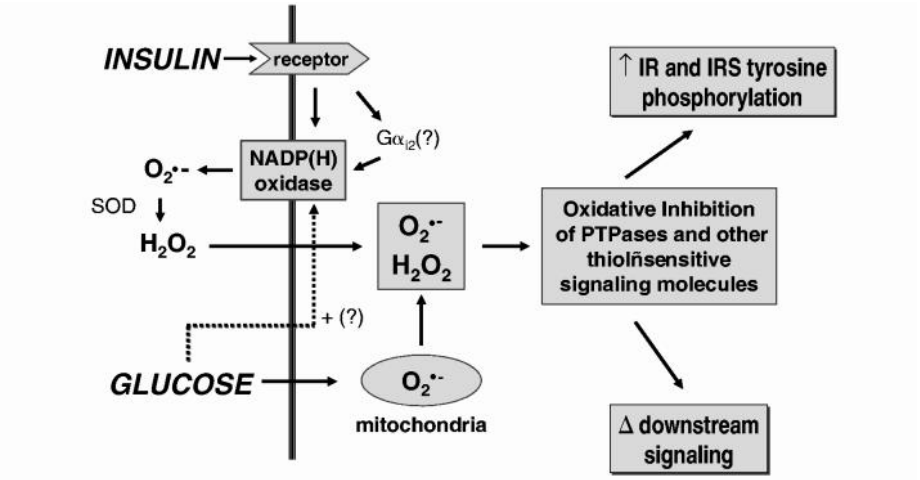

Fig.1.9. Insulin stimulated mitochondrial free radicals production. The generation of cellular reactive oxygen species (ROS) to insulin is coupled to the plasma membrane NADPH oxidase mechanism. Superoxide generated by the NADPH system is converted to H_2O_2 by superoxide dismutase. Both of these ROS can play a role in regulation of the catalytic activity of thiol dependent regulatory enzymes in the cells. The generation of ROS by insulin may be enhanced by high glucose conditions, which increase mitochondrial superoxide production and may also activate NADPH oxidase system. Taken from (Goldstein et al., 2005).

Another pathway of glucose action has also been observed; generation of glucose derived metabolites such as pyruvate (created in the process of glycolysis) also contributes to ROS production. Pyruvate is transported into mitochondria and after being metabolised, it increases the ATP/ADP ratio, consequently enhancing ROS/RNS formation (Szabadkai and Duchen, 2009). Free radicals serve as intracellular messengers and can also stimulate the same pathway as glucose (e.g. activation of the PKC). Excessive activation of PKC leads to tissue injury, through activation of transforming growth factors and NF-κB, causing an inflammatory response within the cells (Pugliese et al., 1994). Lee et al.,(2003) demonstrated that culturing renal cells under high glucose conditions augments the production of ROS and that this stimulation of free radical generation can be effectively blocked by PKC inhibitors (Lee et al., 2003). Catherwood et al., (2002) used *in vitro* cultured mesangial cells and observed unpaired antioxidant activity, including MnSOD under high glucose conditions

(Catherwood et al., 2002). These studies show an increased formation of free radicals and defective antioxidants systems in cells exposed to hyperglycaemia.

The key evidence of mitochondrial contribution and importance in hyperglycaemic damage was demonstrated previously by Nishikawa et al., (2000), who by using pharmacological inhibitors and over-expressed proteins, showed three different pathways potentially involved in mitochondrial superoxide ion production in bovine aortic epithelial cells cultured in high glucose. Normalising high glucose-induced ROS levels prevented increased activation of protein kinase C and NF-κB, aldose reductase pathway and formation of AGE (Nishikawa et al., 2000). Oxidative stress markers have been reported previously in the urine and serum of the diabetes patients with DN and microalbuminuria (Cvetkovic et al., 2009) and in the kidneys of diabetic rats (de Haan et al., 2005)

Altered MtDNA content in circulating cells has been previously reported in diabetes, some reports showing an increase (Malik et al., 2009, Weng et al., 2009b, Khan et al., 2011), whereas others show a decrease (Lee et al., 1998, Gianotti et al., 2008b, Chien et al., 2012) or no change (Asmann et al., 2006, Garcia-Ramirez et al., 2008). The discrepancies observed in the results from different studies are caused by the problems/variations with the methodologies used, including different methods of DNA extraction and accurate detection MtDNA content, without measurement of the pseudogenes (Malik et al., 2011). Also, the direction of changes may vary between different tissues and the way they responded to glycaemic stress may be dependent on their energy requirements.

Dysfunction of mitochondria in correlation to MtDNA levels has been shown in diabetic mouse muscle tissues (Bonnard et al., 2008), in connection with increased ROS. A recent study identified 12 differentially expressed urinary metabolites linked to mitochondrial metabolism, lower MtDNA content and mitochondrial activity in the DN patients (Sharma et al., 2013). Altered mitochondrial structure and lower mitochondrial membrane potential have been highlighted in ischemic kidney injury in the rat kidney (Plotnikov et al., 2007), and

depleted mitochondrial function, which correlated with increased mitochondrial fragmentation in mouse *in-vitro* model of acute kidney injury (Brooks et al., 2009).

1.5 Model systems used in the current study to assess early stages of diabetic nephropathy.

Diabetic nephropathy is a very complex disease and it takes more than 10 years to develop in patients with diabetes. Therefore using animal models and *in-vitro* systems proved to be challenging to study this disease. The most commonly used animal models to study DN are hypertensive rodents as hypertension is one of the contributing factors in renal morbidity (Kopp, 2013, Herrera and Coffman, 2012). However studies of diabetic mice suggest that, like diabetes patients, mice can exhibit susceptibility to diabetes and also renal and cardiovascular diseases (Sugiyama et al., 2001, Paigen et al., 1987). The Animal Models of Diabetic Complications Consortium (AMDCC) defined criteria for validating murine models of human diabetes and diabetic complications: with more than 50% decline in GFR over the lifetime of the animal, more than 10-fold increase in albuminuria (when compared with controls from the same strain) and with distinct pathology of the kidneys (advanced mesangial matrix expansion, basement membrane thickening by more than 50% over baseline and tubulointerstitial fibrosis) (Brosius et al., 2009).

1.5.1 *In-vivo*: rodent models

In the current study three different mouse models of diabetes were used (Table 1.5) in order to investigate early changes in organs and circulating cells caused by hyperglycaemia. Streptozotocin-induced (STZ-induced) diabetic mouse were used as a mouse model of T1D. The chemical structure of STZ is similar to glucose; therefore the compound is delivered to the cells through GLUT-2 transporter. STZ specifically targets β-cells and causes cell necrosis through the depletion of ATP (King, 2012). Second mouse model of T1D were Prohibitin 2 knockout mice (β-PhB2$^{-/-}$) which represent a model of spontaneous diabetes progression, through a series of molecular events which appear after 3 weeks and not require administration of chemicals such as STZ (Supale et al.,2013).

Therefore, we used this spontaneous model of diabetes for an examination of the MtDNA content in the presence of hyperglycaemia in parallel to STZ-induced diabetic mice. The Lep ob/ob (ob/ob) recessive obese mice were also used in current study, as a mouse model of T2D. Ob/ob mice carry a mutation in the leptin gene which leads to uncontrolled appetite and quick weight gain (Chua et al., 1996). Detailed information about mouse models used is provided in chapter 4.

Table 1.5. Mouse models used in the study

Acronym	Type 1 diabetes	Method of generation	References
STZ	T1D	Chemical	(Rackham et al., 2013)
β-PHB2$^{-/-}$	T1D	Knockout	(Supale et al., 2013)
ob/ob	T2D	Mutation selection	(Ingalls et al., 1950)

While *in-vivo* studies provide valuable information about the disease, since the changes are systemic, it makes it difficult to study individual pathways and establish direct effects of hyperglycaemia on single type of cells. Using *in-vitro* models of cultured renal cells allows the researcher to manipulate experimental conditions in a way it might not be ethically possible in the *in-vivo* experiments and study early stages of the disease.

1.5.2 *In-vitro*: cultured kidney cells

1.5.2.1 Mesangial cells

Mesangial cells are specialised cells located around the glomerular capillaries within the renal corpuscle of the kidney. They have several functions, including carrying out the deposition of the matrix which results from increased glomerular filtration pressure. However, in DN, these cells contribute to the development of the disease, through expansion of the matrix into the capillary lumens and the secretion of pro-inflammatory cytokines (Wada et al., 2001) and are considered to be key mediators of glomerular inflammation and fibrosis (Wani et al., 2007). Progression of diabetic nephropathy is associated with structural changes in the kidney like thickening of the glomerulal basement

membrane and expansion of extracellular matrix with deposition of collagen type IV and VI, fibronectin and laminin (Wolf, 2004). The diabetic glomerulosclerosis is characterised by mesangial accumulation of extracellular matrix proteins such as laminin, collagen IV and fibronectin genes (Tervaert et al., 2010).

A number of *in-vitro* studies have suggested that hyperglycaemia can modify mesangial cell function and could contribute to changes observed in the DN. A study by Wolf et al., (1992) showed a different rate of proliferation in mouse mesangial cells exposed to high glucose (Wolf et al., 1992). Clarkson at el. (2002) by using a hybridization technique identified 200 genes differentially expressed in human mesangial cells incubated in high glucose. Most of the identified genes included modulators and products of extracellular matrix protein metabolism and regulators of cell growth and turnover (Clarkson et al., 2002). Many reports also showed an increased ROS and ROS-induced inflammatory pathways in mesangial cells in response to hyperglycaemia (Catherwood et al., 2002, Ha and Lee, 2003, Zhang et al., 2011, Al-Kafaji and Malik, 2010). These reports support the idea, that the alterations in pathways signalling in mesangial cells in response to hyperglycaemia may be involved in the development of DN.

1.5.2.2 Tubular cells

DN is often considered to be primarily a glomerular disease however glomerulopathy is only found in a one-third of a patients with T2D and microalbuminuria while other patients have a normal glomerular structure but present severe tubulointerstitial lesions (Gilbert and Cooper, 1999, Dalla Vestra et al., 2000). The progression of renal disease, characterized as pathogenic mechanisms that lead to progressive interstitial fibrosis, peritubular capillary loss and destruction of functioning nephrons due to the tubular atrophy (Eddy, 2005). Proximal tubule epithelial cells create the lining of the duct within nephrons leading to the Bowman's capsule. Although major pathogenic mechanisms in DN development involves glomerular fibrosis, through mesangial expansion, it is now known that tubular epithelial cells are also affected by inflammation (Bohle et al., 1991).

In addition to inflammation, interstitial fibrosis is a major determinant of progressive renal disease. For instance, albumin stimulated proximal tubular epithelial cells to produce TGF-β which is the most effective cytokine for renal fibrogenesis (Liu and Butow, 2006). Another study demonstrated increased expression of toll like receptor 4 (TLR4) via PKC activation in proximal tubular cells cultured in high glucose (Lin et al., 2012). Kidney injury molecule-1 (KIM-1) was demonstrated to be released from proximal tubular cells by the exposure to high glucose and AGE in parallel with increased ROS (Lim et al., 2014a). Lee at al., (2014) showed increased mitochondrial respiration and complexes activity in mitochondrial renal tubule cells from spontaneously hypertensive rats (Lee et al., 2014). Peng at al., (2014) demonstrated activation of mitochondrial mediated apoptosis and ATP depletion in high glucose-conditioned renal proximal tubular cells (Peng et al., 2014). These studies support the view that tubular cells can also contribute to the development of DN.

1.6 Background of the study

A number of novel genes that are regulated by high glucose in rodent models of diabetes and mesangial cells grown in high glucose have been identified previously in our group, in an attempt to find novel therapeutic targets for DN. In 1997, using mRNA fingerprinting in rat model of diabetes, our group identified several genes that were up regulated in the kidney, during the development of diabetes. A number of changes in mRNA expression under hyperglycaemic state were detected in genes specific for mitochondrial genome (Table 1.6.) (Page et al., 1997). This led to further research and more focus on the possible correlations between mitochondria, progression of diabetes mellitus and development of DN.

Further findings showed that patients with diabetes and proteinuria had elevated levels of MtDNA circulating in their blood, when compared to the healthy controls and patients with diabetes, but without proteinuria (Malik et al., 2009). Also unpublished results from our group obtained from two experiments; a diabetic Goto-Kakizaki rat (GK-rat) study and *in-vitro* cultured renal cells suggested increased MtDNA copy caused by hyperglycaemia. MtDNA content was significantly increased in kidneys of diabetic animals, when compared to the

age matched controls (Malik and Al-Kafaji unpublished) and also significantly up-regulated in renal cells cultured for 3 days in 25mM glucose (Malik unpublished). These results suggest there may be a correlation between mitochondrial biogenesis and development of kidney disease in diabetes.

Table 1.6. Increased mitochondrial mRNAs in the diabetic rat kidney. cDNA fragments corresponding to mitochondrial genes up-regulated in hyperglycaemia in diabetic GK rat kidneys. CDK stands for candidate diabetes associated kidney clones.

Clone	Identity
CDK2	NADH ubiquinone oxidoreductase 42KD subunit precursor
CDK110	mitochondrial cytochrome b
CDK116	RM NADH dehrogenase subunit
CDK117	RM cytochrome C oxidase subunit I
CDK118	RM cytochrome C oxidase subunit I
CDK120	RM cytochrome C oxidase subunit II
CDK121	RM NADH dehrogenase subunit 5
CDK123	RM cytochrome C oxidase subunit I
CDK124	RM cytochrome C oxidase subunit I
CDK125	RM cytochrome C oxidase subunit I
CDK126	RM cytochrome C oxidase subunit I

To date, very little is known about mitochondria biogenesis, replication and degradation and there are many discrepancies in the literature about MtDNA content in diabetes, probably due to the pitfall of the methodology used for the quantification (Lee et al., 1998, Rolo and Palmeira, 2006, Hsieh et al., 2011, Singh et al., 2007, Gianotti et al., 2008, Weng et al., 2009). A common method for measuring MtDNA content is by using real-time qPCR assay and mitochondrial encoded gene to nuclear encoded gene ratio. However there are several problems with using mitochondrial specific primers as mitochondrial genome is widely duplicated in the nuclear genome (Fig.1.10), therefore many of the commonly used MtDNA primers co-amplify homologous pseudogenes.

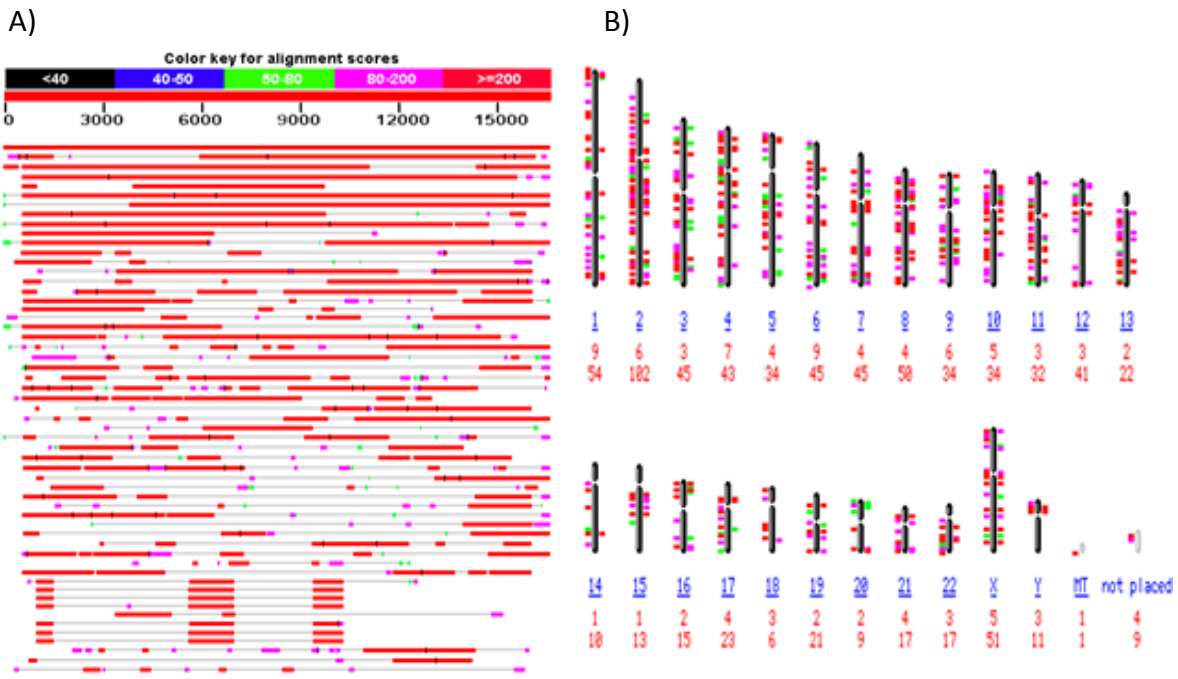

Fig.1.10. Duplication of the mitochondrial genome in the nuclear genome: The mitochondrial genome sequence accession number NC-001807, was blasted against the reference sequence of the human genome using blast, the first 50 best matching sequences are shown, the top red line being an exact match to the mitochondrial genome, whereas the remaining 49 lines are regions of the nuclear genome showing a high degree of identity. The colour key for alignment scores is given at the top of the figure with red being the highest alignment score (A). Mitochondrial pseudogenes in the nuclear genome are shown as bars against the relevant human chromosome, the extent of the homology is shown as a colour code indicated in and the number of hits is shown in red numbers below the chromosome number shown in blue (B).Taken from (Malik et al., 2011).

Secondly, using regions from nuclear genes such as β-actin and 18S rRNA as experimental controls which are repetitive and/or highly variable leads to errors. Also errors during DNA extraction, dilution (the size difference of mitochondrial and nuclear genomes cause a ‘‘dilution bias’’ when template DNA is diluted) and storage may affect the results. A unique assay developed in our group previously, for assessing MtDNA content using mitochondrial genome specific primers and optimised preparation of the samples, allows avoiding bias in co-amplifying mitochondrial sequences, which are duplicated in the nuclear genome. The content of MtDNA is assesed as a ratio of mitochondrial to nuclear genome and Beta-2 microglobulin (B2M) is used as a single copy gene for the nucelar control (Malik et al., 2011).

1.7 Hypothesis and Aims

Although mitochondrial dysfunction has been proposed to be a key mechanism in the development of DN and diabetic complications, the main mechanisms leading to this are not fully understood. DN develops over decades of clinical silence and currently there are no biomarkers which allow detetction of the early clinically silent stages of DN. The main hypothesis that will be tested in this thesis is that hyperglycaemia/high glucose can cause early changes in mitochondrial DNA (content/quality) and that these changes can contribute to mitochondrial dysfunction.

Aims and objectives:

The major aim of this thesis is to test the hypothesis that glucose-induced changes in MtDNA contribute to mitochondrial dysfunction and that this process is involved in the damage to the kidney that results in development of DN.

This aim will be met by undertaking the following objectives:

1. I will examine whether hyperglycaemia can alter MtDNA content in cultured renal cells and whether any such changes are permanent.
2. I will investigate, using *in-vivo* models of diabetes, whether hyperglycaemia can alter MtDNA content in organs and circulating cells of diabetic mice.
3. I will examine whether glucose-induced changes in MtDNA occur in parallel with functional changes in mitochondria in cultured renal cells.
4. I will examine whether glucose-induced changes in MtDNA occur in parallel with altered mitochondrial respiration in renal cells.

The above specific objectives will be met using different experimental models (*in-vitro* and *in-vivo*) and a range of molecular/cellular biology and biochemical techniques to understand the relationship between MtDNA content and mitochondrial dysfunction and their contribution to early glucose-induced changes which may be involved in the development of DN.

Chapter 2

Materials and Methods

Chapter 2

2.1 Chemicals and reagents

All chemicals and reagents used in this study were of molecular biology grade. A list of the chemical and reagents along with their suppliers are shown in table 2.1.

Table 2.1. List of chemicals, reagents and their suppliers

Materials and kits	Supplier
Dulbecco's modified eagle's medium (DMEM),Penicillin-Streptomycin, Ampicillin, Trypsin, Chloroform, Transfer ribonuclease (tRNA), Bromophenol blue, Ethidium bromide, Trypan blue, Sodium dedeocylsulfate (SDS), Tris base (Tris-HCl), Ammonium persulphate, Glycine, Nonfat milk, Tween 20, Bovine serum albumine (BSA)	Sigma-Aldrich Ltd (UK)
Mouse polyclonal horseradish peroxidase conjugated (HRP) antibody,	Santa Cruz Biotechnology Inc. (UK)
Hybond nitrocellulose paper, 3MM Chromatography papers	Amersham Biosciences Ltd (UK).
Insulin-transferrin-selenium (ITS), HEPES buffer, Foetal bovine serum (FBS), Phosphate buffer saline (PBS), L-glutamine, SeeBlue®Plus2 Pre-Stained Standard marker, Agarose, MitoTracker Orange CMTMRos, Countess cell counting chambers	Invitrogen, Life Technologies (UK)
DreamTaq PCR master mix, 100 base pair DNA ladder, Molecular grade DNAse, RNAse free water, BCA kit	Thermo Scientific
DNeasy Blood or Tissue kit, RNeasy Mini kit , Proteinase K, Quantifast SYBR Master Mix (2x), Qiaquick gel extraction kit	Qiagen (UK)
Cell culture flask (25; 75; 162 cm^2), 6-well cell culture cluster, Polypropylene conical falcon tube (15; 50 ml), sterile pipette (5; 10; 25 ml), 0.22 mM sterile filters, 1 ml Cryo-vials	Beckton Dickinson Ltd. (UK)
Filter, Rnase, DNase free tips, 1.5ml tubes	STar Lab (UK)
Molecular Biology Grade : Ethanol, Methanol, Isopropanol, 96-well PCR plates	VWR International Ltd.(UK)
XF^e96 FluxPak, XF Cell Mito Stress Test Kit	Seahorse Bioscience Ltd
HK-2 cells	ATCC
Total OXPHOX human WB antibody cocktail, β-actin antibody	Abcam

2.2 Solutions and buffers

All solutions and buffers were prepared according to the manufacturer's instructions and were sterilized by autoclaving, except those supplied in kits. Table 2.2 shows the buffers and reagents that were prepared according to the manufacturer's instruction.

Table 2.2. preparation of reagents and buffers

Solution	Chemical components
0.5 M EDTA pH 8.0/ 500 ml	Disodium ethylenediaminetetra-acetate.$2H_2O$ 186.1 g (pH 8.0 adjusted with NaOH)
10 X Tris-borate (TBE)/ 1000ml	Tris base 108 g, boric acid 55 g, 0.5 M EDTA (40 ml, pH 8.0)
10 X Tris-acetate /100ml	Tris base 108 g, glacial acetic acid 11.42g, 0.5 M EDTA (20 ml, pH 8.0)
1 M Tris/ 500 ml	Tris-base 60.55 g pH 7.0, 70 ml HCl added
10% SDS/ 500ml	Electrophoresis-grade SDS 50 g, pH 7.2 with few drops of HCl

2.3 Cell culture

2.3.1 Culturing of renal cells

Three types of human renal cells were used in the study, primary cultured human mesangial cells (HMCs, kindly provided by Prof Luigi Gnudi from Cardiovascular Division at KCL), human mesangial immortalised cells (HMCL, kindly provided by Dr Ruan Xiongzhong from Nephrology Department at UCL) and human cortex proximal tubular immortalized cells (HK-2, ATCC, LGC Standards). HMCL, HMCs and HK-2 cells were grown in Dulbecco's Modified Eagle's Medium (DMEM) enriched with supplements. Complete growth medium was supplemented with: 10% of fetal bovine serum (FBS, Gibco), 1ml of Insulin-Transferrin-Selenium (ITS, 5ug/ml, Life Technologies Ltd.) 1ml of Amphotericin B (0.25ug/ml, Life Technologies Ltd.), and 5ml of mixture of penicillin and streptomycin (100 units/ml, Sigma Aldrich, UK). Cells were cultured in 5ml or 15

ml of the complete growth medium in T-25 or T-75 culture flasks respectively; when 6-well plates dishes were used, cells were grown in 2 ml of media/well. Cells were cultured at 37°C in a humidified atmosphere containing 5% CO_2 until 80% confluent before passaging. Confluence was assessed under the inverted microscope. The growth medium was replaced every 2-3 days.

2.3.2 Subculturing

During routine culture complete growth media was renewed every 2-3 days and cells growth density was carefully inspected under the microscope. When cells reached approximately 80% of confluence, flasks were removed from the incubator and media was aspirated and discarded. Cell layer were then washed once with calcium free phosphate buffered saline (PBS, Sigma Aldrich ,UK) in order to remove any traces of FBS which has an inhibitory effect on Trypsin-EDTA (Sigma Aldrich, UK) solution used for cells' detachment. Trypsin actively digests the anchorage sites between the cells and the growing surface, and EDTA binds to Ca^{2+} that is required for Ca^{2+}-dependent adhesion due to its divalent ion chelating property. Between 2-5 ml of pre-warmed Trypsin-EDTA solution was added to the cells and incubated for approximately 3-5 min at 37°C to detach the cells from the flask. After 3 min of incubation cells were inspected under the inverted microscope in order to assess cell layer dispersion. 5ml of complete growth medium was then added to the flask to stop the digestion. Cell mixture was then gently aspirated and placed in a sterile 15 ml falcon tube and centrifuged at 100x g for 5min. To remove Trypsin-EDTA solution supernatant was discarded and the cell pellet resuspended in fresh 5.5mM of glucose complete growth medium and transferred the culture flask. A subcultivation ratio of 1:4 was used in all grown cell types. After plating cells were inspected under the inverted microscope and returned to the incubator.

2.3.3 Counting the cells

For the purpose of the experiments cells were counted and their viability assessed by using Countess Automated Cell Counter (Life technologies, Ltd.) which allowed accurate and reproducible assessment of cell number within 30 sec. After trypsinisation, 10µl of cell suspension was thoroughly mixed with equal

volume of 0.4% trypan blue (Life technologies, Ltd.) and pipetted into Countess chamber. Reactivity of trypan blue is based on the fact, that it is negatively charged and does not interact with the cell unless the membrane is damaged. Therefore, all the cells which exclude the dye are viable. Total cell number and viability was assessed and cell solution was diluted in order to obtain required cell number per ml of growth media. Cells were next plated in 6- well culture plates at the density: $1x10^4$ (HMCs and HMCL) - $1x\ 10^5$ (HK-2) cells per well. Before the start of the experiments growth of the cells was arrested for 24h by culturing them in DMEM supplemented with 0.5% FBS only. This step helps to synchronize the growth of the cells before the start of the treatment.

2.3.4 Freezing down and thawing the cells

Cells which are in the logarithmic phase of growth and just approaching confluency (80-85%) were harvested as described above, and re-suspended with pre-warmed freezing medium containing: DMEM (10 %), DMSO (10%) and FBS (80%). Cell suspension was dispensed in 1 ml aliquots into sterile freezer Cryo-vials. The Cryo-vials were placed in a Nalgene Cryo freezing container filled with appropriate volume of isopropanol and placed at -80^{o}C overnight (ideally, the temperature should decrease 1^{o}C per minute). Frozen vials were then stored in a liquid nitrogen for permanent storage. To recover the cells, frozen cryo vials with cells were thawed in a 37˚C water bath, after partial defrosting, 500 ul of pre-warmed complete growth medium was added to the vials and cell solution was gently transferred to the sterile 15 ml falcon tube containing growth media. Cell mixture was then centrifuged at 100x g for 5 min. To remove any residue of DMSO which can be toxic to the cells, supernatant was discarded and the cell pellet was gently re-suspended in fresh 5.5mM of glucose complete growth medium and transferred the culture flask. Cells were inspected after under the inverted microscope and maintained under the same culture conditions as described previously.

2.3.5 Culturing mesangial and tubular cells in the presence of high glucose

In order to perform *in-vitro* experiments cells were grown under four different conditions including: 5mM D-glucose (normal glucose-NG), 25 mM D-glucose

(high glucose-HG) and 5mM glucose plus 20mM D-mannitol (osmotic control, NGM) which served as an osmotic control. In one of the high glucose group medium was reverted to normal glucose (HG/NG). Before starting the experiment cells were counted and synchronized as described previously. Experiment was carried out in 6 replicates for 4-12 days, with medium changed every 2-3 days. After finishing the experiment, medium was aspirated and cell layers washed twice with ice cold PBS. Cells were then trypsinized, transferred into 1.5ml microcentrifuge tubes and centrifuged at 300xg for 3 min. Supernatants were removed and cell pellets were snap frozen in liquid nitrogen and stored at -80°C for further processing.

2.4 Mouse tissue and peripheral blood samples

2.4.1 Streptozotocin mouse model of type 1 diabetes

STZ-diabetic mouse model was kindly provided by Dr Chloe Rackham from King's College London. 8 week old male C57BL/6 mice were made diabetic with an injection of 180 mg/kg streptozotocin (STZ, Sigma Aldrich, UK) dissolved in citrate buffer (Citric Acid: 0.21g, 0.9% NaCl: 00ml at pH 4.5) and administered within 10 minutes. To measure blood glucose, a needle prick was made at the end of the tail and blood glucose concentrations were determined using blood and an Accu-Chek glucose meter and strips (Roche). Islets were isolated from the pancreases of 8-10 week old male C57BL/6 mice using collagenase digestion followed by gradient purification, as described previously (King et al., 2007). Three days after STZ injection, diabetic mice (>15 mM) received a suboptimal islet graft of 150 islets transplanted under the left kidney. Islets were implanted into isoflourane anaesthetized mice using PE50 tubing and a Hamilton syringe (Rackham et al., 2013). 1 week and 4 weeks after transplantation, kidneys were obtained from animals which had not been treated and thus remained diabetic throughout the study (blood glucose level > 15 mM) or from treated mice (blood glucose level < 11.1 mmol/L for 4 weeks after transplantation). In addition, 12 week-old non-transplanted, non-diabetic mice were used as controls (glucose level <11 mmol/L). Tissues were removed and immediately frozen in liquid nitrogen, and stored at −80°C until further processed.

2.4.2 Prohibitin2 knockout mouse model of type 1 diabetes

ß-*Phb2*$^{-/-}$(beta-cell specific prohibitin 2 knockout) mice were bred from crossing of flox-Phb2-flox mice with Rat-Insulin promoter driven Cre mice so that PHB2 is specifically deleted in the pancreatic beta-cells. This spontaneous mouse model of T1D was kindly provided by Dr Sachin Supale and Prof Pierre Maechler from University of Geneva. These ß-*Phb2*$^{-/-}$mice developed mild diabetes at the age of 5-6 weeks and then became severely diabetic at 8-9 (Supale et al., 2013). Blood samples from control and diabetic mice were taken weekly between weeks 4 to 11 and kidney samples were collected at week 11. Tissues were removed and snap frozen in the liquid nitrogen, and stored at −80°C until further processed.

2.4.3 Lep $^{ob/ob}$ mouse model of type 2 diabetes

Lep$^{ob/ob}$ (ob/ob) mice were used as a mouse model of T2D. The ob/ob mice were kindly provided by Dr Aileen King from King's College London. Ob/ob mice have a mutation in the leptin gene which leads to uncontrolled appetite and quick weight gain. Mutants were discovered in the out-bred colony in the Jackson Laboratory in 1949 and later bred into C57BL/6 mice (King, 2012, Ingalls et al., 1950). Ob/ob mice are a very good model for insulin resistance caused by obesity as they start gaining weight within 2 weeks following birth and develop hyperinsulinaemia and moderate hyperglycaemia after 4 weeks. Tissues were removed and snap frozen in the liquid nitrogen, and stored at −80°C until further processed.

2.5 DNA extraction

2.5.1 DNA extraction from human cells

To prepare genomic DNA from the cell pellets a column base method (Qiagen DNeasy Blood and Tissue kit) was used according to manufacturer's instructions. Following termination of the experiments cells were collected as described above. Cell pellets were snap frozen in liquid nitrogen and stored at -80°C. 200µl of PBS was added to the cell pellets, followed by 20µl of proteinase K (>600mAU/ml, Qiagen, UK). All samples were vortex for about 30s in order to completely disperse cell pellets. Buffers AL, AW1, AW2 and AE were provided

with the DNeasy kit. To lyse the cells 200µl of lysis buffer (buffer AL, without added ethanol) was added and mixed by vortexing. Samples were then incubated at 56°C for 10 min. Following incubation, 200µl ethanol (96–100%) was added and mixed thoroughly by vortexing. Lysates were transferred into the DNeasy Mini spin column placed in a 2 ml collection tube and centrifuged at 9300x g for 1min. In order to wash the columns, 500µl wash buffer AW1 was added to the columns and spun down at 9300x g for 1 min. Wash step was repeated with 500µl of buffer AW2 and columns were dried by spinning down at 12000x g for 3 min. To elute the DNA, 30µl of elution buffer (buffer AE) was added directly onto the DNeasy membrane, incubated at room temperature for 1 min, and then centrifuged for 1 min at 9300x g. For maximum DNA yield, elution step was repeated once again in 30µl buffer AE to make 60µl of total volume. Between 1-2µl of DNA was used to determine the concentration and quality of the DNA using the NanoDrop or equivalent instrument as described in section 2.6.3.

2.5.2 DNA extraction from mouse tissue and mouse blood samples

- DNA extraction from mouse tissues

To prepare genomic DNA from the tissues and whole mouse blood a column base method was used (Qiagen DNeasy Blood and Tissue kit), according to manufacturer's instructions. Lysis buffers ATL, AL, wash buffers AW1 and AW2 and elution buffer AE were provided with the kit (Qiagen). First step in the total DNA extraction from mice tissues was the homogenisation of approximately 0.3-0.5g of tissue in 180µl of ATL lysis buffer in 2ml microtubes (QIAGEN, UK) using Tissue lyser (Qiagen, UK) for 3-5 minutes at 20MHz. Following homogenisation, samples were briefly spun down and 20µl of proteinase K was added to each tube. Samples were then incubated at 56°C for 2-3h to allow complete lysis. Following incubation, 200µl ethanol (96–100%) was added and mixed thoroughly by vortexing. Lysates were transferred into the DNeasy Mini spin column placed in a 2 ml collection tube and centrifuged at 9300x g for 1min. In order to wash the columns, 500µl wash buffer AW1 was added to the columns and spun down at 9300x g for 1 min. Wash step was repeated with 500µl of buffer AW2 and columns were dried by spinning down at 12000x g for 3 min. To elute the DNA,

50µl of elution buffer (buffer AE) was added directly onto the DNeasy membrane, incubated at room temperature for 1 min, and then centrifuged for 1 min at 9300x g. For maximum DNA yield, elution step was repeated once again in 50µl buffer AE to make 100µl of total volume.

- DNA extraction from mouse whole blood

Between 10-50µl of blood samples was used and adjusted to 200µl with PBS buffer. 20µl of proteinase K (>600mAU/ml, Qiagen, UK) was added to the PBS/blood mixture and mixed for 15s. To lyse the cells 200µl of lysis buffer (buffer AL, without added ethanol) was added and mixed by vortexing. Samples were then incubated at 56°C for 10 min. Following incubation, 200µl ethanol (96–100%) was added and mixed thoroughly by vortexing. Lysates were transferred into the DNeasy Mini spin column placed in a 2 ml collection tube and centrifuged at 9300x g for 1min. In order to wash the columns, 500µl wash buffer AW1 was added to the columns and spun down at 9300x g for 1 min. Wash step was repeated with 500µl of buffer AW2 and columns were dried by spinning down at 12000x g for 3 min. To elute the DNA, 30µl of elution buffer (buffer AE) was added directly onto the DNeasy membrane, incubated at room temperature for 1 min, and then centrifuged for 1 min at 9300x g. For maximum DNA yield, elution step was repeated once again in 30µl buffer AE to make 60µl of total volume.

Between 1-2µl of DNA was used to determine the concentration and quality of the DNA using the NanoDrop or equivalent instrument as described in section 2.6.3.

2.5.3 Pre-treatment/fragmentation of DNA

In order to avoid dilution bias, DNA template had to be sheared via sonication method. Between 30-50µl of DNA was transferred into a clean 1.5ml micro centrifuge tube, placed in a Bath sonicator (Kerry, Pulsatron 55) which uses 38 kHz +/- 10% and sonicated for 5 to 10minutes. After sonication, concentration of DNA was determined again and adjusted between 1ng/µl to 10ng/µl. Following the pre-treatment and dilution, samples were checked by amplifying hMito3 and

hB2M1 genes or mMito and mB2M using PCR method and specific primers given in table 2.3 and table 2.4.

Following extraction and sonication, samples were stored at 4°C to avoid freezing for the duration of the study.

2.6 RNA extraction

There are four types of RNAs in living cells, messenger RNA (mRNA), transfer RNA (tRNA), ribosomal RNA (rRNA) and microRNA (miRNA). A good quality of total RNA is required to detect specific gene expression by complementary DNA (cDNA) amplification using polymerase chain reaction (PCR).

2.6.1 RNA Extraction from human cells

Total RNA was extracted from collected cell pellets according to manufacturer instruction by using RNeasy Mini kit (Qiagen,UK). Lysis buffer RLT, wash buffers RW1 and RPE were provided with the kit (Qiagen , UK). Renal cells were grown as monolayers in a 6-well plates and harvested by trypsinisation when reached 75-80% confluency. Cell pellets were re-suspended in 600µl of lysis buffer (RLT) and briefly mixed by vortexing. Lysate was then transferred to into QiaShredder column in order to homogenize cell membranes and spun down for 3 min at 12000x g. Following centrifugation, column was discarded and 600µl of 70% ethanol was added to the homogenised lysate. Following mixing by pipetting, 700µl of homogenate was transferred to a RNeasy spin column and centrifuged for 15s at 12000x g. Flow through was discarded after the centrifugation and membrane with bounded RNA was washed with 700µl of washing RW1 buffer. Following another centrifugation step (15s, at 12000x g), membranes were washed with 500µl of RPE buffer. After final centrifugation step (2min, 12000x g), columns were transferred into new 1.5ml collection tubes. Extracted RNA was eluted with 50µl of the RNase-free water. RNA samples were stored at -80 °C.

2.6.2 RNA extraction from mouse tissue

Total RNA was extracted from mouse kidney tissues using Qiazol-based extraction method (Qiagen, UK) according to manufacturer guidelines.

Approximately 0.1-0.5g of tissue was homogenised in 2ml microtubes (QIAGEN, UK) the 800µl of Qiazol using Tissue lyser (Qiagen, UK) for 3 minutes at 20MHz. Following homogenization, RNA was separated from protein and DNA by adding 200 µl of Chloroform (Sigma- Aldrich) and mixed vigorously for 15s. Next, homogenate was incubated at room temperature for 3 minutes. Samples were centrifuged for 15 min at 14500x g at 4 °C and the aqueous phase (approximately 60% of the total volume) was transferred to a fresh nuclease-free tube. 500µl isopropyl alcohol (Sigma-Aldrich, UK) was added to the aqueous phase, inverted to mix and incubated at room temperature for 10 minutes. RNA pellets were recovered by centrifugation (14500x g, 20 min, 4 °C) and washed with 0.5ml of 75 % chilled ethanol (Sigma-Aldrich, UK). Pellets were re-precipitated by centrifugation (5000x g, 20 min, 4 °C) and left to air dry to remove the ethanol. RNA was re-suspended in 50 µl dH_2O and stored at - 80 °C.

2.6.3 Determination of RNA concentration

Concentrations of RNA in the extracts were quantified using the ND1000 spectrophotometer (Nanodrop). This device is able to measure 260 and 280nm absorbance from samples in only 1µl of extract. A_{260nm} is automatically converted to give an accurate estimation of RNA content in ng/µl. Moreover, the ratio of A_{260nm}/A_{280nm} can be further used as an indication of RNA quality. A ratio of <1.6 indicates contamination of samples with protein, phenol or other compounds which absorb at 280nm. Sample RNAs with $A_{260}nm/A_{280nm}$ > 1.6 were stored at -85˚C and used subsequently for complementary DNA (cDNA) synthesis.

2.6.4 DNase-1 treatment of RNA

No RNA isolation procedure can guarantee the complete removal of trace amount of DNA below the limit of detection by real-time qPCR. Therefore, to effectively remove the DNA contamination from RNA, a DNA inactivation kit based on DNase I treatment (Life Technologies-Ambion, UK) was used. A 50µl RNA was mixed gently with 5µl of DNase-1 buffer (10 X), DNase I enzyme (0.5µl) and incubated at 37 °C in a heat block for 30 min. After this step, the RNA should be free from contaminating DNA. The DNase I must be now removed from RNA that will be subjected to RT-PCR because it could degrade DNA made in the PCR.

Consequently, the reaction was stopped by adding 5µl of DNase inactivation reagent and mixed by gentle flicking to disperse the DNase inactivation reagent in the reaction. Samples were incubated at room temperature for 2 min and were flicked once more to re-disperse the reagent. The DNase inactivation reagent removes divalent cations introduced by the DNase-1 buffer and these cations can degrade RNA at temperature typically used for RNA denaturation prior to reveres transcription. To recover the RNA, samples were centrifuged at 14,000 rpm for 1 min and the upper layer was carefully transferred to 1.5ml DNA-free microcentrifuge tube (with avoiding any transfer of the DNase inactivation agent). The treated RNA samples were then kept at -80 °C.

2.6.5 cDNA synthesis

Reverse transcription is a process, in which single-stranded mRNA is transcribed into complementary DNA (cDNA) using the reverse transcriptase enzyme. Equal amounts of the DNA-free RNA (2 µg) were reverse transcribed to cDNA using High Capacity RNA-to-cDNA KIT (Life-Technologies, Applied Biosystems, UK).

According to the protocol provided with the kit, cDNA synthesis was carried out as following:

Preparation of RNA: RT primer mix:

11 µl of RT –mix (including Oligo-dT and random hexamer primers, RT buffer) was gently mixed with 9 µl of RNA and 1 µl of RT enzyme mix. The RNA:RT mixture was then incubated at 37 °C for 60 min. The cDNA samples were stored at -20°C.

2.7 Assessment of the gene expression

2.7.1 Polymerase chain reaction- PCR

Polymerase chain reaction (PCR) technology was invented by Dr. Kary Mullis in 1983 for which he received a Nobel Prize in chemistry in 1993. PCR is a technique to amplify DNA sequences of interest *in-vitro* (Fig.2.1).

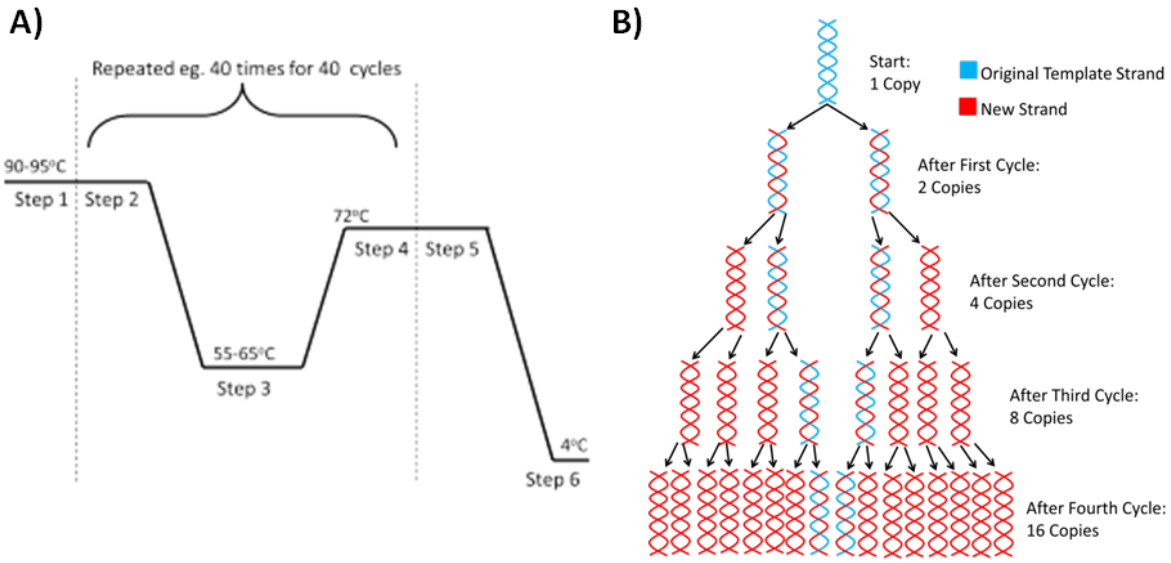

Fig.2.1. Schematic illustration of PCR amplification. A)The double stranded cDNA is dissociated at 95˚C (melting) and cooled down to an appropriate temperature to allow binding of primers to complementary sequences within the template DNA (annealing). The primers serve as initiation points for DNA polymerase which, at 72˚C, extends the primers in the 5' to 3' direction thereby facilitating DNA synthesis (extending). B) As PCR cycles are repeated, new DNAs sequences are generated exponentially. Adapted from (Hollis, 2013).

DNA polymerase is required to synthesise specific regions of template DNAs. Pairs of sequence-specific oligonucleotide primers are essential to define replicating regions by binding to complementary sequences on the DNA template where amplification starts and stops. PCR amplifications are carried out in thermal cyclers in repeated cycles of three phases: denaturation of double stranded DNAs at 95˚C, annealing between primers and DNA templates at ~60˚C, and extension of newly amplified DNAs of interest at 72˚C (Fig.2.2.A). The annealing temperatures are usually determined by the percentage of guanosine and cytidine nucleosides in the DNA sequence of interest and by primer length.

In the experiments described in this thesis, real time qPCR was performed with cDNAs of renal cells, and DNA extracted from cells and mouse kidneys and mouse blood samples. Specific sets of primers were designed and selected using the Roche Universal ProbeLibrary System technology (Roche, 2012) and used to amplify regions of interest. List of primers used in this thesis are shown in tables 2.3 and 2.4.

Table 2.3. Human oligonucleotide primers used in this study

Gene	Accession number	Primers (5'->3')	Amplicon Length (bp)
TFAM	NM_003201.2	F:GAACAACTACCCATATTTAAAGCTCA	95
		R: GAATCAGGAAGTTCCCTCCA	
PGC1a	NM_013261.3	F: ACTGCAGGCCTAACTCCACCCA	190
		R: ACTCGGATTGCTCCGGCCCT	
NFkB p65	NM_021975.3	F: CCTGGAGCAGGCTATCAGTC	213
		R: ATCTTGAGCTCGGCAGTGTT	
MYD88	NM_001172567.1	F: TTTGCACTCAGCCTCTCTCC	121
		GGTTGGTGTAGTCGCAGACA	
MFN1	NM_033540.2	F:GAGAAAATACAAAACAATTCAAAGCTC	96
		R:GCTTGAAGGTAGAAACTGCTTAGTAAA	
MFN2	NM_014874.3	F: AGCCACCAAGTCCAGCAG	117
		R: AACCTCAATTTTCTTGTTCATGG	
OPA1	NM_015560.2	F: GAGCCAGGTTACACCAAAACA	120
		R: GTTCCTGAATTCATGGTCTGC	
Pink1	NM_032409.2	F: CTTACAGAAAATCCAAGAGAGG	199
		R: CAGGGATAGTTCTTCATAACG	
Park2	NM_004562.2	F: GAGGATTTAACCCAGGAGAG	113
		R: ACAAACACTATCATGGTCAC	
Drp1	NM_012063.3	F: TCACGAGACAAGTTAATTCAGGA	344
		R: GCCTTTGGCACACTGTCTTG	
ND1	NC_012920.1	F: GAGCAGTAGCCCAAACAATCTC	140
		R: GGGTCATGATGGCAGGAGTAAT	
ND6	NC_012920.1	F: TGGGGTTAGCGATGGAGGTAGG	140
		R: AATAGGATCCTCCCGAATCAAC	
COX3	NC_012920.1	F: TCCTCACTATCTGCTTCATCCG	140
		R: CCCTCATCAATAGATGGAGACA	
β-actin	NM_001101.3	F: GACGACATGGAGAAAATCTG	131
		R: ATGATCTGGGTCATCTTCTC	
hMito3	NC_012920.1	F: CACTTTCCACACAGACATCA	127
		R: TGGTTAGGCTGGTGTTAGGG	
hB2M1	NC_000015.10	F: TGTTCCTGCTGGGTAGCTCT	187
		R: CCTCCATGATGCTGCTTACA	
Mito primer[b] (damage)	J01415	F: TCTAAGCCTCCTTATTCGAGCCGA	8.9 kb
		R: TTTCATCATGCGGAGATGTTGGATGG	

Table.2.4. Mouse oligonucleotide primers used in this study

Gene	Accession number	Primers (5'->3')	Amplicon Length (bp)
mMito	NC_012387.1	F: CTAGAAACCCCGAAACCAAA	125
		R: CCAGCTATCACCAAGCTCGT	
mB2M	NC_000068.7	F: ATGGGAAGCCGAACATACTG	177
		R: CAGTCTCAGTGGGGGTGAAT	

PCR reaction mixes was performed in 0.2 ml PCR tubes and a reaction mix was prepared by adding 12.5µl of DreamTaq PCR master mix, 0.5µl of forward and reverse primer (10 µM) and 10.5µl RNase free H_2O. Between 1-2µl of DNA template was added and gently vortexed and spun down. DNA templates were amplified using a Thermal Cycler (Thermal Cycler, Bioer) using following conditions: initial denaturation at 94^oC for 15 minutes (1cycle), followed by denaturation at 94^oC for 30 seconds, annealing at 60^oC for 30 seconds and extension 72^oC for 1 minute and 30 seconds (30 cycles). Final extension was at 72^oC for 7 minutes. Once the amplifications had been completed, 10µl of each PCR product were loaded into a 2% agarose gel, which was prepared using 2g of agarose (Invitrogen), 50ml of 0.5X TBE buffer and 10µl ethidium bromide (Sigma 100ng/µl). The agarose was melted in a microwave oven (medium power, 5 min) and cooled to approximately 60°C. when it is cooled down, ethidium bromide (0.5 µg/ ml) was added. Ethidium bromide stained gel was then cast to a thickness of 5 mm comb. The gel was placed in horizontal gel electrophoresis apparatus and covered with 1X TBE buffer. Loading buffer (2 µl) was added to each DNA sample (5-10 µl), mixed and loaded into the well of the agarose gel. Electrophoresis (50-100 V, 1-2 hrs) was carried out at to allow a sufficient separation of the DNA fragments. Ethidium bromide stained agarose gels were then placed on a UV transilluminator in order to assess specificity of the PCR reaction.

2.7.2 Preparation of standards for absolute quantification

- *Purification of DNA from the gel band*

Following PCR amplification with the appropriate primers (*see* table 2.3 and 2.4) and gel electrophoresis of PCR products, DNA fragments were excised from the gel with a clean scalpel using a UV transilluminator (Transilluminator UVP) to visualise the bands. Excised agarose chunks with DNA were placed in a clean tube and QIAquick Gel extraction Kit was used, according to the manufacturer's protocol. The excised gel was weighed and three gel volumes of buffer QG was added to the gel. The gel was then incubated at 50°C for 10min to dissolve the gel, vortexing it every 2-3mins to mix the solution. One gel volume of isopropanol was then added and the solution was mixed by vortexing. 800µl of the sample mix was then added to a QIAquick spin column in a 2ml collection tube and centrifuged for 1min at 14500x g. The flow through was discarded, and the remaining sample was loaded and spun again repeatedly until all the sample had been used up. 500µl of buffer QG was added and centrifuged for 1min at 14500x g. The sample mix was then washed with 750µl of buffer PE and centrifuged for 1min at 14500x g. The flow though was discarded and the sample was spun again. The QIAquick column was then placed in a 1.5ml microcentrifuge tube and the DNA was eluted by 30µl of the elution buffer EB added to the centre of the membrane and then the sample centrifuged for 4min at 14500x g. 10µl of purified DNA was run on the 2% agarose gel, to ensure, that PCR product was purified successfully before proceeding to standards preparation.

- *Standards preparation*

It is essential that the dilution series from which the standard curve is generated be carefully prepared. To prepare standards for the generation of standard curves, PCR products were purified using the GFX PCR DNA and gel band purification kit as described above. Concentration of the purified DNA was assessed using NanoDrop instrument. The exact DNA copy numbers of the purified PCR product were calculated using Avogadro's number and the formula shown on Fig.2.2. A dilution series containing 10^7, 10^6, 10^5, 10^4, 10^3 and 10^2 copies/µl of the gene to be quantified were prepared in the presence of carrier

transfer ribonucleic acid (tRNA, 10 mg/ ml; Sigma, UK) and used as a calibration curve in every run with the Roche LC480. Standards prepared for a target gene and a reference gene were used to establish standard curves by amplification in 10-fold dilutions of PCR product of each gene to be quantified.

$$\frac{Avogadro's\ constant}{MW\ x\ 10^9} x\ Concentration = copies/\mu l$$

Avogadro's constant = 6.02 x 10^{23}

MW = 330Da x 2 x template length (bp)

Concentration of DNA = ng/µl

Fig.2.2. Calculation of the copy number per µl of the PCR product. Following gel purification, DNA concentration was measured on NanoDrop and copy number of gene of interest per µl of extracted PCR product was calculated using the formula presented on a figure.

2.7.3 Real time quantitative PCR -amplification of required product

Quantitative real-time polymerase chain reaction is a sensitive and specific technique used to characterise gene expression patterns. Total RNA is extracted from tissues and cDNA is synthesised from the messenger RNA (mRNA) present in the total RNA using the reverse transcriptase enzyme. The target amplicon specific to the gene of interest in the cDNA is then amplified to detectable levels using PCR. The amplification process is monitored in real time by measuring the fluorescent signal emitted when SYBR Green binds to the double stranded DNA. The rate at which the fluorescent signal reaches a threshold level in the exponential phase correlates with the amount of original cDNA target sequence, which in turn reflects the original amount of mRNA in the starting material. We examined the mRNA expression of genes involved in mitochondrial biogenesis (*TFAM, PGC-1α*), fission (*DRP1*), fusion *(MFN1* and *MFN2; OPA1*) and mitophagy (*PINK1, PARK2*). The mRNA expression of mitochondrial encoded subunits; *ND1*,

ND6 and *COX3* was also measured. For mRNA quantification, following RNA extraction and reverse transcription, qPCR was carried out for the target gene and *β-actin* as a stably expressed reference gene in triplicate. Expression of several reference genes was tested by using GeNorm software (Vandesompele et al., 2002). For MtDNA quantification, following DNA extraction and template pre-treatment qPCR was carried out in triplicates for a target mitochondrial gene and Beta-2 microglobulin (B2M, nuclear control). Absolute quantification was carried out in the presence of dilution standards for each gene. For each DNA or cDNA sample under investigation, the reaction was carried out in duplicate or triplicate.

Real-time qPCR was carried put in a total volume of 10µl, containing 5µl of Quantifast SYBR Master Mix, 0.5µl of forward and reverse primer (500nM final concentration each), 2µl template DNA (sample or standard) and 2µl of RNase free-water.

The reactions were performed in Roche LighCycler (LC) 480 instrument using the following program protocol: pre-incubation at 95°C for 5 minutes (1 cycle); denaturation at 95°C for 10 seconds, annealing and extension at 60°C for 30 seconds (repeat denaturation and extension steps for 40 cycles), melting at 95°C for 5 seconds, 65°C for 60 seconds, and 95°C continues (melt curve analysis -1 cycle) and the last step, cooling at 40°C for 30 seconds .In order to obtain copy numbers for tested samples the threshold was set up above the noise and on the linear/exponential part of amplification curves (example for hMito3 is shown on Fig.2.3A and for the rest of the genes see Appendix II). When running 10-fold dilutions standards and after setting up the values for each standard were plotted against their concentration, giving also values for reaction efficiency (recommended coefficiency of reaction [R^2] is 1.0 (Fig.2.43.C, Appendix II). Specificity of the primers was also checked by using melt curve analysis; one clear peak was visible for each investigated PCR product (Fig.2.3.B, Appendix II). The mRNA copy numbers were calculated by dividing the mean values of target gene relative to the mean values of *β-actin*, MtDNA copy numbers were assessed as mitochondrial to nuclear gene ratio and B2M served as a nuclear control.

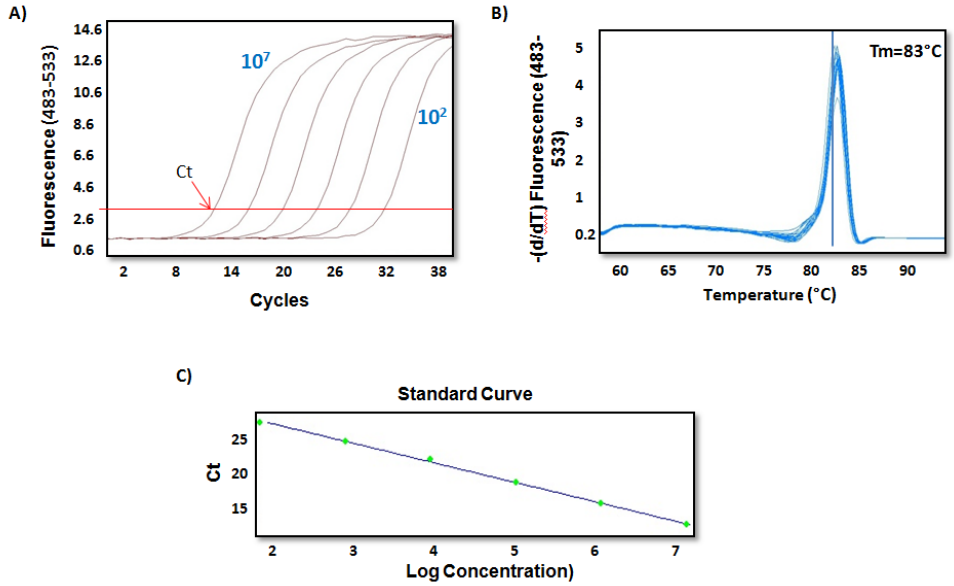

Fig.2.3.Amplification of hMito3 in 10-fold dilutions and standard curve generation. Dilution standards of hMito3 were prepared and 2ul of each standard was used in qPCR reaction and amplified. Fluorescence data was acquired once per cycle and amplification curve (A) was generated showing dilution series from 10^2 to 10^7 copies of hMito3. Melting point analysis (B) represents specificity of multiplied product as one single melt peak is visible at 83°C. (C) Standard curve showing the crossing point (Ct) for each of the 10-fold dilutions plotted against a log concentration. Threshold line is shown in red.

2.8 Western blot and detection of the OXPHOS proteins

2.8.1 Protein extraction

Mesangial cells were maintained as monolayers in 6-well plates up to 75% confluence. The cells were harvested by trypsinisation and washed with PBS. Lysis buffer (Table 2.5) supplemented with protease and phosphatase inhibitors to protect the proteins from being degraded and dephosphorylated, was added to mesangial cells, followed by sonication in the water bath for 3 min. Protein content of samples was quantified using 10µl of each cell lysate. The remaining protein extracts were kept at -80˚C.

2.8.2 Determination of protein concentration

To ensure equal loading for SDS-PAGE, protein concentration was determined by the bicinchoninic acid (BCA) assay kit (Pierce; distributed by Thermofisher Scientific, Cramlington, UK). This colorimetric method is based on the reduction of Cu^{2+} to Cu^{1+} by protein in an alkaline medium and the formation of a purple-

coloured reaction product by the subsequent chelating of the reduced Cu^{1+} with BCA. The amount of protein in the sample is directly proportional to the amount of purple coloured reaction complex.

Protein standard curve was made by a serial dilution of the stock solution (2 mg/ml of BSA) to final concentrations of 0.25, 0.5, 0.75, 1.0, 1.5and 2.0 mg/ml. Protein lysates were further diluted 1:4 in the lysis buffer. The working reagent was prepared by mixing 50 parts reagent A (containing BCA in a 0.1 M sodium hydroxide solution) with 1 part reagent B (containing 4 % cupric sulphate).

10µl of blank (lysis buffer), standards and samples were added in triplicate to the wells of a 96 well plate. 200µl working reagent was then added to each well. The plate was thoroughly mixed on a plate shaker for 30 s and incubated for 30 min at 37 ^{o}C. The plate was cooled to room temperature and the absorbance read at 570 nm on a spectrophotometer (Chameleon microplate reader, Hidex). The absorbances of each standard point were plotted and the concentration in the unknown sample derived from the regression equation of the standard curve (Fig.2.4).

Table 2.5. Preparation of cell lysis buffer.

Reagent	Amount for 100ml	Final Conc.
Tris-base	790mg	50mM
NaCl	900mg	150mM
NP-40 (10%)(v/v)	10ml	1% (v/v)
Na-deoxycholate (10%) (v/v)	2.5ml	0.25% (v/v)
EDTA (100 mM)	1ml	1mM

Tris base and NaCl were first dissolved in 75ml DI H_2O, the pH was adjusted to 7.4 with concentrated HCl followed by addition of NP-40, Na-deoxycholate and EDTA. DI H_2O was then added to make up the final volume to 100ml.

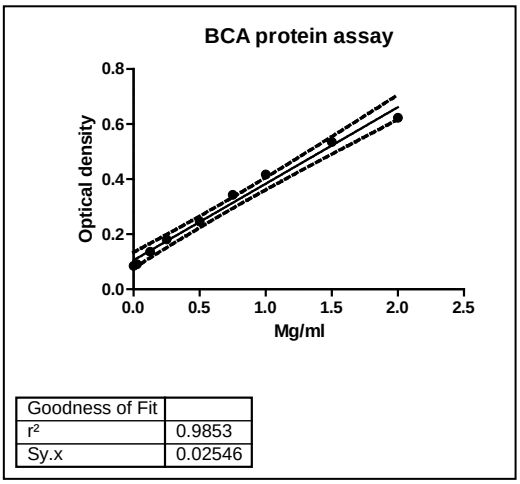

Fig.2.4.Representative example of a BCA assay standard curve. Absorbance was plotted against total protein concentration of the BSA standards. Equations for the regression line and the goodness of fit ($R^{2)}$ value are shown.

2.8.3 Sodium dodecyl sulfate polyacrylamide gel electrophoresis (SDS-PAGE)

SDS-PAGE is a method commonly used to separate proteins across an electric field based on their molecular weight. SDS is a negatively charged detergent that binds to and unfolds the protein to its primary structure, and applies a net negative charge. In the presence of an electric field, the negatively charged proteins migrate towards the positive pole through a porous gel matrix of polyacrylamide. The amount of polyacrylamide determines the pore size, and effectively causes separation of the polypeptides according to their lengths. The NuPAGE Bis-Tris electrophoresis system was used in the experiments described in this thesis. Equal amounts of total protein from mesangial cell protein extracts were loaded on to a 10% Bis-Tris-HCl buffered (pH 6.4) polyacrylamide gels. The gel was arranged and placed in the Xcel Surelock mini cell apparatus, and the inner chamber, containing sample proteins was filled with antioxidant-supplemented MOPS running buffer (Table 2.6). The outer chamber was filled with approximately 600ml of MOPS running buffer and the gel was run at 200V for 50min. A Rainbow® coloured protein molecular weight marker, labelled with chromophores for detection, was also loaded and run in parallel to the sample protein extracts for identification of sample protein molecular weights.

Table 2.6. Preparation of MOPS running buffer

Reagent	Amount for 500ml	Final Conc.
MOPS	104.6g	1M
Tris Base	60.6g	1M
SDS	10g	69.3mM
EDTA	3g	20.5mM

Reagents listed above were dissolved in 400ml DI H_2O and adjusted to a final volume of 500ml. The 20×MOPS running buffer was kept at 4˚C and diluted 1 in 20 (50ml 20×MOPS running buffer in 950ml DI H_2O) before use.

2.8.4 Western blot

After SDS-PAGE, the separated proteins are usually transferred to a suitable membrane such as polyvinylidene difluoride (PVDF) to allow access of specific antibodies for immuno-detection of proteins of interest. The transfer process is carried out by sandwiching the polyacrylamide gel and PVDF membrane between layers of filter paper, pre-soaked in a Tris-based transfer buffer (Table 2.7) while an electric current is used to pull the proteins from the gel onto the PVDF membrane.

After immunoblotting, the membrane was incubated in a protein-rich solution (5% w/v skimmed milk powder dissolved in TBS-Tween), for 1 hour at room temperature to block non-specific binding sites. Following the blocking process, the protein of interest was probed by incubating the membrane with a primary antibody raised against the target protein overnight at 4˚C. (The primary OXPHOS antibody cocktail antibody was diluted the ratio 1:2000 in 5% in w/v milk TBS-T to increase specificity.). After primary antibody incubation, the membrane was washed with blocking buffer (5% w/v milk in TBS-T/1× TBS-T, 15min each) 3 times to remove unbound primary antibody. The membrane was then incubated for 1 hour in a horseradish peroxidase-conjugated secondary antibody solution (1:7500 dilution in 5% w/v milk TBS-T) at room temperature. After 5 washes with TBS-T (5min each), immunoreactive proteins were identified by chemiluminescent detection following addition of enhanced chemiluminescent reagents. Photographic film which detects light signals was used and protein

identification was carried out by comparing the immunoreactive bands with those of the Rainbow® markers loaded during SDS-PAGE.

Table 2.7. Preparation of ×1 Transfer buffer.

Reagent	Volume
DI H_2O	849ml
20× NuPAGE transfer buffer (Invitrogen)	50ml
NuPAGE sample antioxidant	1ml
Methanol	100ml

2.8.5 Semi-quantitative analysis using ImageJ

To analyze protein expression, densitometry of both the protein of interest and reference protein was performed using ImageJ (version 1.43: National Institutes of Health; www.rsb.info.nih.gov/ij), a program that quantifies protein band intensity based on peak area. The amount of the protein of interest was expressed relative to the reference protein (β-actin) for each sample.

2.9 Mitochondrial network visualisation

2.9.1 Staining mitochondrial network with MitoTracker orange

Cells were cultured in different medium condition as follow: 5mM (NG) and 25mM (HG) glucose at various time points. To visualise mitochondria, MitoTracker (Invitrogen) fluorescent probes was added into the culture medium (100nM working concentration) and incubated at 37°C for 30 minutes. Cells were then washed three times with PBS and fixed by incubation with paraformaldehyde for 30 minutes at 4°C. After fixation, cells were rinsed three times with PBS and then visualized using the Nikon Eclipse Ti-E Inverted Microscope. Mitochondrial network (Fig.2.5) was analysed by ImageJ free software.

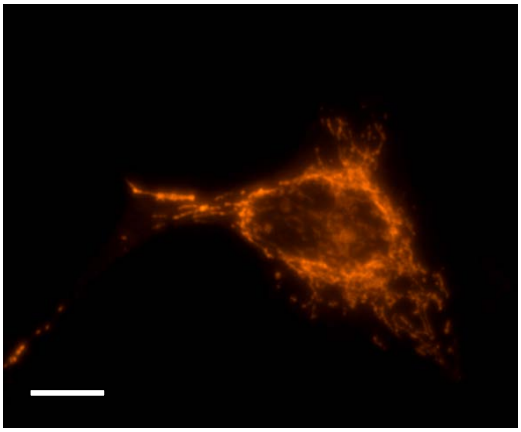

Fig.2.5. Mitochondria stained with MitoTracker Orange. To visualise mitochondria, MitoTracker (Invitrogen) fluorescent probes was added into the culture medium (100nM working concentration) and incubated at 37°C for 30 minutes. Cells were then washed three times with PBS and fixed by incubation with paraformaldehyde for 30 minutes at 4°C. Magnification 40x, Scale bar 10µm

2.9.2 ImageJ analysis of mitochondrial morphology

To visualise mitochondrial morphology, cells were grown in 96-well plates with clear bottoms, fixed with paraformaldehyde and visualized by staining with Mitotracker Orange (Invitrogen) according to the manufacturer's instructions. Cells were viewed under Nikon Eclipse Ti-E Inverted Microscope, using CFI S Plan Fluor ELWD 20x/0.45NA objective, at room temperature 25°C, in PBS. Images were captured using a PhotometricsCoolsnap HQ CCD camera, and images were acquired using NIS Elements V4.20. The stained mitochondrial network was assessed using ImageJ software (version 1.47q: National Institutes of Health; www.rsb.info.nih.gov/ij) using an image-processing algorithm as described by Koopman at al. (Koopman et al., 2005). Briefly, after adjusting brightness and contrast, a spatial filter was applied and by adjusting the threshold, mitochondrial network was distinguished from the background. Two different parameters, formfactor F (calculated as a perimeter^2/4П*area) and the aspect ratio AR (ratio between major and minor axes) were used to quantify mitochondrial morphology. Both formfactorF and aspect ratio AR are independent of image magnification, and have a minimal value of 1. Formfactor

F is a measure of the length and degree of branching and aspect ratio AR is a measure of mitochondria length.

2.10 Measurement of cell viability in human mesangial cells

Cell viability was measured using CellTiter-Glo luminescence assay (Promega, UK) in the microplate reader (according to the manufacturer's instructions). The assay detects number of viable cells, based on the measurement of ATP present, an indicator of metabolically active cells.

2.11 Measurement of cellular ROS production

Intracellular ROS in cultured cells was measured using cell-permeant 2',7'-dichlorodihydrofluorescein diacetate (H2DCFDA) oxidation in the microplate reader (according to the manufacturer's instructions). Cells well grown in various glucose concentrations in 6-well plates for 4 or 8 days. 4 days before the assessment cell were trypsinised and seeded in 96-well plates at the density of 10^3cells/well. On a day of the assessment, cells were treated with H_2DCFDA, washed 3 times with PBS and fluorescence signal was measured in the Chameleon microplate reader (Hidex) using excitation/emission: ~ 495/540 filters. DCFDA is a fluorogenic dye that measures hydroxyl, peroxyl and other ROS activity within the cell. After diffusion in to the cell, DCFDA is deacetylated by cellular esterases to a non-fluorescent compound, which is later oxidized by ROS into 2', 7' –dichlorofluorescein (DCF), which is highly fluorescent.

2.12 Mitochondrial DNA damage

MtDNA damage was assessed using the PCR based elongase method (Furda et al., 2014).15 ng of genomic DNA isolated as described above was amplified using the primers 14841 and 5999 as described by Furda et al which amplifies an 8.9kb region of the mitochondrial genome. Cycling conditions used the standard program (following the hot start of 75°C for 2 min and the addition of the polymerase) includes an initial denaturation step at 94°C for 1 min followed by a variable number of cycles of 94°C for 15 seconds and a set annealing/extension temperature for 12 min, with a final extension at 72°C for 10 min (Hunter et al., 2010). The thermocycler profile for the amplification of short DNA fragments

(127bp) includes an initial denaturation step at 94°C for 15 min, 21 cycles of denaturation at 94°C for 30 seconds, a specified annealing for 30 seconds, and 72°C for extension for 1 minute, with final extension at 72°C for 7 min. PCR assay included treated DNA samples, positive control, 50% DNA positive control and a negative control. DNA damage is quantified by comparing the relative amplification of large fragments (8.9 kb) of DNA from treated samples to those of controls and normalizing this to the amplification of small (127 bp) fragments.

2.13 Extracellular flux experiments using Seahorse XF ^{e}96 analyzer

The metabolic profiles of cultured HMCs and HK-2 cells were assessed using the XF^{e}96 Seahorse analyser and XF cell mito stress test kit and XF-FluxPaks containing 96-well plates and cartridges (Seahorse Biosciences, Fig.2.6). Oxygen consumption rate (OCR), a measurement of mitochondrial respiration, and extracellular acidification rate (ECAR) which correlates to amount of protons released from the cell with potential contribution from glycolysis and the Krebs cycle, were measured in the presence of specific mitochondrial activators and inhibitors.

Oligomycin (ATP synthase blocker) was used to measure ATP turnover and to determine proton leak, the mitochondrial uncoupler FCCP (carbonyl cyanide 4-[trifluoromethoxy] phenylhydrazone) was used to measure maximum respiratory function (maximal OCR). Reserve capacity was calculated as maximal OCR minus the basal respiration. At the end of the experiments, rotenone (inhibitor of complex I) and antimycin A (a blocker of complex III), were injected to completely shut the mitochondrial respiration down, to confirm that any changes observed in respiration were mitochondrial. In order to determine optimal cell number and drug concentration, optimisation experiments with a different cell seeding number and titration of electron transport chain activators and inhibitors were carried out to accurately assess OCR and ECAR which are explained in details in chapter 6. HMCs were grown in 5mM glucose (NG), 25mM glucose (HG) and in 5mM glucose plus 20mM mannitol (osmotic control, NGM) for 4, 8 and 12 days. One day prior to the flux analysis, cells were seeded at the concentration of 35000cells/ well in 96-well assay plates in complete growth

medium containing NG, HG glucose and NGM. 1hr prior to the experiment the growth medium was removed, cells washed 3 times and then incubated in low buffered assay medium (Seahorse bioscience) supplemented with 5mM glucose and 1mM sodium pyruvate, pH 7.4.

b

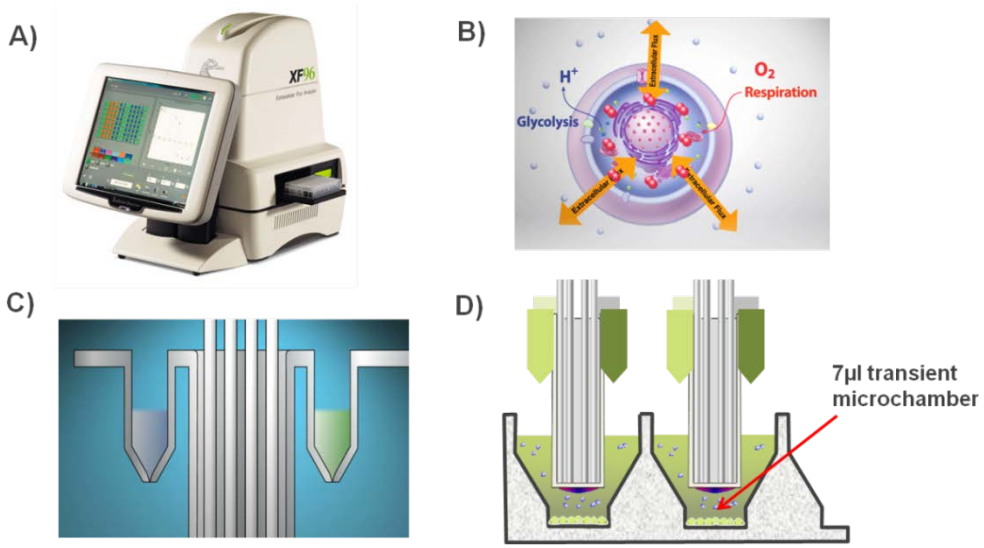

Fig.2.6.Measurement of mitochondrial function (respiration and glycolysis) via Seahorse XF^{e}96 analyzer. Seahorse XF^{e}96 analyzer (A), Oxygen consumption rate (OCR), a measurement of mitochondrial respiration, and extracellular acidification rate (ECAR) which correlates to amount of protons released from the cell with potential contribution from glycolysis and the Krebs cycle, were measured in the presence of specific mitochondrial activators and inhibitors (B), drug injection ports (C), 7µl volume transient micro chamber allowing real-time measurement of the mitochondrial respiration and glycolysis above monolayer of cells (D). Adapted from (SeahorseBioscience, 2014).

The microplates were then assayed in the XF-96^{e}analyzer. For a measurement of steady basal respiration 4 to 5 measurements were taken before injecting ATP synthase inhibitor, oligomycin at 1µM (final concentration). Mitochondrial membrane uncoupler FCCP was then injected at 0.75µM. Finally a mixture of rotenone and antimycin A (1µM) was injected. Mitochondrial basal respiration, proton leak, spare capacity and maximal respiration were measured after correcting for non-mitochondrial respiration. After finishing the experiments 20µl of cell lysis buffer [10mmM Tris, pH 7.4, 0.1% Triton X-100] were added per well and protein content measured by BCA assay (Fisher Scientific). OCR and

ECAR rates were normalised to the protein content and presented as pmolesO_2/min/μg protein.

Table 2.8. Preparation of protein lysis buffer for Seahorse flux analyzer experiments.

Reagent	Volume	Final concentration
Tris-HCL 100mM	10	10mM
Triton X-100	0.1	0.1%
DI H_2O	89	-

100mM Tris-Hcl was prepared by adding 242mg of Tris-HCl powder (MW=121.14) to 20ml of DI H_2O.

2.14 Statistical analysis

All tests were performed using GraphPad analysis software. Data are presented as mean ± standard deviation (SD). Gaussian distribution of the data was tested using the Kolmogorov-Smirnov test if possible or by the assessment of scatter plots. If data didn't follow normal distribution a log10 function was performed and Kolmogorov-Smirnov test was run on samples again Student*'s* independent *t*- test or Mann-Whitney *U*-tests were used depending on the distribution of the data. When comparing means between more than 2 groups 1 way analysis of variance was used (1 way ANOVA) with post-hoc Tukey's multiple comparison test. The null hypothesis was rejected where $P < 0.05$.

Chapter 3

Hyperglycaemia-induced changes in mitochondrial DNA content in human renal cells

3.1 Abstract

Background/Aims: The main hypothesis of this thesis is that hyperglycaemia/high glucose can cause early changes in mitochondrial DNA (content/quality) and that these changes can contribute to mitochondrial dysfunction. In the current chapter this theory was investigated using cultured renal cells.

Methods: Human renal immortalised and primary cultured mesangial cells (HMCL, HMCs) and transformed tubular epithelial cells (HK-2) were cultured in 5mM (NG) and 25mM (HG) glucose and in 5mM glucose plus 20mM mannitol (NGM). Total DNA was extracted and MtDNA content was determined as the mitochondrial genome to nuclear genome ratio using real time qPCR. Changes in MtDNA content in response to fluctuations of glucose concentration were also assessed. Moreover a reversal experiment was performed, where growth medium with HG was replaced with NG, and the effect of change on MtDNA copy number was measured.

Results: Culture in HG had no effect on MtDNA copy number in immortalized cells (HMCL and HK-2). Contrary to the cell line data, in primary cultured mesangial cells, there was a highly significant, almost 3-fold higher up-regulation of MtDNA copy number in response to HG when compared to the control ($P<0.01$) after 4 days of culture. 8 days of the exposure to HG caused an alteration in the MtDNA copy number, but the result was no longer significant ($P>0.05$). Fluctuations of glucose concentration every 24 hours (HG/NG/HG), caused a significant increase in MtDNA copy number ($P<0.05$). In a reversal experiment, the change in MtDNA copy number was reversible after 2 days of culture in HG, followed by 2 days in NG, but was not reversible after longer exposure to HG.

Conclusion: These results show that cellular MtDNA can be increased in response to hyperglycaemia in cultured primary mesangial cells. The functional consequences of this increase are unknown.

3.2 Introduction

MtDNA exclusively codes for 13 proteins of the OXPHOS which are crucial for proper cell function (Falkenberg et al., 2007). The number of mitochondria in a particular cell type can change depending on many factors, including the stage in the cell cycle, the environment and redox balance of the cell, the stage of differentiation, and a number of cell signalling mechanisms (Michel et al., 2012; Rodriguez-Enriquez et al., 2009). It has been assumed, that cellular MtDNA content is proportionate to the mitochondrial function and respiratory complex activity, and can be regulated by the cellular energy demand and linked to the bioenergetic requirements of the cells (Hock and Kralli, 2009). However, work from our group and others has supported that in certain conditions of disease, MtDNA content can be altered. The work started in our laboratory led to the identification of genes that change at the mRNA level during the progression of hyperglycaemia. Using the technique of differential screening, Page et al., (1997) detected transcriptional changes in both, mitochondrial encoded and nuclear encoded mRNAs in the kidney during the development of diabetes in the GK rat (Page et al., 1997). These results led to further research on possible links between MtDNA content and changes in the kidneys caused by hyperglycaemia. Unpublished results from our group obtained from two pilot experiments; a diabetic GK-rat study and *in-vitro* cultured renal mesangial cells suggested increased MtDNA copy caused by hyperglycaemia. MtDNA content was significantly increased in kidneys of diabetic animals, when compared to the controls (Figure 3.1.) and also significantly up-regulated in renal cells cultured in high concentration of glucose (Figure 3.2.). These data suggest there may be a correlation between mitochondrial biogenesis and development of kidney disease in diabetes.

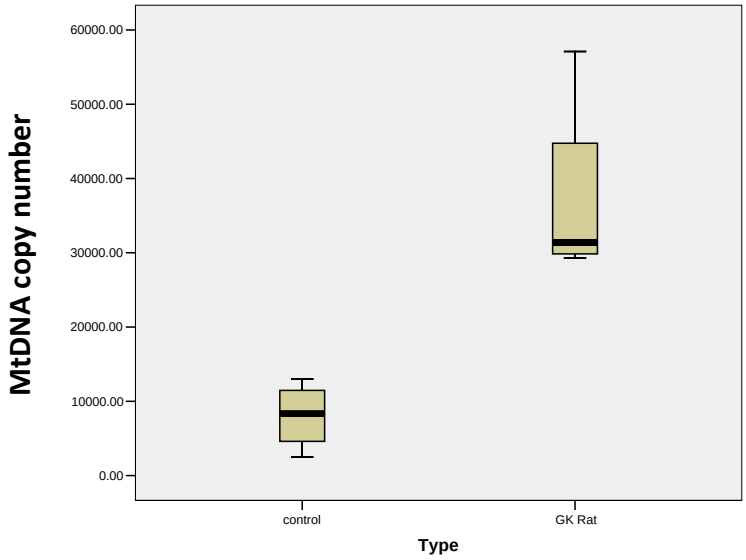

Fig.3.1. Mitochondrial DNA is up-regulated in diabetic rat kidneys. Goto Kakizaki (GK) rat study results. Diabetic rat kidneys contain more MtDNA per cell than control kidneys. Data presented as median and range (Malik and Al-Kafaji, unpublished).

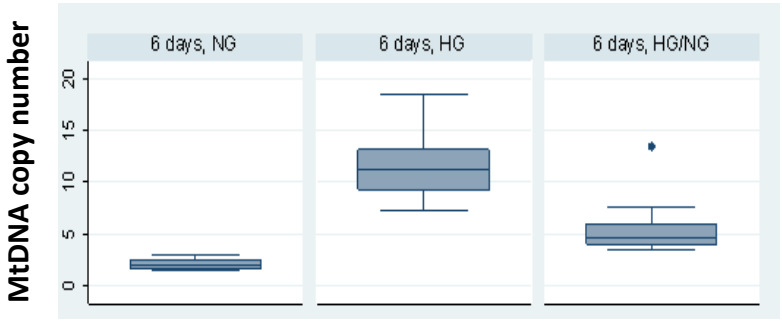

Fig.3.2. Mitochondrial DNA is increased by hyperglycaemia in human primary mesangial cells. HMCLs were cultured in 5mM (NG) and in 25mM (HG) for 6 days. Growth of mesangial cells in HG leads to increased MtDNA copy number. This increase can be reversed by removing the HG after 3 days. Data presented as median with range (Malik and Al-Kafaji, upublished).

Several animal and human studies have described variations in MtDNA content in diabetes and diabetic complications, including DN, showing alterations in MtDNA in peripheral white mononuclear cells (Song et al., 2001, Khan et al., 2011, Malik et al., 2009, Cormio et al., 2009), decrease in MtDNA copy number in blood vessel in patients with diabetic atherogenesis (Chien et al., 2012) and in skeletal muscle from patients with T2D (Kelley et al., 2002). The discrepancies observed in the results from different studies are caused by the

problems/variations with the methodologies used, including different methods of DNA extraction and accurate detection MtDNA content, without measurement of the pseudogenes (Malik et al., 2011).

Although changes in the MtDNA levels were reported in patients with diabetes and diabetic complications (reviewed in the main introduction section), to date it is not known how glucose causes alteration in MtDNA levels, how these changes correlate with mitochondrial function and possible contribution to the disease development.

While *in-vivo* studies provide physiological information about the disease, since the changes are systemic, it makes it difficult to study individual pathways and establish direct effects of hyperglycaemia on single cell types. Using *in-vitro* models provides valuable information and allows the researcher to manipulate experimental conditions in a way it might not be ethically or practically possible in the *in-vivo* experiments. Cells chosen in this study were human primary cultured mesangial cells (HMCs) and immortalised proximal tubule epithelial cell line (HK-2), as these two cell types are involved in the development of DN. Mesangial cells are specialised cells located around the glomerular capillaries within the renal corpuscle of the kidney. They have several functions, including carrying out the deposition of the matrix which results from increased glomerular filtration pressure. However, in DN, these cells contribute to the development of the disease, through expansion of the matrix into the capillary lumens (Wada et al., 2001). Proximal tubule epithelial cells create the lining of the duct within nephrons leading to the Bowman's capsule. Primarily, it was thought that major pathogenic mechanisms in DN development involves glomerular fibrosis, through mesangial expansion, but it is now known that tubular epithelial cells are also affected by inflammation and later fibrosis (Bohle et al., 1991).

Both mesangial and tubular cells are highly energetic and contain many mitochondria due to the active filtration processes they are involved with (Brown and Breton, 1996, Hall et al., 2008).

3.3 Hypothesis and aims

3.3.1 Hypothesis

The main hypothesis under study in this work is that hyperglycaemia can cause early changes in mitochondrial DNA (content/quality) and that these changes can contribute to mitochondrial dysfunction. In the current chapter the first part of this hypothesis was investigated using cultured renal cells.

3.3.2 Aims and objectives

The main objective of this chapter was to demonstrate using cultured renal cells whether hyperglycaemia can alter MtDNA content in cells and whether any such changes are permanent.

This aim will be met as follows:

1. The effect of growth of renal cells in high glucose on MtDNA content will be evaluated.
2. Time course experiments will be performed on renal cells which display glucose induced MtDNA changes.
3. The effect of the reversing and oscillation of the glucose concentration on MtDNA content will be evaluated.

The experimental strategy to carry out the above will be as follows:

1. Three different renal cells will be used, immortalized mesangial and epithelial proximal tubular cells (HMCL and HK-2) and primary cultured mesangial cells (HMCs).
2. Cells will be cultured in 5mM (normal, NG) and 25mM (high, HG) glucose, for various time points. 20mM mannitol in 5mM glucose (Man) will be used as an osmolarity control.
3. Following DNA extraction, MtDNA content will be measured as a mitochondrial to nuclear genome ratio using real-time qPCR.

3.4 Results

Changes in the MtDNA content were investigated in cells cultured in different glucose concentrations. Three different *in-vitro* models of hyperglycaemia were used, immortalized mesangial (HMCL) and tubular cells (HK-2), and primary cultured mesangial cells (HMCs). Cells were cultured in 5mM (NG) or 25mM (HG) glucose for 4 or 8 days. To exclude the possibility that change in MtDNA content occurs as a result of osmotic stress, cells were incubated in 5mM glucose plus 20mM mannitol (NGM). A general overview of the chapter is illustrated on the Fig. 3.3..

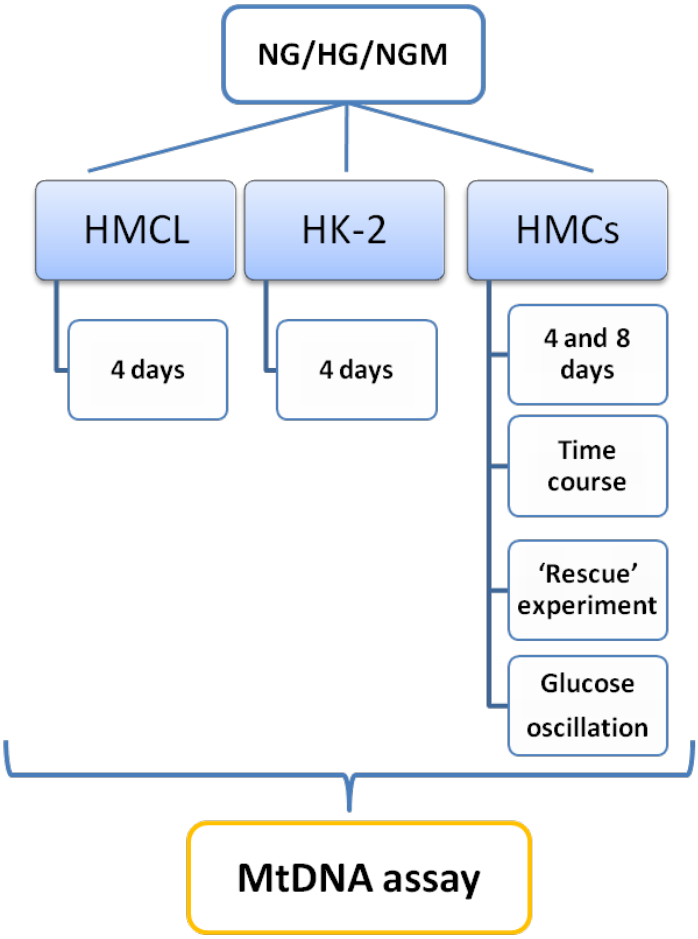

Fig.3.3. Overview of chapter 3. Immortalized and primary mesangial cells (HMCL and HMCs) and tubular epithelial (HK-2) cells were cultured in DMEM containing 5mM (NG) or 25mM glucose (HG) and in 5mM glucose plus 20mM mannitol for the times shown.

3.4.1 Does high glucose affect mitochondrial DNA copy number in renal cells cultured for 4 days?

The aim of this experiment was to evaluate the effect of high glucose on MtDNA copy number in cultured renal cells. Three types of human renal cells were used in the study; HMCs, HMCL and HK-2 cells. Following growth arrest in DMEM containing 0.5% FBS for 24 h to allow cell synchronisation, cells were cultured for 4 or 8 days in DMEM containing 5mM (NG), 25mM (HG) or the 5mM glucose plus 20mM D-mannitol (NGM). Total genomic DNA was extracted as described in the main methods section of this thesis (section 2.5.1), and template was sheared by sonication in order to avoid dilution bias [methods section 2.5.3. (Malik et al., 2011)].

As shown in table 3.1, average concentration of DNA extracted from immortalized mesangial cells exposed to high glucose for 4 days was almost 2-fold lower when compared to the controls ($P<0.05$). No statistically significant difference was observed in the average DNA yield extracted from HK-2 or HMCs cells cultured in media with different concentrations of glucose (table 3.1, $P>0.05$).

To assess MtDNA content, ratio of mitochondrial to nuclear genome was measured using real-time qPCR. Oligonucleotides against human mitochondrial genome (hMito 3; accession number: NC_012920.1) and reference gene (hB2M1; accession number: NC_000015.10) were design and optimized previously in our group. These hMitoF3 (CACTTTCCACACAGACATCA) and hMitoR3 (TGGTTAGGCTGGTGTTAGGG) designed against human mitochondrial genome (NC_012920) amplified a unique region of 127 bp, which is not duplicated in the nuclear genome (Fig.3.4.A). hB2MF1 (TGTTCCTGCTGGGTAGCTCT) and hB2MR1 (CCTCCATGATGCTGCTTACA) designed against B2M precursor (NC_000015.10) amplified a 188 bp fragment (Fig.3.4.B). The specificity of the primers (one PCR product multiplied) was recognized as a single band when run on 2% agarose gel for both genes of interest (Fig.3.4.).

Table 3.1. DNA concentration extracted from human renal cells cultured in different glucose concentration for 4 days.

Cell type	Treatment	Average DNA concentration [ng/µl]
HMCL	NG	33 ± 12
	HG	18 ± 5 *
	NGM	30 ± 3
HK-2	NG	16 ± 13
	HG	14 ± 7
	NGM	16 ± 11
HMCs	NG	25 ± 8
	HG	18 ± 8
	NGM	30 ± 7

Cells were cultured for 4 days in 5mM (NG), 25mM glucose (HG) and in 5mM glucose plus 20mM D-mannitol (NGM). Cells were washed in ice cold PBS, trypsinized and cell pellets collected for DNA extraction. NanoDrop instrument was used to determine DNA concentration in each sample. 5-6 observations of each condition were used in the study (HMCL) or 3-4 independent experiments (HK-2, HMCs). Data presented as Mean ± SD, One Way ANOVA with Post hoc Tukey's test where *P<0.05

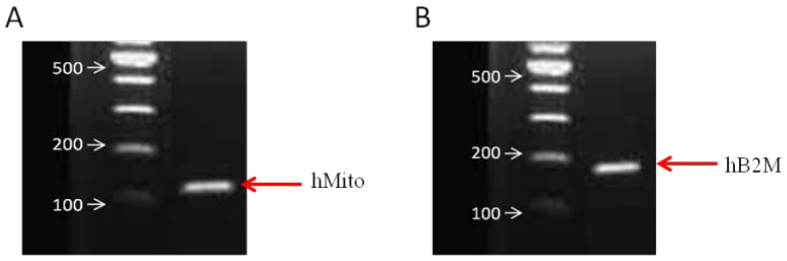

Fig.3.4. Agarose gel electrophoresis of hMito3 and hB2M1 PCR products. The PCR products obtained from primers hMito F3and hMito R3 (Figure A) and primers hB2M F1 and hB2M R1 (Figure B) electrophoresed on a 2% agarose gel. The 127bp hMito and 189bp hB2M PCR products are indicated by the red arrows. Ladder bands are marked with white arrows and labelled with appropriate molecular weight sizes

To detect copy number of mitochondrial and B2M gene fluorescence based qPCR assay and absolute quantification method were used as described in section 2.7.2. Briefly 10 fold dilution of each transcript was used to create a standard curve (Fig3.5.A, 3.6A) and specificity of the primers was recognised as a single

melt peak (Fig.3.5B, 3.6B). MtDNA content was determined as mitochondrial to nuclear gene ratio after extrapolating the values from the standard curves for specific targets (Fig.3.5C, 3.6C).

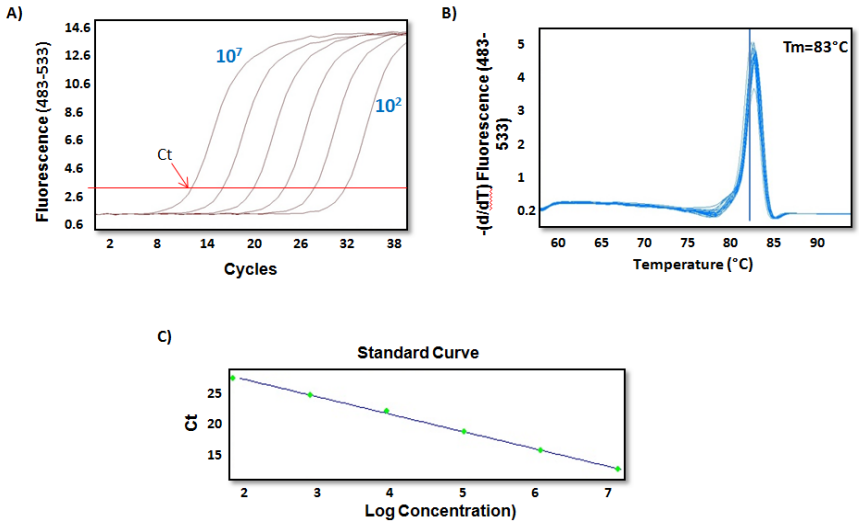

Fig.3.5. Amplification of hMito3 in 10-fold dilutions. Dilution standards of hMito3 were prepared and 2ul of each standard was used in qPCR reaction and amplified. Fluorescence data was acquired once per cycle and amplification curve (A) was generated showing dilution series from 10^2 to 10^7 copies of hMito3. Melting point analysis (B) represents specificity of multiplied product as one single melt peak is visible at 83°C. (C) Standard curve showing the crossing point (Ct) for each of the 10-fold dilutions plotted against a log concentration. Threshold line is shown in red.

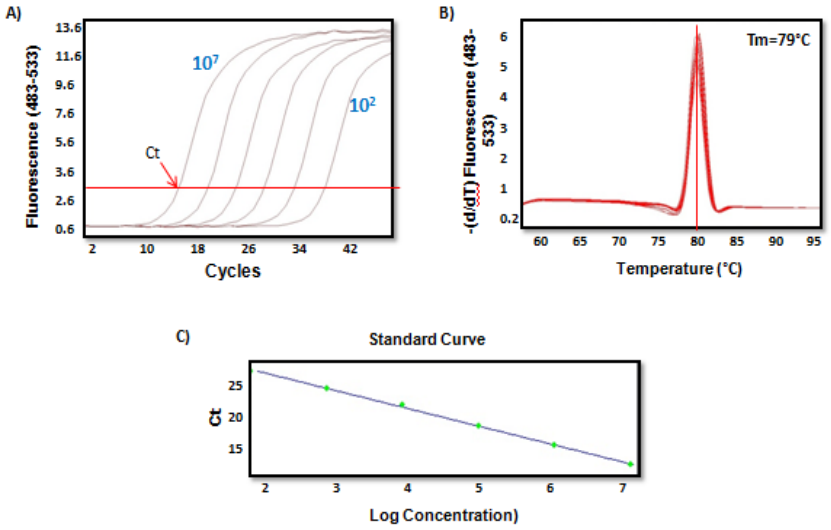

Fig.3.6. Amplification of hB2M1 in 10-fold dilutions. Dilution standards of hB2M were prepared and 2ul of each standard was used in qPCR reaction and amplified. Fluorescence data was acquired once per cycle and amplification curve (A) was generated showing dilution series from 10^2 to 10^7 copies of hB2M1. Melting point analysis (B) represents specificity of multiplied product as one single melt peak is visible at 79°C. (C) Standard curve showing the crossing point (Ct) for each of the 10-fold dilutions plotted against a log concentration. Threshold line is shown in red.

As illustrated on Fig.3.7. hyperglycaemia had no significant effect on MtDNA copy number in renal cell lines. MtDNA copy number seems to be lower in HMCL cells exposed to high glucose (293± 197) when compared to the control (478± 281), in contrary to H2-2 cells grown in high glucose, which MtDNA content was 1.5-fold higher (430± 187) when compared to the control (298±178), but none of these results were significant (P>0.05, Fig.3.7). However in primary mesangial cells exposed to high glucose for 4 days, MtDNA content was approximately 2.5-fold higher when compared to the control (717± 157 vs. 280±53, respectively P<0.01). MtDNA copy number detected in primary mesangial cells was similar to the one measured in tubular cells (280±53 vs. 298±178) but lower than in HMCL cells (478± 281), when cells were culture in normal glucose (Fig.3.7). Osmotic control had no effect on MtDNA content (P>0.05, Fig.3.7).

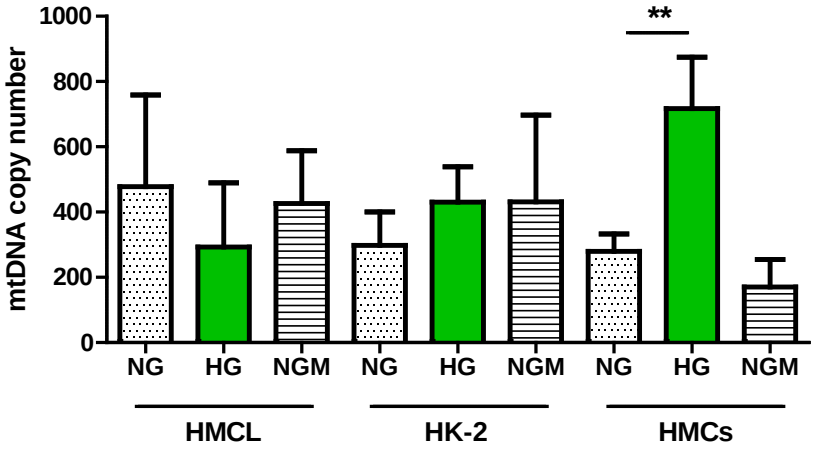

Fig.3.7.Mitochondrial DNA content in human renal cells cultured in different concentrations of glucose. Cells were synchronized FBS for 24hr and then cultured in DMEM containing 5mM (NG) and 25mM (HG) glucose for 4 days. 5mM glucose plus 20mM mannitol (NGM) was used as an osmotic control. MtDNA copy number was assessed as a mitochondrial to nuclear gene ratio using real-time qPCR method. Data presented as a mean ± SD, n=5-6 observations for HMCL cells and n=3-4 independent experiments for HK-2 and HMCs, One way ANOVA with Tukey's post hoc test where, **P <0.01

The above data show, that exposure to hyperglycaemia had no significant effect on MtDNA content in any of the examined immortalized renal cells but did significantly affect the cell growth and resulted in lower DNA yield in mesangial

cell line. In the primary mesangial cells cultured in high glucose for 4 days MtDNA copy number was significantly up-regulated and no significant effect on cell growth was observed.

3.4.2 Time course study of the effect of high glucose on mitochondrial DNA copy number in human primary mesangial cells

As shown above, MtDNA copy number in HMCs was elevated after 4 days of culture in high glucose, therefore the aim of this experiment, was to assess MtDNA copy number in response to different exposure time to hyperglycaemia. HMCs were grown in NG and HG glucose for 1, 2, 3 and 4 days in order to assess effect of high glucose on MtDNA changes over time.

MtDNA content was almost 2 fold higher after 24h of culture in HG (421 ± 112) when compared to time matched control (242 ± 47), but the difference was not significant (P>0.05). 72 and 96 h of high glucose treatment caused a significant up-regulation of MtDNA, when compared to the controls (537 ± 68 and 647 ± 32 vs. 278± 120 and 285± 34, P<0.05 and P<0.01 respectively Fig.3.8).

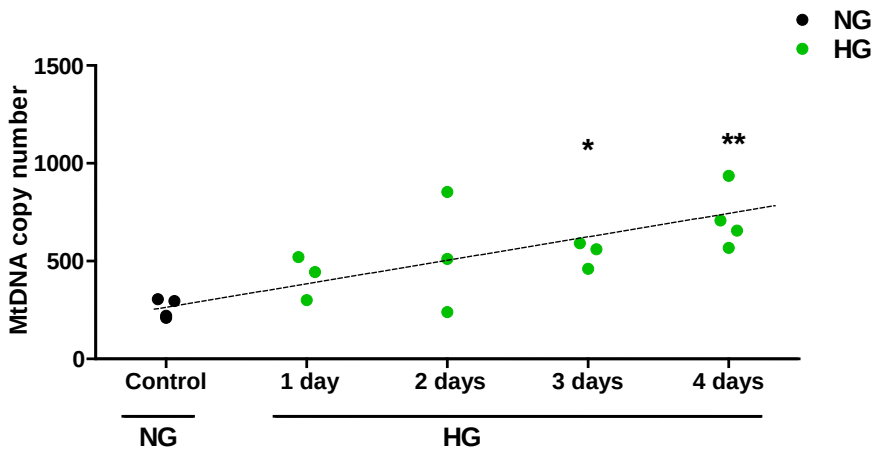

Fig.3.8. Time course study of mitochondrial DNA content in primary mesangial cells cultured in different glucose concentrations. HMCs were synchronized in 0.5% FBS for 24hr and then cultured in DMEM containing 5mM (NG), 25mM (HG) for 4 days. Samples were collected every 24 h. Following DNA extraction, MtDNA copy number was assessed as a mitochondrial to nuclear gene ratio using real-time qPCR method. Representative control for MtDNA content in cells cultured in NG for 4 days is shown. Data presented as a mean ± SD, n=3-4, Student's t-test where, *P<0.05, **P <0.01

The above data show that MtDNA copy numbers in HMCs were up-regulated as quickly as within 24 h after the exposure to hyperglycaemia and this increase became statistically significant after 72 hours.

3.4.3 Does mitochondrial DNA copy number remain up-regulated in human primary mesangial cells after 8 days of culture in high glucose?

In order to see, if the increase in MtDNA content persists in HMCs exposed to high glucose for a longer period of time, cells were cultured in 25mM glucose for 8 days. As there was no effect of the osmotic control observed on MtDNA copy number in the previous study, mannitol was not used in this part of the experiment. Although MtDNA content was still elevated in cells cultured in high glucose for 8 days, the difference was no longer statistically significant in cells grown in high glucose when compared to the control (792 ± 575 vs. 263 ± 120, P>0.05, Fig.3.9). No effect of passage on MtDNA in cells cultured in NG was observed between 4 and 8 days (279 ± 53 vs. 263 ± 120 respectively, P>0.05, Fig. 3.9).

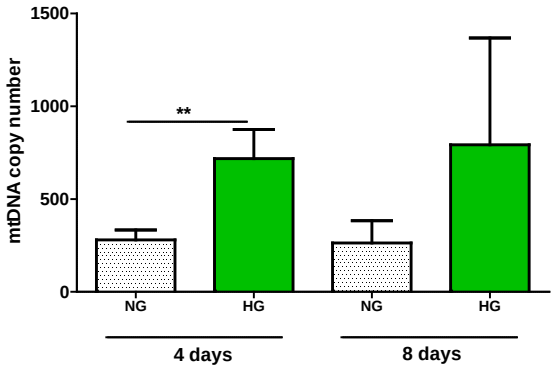

Fig. 3.9. Mitochondrial DNA content in human primary mesangial cells after 8 days of culture. Cells were synchronized in 0.5% DMEM for 24hr and then cultured in 5mM (NG), 25mM (HG) glucose for 4 and 8 days. Following DNA extraction, MtDNA copy number was assessed as a mitochondrial to nuclear gene ratio using real-time qPCR method. Data presented as a mean ± SD, n=3 -4, Student's t-test where, **P<0.01

To summarize, MtDNA content in HMCs cultured for 8 days in high glucose was still increased but the difference was not significant.

3.4.4 Is glucose-induced up-regulation of mitochondrial DNA content in mesangial cells reversible?

It was shown above, that exposure of HMCs to high glucose for 4 and 8 days increases MtDNA content. To assess if these changes were permanent or possibly reversible, a 'rescue' study was designed to examine MtDNA content in cells which were cultured in high glucose growth medium followed by low glucose. Three time points were chosen for 4 and 8 days respectively, as illustrated (Fig.3.10).

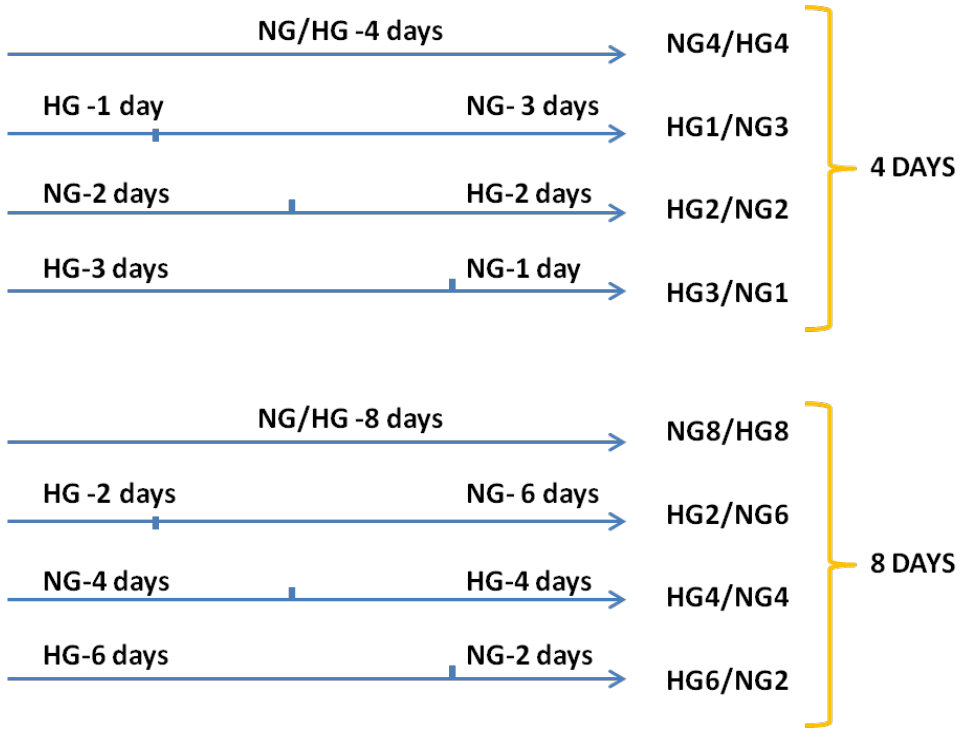

Fig.3.10. Schematic representation of the experimental strategy. 5mM glucose (NG), 25mM glucose (HG). HG/NG, growth medium reversed from HG to NG.

As shown on Fig.3.11, short exposure to 25mM, following longer 'recovery' with 5mM glucose medium (HG1/NG3), had no effect on MtDNA content ($P>0.05$, Fig.3.11. MtDNA copy number was significantly reduced in HG2/NG2 group when compared to the cells cultured in the HG for 4 days (218 ±40 vs. 936 ±383 respectively, $P<0.05$).). 3 days exposure to 25mM glucose following 1 day of

treatment with 5mM glucose (HG3/NG1) did not significantly altered MtDNA copy number when compared to the control and cells cultured in HG (P>0.05, Fig.3.11). 4 days of the exposure to 25mM glucose significantly up-regulated MtDNA copy number when compared to the control (Fig.3.11).

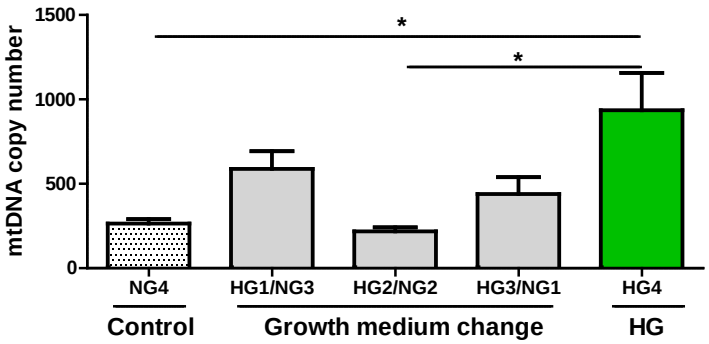

Fig. 3.11. Glucose-induced mitochondrial DNA content change in human primary mesangial cells. Cells were synchronized in 0.5% DMEM for 24hr and then cultured in 5mM (NG), 25mM (HG) glucose or in reversed conditions (HG/NG) for 4 days. Following DNA extraction, MtDNA copy number was assessed as a mitochondrial to nuclear gene ratio using real-time qPCR method. Data presented as a mean ± SD, n=3 observations, one way ANOVA with Tukey's post hoc test where, *P<0.05

After 8 days of culture and with media change, there was no difference between the groups as shown on Fig.3.12. MtDNA content seem to be dys-regulated in all groups in which cells were exposed to high glucose, but none of the results was significant, when one way ANOVA was performed (P>0.05, Fig.3.12).

Short exposure to high glucose, following longer 'recovery' with medium with physiological glucose concentration (HG2/NG6), did not normalise MtDNA copy, which was almost two fold higher than the control (P>0.05, Fig.3.12 A, B).

4 days exposure to high glucose flowing 4 days treatment with normal glucose did not significantly alter MtDNA copy number in any of the experiments, but MtDNA content in this group was almost 3 fold higher than in the control (P>0.05, Fig.3.12A, B). Prolonged, 6 days of the exposure to high glucose, following the media change to normal glucose for 2 days (HG6/NG2), had no

significant effect on MtDNA copy number, but there were contradictory results observed in this group between the two experiments (P>0.05, Fig.3.12). There was a stimulating effect (although not significant) of high glucose on MtDNA copy number observed in the experiment shown on Fig3.12A and no effect of hyperglycaemia observed in experiment illustrated on Fig.3.12B.

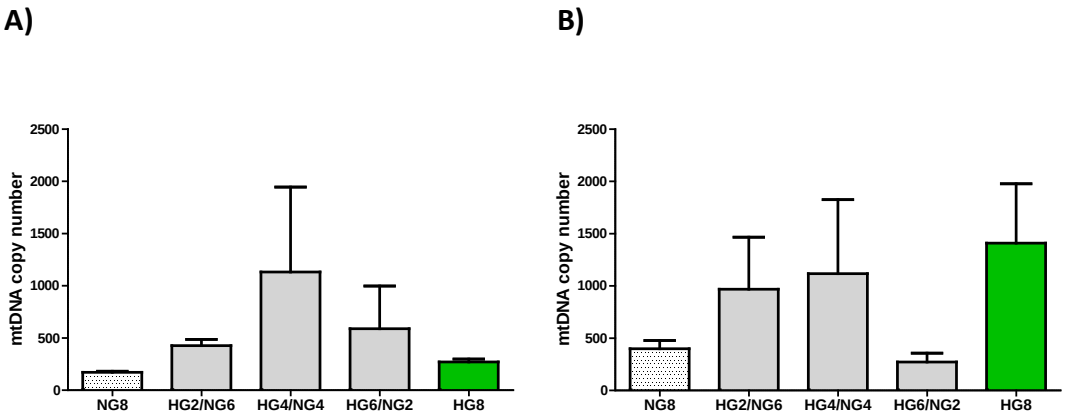

Fig. 3.12. Mitochondrial DNA content in human primary mesangial cells is not affected in glucose reversal experiment after 8 days. Cells were synchronized in 0.5% DMEM for 24hr and then cultured in 5mM (NG), 25mM (HG) glucose or in reversed conditions (HG/NG) for 8 days in two independent experiments (A-B). Following DNA extraction, MtDNA copy number was assessed as a mitochondrial to nuclear gene ratio using real-time qPCR method. Following DNA extraction, MtDNA copy number was assessed as a mitochondrial to nuclear gene ratio using real-time qPCR method. Data presented as a mean ± SD, n=3 observations per experiment, one way ANOVA where, P>0.05

Pilot data from the 4-days glucose reversal experiment showed, that MtDNA content can be altered by reversing glucose concentration, but two independent experiments for 8 days proved to be inconclusive (Fig.3.12). Therefore, I have repeated the experiment on different batch of primary mesangial cells, choosing only two reversal time points for 4 and 8 days, in order to see if the MtDNA is still dys-regulated or if it can be normalised by a glucose concentration change.

As illustrated on Fig.3.13, in cells, which were cultured in high glucose for 2 days and had the media changed to normal glucose for 2 days (HG2/NG2), MtDNA copy number was not significantly different when compared to the control (404±254 vs. 280±53, P>0.05, Fig.3.13). However, in the HG4/NG4 group MtDNA

copy number remained significantly higher when compared to the control (1113± 20 vs. 263± 120, P<0.05, Fig.3.13).

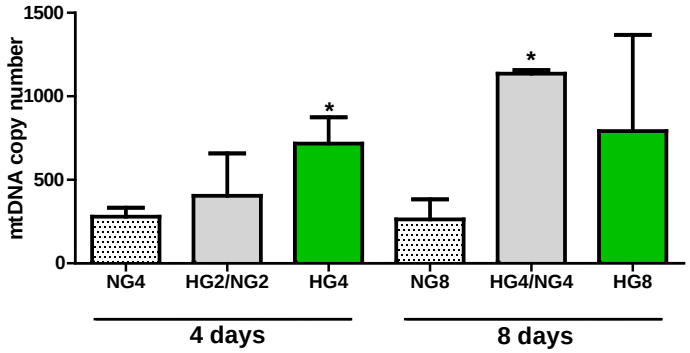

Fig.3.13. Mitochondrial DNA content in human primary mesangial cells can be changed by reversing glucose concentrations. Cells were synchronized in 0.5% FBS for 24hr and then cultured in DMEM containing 5mM (NG), 25mM (HG) glucose or in reversed conditions (HG/NG) for 4 and 8 days. Following DNA extraction, MtDNA copy number was assessed as a mitochondrial to nuclear gene ratio using real-time qPCR method. Data presented as a mean ± SD, n=3-4, one way ANOVA with Tukey's post hoc test where, *P<0.05

In summary, data from the glucose reversal experiment showed that the increase in MtDNA copy number is dependent on the exposure time to high glucose, and that this increase cannot be reversed after 4 days of the high glucose treatment.

3.4.5 Does oscillation of the glucose concentration in the growth medium affect MtDNA content in human mesangial cells?

Primary mesangial cells were cultured for 4 or 8 days, and had their growth medium changed from high glucose to normal (HG/NG) or from normal to high glucose (NG/HG) every 1 day (HG1/NG1), or every 2 days (HG2/NG2) respectively. Two independent experiments for each of the selected times points were performed.

Oscillation of the glucose concentration for 4 days, caused a significant, 2-4 fold up-regulation of MtDNA in HMCs, but only following the exposure to high glucose for the last 24 h before the cells collection when compared to the HMCs cultured in normal glucose (NG1/HG1, P<0.01, P<0.05, Fig.3.14A, B). When the

growth medium glucose levels were returned to physiological concentration, although there was still an up-regulation of MtDNA content, the result was no longer significant (HG1/NG1, P>0.05, Fig.3.14A, B).

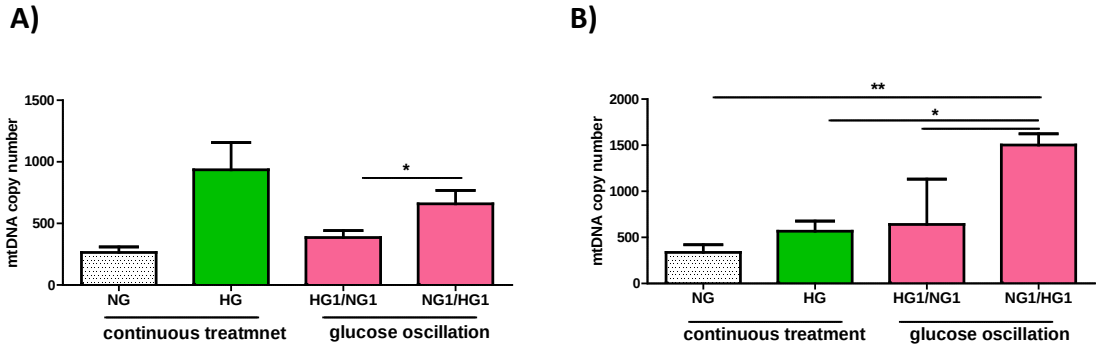

Fig. 3.14. Mitochondrial DNA content in human primary mesangial cells grown for 4 days in various glucose concentrations. Cells were synchronized in 0.5% FBS for 24hr and then cultured in DMEM containing 5mM (NG), 25mM (HG) glucose or in reversed glucose concentrations (HG1/NG1, NG1/HG1, medium changed every 1 day) for 4 days in two independent experiments (A,B). Following DNA extraction, MtDNA copy number was assessed as a mitochondrial to nuclear gene ratio using real-time qPCR method. Data presented as a mean ± SD, n=3 observations per experiment, one way ANOVA with Tukey's post hoc test where, *P<0.05, **P<0.01

Oscillation of the glucose concentration every two days for 8 days caused an increase in MtDNA copy number but result was not statistically significant in any of the investigated group (HG2/NG2 or NG2/HG2) when compared to the control (P>0.05, Fig.3.15).

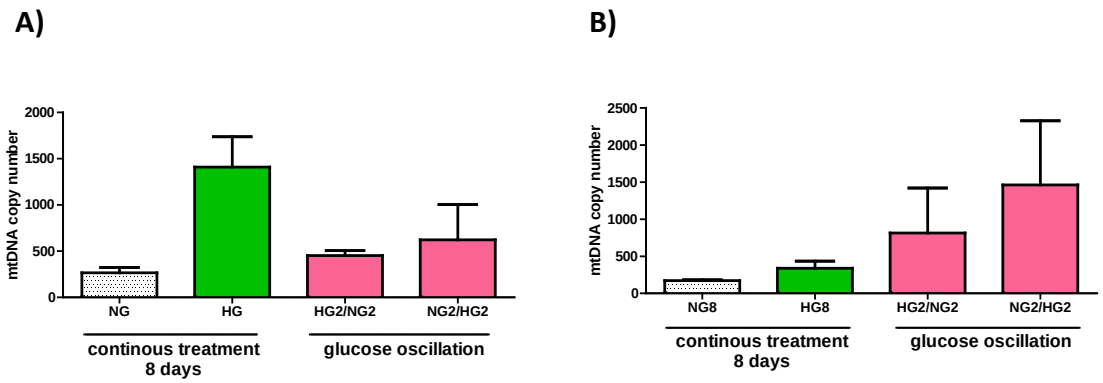

Fig.3.15. Mitochondrial DNA content in human primary mesangial cells grown for 8 days in various glucose concentrations. Cells were synchronized in 0.5% DMEM for 24hr and then cultured in 5mM (NG), 25mM (HG) glucose or in reversed conditions (HG2/NG2, NG2/HG2, medium changed every 2 days) for 8 days in two independent experiments (A,B). Following DNA extraction, MtDNA copy number was assessed as a mitochondrial to nuclear gene ratio using real-time qPCR method. Data presented as a mean ± SD, n=3-4 observations per experiment, one way ANOVA

In summary, oscillation of the glucose concentration in the growth medium for 4 days significantly affected MtDNA content. Moreover, final glucose concentration before the cell collection had also a significant effect on the MtDNA content.

3.5 Discussion

Data from the current study show, that MtDNA content is positively regulated by hyperglycaemia in primary cultured human mesangial cells. No significant changes in MtDNA copy number were observed in any of the tested immortalised cell lines, HK-2 and HMCL. In addition increase in MtDNA content occurs as early as 24 hours following the exposure to high glucose. Changes in glucose concentration in the growth medium further contributed to MtDNA number dys-regulation. In the 'rescue' experiment when high glucose growth medium was substituted with a low-glucose one, after 4 days of cells exposure to high glucose, changes in the MtDNA were not reversible.

The lack of any differences in the response to hyperglycaemia in the immortalised cells, was surprising, but in the case of HMCL, the problem may be with the culture system, as this cell line already had a high passage number (>50) when used in these experiments and high passage has been shown to affect cell line's characteristics over time (Chang-Liu and Woloschak, 1997).

Tubular cells seem to have dys-regulated level of MtDNA, which was slightly higher than in controls, but limitation may be, not using the correct, fully optimised experimental time points, as these cells might be slightly more/less sensitive to the high glucose concentrations, therefore this experiment may need further optimising. Another reason for the lack of differences in the immortalized cells may be the different characteristics of the cell lines, which may lose some properties from the primary cells during the viral transfection and therefore respond differently to treatment. As immortalized cell lines are *in-vitro* equivalent of cancerous cells, they may not use their OXPHOS systems as much as the cells they were originated from and rely more on glycolysis.

However, data obtained from primary mesangial cells clearly show MtDNA alteration, when cells were exposed to high glucose. Mesangial cells are the cells surrounding blood vessels in kidney and their excessive proliferation and production of extracellular matrix contribute to the pathophysiological mechanism during the development of DN (Wada and Makino, 2013). It is well established that these cells are susceptible to a high glucose environment and

when exposed to hyperglycaemia, the increased production of free radicals and activation of signalling pathways present in DN is observed (Henningsen et al., 2003, Ha and Lee, 2005, Catherwood et al., 2002). Published data from our group, also suggested increased ROS in human mesangial cells when analyzed by confocal microscopy and flow cytometry in response to hyperglycaemia (Al-Kafaji and Malik, 2010).

However, to my knowledge this is the first study showing up-regulation of MtDNA in human renal cells exposed to hyperglycaemia. In the presence of the oxidative stress, when the redox balance of the cells is disturbed, there might be an alteration in MtDNA copy number and MtDNA function. In healthy cells, mitochondrial mass is regulated through mitochondrial biogenesis and degradation via mitophagy, but in the case of cellular signalling dys-regulation, an adaptive response that leads to increased mitochondrial mass can occur (Michel et al., 2012). MtDNA copy number was increased as early as 24 hours after the exposure to high glucose, which is not surprising, as MtDNA resemble bacterial DNA and can replicate in a very short time (Bogenhagen et al., 1979). Also, unlike nuclear DNA, MtDNA replication happens independently of the cell cycle (Sazer and Sherwood, 1990). Due to the lack of strict restriction in replication (Clayton, 1982), increases in MtDNA could be an adaptive response of cells, trying to cope with the nutrient overload by increasing number of the mitochondria, or a compensatory mechanism to high-glucose induced mitochondrial damage. Induction of the MtDNA might be some sort of a 'rescue mechanism' that would help cells overcome free radical damage to their mitochondria.

However, after 8 days exposure to high glucose, MtDNA was still up-regulated but the result was no longer significant. Possible explanations might be either technical issue with the experiments, or that cells removed the mutated MtDNA, and mitochondria by mitophagy process (Ma et al., 2013). Observed changes in MtDNA following the treatment with high glucose could also be transient and represent an early response of the cells to hyperglycaemia.

The theory of the compensatory mechanism of increased MtDNA content caused by the falling mitochondrial function is supported by a clinical study from Lindinger et al.,(2010). They reported an increase in MtDNA content in adipose tissue from obese patients and suggested that this up-regulation of MtDNA copy number in patients with severe obesity as a form of an adaptation to dysfunctional mitochondria (Lindinger et al., 2010). Wei et al. (2001), reported increased mitochondrial mass and MtDNA content in cybrid cells from skin fibroblasts carrying a 4977 bp deletion when compared to cybrids with wild type MtDNA only. Moreover the relative increase in MtDNA amount correlated positively with increased percentage of the mutated MtDNA content and by treatment with H_2O_2 (Wei et al., 2001).

High glucose-increase in MtDNA copy number, which could not be reduced by normalizing glucose levels in a 'rescue' experiment' might imply epigenetic changes caused by glucose as suggested by El-Osta and Brownlee (El-Osta et al., 2008). Results from those studies suggested that even transient exposure of vascular cells to high glucose, both *in-vitro* and *in-vivo*, can cause long lasting effects on gene expression and methylation (El-Osta et al., 2008).

One of the limitations of the current study may be a low number of repeats for some of the experiments and not fully optimised experimental time points, especially for HK-2 cells. Also the 'rescue' experiments in mesangial cells, showed some variability in MtDNA content after the exposure to hyperglycaemia and following normalization of glucose levels, therefore this experiment should be repeated with larger numbers. Furthermore, 8 day exposure caused an increase in MtDNA, but because of variability, it was no longer significant. An increased number of repeats would lower the observed variability and enable better definition of the changes in MtDNA replication in response to hyperglycaemia. Finally, extending the treatment time might provide valuable information about the long term effects of hyperglycaemia on the kidney cells.

In summary, I have shown that hyperglycaemia positively regulates MtDNA copy number in primary cultured human mesangial cells and that these were transient and may represent early compensatory response to the hyperglycaemia.

Chapter 4

Hyperglycaemia-induced changes in mitochondrial DNA in mouse models of diabetes

4.1 Abstract

Background/Aims: The hypothesis that will be tested in this thesis is that hyperglycaemia/high glucose can cause early changes in mitochondrial DNA content and that these changes can contribute to mitochondrial dysfunction. In the current chapter, the effect of hyperglycaemia on MtDNA content in organs and circulating cells in different mouse models of diabetes was investigated.

Methods: Tissue and whole blood samples were collected from 3 different mouse models of diabetes representing: T1D (STZ-induced and spontaneous β-PhB2$^{-/-}$ mice) and T2D (Lep$^{ob/ob}$ mice). Following DNA extraction, MtDNA content was determined as the mitochondrial genome to nuclear genome ratio using real time qPCR.

Results: In the STZ-induced diabetic mice MtDNA content was increased by 4 fold in mouse blood after 7 days of induction of diabetes ($P<0.05$). After 4 weeks of hyperglycaemia, there was a significant decrease in MtDNA content in kidneys of STZ- mice. No significant difference between diabetic and control mouse heart, brain, lung and liver were observed ($P>0.05$) but an increase in MtDNA content in STZ-mouse islets was observed ($P<0.05$). In β-PhB2$^{-/-}$ mice, significantly increased MtDNA content was observed in circulating cells sampled weekly ($P<0.05$), but no significant change in the amount of MtDNA in the kidneys was observed ($P>0.05$). In the Lep$^{ob/ob}$ there was a decline in MtDNA copy number in the kidneys, but result was not significant ($P>0.05$).

Conclusion: These results show that hyperglycaemia leads to the increase in MtDNA content in circulating cells in the mouse models of diabetes. These data also suggest that there is a loss in MtDNA in diabetic mouse kidney, which may be a result of either leakage of kidney MtDNA into circulation or increased removal of the damaged mitochondria.

4.2 Introduction

In the previous chapter, I have shown that MtDNA is elevated in renal cells cultured in 25mM glucose. In this chapter the focus is on changes in MtDNA quantity in tissues of three *in-vivo* mouse models of diabetes. It is generally assumed that MtDNA is differentially expressed in various organs and its level correlates with mitochondrial function (Hock and Kralli, 2009). Unpublished results from our group obtained from pilot experiments using diabetic GK-rat samples suggested increased MtDNA copy caused by hyperglycaemia in the rat kidneys (Malik, unpublished). Several animal studies have described variations in MtDNA content and mitochondrial dysfunction in diabetes, including decreased activity of respiratory enzyme complexes, depletion of mitochondrial membrane potential, and decreased ATP production in diabetic rat liver mitochondria (Chen et al., 2011). Another group investigated the role of mitochondrial dysfunction and insulin resistance by using two different mouse models of type 1 and type 2 diabetes, and reported increased ROS and later oxidative stress having an inhibiting effect on mitochondrial function at the molecular, structural and functional level in mouse muscle tissue (Bonnard et al., 2008). Altered mitochondrial structure and lower membrane potential had been highlighted in ischemic kidney injury in the rat (Plotnikov et al., 2007). Brookes at al. (2009) using mice an *in-vitro* mouse proximal tubular cell cultures as models of acute kidney injury, observed changes in mitochondrial structure (increased fragmentation) and depleted mitochondrial function (Brooks et al., 2009).

The specific hypothesis of this chapter will be addressjed using the following models:

a) Chemically induced model of T1D: a streptozotocin-induced diabetic mouse model (STZ-diabetic mice). STZ chemical structure is similar to glucose; therefore the compound is delivered to the cells through GLUT-2 transporter. STZ specifically targets β-cells and causes cell necrosis through the depletion of ATP. Animals become diabetic within 3 days after the injection. (Rackham et al., 2013) (table 4.1). C57BL/6 mice are extensively used for studies of kidney disease which are typically made diabetic by an injection of STZ, as it results in the destruction of the pancreatic β-cells. In humans, diabetic nephropathy is

clinically characterized by the development of microalbuminuria and a decline in renal function. These clinical parameters are observed in the rodent models, although the renal dysfunction is less severe when compared with a patient with DN (Tesch and Allen, 2007). The STZ diabetic mice typically develop extreme hyperglycaemia and insulin deficiency which can be observed as quickly as 3 days following the acute injection of STZ (Rackham et al., 2013).

However STZ can have a toxic effect on the kidney, especially the tubular epithelium. Also in humans, DN gradually develops in patients 15 to 25 years after the onset of diabetes (Caramori et al, 2000). Most of the studies of DN in animals, such as the progression of albuminuria and histopathologic changes have focused on the earlier indication of DN due to the cost and convenience and not openly used renal deficiency as an end point (Sharma et al, 2003). In the current study the effect of hyperglycaemia on mitochondrial biogenesis in mouse kidneys as an indication of early change in diabetes and DN is investigated.

b) Knockout mouse model of T1D: prohibitin 2 knockout (β-PHB2$^{-/-}$) mice. Prohibitins are conserved proteins found as heterodimers (built from subunits of prohibitin 1 and prohibitin 2), localised mainly in mitochondrial membranes. They are responsible for a cell cycle, apoptosis, and more importantly functionally associated with MtDNA and mitochondrial biogenesis (Artal-Sanz and Tavernarakis, 2009). β-*PHB2*$^{-/-}$ mice were generated as a crossbred between flox-PHB2-flox (PHB2$^{fl/fl}$) mice and rat-insulin promoter driven Cre mice (RipCre). The mix of the two breeds causes deletion of the PHB2 gene exclusively in β-cells in the pancreas. PHB2 mutants spontaneously developed diabetes at 6 weeks of age (glucose levels > 11.1mM) and progressed to severe hyperglycaemia afterwards (glucose levels >25mM). Blood samples were collected weekly, starting from animals at pre-diabetic state (week 4), till the end the termination of the experiment (week 11, which was equal to 5 weeks of the duration of severe diabetes). This knockout mouse model of diabetes has proven to be quite severe, with mice not surviving more than 14 weeks due to severe diabetes (Supale et al., 2013).

This model represents a model of spontaneous diabetes progression, through a series of molecular events which appear after 3 weeks and does not require administration of chemicals such as STZ. Therefore, we used this spontaneous model of diabetes for an examination of the expression of our genes of interest in the presence of hyperglycaemia parallel to STZ-induced diabetic mice.

c) $Lep^{ob/ob}$ (ob/ob) mice are a mouse model of T2D. These animals have a mutation in the leptin gene which leads to uncontrolled appetite and quick weight gain. Mutants were discovered in the out-bred colony in the Jackson Laboratory in 1949 and later bred into C57BL/6 mice (King, 2012, Ingalls et al., 1950). Ob/ob mice are a very good model for insulin resistance caused by obesity as they start gaining weight within 2 weeks following birth and develop hyperinsulinaemia and moderate hyperglycaemia after 4 weeks (King, 2012) (table 4.1). Although changes in renal structure and function in response to hyperglycaemia in the ob/ob mice are relatively mild (Soler et al., 2012), Chua et al. (1996) observed increased mesangial matrix expansion in FVB ob mice (Chua et al., 1996). In the current study, ob/ob mice were used as a model of T2D the effect of insulin resistance on mitochondrial biogenesis in mouse kidneys.

4.3 Hypothesis and aims

4.3.1 Hypothesis

The main hypothesis under study in this work is that hyperglycaemia can cause early changes in mitochondrial DNA content and that these changes can contribute to mitochondrial dysfunction. In the current chapter this hypothesis was investigated using mouse models of diabetes.

4.3.2 Aims and objectives

The main aim of this chapter was to, investigate using *in-vivo* models of diabetes, whether hyperglycaemia can alter MtDNA content in organs and circulating cells of diabetic mice.

This aim will be met as follows:

1. The effect of hyperglycaemia on MtDNA content in various mouse organs and circulating cells will be evaluated in three different mouse models representing T1D and T2D.

The experimental strategy to carry out the above will be as follows:

1. Three different mouse models of diabetes were used:
   a) Mice made diabetic using STZ were used as a model of T1D.
   b) Prohibitin2 knockout mice (β-PhB2$^{-/-}$) were used as a spontaneous model of T1D
   c) Leptin deficient ob/ob mice were used as a model of T2D
2. Blood and tissue samples will be collected after 7 and 31 days of hyperglycaemia in STZ-model from control mice, normoglycaemic transplanted mice and diabetic transplanted mice.
3. Blood samples will be sampled weekly and kidney tissues will be collected after 6 weeks of diabetes in β-PhB2$^{-/-}$ model.
4. Kidneys will be collected from 8-week old leptin deficient ob/ob mice.
5. Following DNA extraction, MtDNA content will be measured as a mitochondrial to nuclear genome ratio using real-time qPCR.

4.4 Results

In this chapter changes in MtDNA content in response to hyperglycaemia were investigated. Three different mouse models of diabetes were used; STZ-induced model of T1D, a β-PHB2$^{-/-}$ model of T1D and insulin resistant ob/ob mice as a model of T2D. A general overview of the content of this chapter is shown on Fig.4.1.

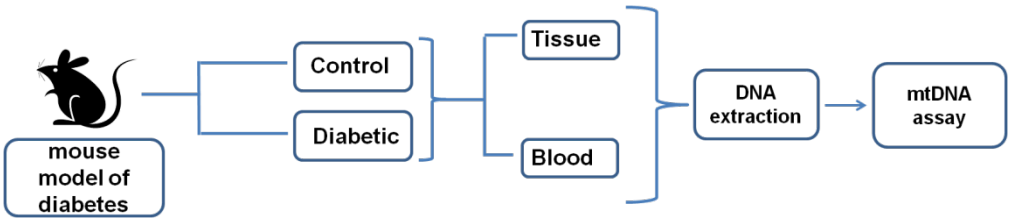

Fig.4.1. Overview of chapter 4.

To measure MtDNA content, total DNA extraction was performed as described in the methods section 2.5 and following template pre-treatment MtDNA assay was performed. Unique regions in the mitochondrial and nuclear genome were used to design an assay which does not co-amplify pseudogenes (Malik et al., 2011). Oligonucleotides against mouse mitochondrial genome (mMito; accession number: NC_012387.1) and a single copy reference gene (mB2M; accession number: NC_000068.7) were designed and optimized previously in Malik's lab. These mMitoF1 (CTAGAAACCCCGAAACCAAA) and mMitoR1 (CCAGCTATCACCAAGCTCGT) designed against mouse mitochondrial genome (NC_012387) amplified a unique region of 125bp (Fig4.2.D), which is not duplicate din the nuclear genome. mB2MF (ATGGGAAGCCGAACATACTG) and hB2MR (CAGTCTCAGTGGGGGTGAAT) designed against B2M precursor amplified a 177bp fragment (Fig.4.3D). Fluorescence based qPCR assay was used to detect copy number of mitochondrial and B2M gene (nuclear control) by absolute quantification method by applying 10 fold dilution of each transcript to create standard curve. The specificity of the primers (one PCR product amplified) was recognised as a single melt peak and single band when run on 2% agarose gel for

both genes of interest (Fig. 4.2 and Fig. 4.3). MtDNA content was measured as mitochondrial to nuclear gene ratio.

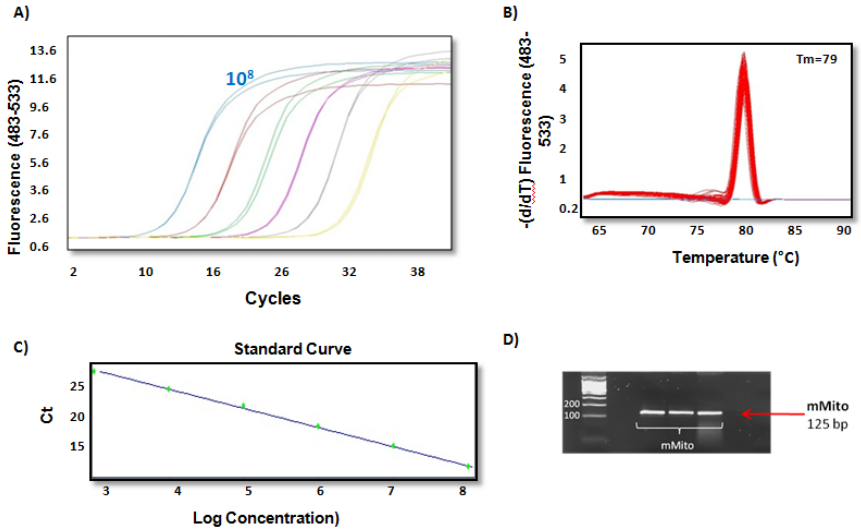

Fig.4.2. Mouse mitochondrial qPCR assay. Standard curve of mMito1 showing dilution series from 10^8 to 10^3, fluorescence data acquired once per cycle (A). Product melting temperature (Tm) representing the specificity of the multiplied product as one single melt peak at 79°C (B). Standard curve efficiency showing the crossing point for each of the 10-fold dilutions with efficiency: 1.96 and error = 0.037 (C). Agarose electrophoresis of PCR product run alongside 100bp marker. A single product of PCR reaction is shown with red arrow with comparison to 200bp of the ladder (D).

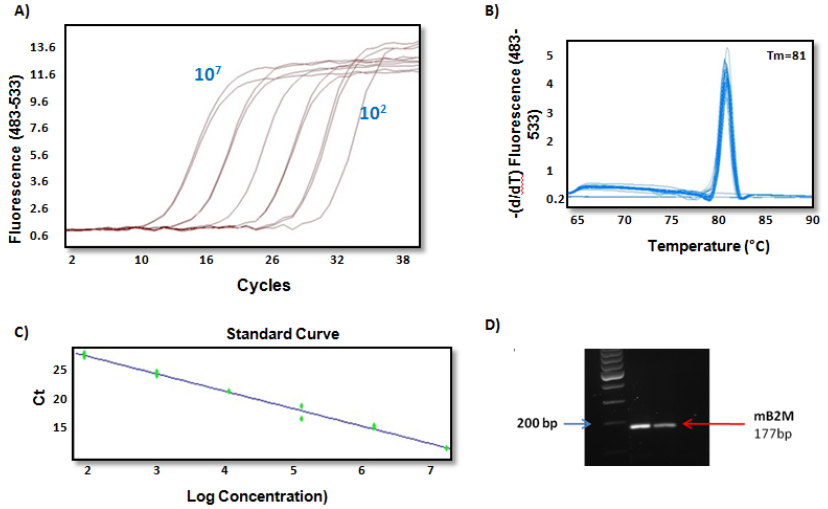

Figure 4.3. Mouse B2M qPCR assay. Standard curve of B2M product showing dilution series from 10^7 to 10^2, fluorescence data acquired once per cycle (A). Product melting temperature (Tm) representing the specificity of the multiplied product as one single melt peak at 81°C (B). Standard curve efficiency showing the crossing point for each of the 10-fold dilutions with efficiency: 1.92 and error =0.14 (C). Agarose electrophoresis of PCR product run alongside 100bp marker. Single product of PCR reaction (177bp) shown with red arrow (D).

4.4.1 Mitochondrial DNA content in the streptozotocin induced mouse model of type 1 diabetes

The experimental design and detailed description of the groups used in the study are presented in the Fig.4.4 and table 4.1. Three groups of mice were used; control untreated C57Bl/6 mice, diabetic (D) which had been injected with STZ and didn't cure after transplantation of islets and treated (T) mice in which hyperglycaemia was reversed by the transplant (Table 4.1). Kidneys and blood samples of these mice were collected after 1 week (T7, D7) and 4 weeks (T31, D31) post-transplantation and compared to samples collected from non-diabetic control mice of the same strain.

Table 4.1. Experimental mouse groups used in STZ study. Groups were divided based on duration of diabetes and treatment.

Group	N (kidneys)	N (blood samples)	Treatment	Duration of diabetes	Glucose levels [mM]
Control (Ctr)	6	6	non treated animals, non-diabetic - 8-12 weeks old	-	<11.1
Diabetic 7 (D7)	3	3	treated with streptozotocin, 3 days after injection islets were transplanted and mice were diabetic for 7 days (transplantation failed)	7-9 days	14-24
Treated 7 (T7)	5	2	treated with streptozotocin, 3 days after injection islets were transplanted and mice were normoglycaemic for 7 days (transplantation successful)	3 days	<11.1
Diabetic 31 (D31)	3	5	treated with streptozotocin, 3 days after injection islets were transplanted and mice were diabetic for 31 days (transplantation failed)	31 days	21-28
Treated 31 (T31)	5	6	treated with streptozotocin, 3 days after injection islets were transplanted and mice were normoglycaemic (transplantation successful)	3 days	<11.1

[a] See also Fig.4.4

The glucose levels in the mice used for this experiment are shown in Fig.4.4. As can be seen, the controls remained normoglycaemic (<11mM glucose) for the duration of the experiment. The treated mice were diabetic (>20mM glucose) for 3 days and following islets transplant had hyperglycaemia reversed to blood glucose concentration of <11mM, whereas the diabetic mice remained hyperglycaemic throughout the study (Fig.4.4).

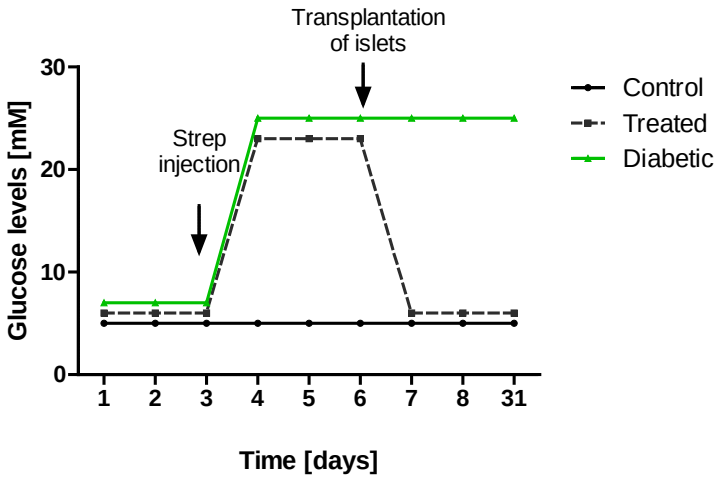

Fig.4.4. Schematic illustration of the treatment in the STZ model of diabetes used in this study. Mice were made diabetic by streptozotocin injection, three days after the injection diabetic mice received a suboptimal islet graft of 150 islets transplanted under the left kidney. Time points representative for 7 and 31 days of duration of the experiment. Control mice were not given any injections.

- *Mitochondrial DNA content in the kidneys of STZ-diabetic mice*

The aim of this experiment was to evaluate the effect of high blood glucose on MtDNA copy number in the kidneys of diabetic mice.

MtDNA content was quantified by using real-time qPCR method in DNA extracted from kidney sections of the 3 groups, healthy controls, treated and diabetic mice as described in the methods section. MtDNA copy number was estimated at approximately 400 copies per nuclear genome in healthy control mouse kidneys (Fig.4.5). In the kidneys of mice treated with islets' transplant, and subsequently cured for 7 days, there was a reduction in the MtDNA copy number when compared to the controls (258±72 vs. 385±42 respectively,

P>0.05), and this trend remained after 31 days of treatment (283±71), but it was not significant. Mice which were diabetic for 7 days had reduced MtDNA levels (232±112), when compared to the control group (385±42), but result was not significant (P>0.05). After 31 days, the depletion in MtDNA content was greater than 2 fold when compared to non treated controls in the diabetic mice (183±88, P<0.05, Fig.4.5).

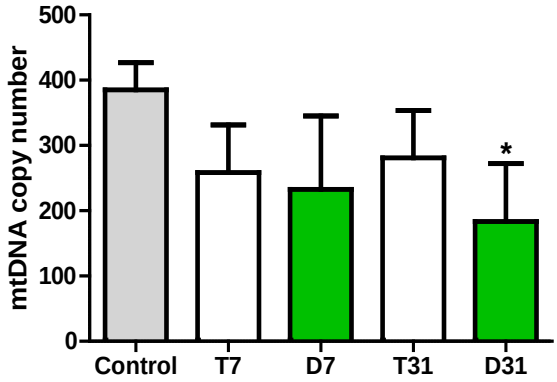

Fig.4.5. Hyperglycaemia affects mitochondrial DNA copy number in diabetic mouse kidneys in streptozotocin induced model of diabetes. C57BL/6 mice were made diabetic by streptozotocin injection, three days after the injection; some of the diabetic mice received a suboptimal islet graft of 150 islets transplanted under the left kidney (T7 and T31).Tissue samples were collected 7(D7) and 31 (D31) days after induction of diabetes in mice and also from healthy controls. Following DNA extraction, MtDNA content was assessed as a ratio of mitochondrial to nuclear gene using qPCR method. Data are shown as mean ± SD, n =3-6, one way ANOVA with Tukey's post hoc test where, *P<0.05 vs. Control

- *Mitochondrial DNA content in the circulating cells in STZ-diabetic mice*

Peripheral whole blood samples collected from STZ-induced diabetic mice were used in order to assess MtDNA content in circulating cells. As shown on Fig.4.6, MtDNA content in circulating cells in control animals was approximately 200 copies per nuclear genome. D7 group showed a highly significant, 4 fold increase in MtDNA copy number when compared to the healthy control group (854 ± 636 vs. 202±96 respectively; P<0.01). After 31 days of diabetes, MtDNA content returned to the control levels (113± 53 copies of MtDNA) and was significantly down-regulated when compared to D7 group (P<0.05). There was no difference in treated mice after 7 (T7) and 31 days (T31), when compared to the control group (Fig.4.6, P>0.05).

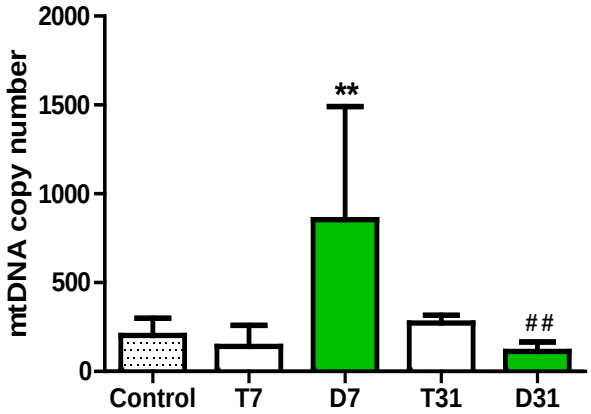

Fig.4.6. Hyperglycaemia affects mitochondrial DNA copy number in circulating cells in mouse blood in streptozotocin induced model of diabetes. C57BL/6 mice were made diabetic after single injection of streptozotocin. Some of the diabetic mice received a suboptimal islet graft of 150 islets transplanted under the left kidney (T7, T31) .Blood samples were collected 7(D7) and 31 (D31) days after induction of diabetes and from healthy controls. Following DNA extraction, MtDNA content was assessed as a ratio of mitochondrial to nuclear gene using qPCR method. Data are shown as mean ± SD, n =2-6, one way ANOVA with Tukey's post hoc test where, **P<0.01 (D7 vs. Control), $^{\#\#}$P<0.01 (D7 vs. D31).

- *Mitochondrial DNA content in different organs in control and diabetic mice*

Having established that hyperglycaemia caused a reduction in MtDNA content in the diabetic mouse kidney (D31) and a transient increase in circulating cells (D7), the next aim was to assess levels of MtDNA in other organs in control and diabetic mice (31D), in order to assess if changes were organ specific or systemic. Following DNA extraction, MtDNA copy number was measured in various control (table 4.2 and Fig.4.7) and diabetic (table 4.3 and Fig.4.8) mouse tissues.

The results from control mice showed that MtDNA levels were the highest in the heart (~600 copies), followed by the kidney (~400 copies) and lowest in the lung and islets (~40 copies) (table 4.2). A similar trend was observed in the diabetic mouse tissues after 31 days of hyperglycaemia, with the highest MtDNA levels detected in mouse heart (~700 copies) and lowest in the lung (~30copies) and islets (~60 copies) (table 4.3).

Table 4.2. Mitochondrial DNA copy number in healthy mouse tissues.

	Lung	Liver	Heart	Kidney	Whole blood	Brain	Islets
N	6	6	6	6	6	3	4
Mean	38	290	577	385	199	131	44
SD	16	46	406	41	102	67	8
Minimum	9	234	156	331	79	80	32
Maximum	60	371	1273	439	344	207	50

The tissues were collected from healthy, 8-12 weeks old C57BL/6 mice and following DNA extraction, MtDNA copy number was assessed via real-time qPCR method.

Table 4.3. Mitochondrial DNA copy numbers in diabetic mouse tissues.

	Lung	Liver	Heart	Kidney	Whole blood	Brain	Islets
N	3	3	3	3	5	4	4
Mean	24	190	657	183	113	147	61
SD	7	61	595	89	53	29	10
Minimum	19	120	277	80	57	106	50
Maximum	33	235	1473	237	190	170	75

The tissues were collected from diabetic C57BL/6 mice (D31) and following DNA extraction, MtDNA copy number was assessed via real-time qPCR method.

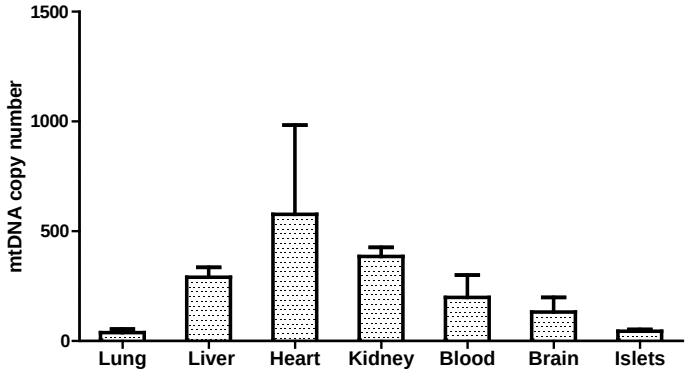

Fig.4.7. Mitochondrial DNA copy numbers in control mouse tissues. Tissue samples were collected from healthy control C57BL/6 mice. Following DNA extraction, MtDNA content was assesses as a ratio of mitochondrial to nuclear gene using real-time qPCR method. Data are shown as mean ± SD, n =3-6

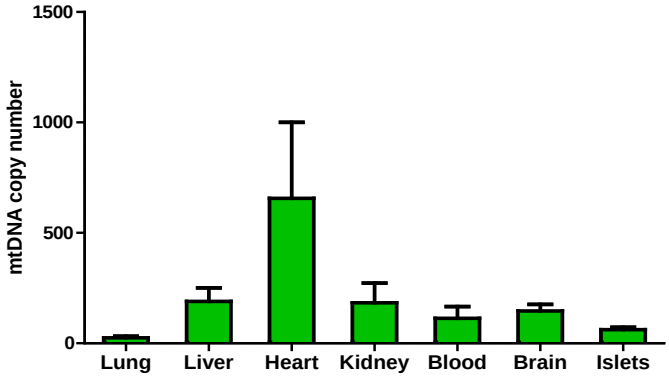

Fig.4.8. Mitochondrial DNA levels in diabetic mouse tissues. C57BL/6 mice were made diabetic after single injection of streptozotocin. Tissue samples were collected 31days after the induction of diabetes in mice. Following DNA extraction, MtDNA content was assesses as a ratio of mitochondrial to nuclear gene using qPCR method. Data are shown as mean ± SD, n =3-6.

Interestingly, when using independent Student's t-test to compare the direction of changes in the MtDNA levels between control and diabetic mouse tissues, we observed a significant decrease in MtDNA in diabetic kidney (as reported above) and a significant increase in diabetic islets ($P<0.05$), after 31 days of diabetes duration. No other significant changes in any other tissues were observed. However, there was a decrease MtDNA content in diabetic liver, and although it only approached significance ($P=0.05$; Table 4.4).

Table 4.4. Results from statistical analysis of changes in mitochondrial DNA content between control and diabetic mouse tissues.

	Ctr Lung	Ctr Liver	Ctr Heart	Ctr Brain	Ctr Islets	Ctr Kidney	Ctr Blood
D31 Lung	P=0.22	-	-	-	-	-	-
D31 Liver	-	P=0.05	-	-	-	-	-
D31 Heart	-	-	P=0.82	-	-	-	-
D31 Brain	-	-	-	0.7	-	-	-
D31 Islets	-	-	-	-	↑P=0.04	-	-
D31 kidney	-	-	-	-		↓P=0.02	
D31 Blood							P=0.13

Diabetes was induced in mice by administration of STZ. Samples were collected from diabetic mice 31 days after induction of diabetes (D31) and from healthy controls (Ctr). Following DNA extraction, the mitochondrial DNA (MtDNA) copy number was assessed as a ratio of mitochondrial to nuclear gene via qPCR method. Student's t-test was performed to assess the differences in the MtDNA content between Ctr and D31 mouse tissues. The tissues tested were lung, liver, heart, brain, islets, kidney, and whole blood samples. ↑, increased; ↓, decreased

To summerize, these data show that MtDNA content was significantly reduced in STZ-diabetic mouse kidneys after 4 weeks of the duration of diabetes. Treatment of diabetes (T7, T31) appeared to prevent the depletion of MtDNA observed in D31 group.

A transient increase in MtDNA content in peripheral blood samples after 7 days of hyperglycaemia, which was different to the results obtained from diabetic mouse kidney, where a slight reduction was seen. There was no significant difference in MtDNA content in circulating cells in the treated groups (T7 and T31). The above data show, that MtDNA copy number varies between different mouse tissues and hyperglycaemia had up-regulatory effect on MtDNA content in the mouse islets and a down-regulatory in the mouse kidneys after 31 days. No changes in the MtDNA copy number between any other diabetic and control tissues were detected, although there was a trend in the diabetic liver towards the reduction of MtDNA.

4.4.2 The effect of hyperglycaemia on mitochondrial DNA content in the β-PHB2$^{-/-}$ mouse model of type 1 diabetes

As STZ-diabetic mice are a chemically induced mouse model of T1D, to exclude any direct toxic effect of STZ on MtDNA content, a different mouse model of hyperglycaemia representing T1D, β-PHB2$^{-/-}$ mice was used (Supale et al., 2013). The aim of this part of the work was to determine if hyperglycaemia affects MtDNA content in kidney, heart and in circulating cells of β-PHB2$^{-/-}$.

- *Mitochondrial DNA content in organs in control and β-PHB2$^{-/-}$ diabetic mice*

MtDNA copy number in kidneys of control animals was slightly lower to the one which was observed in C57BL/6 control mice and estimated at around 300 of copies of MtDNA per nuclear genome. There was no difference in the MtDNA content between control and β-PHB2$^{-/-}$ diabetic mouse kidneys (287 ± 174 vs. 379 ± 192, respectively, Fig. 4.8A). The next goal was to look at the MtDNA copy number in the diabetic mouse hearts, as kidney and heart are organs with the highest MtDNA content therefore possibly with rapid changes in mitochondrial biogenesis in response to oxidative stress. No statistically significant changes in the levels of MtDNA copy number in control and diabetic hearts (821 ± 246 vs. 765 ± 396, respectively) were observed. Mean MtDNA copy number in the control animals were measured at around 800 copies and were slightly higher to the number detected in C57BL/6 mice used in the STZ model (4.9B).

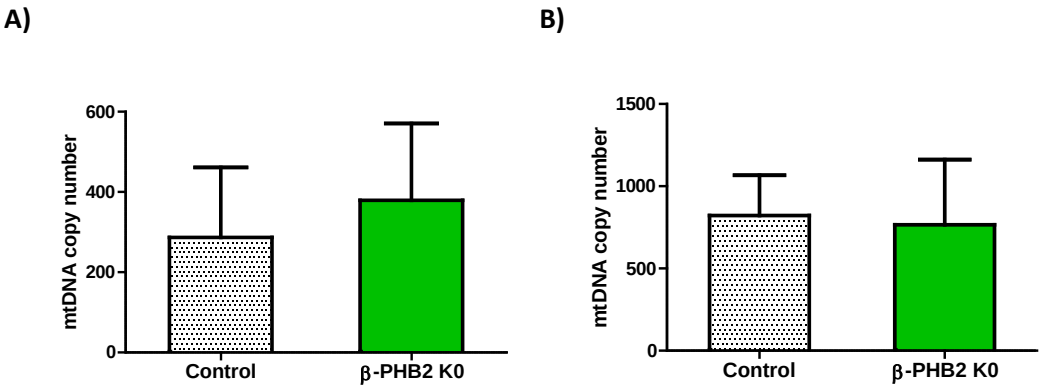

Fig.4.9. Mitochondrial DNA content is not affected by diabetes in β-PHB2$^{-/-}$ mouse tissues. Kidney (A) and heart (B) samples were collected from 11-week old healthy control and β-PHB2$^{-/-}$ diabetic mice. Following DNA extraction, MtDNA content was assessed as a ratio of mitochondrial to nuclear gene using qPCR method. Data are shown as mean ± SD, n =6-8, Student's t-test where, P>0.05.

- *Mitochondrial DNA content in circulating cells in control and* β-PHB2$^{-/-}$ *- diabetic mice*

MtDNA content detected in the control mouse blood samples was similar to that observed in C57BL/6 mice, and estimated at approximately 200-300 of copies (Fig.4.10). There was no significant difference in MtDNA content between the knockout and control group at the beginning of the study (week 4). However, after β-PHB2$^{-/-}$ became hyperglycaemic (week 6), there was a significant difference in MtDNA content between control and diabetic group, the latter having a higher number of MtDNA in circulation (277 ± 172 vs. 898 ± 343, respectively, P<0.05). Diabetic mice sustained high levels of MtDNA content in the blood throughout the duration of the study. The MtDNA copy number was almost 3 fold higher when compared to age-matched healthy controls and peaked to approximately 1100 copies at week 11 (Fig.4.10).

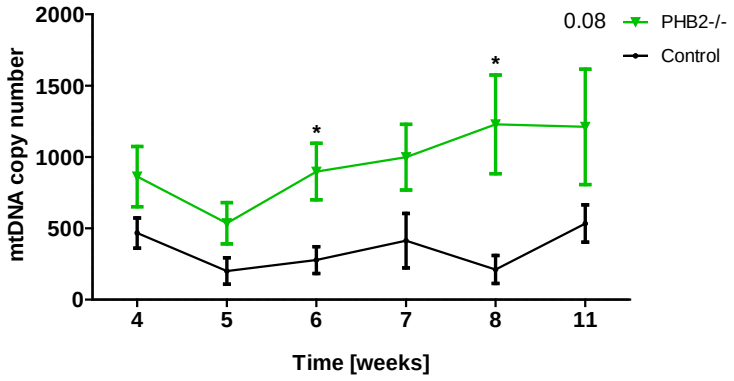

Fig.4.10. Mitochondrial DNA content in circulating cells is affected by hyperglycaemia in β-PHB2 knockout mice. Blood samples were collected from weekly form healthy control and β-PHB2$^{-/-}$ diabetic mice. Following DNA extraction MtDNA copy number was measured as a ratio of mitochondrial to nuclear gene copy number by qPCR method. Data shown as a mean ± SD, n =3-4, Student's t-test, where, *P<0.05

These data show that unlike to the reduction in MtDNA content observed in STZ-diabetic model no changes in MtDNA copy number in β-PHB2$^{-/-}$ diabetic kidneys were observed. No change in MtDNA content in diabetic heart was also observed. There was a clear and significant 3 fold increase in MtDNA copy number in circulating cells in diabetic β-PHB2$^{-/-}$ mice.

4.4.3 The effect of hyperglycaemia on mitochondrial DNA content in the Lep ob/ob mouse model of type 2 diabetes

Both, β-PHB2$^{-/-}$ and STZ mouse models used in the study were highly hyperglycaemic (Rackham et al., 2013, Supale et al., 2013). The aim of this study was to evaluate MtDNA levels in the kidneys of type 2 diabetic mouse model, with relatively moderate obesity and hyperglycaemia. Mice used in this study were 8 weeks old and contained approximately 10x more abdominal fat than their aged matched lean controls. As shown on figure 4.11 ob/ob animals were also two times heavier than their lean controls (43 ± 1.6 vs. 21 ± 0.4). Moreover ob/ob mutants also had bigger pancreas and kidneys (personal communication, Dr Aileen King). MtDNA copy number in kidneys of control mice was also lower to the one which was observed in C57BL/6 control mice (approx.400 copies per nuclear gene) and controls in the knockout study (approx.300 copies per nuclear gene) and estimated at around 150 of copies of MtDNA.

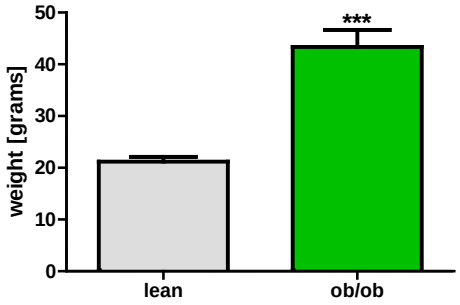

Fig.4.11. Ob/ob mutant mice are heavier than the lean controls. Body weights were taken from 8-weeks old C57BL/6 lean control and ob/ob mice. Data shown as a mean ± SD, n =4, Student's t-test where,*** P<0.001

As presented on Fig.4.12, MtDNA copy number was reduced by almost a half in the diabetic, obese mice when compared to the lean controls (63 ± 22 vs. 140 ± 74), but the difference only approached significance (P=0.08).

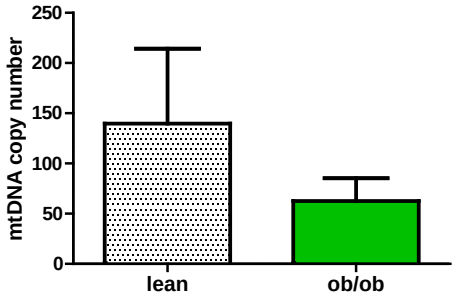

Fig.4.12. Insulin resistant ob/ob mice seem to have less mitochondrial DNA content in the kidneys. Following DNA extraction MtDNA copy number was measured as a ratio of mitochondrial to nuclear gene copy number using qPCR technique. Data shown as a mean ± SD, n =4, Student's t test where, $P<0.05$

These data suggest a trend towards down-regulation of MtDNA copy number in ob/ob mouse model of T2D, however a major limitation was the sample size used in the experiment.

4.5 Discussion

Three different mouse models of diabetes were used in this chapter to study the effect of hyperglycaemia on MtDNA content in circulating cells and tissues. Two models of T1D (chemically induced by STZ, and by using β-PHB2$^{-/-}$ mice), and one model of T2D were used. Healthy, non diabetic mice were used as a controls.

In the STZ-induced diabetic model, lower MtDNA content was found in the kidneys of diabetic mice after 7 days, and this reduction became statistically significant after 31 days of the duration of diabetes. MtDNA content in circulating cells was increased after 7 days and returned to normal levels after 31 days. As shown in Fig.4.3 the treated groups (T7and T31), which received STZ injection, also seem to have slightly reduced MtDNA content in the kidney, but this reduction was not statistically significant. STZ is a toxic compound, which specifically targets β-cells and causes cell necrosis through the depletion of ATP. This complex acts via ROS and when is transported to the cells causes DNA damage and activation of poly-ADP-ribosylation, NAD^+ depletion, which causes a reduction in ATP produced (Szkudelski, 2001). The main controversy in using this chemically induced model of diabetes is that STZ is a broad spectrum toxin, which can also affect other organs. Lee at al. (2010) reported changes in protein levels of cytochrome P450(CYP) proteins in various rat tissues, showing up-regulation of the CYP in the kidney, and dys-regulation in the liver, brain and intestines (Lee et al., 2010). On the other hand, Sandler and Swenne (1983) reported STZ-induced DNA repair in isolated mouse islets (Sandler and Swenne, 1983). Additionally, glucose measurement data from our lab suggest, that in treated animals, glucose levels tend to oscillate between normal and diabetic levels, especially within the first week after transplantation of the islets (Dr Chloe Rackham, personal communication). This could explain why there seem to be (although not significant) dys-regulation of the MtDNA content in the treatment groups.

In contrast to the kidney, circulating cells showed a significant up-regulation of MtDNA after a short duration of diabetes (7 days), and MtDNA content returning to normal after 31 days of hyperglycaemia. These results suggest possibly, an

increased mitochondrial biogenesis in response to hyperglycaemia, or leakage of MtDNA into the circulation from the tissues. Increased biogenesis is supported indirectly by the findings in the previous chapter, where up-regulation of MtDNA copy number in HMCs exposed to HG for 4 days was observed (Fig.3.6, chapter 3). Also recent work of a Taiwan group assessed MtDNA content in leg muscle, blood vessels and peripheral leukocytes in type 2 diabetic patients in comparison to the healthy controls (Hsieh et al., 2011). Their results also showed discrepancies between the level of MtDNA in different tissues, with significant increase of MtDNA in blood cells, decrease in muscle tissue and no variation in MtDNA content in blood vessels, between diabetic and healthy patients, suggesting a varying effect of hyperglycaemia on different type of cells (Hsieh et al., 2011).

Decreased MtDNA content in diabetic mouse kidneys, which is observed in this study in the STZ-diabetic mice and also in the ob/ob mice, correlate with data reported by others. Fedorova et al. (2013), using a proteomics approach in a partially nephrectomised rat model of chronic kidney disease (CKD), showed dysregulation of proteins involved in metabolism in rat kidney cortexes. They observed a 50% reduction in mitochondrial OXPHOS and structural proteins and approximately 30% reduction in the MtDNA content (Fedorova et al., 2013).

The possible mechanism behind the reduction of the MtDNA amount in diabetic mouse kidneys might be damage of MtDNA by increased ROS. It has also been reported that in insulin resistant mice fed with high fat diet, there was an induction of MtDNA damage in mouse muscle and liver due to the dys-regulation of the repair enzyme, which eventually contributes to increased ROS production by mitochondria, dysfunction in OXPHOS and induction of apoptosis (Yuzefovych et al., 2013). However Dugan at el. (2013) by using *in-vivo* real-time transcutaneous fluorescence observed decreased oxygen production in diabetic mice kidneys by mitochondria and this result correlated with decreased mitochondrial function and biogenesis. By using STZ model they also observed a reduction in both, mitochondrial biogenesis and mitochondrial glucose oxidation (Dugan et al., 2013).

On the other hand, Ruggiero at al., (2011) reported increased mitochondrial bioenergetics in diabetic mouse kidneys as an adaptive response to oxidative stress. By using C57BL/6 mice fed on high fat diet, they reported structural changes in mouse kidneys (fibrosis and hypertrophy), which correlated with increased ROS production and pro-inflammatory markers. Increased levels of mitochondrial superoxide dismutase (MnSOD) and increased mitochondrial ATP-linked respiration in animals kept for 12-weeks, which was not present at later stages, suggesting that there is an adaptive phase to the nutrient overload, but over time, mitochondria became exhausted and their function starts to fail (Ruggiero et al., 2011).

In humans DN is characterised by different stages with hyperfiltration occurring first, followed by a decline in the filtration and lesion in the kidney (Mogensen et al., 1983). This could explain various reports from animal studies regarding mitochondrial biogenesis and function. Reduction in MtDNA levels, which was observed in two different diabetic mouse models used in current study may reflect adaptive mechanism in which excessive glucose load inhibits proximal re-absorption of the glucose. Glucose is actively reabsorbed from the blood , through NA^+/K^+ pumps which require constant energy provided by mitochondria ATP (Vallon, 2011).

The lack of changes in the kidneys observed in the knockout mice might be caused by slightly different mechanisms. In STZ-induced diabetic model we observed changes in circulating cells very quickly (after 7 days), and after 4 weeks they return to normal levels. In the β-$PHB^{-/-}$ mice a constant induction of MtDNA in blood samples collected weekly was observed, and no difference in the kidney or heart tissues. Interestingly elevated MtDNA content, which we observed in circulating cells in the knockout animals correlates with the time when they develop diabetes (week 6). This data is supported by a study of Bonnard et al. (2008), in which diabetes-induced structural and functional changes in mitochondria in mouse muscle tissue were shown. A reduction in both MtDNA content and protein expression of mitochondrial transcription factor PGC-1α in two different mouse models of diabetes was also observed. Interestingly, in this report no changes in MtDNA content when animals were at

pre-diabetic state were observed, but only at fully developed disease state. The *in-vitro* study showed that hyperglycaemia induced changes in mitochondrial function could be reverted by antioxidant treatment, suggesting that mitochondrial dysfunction was due to the increased oxidative stress also observed in experimental animals (Bonnard et al., 2008).

I also compared MtDNA content in other tissues from the control and diabetic mice, and in both groups, tissues with the highest number of MtDNA were heart and kidney. Lowest MtDNA content was determined in the lung tissue. These findings correlate with results reported by others in human (Mercer et al., 2011) and in rat tissues (Fernandez-Vizarra et al., 2011), which confirm the MtDNA content test reliability. Islets proved to be among the organs with one of the lowest levels of MtDNA content, which might suggest they are particularly susceptible to the toxic effects of chronic hyperglycaemia. In this study, there was a significant increase of MtDNA in diabetic islets, when compared to the controls, which is in contrast to the findings reported by Lu et al. (2010), who observed no changes in MtDNA in beta-cells after the onset of diabetes and a decline during the progression of the disease in diabetic knockout mice (Lu et al., 2010). However, we measured MtDNA after only 31 days of the onset of diabetes, therefore our results may suggest and adaptive response of the islets to their failing function.

This study could be criticized for not using a specific animal model of diabetic nephropathy. However my aim was to examine the effect of hyperglycaemia on MtDNA levels in mouse organs and circulating cells. To date there are no ideal animal models of DN, since it takes approximately 15-20 years in humans to develop kidney disease, this makes it difficult to study the disease using animal models. Another limitation of this study is the lack of measurement of oxidative stress and enzyme activities. It was shown by others that mitochondrial biogenesis correlates with function in diabetic animal models, therefore falling levels of MtDNA in our study in the kidney tissues, suggest reduced mitochondria function in these animals. A further limitation may be use of relatively young animals. Some of the sample number used in the study was low, especially in the ob/ob mouse model and some of the groups in the STZ-model. In the kidneys of

ob/ob mice as the result was approaching significance and might become significant if a larger sample size was used.

In summary, I have observed increased MtDNA level in circulating cells in the *in-vivo* diabetic mouse models, and this increase preeceded changes observed in the mouse kidneys. To my knowledge this is the first report of altered levels of MtDNA in circulating cells in diabetic mouse models. Increased MtDNA content in circulation may be an adaptation to the nutrient overload or may be a cellular free MtDNA released from tissues. Decrease in MtDNA in diabetic mouse kidneys may be a sign of the failing mitochondrial function and cell death.

Chapter 5
Functional consequences of hyperglycaemia in kidney cells

5.1 Abstract

Background/Aims: The hypothesis that will be tested in this thesis is that hyperglycaemia/high glucose can cause early changes in mitochondrial DNA (content/quality) and that these changes can contribute to mitochondrial dysfunction. In the current chapter functional consequences of the altered MtDNA were examined in human mesangial cells.

Methods: RNA was extracted from: human mesangial cells (HMCs) cultured in DMEM containing 5mM (NG) and 25mM (HG) glucose. Following reverse transcription, quantitative measurement of genes involved in mitochondrial life cycle (biogenesis and mitophagy) and mitochondrial encoded mRNAs were measured using real-time qPCR. ROS production and cell viability were also assessed in HMCs grown in normal and high glucose using fluorescence and luminescent assays. Moreover high glucose-induced mitochondrial DNA damage in renal cells was assessed using PCR. Mitochondrial morphology and protein content were assessed using MitoTracker staining and Western blot respectively.

Results: Growth of HMCs in HG resulted in 2-fold higher *TFAM* ($P<0.05$). The expression of two mitochondrial genome encoded mRNAs was reduced ($P<0.05$) in parallel with increased MtDNA damage, cellular ROS and apoptosis ($P<0.05$) in HMCs exposed to HG. Mitochondrial length and degree of branching were reduced in HMCs cultured in HG ($P<0.01$, $P<0.001$). *NF-κB* and *MYD88* expression were up-regulated in HMCs exposed to HG ($P<0.05$).

Conclusion: These data suggest that exposure to hyperglycaemia caused a dys-regulation between mitochondrial DNA content and mitochondrial transcription and translation. Moreover high glucose-induced stress caused damage to mitochondrial DNA, which suggest that although as previously shown mitochondrial DNA is up-regulated, it is not functional. Changes in mitochondrial morphology and network which occurred very quickly after the exposure to high glucose may also contribute further to mitochondrial dysfunction in the renal cells.

5.2 Introduction

In this chapter the focus is on changes in MtDNA quality, morphology and expression of nuclear-encoded transcription factors and on the assessment of cellular ROS and apoptosis in human mesangial cells cultured in high glucose. It has been shown in the previous chapters, that MtDNA is elevated in renal cells cultured in high glucose and also in peripheral blood in diabetic mice but decreased in the diabetic mouse kidneys.

Free radicals serve as intracellular messengers and can also stimulate the same pathway as glucose e.g. activation of protein kinase C (PKC); but excessive activation of PKC leads to tissue injury trough activation of transforming growth factors and also NF-κB, which then activates inflammatory response within the cells (Pugliese et al., 1994). Lee et al (2003) demonstrated that culturing renal cells under high glucose conditions augments production of ROS and that this stimulation of free radicals generation can be effectively blocked by PKC inhibitors (Lee et al., 2003). Catherwood et al., (2002) using *in-vitro* cultured porcine mesangial cells, showed also high glucose-induced impaired antioxidant activity including mitochondrial superoxide dismutase (MnSOD) (Catherwood et al., 2002). Nishikawa et al, (2000) had shown that culturing bovine endothelial cells in 30mM glucose induces ROS production and by using mitochondrial complex I and II inhibitors and uncoupler (CCCP) they were able to abolish stimulating effect of hyperglycaemia on free radicals production (Nishikawa et al., 2000). An adaptive response of mitochondria to oxidative stress might be to increase mitochondrial biogenesis via replication of the mitochondrial genome and increasing mitochondria mass. However, it has been shown that under persistent oxidative stress, mitochondrial DNA mutations ratio increases (Xie et al., 2008, Wei and Lee, 2002).

Mitochondrial biogenesis is regulated by the nuclear transcription factors like mitochondrial transcription factor A (TFAM) and Peroxisome proliferator-activated receptor gamma coactivator 1-alpha (PGC-1α) (Hock and Kralli, 2009). Mitochondria are not static organelle and they are frequently undergoing processes called fusion and fission; non-functional mitochondria are removed by a process called mitophagy. Fusion is maintained by mitofusin 1 and 2 (MFN1

and MFN2) and optic atrophy gene 1 (OPA1) and mitochondrial fission by mitochondrial fission protein 1 (FIS1), mitochondrial fission factor (MFF) and dynamin-related protein 1 (DRP1) (Twig and Shirihai, 2011). Non-functional mitochondria are removed during the mitophagy process which is orchestrated by PTEN induced putative kinase 1 (PINK-1) and parkin (PARK2), but it is not know how the faulty mitochondria are selected for disposal [reviewed in (Ashrafi and Schwarz, 2013)]. One possibility is a membrane potential, as by the fusion process some mitochondria can rescue their falling membrane potential. Mitochondrial fusion and fission occurs every 20 minutes which possibly allows mitochondria recover their membrane potential by fusing with mitochondria with the higher membrane potential (Twig and Shirihai, 2011).

The mitochondrial mitophagy and fusion proteins are also important for the MtDNA maintenance (Chen and Chan, 2009). Moreover it has been reported that mutation in the OPA1 gene caused MtDNA deletion (Hudson et al., 2008). A disturbance in mitochondrial cycle, caused by oxidative stress might have a detrimental effect for the proper function of the cells, which have been shown in several studies. In mouse neuronal cells exposed to the oxidative stress, induced secondary ROS production was shown, as well as changes in mitochondrial morphology which also correlated with decreased mitochondrial function, measured as a membrane potential (Grohm et al., 2010). Makino at al., (2010) using cultured endothelial cells extracted from diabetic mice also reported an increased fragmentation of mitochondria which was reverted by a treatment with antioxidant which suggest effect of oxidative stress on mitochondrial morphology (Makino et al., 2010).

Diabetic nephropathy is a complex disease associated with induced inflammation (Wada and Makino, 2013). Inflammation has been reported to be up-regulated through the AGE production and activations of the AGE-receptor (RAGE), which then induces NF-κB cascade and cytokine production (Mosquera, 2010). NF-κB is a regulatory switch for more than 400 genes involved in the inflammatory response, including cytokines, and pro-inflammatory enzymes (Sethi et al., 2008). MtDNA can also contribute directly to pathology in acquired diseases such as diabetic complications because, like bacterial DNA, it is un-methylated and

initiates immune responses via the intracellular Toll like receptor 9 (TLR9) (Barbalat et al., 2011, Sparwasser et al., 1997).

In overall, the main aim of this chapter is to assess functional changes in mitochondrial life cycle caused by hyperglycaemia in order to see if they correlate with increased MtDNA in renal cells. Mitochondrial transcription factors and the expression of the *NF-κB* and Myeloid differentiation primary response gene 88 (MYD88, downstream activator of TLR9 pathway) were also measured.

5.3 Hypothesis and aims

5.3.1 Hypothesis

The main hypothesis under study in this work is that hyperglycaemia can cause early changes in mitochondrial DNA (content/quality) and that these changes can contribute to mitochondrial dysfunction. In the current chapter hyperglycaemia-induced functional changes in mitochondria and cells were investigated.

5.3.2 Aims and objectives

The main aim of this chapter is to demonstrate, using cultured renal cells, whether glucose-induced changes in MtDNA occur in parallel with functional changes in mitochondria and renal cells.

This aim will be met as follows:

1. The effect of culture of renal cells in high glucose on mitochondrially encoded mRNAs will be measured.
2. The effect of hyperglycaemia on the nuclear control of MtDNA replication in the human mesangial cells will be determined.
3. The effect of hyperglycaemia on the mRNAs expression of the genes involved in mitochondrial life cycle will be assessed in renal cells.
4. The effect of hyperglycaemia on the activation of inflammatory associated mRNAs will be measured in renal cells.
5. The effect of hyperglycaemia on cell viability and ROS production in human mesangial cells will be measured.
6. MtDNA damage in human mesangial cells exposed to hyperglycaemia will be assessed.
7. The effect of glucose-induced changes in mitochondrial protein levels and mitochondrial morphology in renal cells will be evaluated.

The experimental strategy to carry out the above will be as follows:

1. Primary mesangial cells will be cultured in 5mM (normal, NG) and 25mM (high, HG) glucose for 4 and 8 days.

2. Following RNA extraction and reverse transcription, mitochondrial and nuclear encoded mRNAs will be measured using real-time qPCR following normalization to β-actin.

3. Following protein extraction protein content will be assessed using Western blotting technique.

4. Following staining of mitochondria and by using fluorescent microscopy and ImageJ software, mitochondrial morphology and network structure will be measured.

5. Cellular ROS and cell viability will be assessed using fluorescence and luminescence assays.

6. Following DNA extraction MtDNA damage will be assessed by using PCR and elongase method.

5.4 Results

In this chapter, hyperglycaemia-induced functional changes in mitochondria and cells were investigated. General overview of chapter 5 is shown on Fig.5.1

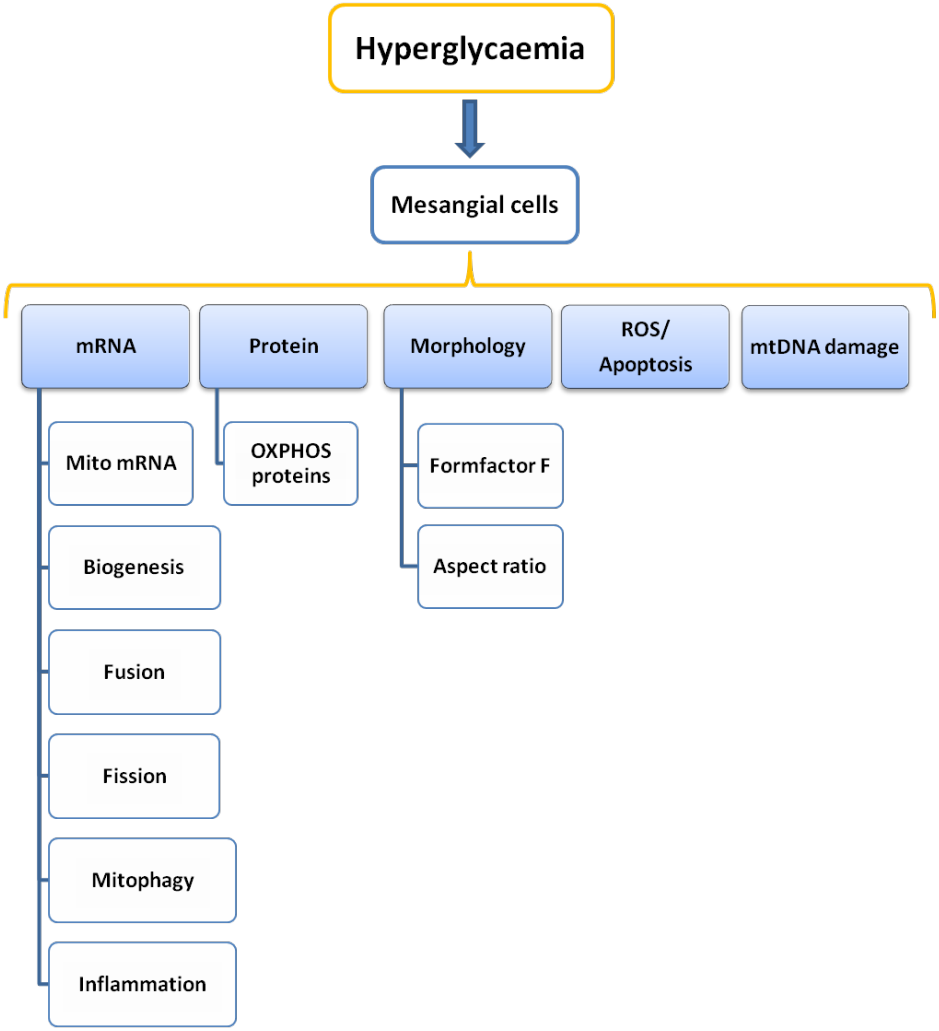

Fig.5.1. Overview of chapter 5.

5.4.1 The effect of hyperglycaemia on mitochondrial mRNAs in human mesangial cells

HMCS were cultured as described in the main methods section 2.3. Cells were seeded at an equal density ($1x10^5$/well) in 6-well plates in DMEM containing either 5mM (normal, NG) or 25mM (high, HG) glucose for 4 and 8 days. To assess copy number of the investigated mRNAs, RNA was extracted, reversely

transcribed and real time qPCR was performed as describe in method section 2.7. *β-actin* was selected for normalization by using GeNorm software.

To examine whether glucose induced MtDNA content in HMCs correlated with changes in transcription of the mitochondrial genome, mRNAs for three mitochondria genome coded OXPHOS subunits were measured, *ND6*, *ND1* and *COX3*. As illustrated on Fig.5.2, exposure to hyperglycaemia had significantly down-regulated expression of mitochondrial *ND6* and *COX3* after 4 days of culture, but had no effect on the expression of *ND1*.

Expression of *ND1* remained at the same level throughout the culture time and was not significantly affected by 25mM glucose ($P>0.05$, Fig.5.2.B). *ND6* expression was significantly decreased after 4 days of exposure to high glucose when compared to the control (64 ± 20 vs. 156 ± 8 respectively, $P<0.01$ Fig.5.2.A). Similar trend was observed in *COX3* expression, as there was a highly significant down-regulation of *COX3* mRNA expression in HMCs exposed to high glucose for 4 days when compared to the control (285 ± 88 vs. 633 ± 44 respectively, $P<0.01$, Fig.5.2.C).

No significant differences between the groups were observed after 8 days of treatment ($P>0.05$, Fig.5.2). However, when the mRNA expressions of the controls were compared there was also observed a trend towards down-regulation of *ND6* expression in NG between 4 and 8 days of culture, but results was not significant ($P>0.05$) (Fig.5.2A). Moreover there was a trend (however not significant), towards the reduction of *COX3* in cells cultured in NG for 8 days, when compared to the cells culture in normal glucose for 4 days ($P>0.05$, Fig. 5.2 C), which may suggest an effect of sub-culturing on mitochondrial mRNAs in HMCs.

In summary, the increased MtDNA in response to high glucose is not acting as a template for mitochondrial encoded mRNAs, as there was either no change or reduction of the mitochondrial encoded mRNAs.

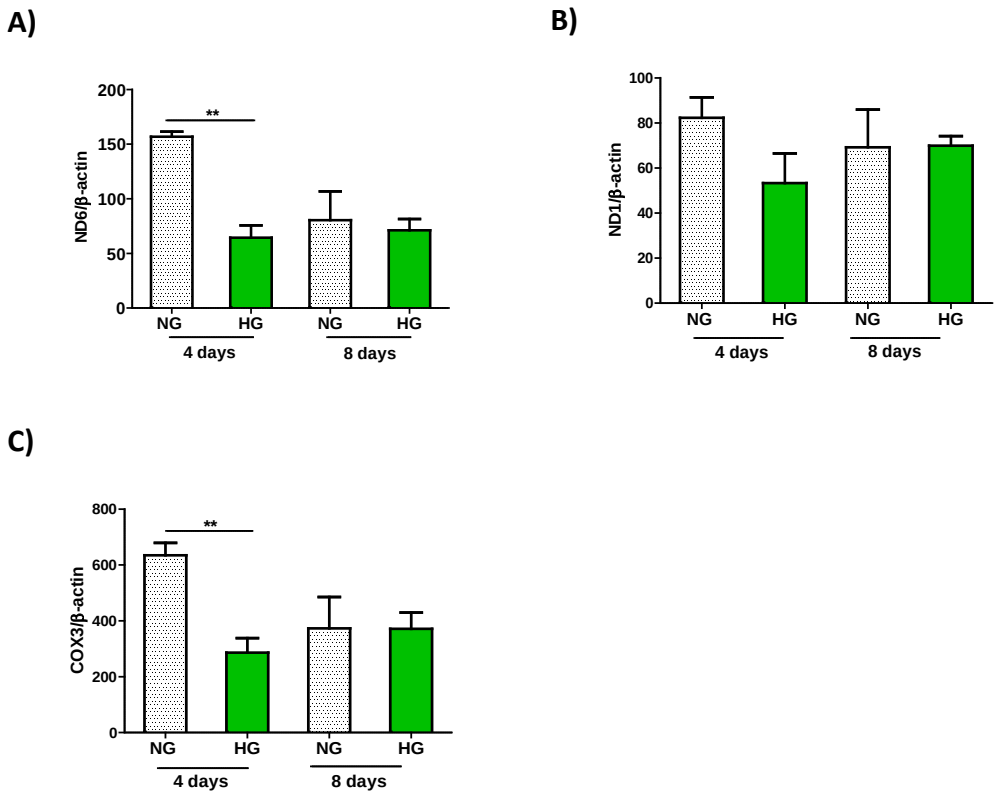

Fig.5.2. The effect of hyperglycaemia on mitochondrial encoded mRNAs in human mesangial cells. After glucose synchronization with 0.5% FBS in DMEM, HMCs were cultured in DMEM containing 5mM (NG) and 25mM (HG) for 4 and 8 days. Following RNA extraction and reverse transcription, copy numbers of ND6 (A), ND1 (B), and COX3 (C) were determined using real-time qPCR. mRNA copy numbers for each gene were determined relative to 1000 copies of reference gene *β-actin*. Data presented as a mean ± SD, n=3, Student's t-test where, **P<0.01 vs. NG

To determine whether hyperglycaemia affects the mRNA expression of genes involved in the mitochondrial life cycle, the mRNAs genes involved in mitochondrial biogenesis (*TFAM* and *PGC-1α*) in HMCs grown in normal and high glucose for 4 and 8 days were examined.

As seen on Fig.5.3, the relative expression of *TFAM* in HMCs was 100 times higher, when compared to the detected levels of *PGC1-α*. *TFAM* expression was significantly increased in high glucose at 4 days when compared to the control (44±23 vs. 19±5, P<0.05, Fig.5.3.A). After 8 days of exposure to high glucose, *TFAM* expression was still elevated when compared to the control (32±11 vs. 20±8) and the result was approaching significance (P=0.07, Fig.5.3 A). The levels

of the *PGC-1α* did not show a statistically significant change in high glucose when compared to control at times shown (Fig.5.3 B, P>0.05).

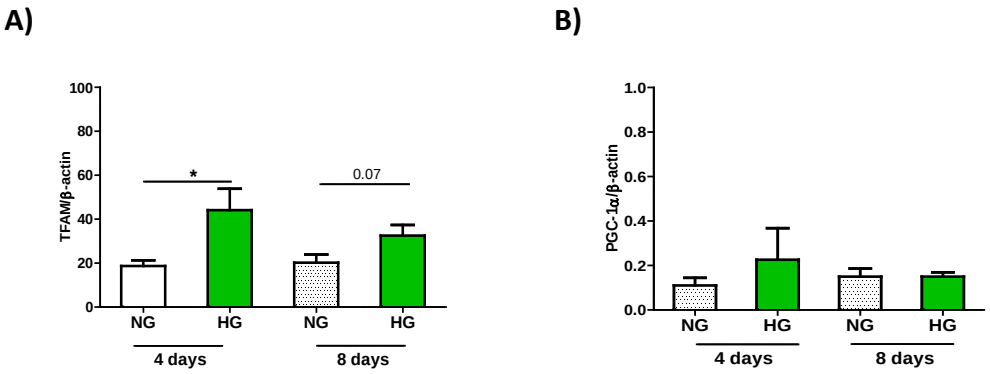

Fig.5.3. The effect of hyperglycaemia on mRNA expression of mitochondrial transcription factors in cultured primary human mesangial cells. After being synchronized, HMCs were cultured in DMEM containing 5mM (NG) and 25mM (HG) glucose for the times shown. Following RNA extraction and reverse transcription, copy numbers of *TFAM* (A) and *PGC-1α* (B) were determined using RT-qPCR. mRNA copy numbers for each gene were determined relative to 1000 copies of reference gene *β-actin*. Data presented as a mean ± SD, n=5-6, Student's t-test where, *P<0.05

These data show that there is an up-regulation of *TFAM* in HMCs after 4 days of culture in HG. The increase in *TFAM* is taking place at the same time as the increase in MtDNA (Fig.3.7), but *PGC-1α* does not show a significant increase during this time.

5.4.2 The effect of hyperglycaemia on fusion, fission and mitophagy mRNAs in human mesangial cells

mRNA expression of the genes involved in mitochondrial dynamics was assessed in HMCs cultured in 5mM and 25mM glucose. Expressions of *MFN1*, *MFN2*, *OPA1* and *DRP1* (as the candidate genes of mitochondrial fusion and fission) and *PINK1* and *PARK2* (genes involved in mitophagy) were assessed using real-time qPCR and primers listed in table 2.4 in the methods chapter. There was no significant difference (P>0.05) in mRNA expression of any of the investigated genes involved in mitochondrial fusion (Fig.5.4 A-C), fission (Fig.5.5) and mitophagy (Fig.5.6A, B) between the groups (P>0.05).

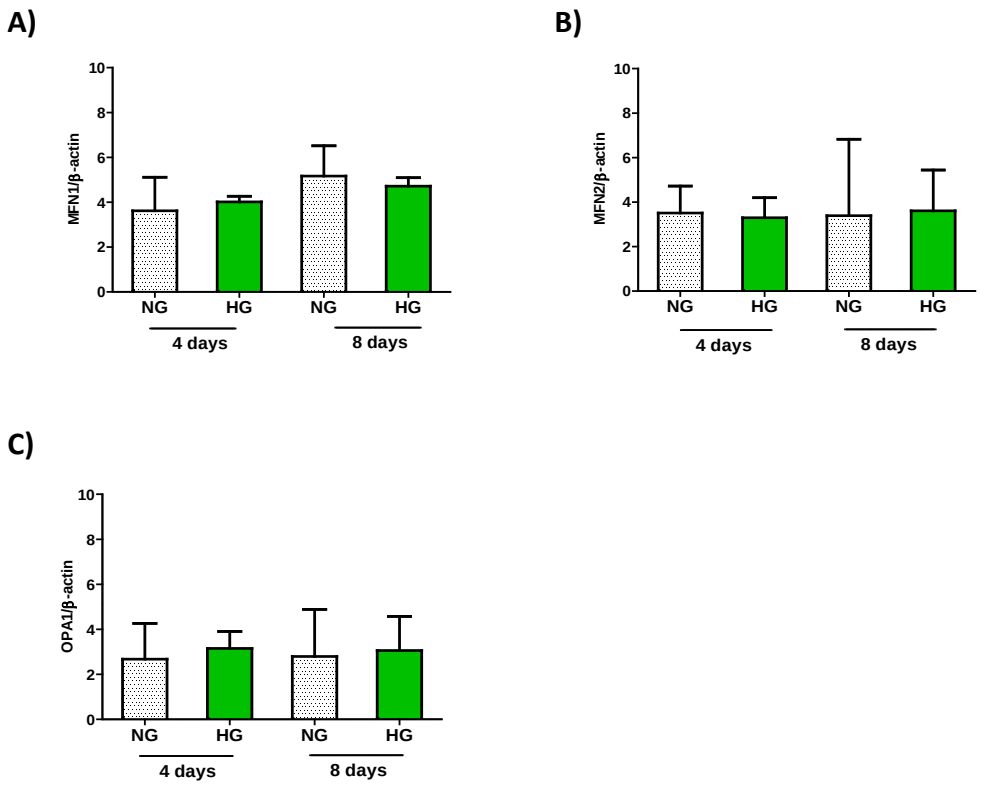

Fig.5.4.Hyperglycaemia has no effect on the expression of mRNAs involved in mitochondrial fusion in cultured primary human mesangial cells. After being synchronized, HMCs were cultured in 5mM (NG) and 25mM (HG) glucose for 4 and 8 days. Following RNA extraction and reverse transcription, copy numbers of *MFN1* (A), *MFN2* (B), and *OPA1* (C) were determined using real-time-qPCR. mRNA copy numbers were determined relative to 1000 copies of reference gene *β-actin*. Data presented as a mean ± SD, n=3, Student's t-test where, P>0.05

There was also no effect of the duration of the culture as the expression levels of *MFN1*, *MFN2*, *OPA1*, *DRP1* in cells cultured in 5mM glucose for 4 and 8 days did not differ (P>0.05, Fig 5.4 and Fig 5.5). Although no significant difference in the expression of the genes involved in mitophagy was observed, expression of *PARK2* was up-regulated by 4-fold, in HMCs exposed to high glucose for 8 days, when compared to the control (0.04 ± 0.06 vs. 0.01 ± 0.005, P>0.05, Fig. 5.6 B). Expression of *PINK1* did not vary between the treatments (P>0.05, Fig.5.6 A).

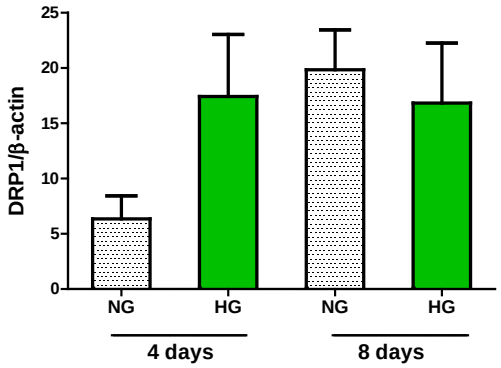

Fig.5.5. Hyperglycaemia does not affect mRNA involved in mitochondrial fission in cultured primary human mesangial cells. After being synchronized, HMCs were cultured in DMEM containing 5mM (NG) and 25mM (HG) glucose for 4 and 8 days. Following RNA extraction and reverse transcription, copy numbers of *DRP1* were determined using real-time qPCR and relative to 1000 copies of reference gene *β-actin*. Data presented as a mean ± SD, n=4-6, Student's t-test where, P>0.05 vs.NG

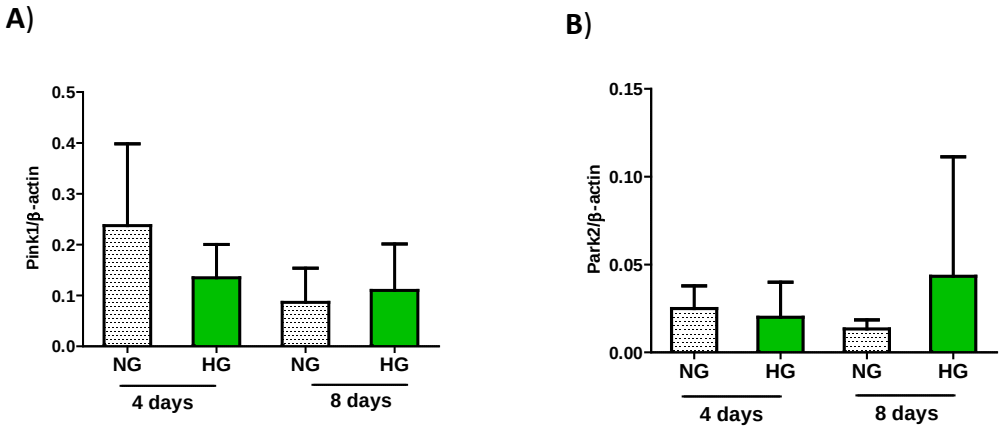

Fig.5.6. Hyperglycaemia does not affect mRNAs involved in mitophagy in cultured primary human mesangial cells. HMCs were cultured in DMEM containing 5mM (NG) and 25mM (HG) glucose for 4 and 8 days. Following RNA extraction and reverse transcription, copy numbers of *PINK1* (A) and *PARK2* (B) were determined using real-time qPCR and relative to 1000 copies of reference gene *β-actin*. Data presented as a mean ± SD, n=4-6, Student's t-test where, P>0.05

Therefore, there was no difference in the mRNA expression of the genes involved in mitochondrial life cycle, including fusion, fission and mitophagy.

5.4.3 The effect of hyperglycaemia on ROS production, viability and mitochondrial DNA damage in primary cultured human mesangial cells.

Since nuclear encoded mRNAs involved in the mitochondrial life cycle did not respond to hyperglycaemia in the time frame in which the MtDNA increase is seen, intracellular ROS, cell viability and MtDNA damage were examined. Briefly, HMCs were cultured in DMEM containing 5mM (NG) and 25mM (HG) glucose, as previously described. Following trypsinisation, cell pellets were collected and MtDNA damage was assessed using the PCR based elongase method (Furda et al., 2014) as described in the main methods chapter (2.12). Data were kindly provided by Ms Chandani Kiran Parsade. Intracellular ROS in cultured cells was measured using cell-permeant 2',7'-dichlorodihydrofluorescein diacetate (H2DCFDA) and viability by using Celltiter-Glo reagent in the microplate reader (as described in methods sections 2.10 and 2.11). Briefly, cells grown in different glucose concentrations were seeded in 96-well opaque plates. Viability assay detects number of viable cells, based on the luminescence signal proportional to the amount of ATP present, an indicator of metabolically active cells. For ROS measurement, on a day of the assessment, HMCs were treated with H_2DCFDA reagent and fluorescence signal from cleavage of the acetate groups by intracellular esterases was measured.

There was a significant increase in intracellular ROS in HMCs grown in HG for 4 (50% increase, $P<0.001$) and 8 days (30% increase, $P<0.01$, Fig.5.7). In parallel to the increased ROS, cell viability was significantly reduced by almost 2-fold in HMCs grown in high glucose after 4 days ($P<0.01$, Fig. 5.8).

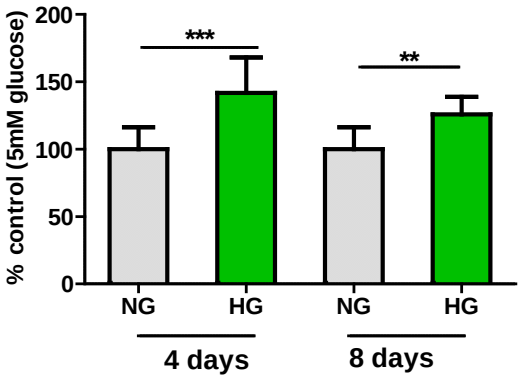

Fig.5.7. Hyperglycaemia induces cellular ROS in human mesangial cells. After being synchronized, HMCs were cultured in DMEM containing 5mM (NG) and 25mM (HG) glucose for 4 and 8 days. H_2DCFDA reagent was used to detect intracellular ROS by measurement of the fluorescence from cleavage of the acetate groups. Data presented as mean ± SD of % of control, n=14-18 observations, Student's t-test where, **P<0.01, ***P<0.001

,

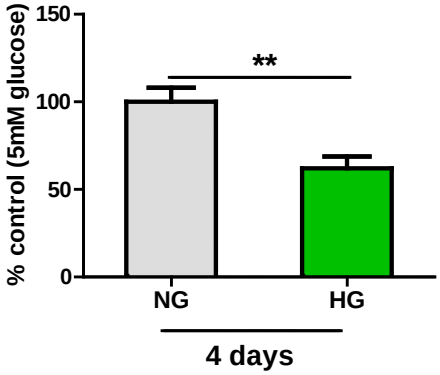

Fig.5.8. Hyperglycaemia decreases cell viability in human mesangial cells. After being synchronized, HMCs were cultured in DMEM containing 5mM (NG) and 25mM (HG) glucose for 4 days. CellTiter Glo luminescence reagent used to detect intracellular ATP as a measurement of metabolically active cells. Data presented as mean ± SD of % of control, n=17-21 observations, Student's t-test, where, **P<0.01

Increase in ROS and reduced viability in parallel with reduction in MtDNA transcription suggest that ROS might damage MtDNA. Therefore the next aim was to assess MtDNA damage in HMCs cultured in high glucose, by using a PCR based elongase method.

MtDNA damage was significantly increased in HMCs exposed to high glucose for 4 days (P<0.05 Fig.5.9) and increased by almost 2-fold after 8 days, although

8 day result was not significant, probably due to the low sample size (P>0.05, Fig.5.9).

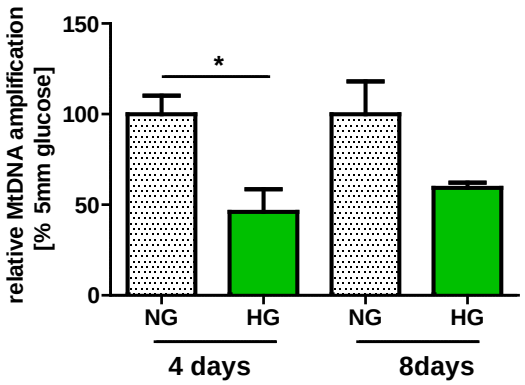

Fig.5.9. Hyperglycaemia-induced mitochondrial DNA damage in mesangial cells. After being synchronized, HMCs were cultured in DMEM containing 5mM (NG) and 25mM (HG) glucose for 4 and 8days. Long elongase PCR method was used to amplify 8.9kb and 127 fragment of MtDNA. Following agarose gel electrophoresis of the long and short fragments, bands intensity was measured and ratio calculated. Data presented as mean ± SD of % of control, n=3-6, Student's t-test, where, *P<0.05

The above data show that growth of HMCs in high glucose results in increased ROS and apoptosis, and in parallel increased damage to MtDNA.

5.4.4 Does high glucose activate inflammatory pathways in human mesangial cells?

HMCs were grown in normal and high glucose as previously described. Expression of the *NF-κB* and *MYD88* mRNAs was assessed using absolute quantification method and real-time qPCR and primers listed in table 2.4 in methods section. Both *NF-κB* and *MYD88* were significantly increased after 4 days of incubation in high glucose by almost two fold when compared to the control (0.21±0.01 vs. 0.73±0.08 and 0.52± 0.12 vs. 0.98±0.3 respectively, P<0.05, Fig.5.10.A, B).

8 days of exposure to high glucose also resulted in the increase of *NF-κB* and *MYD88* expression but result was not significant (0.13±0.03 vs. 0.80±0.6 and 0.67±0.4 vs. 1.37±0.9 respectively P>0.05, Fig.5.10A, B).

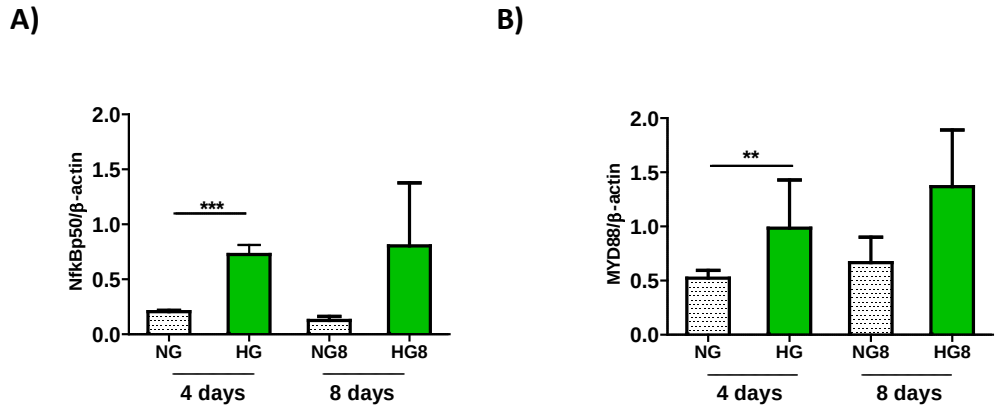

Fig.5.10. Hyperglycaemia-induced activation of toll like receptor 9 pathway. After being synchronized, HMCs were cultured in DMEM containing 5mM (NG) and 25mM (HG) glucose for 4 and 8days. Following RNA extraction and reverse transcription, copy numbers of Nf-kB (A) and MYD88 (B) were determined using real-time qPCR. mRNA copy numbers for each gene were determined relative to 1000 copies of reference gene β-actin. n=3, Student's t-test where, ***P<0.001, **P<0.01

5.4.5 Is mitochondrial protein mass affected by high glucose treatment in human mesangial cells?

Measurement of the mitochondrial OXPHOS protein levels in HMCs cultured in 5mM (NG) and 25mM (HG) for 4 and 8 days, was performed using Western blot method, as described in the main methods section 2.9. Briefly, following SDS-PAGE and a cocktail of primary antibodies against five different subunit of complex I-V (dilution 1:2000) were used to detect protein expression in HMCs cultured in different conditions. HRP conjugated anti-mouse secondary antibody (dilution 1:10000) was used to detect protein content via ECL method. Densitometry and ImageJ was used to quantify the expression levels of OXPHOS proteins, β-actin (dilution 1:5000) was used as a loading control.

As illustrated on Fig.5.11, there was no significant difference in the protein levels of any of the investigated complexes (P>0.05, n=3, Fig.5.11A-F).

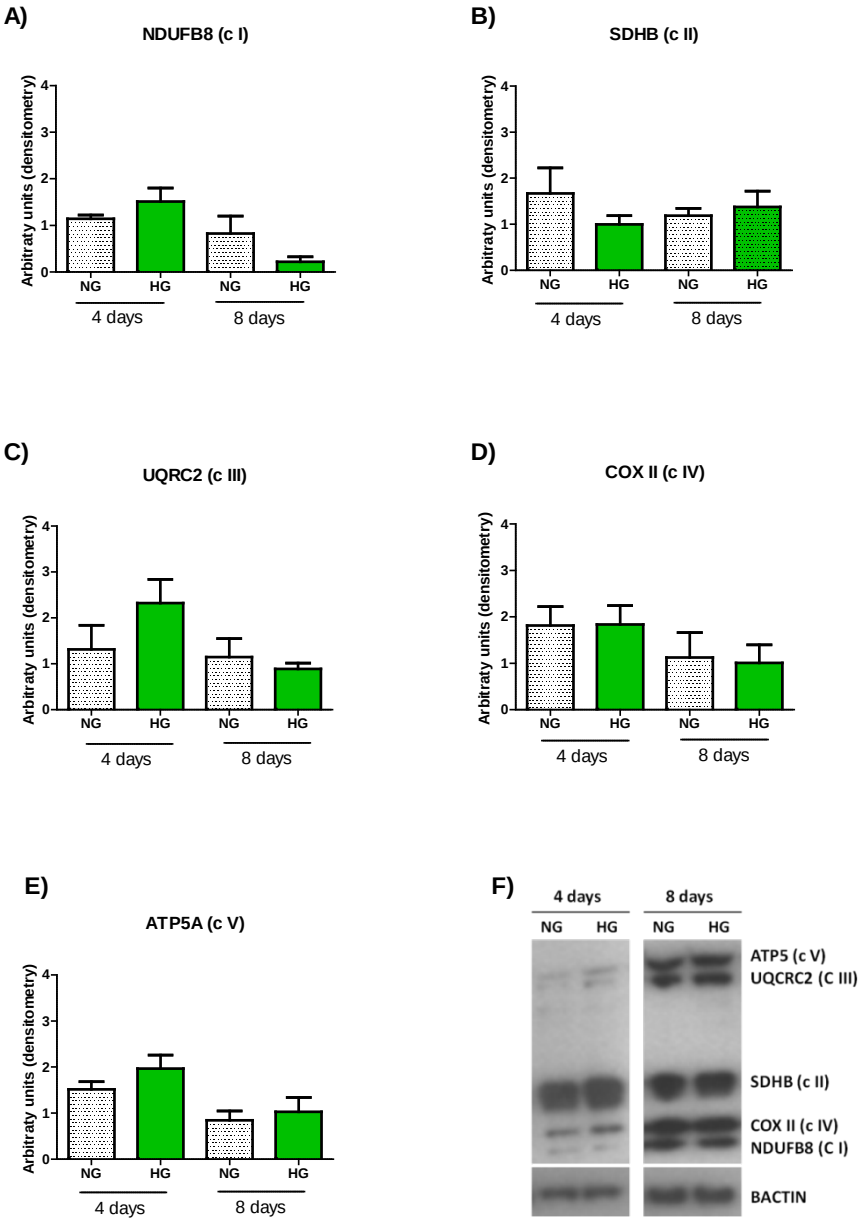

Fig.5.11. Mitochondrial protein content in human mesangial cells culture for 4 and 8 days. HMCs were incubated in DMEM containing 5mM glucose (NG) and 25mM glucose (HG) for the times shown. Western blotting of the mitochondrial respiratory complexes I–V in HMCS cultured in different conditions. Relative intensities of bands were quantified by densitometry and β-actin served as a loading control. CI, complex I (A); CII, complex II (B); CIII, complex III (C); CIV, complex IV (D); CV, complex V (E). Representative western blot (F). Data shown as mean ± SD, n=3, Independent student's t-test, where, P>0.5

5.4.6 The effect of hyperglycaemia on mitochondrial morphology and network in human mesangial cells

To visualise mitochondrial morphology, following culture in 5mM (NG) and 25mM (HG) glucose HMCs were fixed with paraformaldehyde and visualized by staining with Mitotracker Orange (as decribed in method section 2.9) and viewed under Nikon Eclipse Ti-E Inverted Microscope. The stained mitochondrial network was assessed using ImageJ software using an image-processing algorithm as described by Koopman at al. (Koopman et al., 2005). HMCs were incubated in high glucose for the times shown in Fig.5.12 and Fig.5.13. Culture time had no effect on mitochondrial morphology as shown in summary data shown on Fig.5.12, 1st and 2nd panel.

To quantify mitochondrial network and morphology, two different parameters, formfactor F, a measure of the length and degree of branching and the aspect ratio AR, a measure of mitochondrial length, were used. (Fig.5.13, Fig.5.14). In HMCs grown in normal glucose medium, mitochondria were visualised as long, tubular networks throughout the cytoplasm (Fig.5.12 two left panels, Fig.5.13 top panel). As illustrated on Fig.5.13 mitochondrial morphology and connection were not affected after short exposure to hyperglycaemia (2h), but extended exposure to hyperglycaemia (1-8 days) affected mitochondrial structure. More rounded and not connected mitochondria were visible after cells were cultured in high glucose for 8 days (Fig.5.13 left and middle panels). Plotting aspect ratio AF versus formfactor F clearly showed decreasing values for both parameters, correcting with increasing time of cells' exposure to HG (Fig.5.13 right panel).

When calculated individually, both formfactor F and aspect ratio AR were highly significantly down-regulated in HMCs after 24h of incubation in high glucose ($P<0.01$, Fig.5.14A, B). These results became ever more significant after 4 days of incubation in the high glucose ($P<0.001$, Fig.5.14A, B) and the values for both factors showed a progressive reduction with increased time of the high glucose exposure (Fig.5.14A, B).

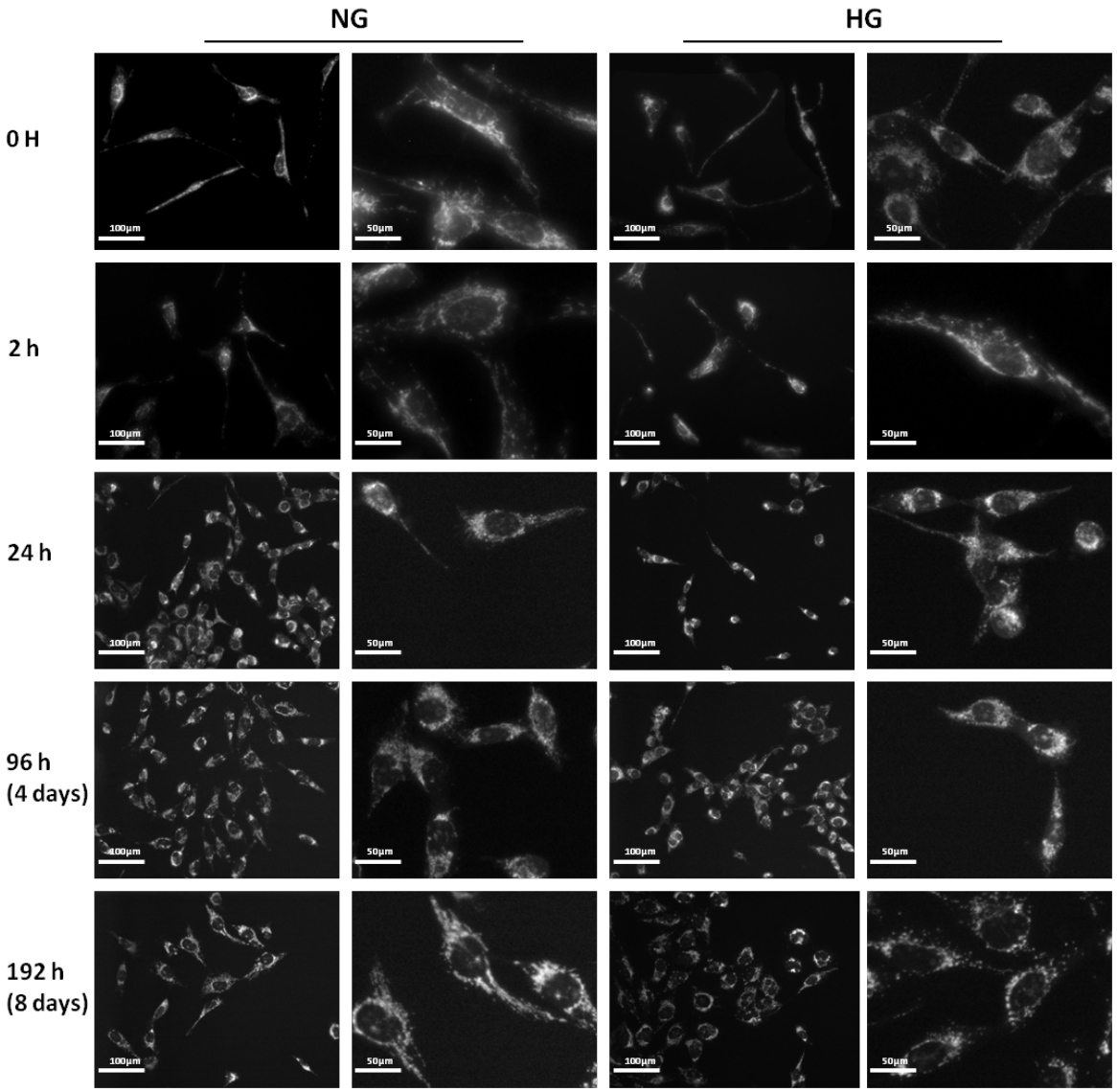

Fig.5.12. Mitochondrial morphology in mesangial cells incubated in high glucose. HMCs were cultured in 96-well plates in DMEM containing 5mM glucose (NG) and 25mM glucose (HG) for the times shown. Mitochondria were labelled with MitoTracker Orange CMXRos and images were captured at magnification x20. (A) Representative images of; time culture controls shown 1st and 2nd panel, cells cultured in Hg in 3rd and 4th panel. . Scale bar, 50µm and 100 µm.

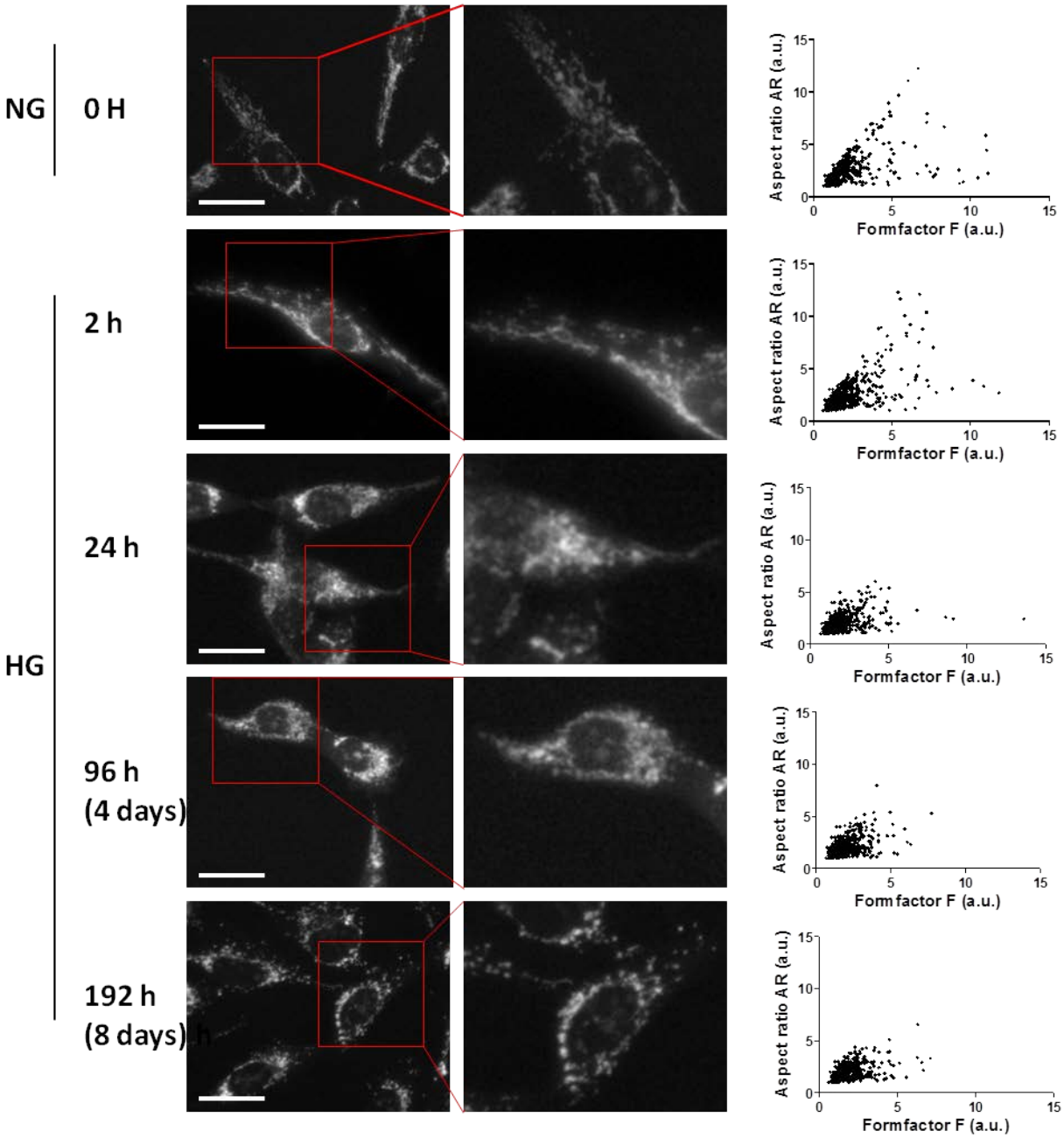

Fig.5.13. High glucose affects mitochondrial morphology in mesangial cells. HMCs were cultured in 96-well plates in 5mM glucose in DMEM containing (NG) and 25mM glucose (HG) for the times shown. Mitochondria were labelled with MitoTracker Red CMXRos and images were captured at magnification x20. (A) Representative images of each condition shown in left panel. Mitochondrial length (Aspect ratio -AR), was plotted against mitochondrial degree of branching (Formfactor F) and shown on the right panel as scatter plots. Data are presented as mean ±SEM, n=10-14 cells. Scale bar, 50µm

A)

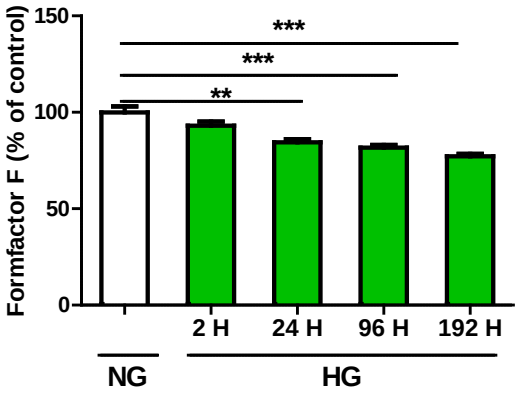

B)

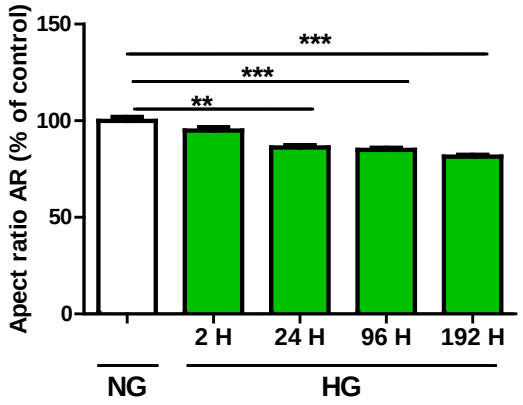

Fig.5.14. High glucose affects mitochondrial length and degree of branching. HMCs were cultured in 96-well plates in 5mM glucose (NG) and 25mM glucose (HG) for the times shown. Mitochondria were labelled with MitoTracker Red CMXRos and images were captured at magnification x20. Mitochondrial length (Aspect ratio -AR), was plotted against mitochondrial degree of branching (Formfactor F). Quantitative analysis of aspect ratio AR (% of the control) (A). Quantitative analysis of formfactor F (% of the control) (B). Data are presented as mean ±SEM, n=10-14 cells, Kruskal-Wallis with Dunn's post hoc test where, **P < 0.01; ***P <0.001

5.5 Discussion

A key finding of current study is the demonstration that although exposure to high glucose leads to a rapid increase in renal mesangial cell MtDNA (as shown in Chapter 3), this does not correlate with increased mitochondrial encoded mRNA transcripts or mitochondrial mass. In contrast a decrease/unchanged transcription of mitochondrial encoded mRNAs and little change in the nuclear encoded mitochondrial mRNAs in renal cells, with the exception of glucose induced up-regulation of *TFAM* mRNA was observed. There was no difference in mitochondrial complexes' protein content, but there was a change in mitochondrial network morphology with increased fragmentation occurring as early as 24 hours of the cells' exposure to high glucose. In parallel, there was an increase in MtDNA damage, increased ROS, decreased viability after 4 days of treatment with high glucose, these results correlated with the activation of TLR9 pathway.

When mitochondria are not meeting ATP demand , the number of mitochondria should eventually increase, as in the balanced environment MtDNA content is proportionate to mitochondrial genome transcription level with a dose dependent effect (Williams, 1986, Hock and Kralli, 2009). Result from mitochondrial encoded mRNAs experiment suggest, that although MtDNA is increased (as shown in chapter 3), it is not functional and there is a disconnect between MtDNA and the mitochondrial transcription/translation. A similar disconnect was reported in a study investigating the mechanisms of insulin resistance in muscle, with increased MtDNA but not increased mitochondrial content in myotubes (Aguer et al., 2013). Simultaneously Aguer et al., demonstrated increased MtDNA damage in parallel with reduced ATP levels (Aguer et al., 2013). Also, a report from Gao group (2010), demonstrates a disconnect in MtDNA replication and transcription in conditions of oxidative stress. Although no changes in DNA copy number in adipose cells cultured in high glucose and also in fatty acid conditions were reported, there was a change in mitochondrial morphology and reduced levels of mitochondrial transcription factors in response to oxidative stress (Gao et al., 2010). Ballinger et al., (2000)

reported decreased synthesis of mitochondrial proteins in vascular endothelial and smooth muscle cells caused by ROS in dose dependent manner, which supports our observation of no changes in the protein level (Ballinger et al., 2000). Xie et al., (2008) also showed a decrease in mitochondrial encoded OXPHOS subunit in human retinal cells following 6 h incubation in 30mM glucose (Xie et al., 2008b).

In the current study no changes in the expression levels with any of the mRNAs involved in mitochondrial life cycles were observed with the exception of the glucose induced up-regulation of *TFAM* mRNA, which has been previously reported in rat muscle cells (Choi et al., 2004). This is contrary to the report by Bonnard et al. (2008), in which diabetes-induced structural and functional changes in mitochondria were shown in parallel with reduction in both, MtDNA content, and protein expression of PGC-1α in mouse muscle tissue of two different mouse models of diabetes (Bonnard et al., 2008). However, Shrepper et al. (2012) reported decreased OXPHOS complex activities, which didn't correlate with any changes in mRNA expression of genes involved in mitochondria biogenesis (Schrepper et al., 2012). However, it has been shown using a transient over-expression of *TFAM* in cultured human embryonic kidney (HEK) cells, that only small increase of TFAM protein can have stimulatory effects on mitochondrial transcription, and high levels of TFAM have an inhibitory effect on the MtDNA transcription rate (Maniura-Weber et al., 2004), which might explain 8 days results with non significant changes in the MtDNA levels and mitochondrial transcription factors. No changes were observed in the nuclear encoded mitochondrial mRNAs in diabetic mouse kidney (data not shown), it might suggest there is a dys-regulation between nuclear and mitochondrial control of MtDNA replication (especially in STZ-induced mice), or possibly expression of the mitochondrial protein content should be measured, as both TFAM and PGC-1α mRNAs have been reported to have a short life time (Lai et al., 2010).

There were no significant changes in the mRNA expression of genes involved in mitochondrial life cycle in renal cells, but interestingly mitochondrial morphology

in renal cells exposed to high glucose changed very quickly, with more short, rounded mitochondria which start losing their network connection within 24 hours of the exposure to the high glucose. Change in the mitochondrial morphology after the exposure to high glucose also suggests a dysfunction in fusion and fission processes, which are necessary to sustain healthy mitochondria (Twig and Shirihai, 2011). Results from current study are in accordance with reports by Molina et al., (2009), where almost complete fragmentation of the mitochondrial network was shown in beta cells within 1 hour of exposure to 20mM glucose with 0.4mM palmitate (Molina et al., 2009) and by Trudeau group (2010), which has shown increased mitochondrial fragmentation in rat retinal cells incubated for 6 days in high glucose (Trudeau et al., 2010). Although most the studies suggest oxidative stress playing a major role in mitochondrial network and motility, publication by Nowak et al. (2003), reported persistent mitochondrial fragmentation in primary tubular cells which could not be abolished by the antioxidant treatment (Nowak et al., 2011). This loss in the connection between mitochondria might have a detrimental effect on mitochondria coping with increased oxidative stress, as during constant fusion and fission mitochondria can actively exchange MtDNA [reviewed in (Chen and Chan, 2009)]. In the current study increased ROS and significantly reduced cells viability was also observed in HMCs incubated in high glucose. These results have been previously reported in the mesangial cells (Al-Kafaji and Malik, 2010, Catherwood et al., 2002).

Moreover in the current report, MtDNA damage was also observed in cells incubated in high glucose. This result might explain the disconnection between MtDNA copy number and amount of mitochondrial encoded mRNA and suggest that most of the detected MtDNA molecules are not functional. MtDNA is very susceptible to damage due to its proximity to ETC (Ma et al., 2009). Publication of Xie et al.,(2008) has shown that in the human retinal cells, first signs of damage to MtDNA can occur within 3 hours and turn into severe changes after 2 days of the exposure to hyperglycaemia (Xie et al., 2008b).

I have also measured expression of the *NF-κB* mRNA as a marker of glucose-induced inflammation, which is known to be induced by hyperglycaemia in, *in-vivo* (Romeo et al., 2002), and *in-vitro* systems (Hattori et al., 2000).

Mitochondria per se can contribute to the systemic inflammation through direct increase and release of the MtDNA. MtDNA resemblance bacterial genome and therefore can be recognised as a pathogen molecule by the system through toll like receptors (TLRs) because it's un-methylated (Rutz et al., 2004). In the *in-vitro* study the expression of both, *NF-κB* and *MYD88*, as downstream signalling molecules of TLR-9 were examined. mRNAs expression of both *NF-κB* and *MYD88* were up-regulated in mesangial cells exposed to high glucose. As there was up-regulation of MtDNA, increased ROS production, decreased mitochondrial transcription and increased rate of the MtDNA damage, taken all together these data might support the theory of damaged MtDNA acting as a danger molecule which by escaping autophagy activates inflammatory pathways via TLKR-9 receptor (Oka et al., 2012).

One of the major limitations of this study is lack of the data from protein expression for each of the investigated mRNAs. Results from mitochondrial staining in HMCs implicate possible changes in mitochondrial proteins responsible for the fusion, fission and mitophagy.

In summary, in the current study we have observed functional changes in mitochondrial cycle following the exposure to high glucose, including induced intracellular ROS and damaged MtDNA, disconnection in mitochondrial transcription in translation (which may affect cellular response to oxidative stress) and also activation of the inflammatory pathways which may contribute further to the toxic effect of hyperglycaemia.

Chapter 6

Hyperglycaemia-induced changes in the bioenergetic profile of kidney cells

6.1 Abstract

Background/Aims: The hypothesis that will be tested in this thesis is that hyperglycaemia/high glucose can cause early changes in mitochondrial DNA (content/quality) and that these changes can contribute to mitochondrial dysfunction. In the current chapter mitochondrial respiration in renal cells exposed to high glucose was examined.

Methods: Primary cultured mesangial cells (HMCs) and tubular epithelial cell line (HK-2) were cultured in 5mM (normal) and 25mM (high) glucose and in 5mM glucose and 20mM mannitol (NGM) at various time points. Cellular bioenergetics was assessed in Seahorse XF^e96 analyzer in cells cultured in NG, HG, NGM and in HMCs and HK-2 cells subjected to the treatment with hydrogen peroxide and acute 20mM glucose treatments. Mitochondrial basal, ATP-linked and maximal respiration in parallel with proton leak and non-mitochondrial respiration were assessed. Moreover a reversal experiment was performed, where growth medium with HG was replaced with NG, and the effect of change of glucose concentration on mitochondrial respiration was measured.

Results: In HMCs cultured in high glucose, maximal respiration and reserve capacity did not change at 4 days, and were significantly reduced at 8 days ($P<0.05$) and at 12 days ($P<0.001$). No changes were seen at any of the time points in the NGM or in cells cultured in NG. No changes were also seen in glycolysis (ECAR) at 4, and 8 days of culture ($P>0.05$), but a significant decrease was observed at day 12 at basal level ($P<0.05$) and after the addition of oligomycin ($P<0.01$) in HMCs. In HK-2 cells, basal, ATP-linked and maximal respiration were significantly down-regulated as early as 4 days of culture in HG ($P<0.001$, $P<0.01$). Acute treatment of HK-2 with H_2O_2 caused a significant decrease in mitochondrial respiration ($P<0.05$) and in basal and oligomycin-induced glycolysis. Acute injection of 20mM glucose to HMCs, which were cultured in NG media, caused a 'metabolic switch' from OXPHOS respiration to the glycolysis but had no effect on cells pre-cultured in HG. Toxic effect of hyperglycaemia on cellular bioenergetics was reverted by correcting the glucose levels; however the outcome was dependent on the time of exposure of the cells to HG prior to media change.

Conclusion: Hyperglycaemia significantly reduced mitochondrial respiration in the HMCs and HK-2 cells. Tubular cells seem to be more sensitive with more profound changes on their OXPHOS function that mesangial cells. Toxic effect of hyperglycaemia in mitochondrial respiration can be reverted; however the result is dependent on the time of exposure. These results show that hyperglycaemia leads to the decrease in energy metabolism in renal cells by down-regulation of their respiratory function.

6.2 Introduction

It was shown in the Chapter 3 of this thesis, that MtDNA copy number was elevated in mesangial cells cultured in 25mM glucose. To my knowledge this is the first report showing increased MtDNA level in human mesangial cells in response to hyperglycaemia. The next question was related to mitochondrial function, and if changes which we observed on molecular level would correlate with altered mitochondrial respiration system. High glucose is known to be a contributing factor in the development of DN, and both clinical and experimental studies have shown, that high concentration of glucose inside the cells directly and indirectly activates a series of complex overlapping pathways. These include induction of oxidative stress and inflammatory responses, inhibition of antioxidant defence, formation of advanced glycation end products and activation of protein kinase C (Brownlee, 2005, Brownlee, 2001). There is also growing evidence that oxidative stress produced by dysfunctional mitochondria is a major contributor in the development of DN [reviewed in (Forbes et al., 2008, Sivitz and Yorek, 2010)].

Generation of reactive oxygen through metabolic processes leads to thickening of glomerular basement membrane, extracellular matrix accumulation in the mesangial cells and interstitial fibrosis which eventually will lead to kidney failure (Brownlee, 2005, Ha and Lee, 2003). Moreover glucose derived metabolites like pyruvate and NADH (created in the process of glycolysis), when transported to mitochondria for further utilization also contribute to ROS production. Pyruvate enters the mitochondrial membrane and after being metabolized, increases the ATP/ADP ratio consequently enhancing ROS/RNS formation. Increased levels of glucose and later pyruvate as a substrate may lead to increased oxidative phosphorylation, but this process is limited and can be ablated due to the changes in ETC caused by nutrient overload and toxic effect of superoxide ions which are produced as side effects of the OHPHOS system (Szabadkai and Duchen, 2009).

The differences in energy demand and the way cells respond to nutrient concentration could explain why changes observed in diabetic complication

mainly involve certain types of cells like retinal, endothelial, tubular, neuronal and mesangial cells (Brownlee, 2005). This process could occur primarily due to the fact that these cells cannot cope with increased levels of glucose which is not removed efficiently and therefore glucose piles up inside the cells. It has been shown that there are differences in energy demands between different organs and cell types within organs in the body. Kidneys are organs requiring large amounts of energy in form of ATP due to the re-absorption processes and although their mass account of less than 1% of total body mass, they use almost 10% of oxygen consumption which is then utilized in cellular respiration (Berg et al., 2002). Mercer et al., (2011) by using deep sequencing observed differences in the amount of each mitochondrial mRNA complexes between tissues and cells, with kidney mitochondrial mRNAs profiling showing one of the highest levels of mitochondrial transcripts, after colon, muscle and heart (Mercer et al., 2011). This data is not surprising, as eukaryotic cells, especially the ones with high energy demands rely mostly on ATP generated through OXPHOS, which is 15 times more productive than the amount produced by aerobic glycolysis (Alberts et al., 2002). In the kidney, during the filtration processes glucose is re-absorbed from plasma and actively co-transported with help of NA^+/K^+ pumps which require constant source of ATP (Vallon, 2011). Moreover, different cells have different amount of mitochondrial transporters, with kidney proximal tubules mitochondria containing more types of transporters than other cell types especially with higher glutamate transporter levels, necessary in glutamine metabolism and formation and excretion of ammonia (Schoolwerth and LaNoue, 1985).

In the current study, I investigated two types of kidney cells involved in the development of DN, primary mesangial cells and transformed proximal tubular cells. Both cell types are known to mostly use ATP through their OXPHOS system and proximal tubules are also known to have limited anaerobic glycolytic capacity (Wirthensohn and Guder, 1986).

The current methodology used to measure mitochondrial function includes a variety of techniques including measurement of: mitochondrial physiology

(measurement of OXPHOS enzymes activity (Fernandez-Vizarra et al., 2011), assessment of proteins via western blotting (Sheng et al., 2012), northern blot analysis (Veltri et al., 1990), mitochondrial network structure via electron or fluorescent microscopy (Medeiros, 2008, Rodriguez-Enriquez et al., 2009) and also measurement of the oxygen consumption rate (Silva and Oliveira, 2012, Perry et al., 2013). The idea of the measurement of oxygen consumption as an indicator of mitochondrial health emerged from Clark oxygen electrode method. Clark electrode, developed by Leland Clark, enables accurate measurement of changes in oxygen levels present in the solution after the addition of mitochondrial extract mixture and mitochondrial activators and inhibitors (Silva and Oliveira, 2012, Clark et al., 1953). Although accurate, this technique requires optimisation and is not suitable for high throughput assessments. The need of high throughput and standardise method to measure mitochondrial function, which could also be used directly on patient cells, lead to the development of extracellular flux analyzers like Seahorse XF analyzer (Ferrick et al., 2008).

Due to allowing more experimental replicates and smaller samples sizes for analysis, Seahorse XF analyzer became a more popular method for the assessment of mitochondrial function in many samples including cell culture, whole mitochondria extracts (Brand and Nicholls, 2011), and also patients' peripheral blood mononuclear cells (PBMCs) for a direct a quick measurement of mitochondrial respiration (function) in healthy and disease state (Chacko et al., 2013, Shikuma et al., 2008, Caimari et al., 2010). By utilizing plate system and fibre optic probes, Seahorse technology assess the levels of O_2 and H^+ ions in 2-7µl micro chamber created over the monolayer of cells. Two different probes allow simultaneous measurement of two aspects of mitochondrial bioenergetics: oxidative phosphorylation /oxygen consumption rate (OCR) and extracellular acidification rate /amount of H^+ ions (ECAR) in intact cells in a plate format (Ferrick et al., 2008, Brand and Nicholls, 2011).

The Seahorse analyzer allows measurement of the oxygen consumption from fundamental parameters of mitochondrial function: mitochondrial respiration (basal, maximal and ATP-linked respiration), glycolysis, and non-mitochondrial

respiration. In order to assess these factors cells are injected with mitochondrial respiration inhibitors and uncoupler such as oligomycin, antimycin A, rotenone and FCCP (Carbonyl cyanide-4 (trifluoromethoxy) phenylhydrazone) (Fig.6.1.). Oligomycin (ATP synthase blocker) is used to observe ATP turnover and to determine if there is any difference in proton leak. In oxidative phosphorylation research, it is used to prevent state 3 respiration. Oligomycin inhibits ATP synthase (complex V) by blocking its proton channel (F_0 subunit), which is necessary for oxidative phosphorylation of ADP to ATP (Brand and Nicholls, 2011). The inhibition of the ATP synthesis by oligomycin will significantly reduce electron flow through the ETC; however, electron flow will not be stopped completely due to a process known as proton leak or mitochondrial uncoupling. This process is due to the facilitated diffusion of protons into the mitochondrial matrix through UCPs (uncoupling proteins) (Affourtit and Brand, 2008). After blocking ATP production through the OXPHOS system, cells tend to switch to glycolysis to balance their ATP levels. FCCP (mitochondrial uncoupler) is used to measure maximum respiratory function. It is called an uncoupling agent because it disrupts ATP synthesis by transporting hydrogen ions through a cell membrane against proton gradient (Schraufstatter et al., 1985). Rotenone (inhibitor of mitochondrial complex I) and antimycin A (blocker of ubiquinol phosphorylation) are used to completely shut mitochondrial respiration down to prove the changes in respiration were mainly in mitochondria. Use of these inhibitors gives us also indication of non-mitochondrial respiration, term used to asses amount of oxygen used by cellular oxidases, like NADPH dependent oxidases (Brand and Nicholls, 2011).

To date there are no published reports describing cellular bioenergetics of human renal cells after the exposure to hyperglycaemia. Published poster data from Chacko et al., (2010) reported down-regulation of the mitochondrial function in primary mouse mesangial cells exposed to hyperglycaemia for 14 days (Chacko et al., 2010a). There are however reports about different cells types in response to hyperglycaemia, Trudeau at al., (2010) assessed mitochondrial bioenergetics in rat retinal endothelial cells cultured for 3 and 6 days in 30mM glucose and also observed a decline in mitochondrial function. In

contrary, Fink at al., (2012) did not observed any changes in the bovine aortic endothelial cells and human platelets cultured in high glucose for 18 hours (Fink et al., 2012).

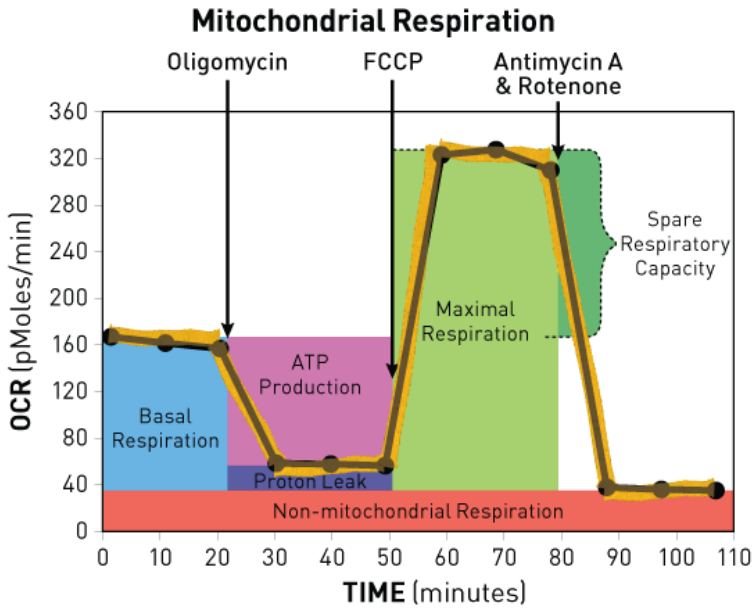

Fig.6.1. Key parameters of mitochondrial function measured by seahorse flux analyzer. The main parameters measured by using cell XF mito stress test kit are: basal respiration, ATP turnover, proton leak, maximal respiration and reserve capacity. In order to assess these factors cells are injected with mitochondrial respiration inhibitors and uncoupler such as oligomycin, antimycin A, rotenone and FCCP. Taken from (SeahorseBioscience, 2014).

6.3 Hypothesis and aims

6.3.1 Hypothesis

The main hypothesis under study in this work is that high glucose can cause early changes in mitochondrial DNA (content/quality) and that these changes can contribute to mitochondrial dysfunction. In the current chapter the mitochondrial respiration was investigated in primary cultured renal mesangial cells.

6.3.2 Aims and objectives

The main aim of this chapter was to demonstrate using cultured renal cells whether glucose-induced changes in MtDNA occur in parallel with altered mitochondrial respiration in renal cells.

This aim will be met as follows:

1. The effect of hyperglycaemia on the bioenergetic profile in the renal cells will be measured.
2. The effect of acute glucose load on the on mitochondrial respiration in renal cells will be determined.
3. The effect of acute oxidative stress on the mitochondrial respiration in renal cells will be determined.
4. The effect of the reversing of the glucose concentration on mitochondrial bioenergetic profile will be evaluated in renal cells.

The experimental strategy to carry out the above will be as follows:

1. Two different renal cell types will be used, primary cultured mesangial cells (HMCs) and immortalized proximal tubular cells (HK-2) cells
2. Cells will be cultured in 5mM (normal, NG) and 25mM (high, HG) glucose, for various time points. 20mM mannitol in 5mM glucose (Man) will be used as an osmolarity control.
3. Bioenergetic profile will be assessed by using a Seahorse XF^e96 analyzer

4. To measure acute effect of high glucose on mitochondrial respiration 20mM glucose will be injected during respiration assessment.
5. To determine effect of direct oxidative stress on metabolic profile of renal cells, HMCs and HK-2 will be treated with 1µM or 5µM H_2O_2 for 15 min prior the respiration assessment.

6.4 Results

In this chapter we investigated changes in bioenergetic profiles in human renal cells cultured under normal (5mM) and high (25mM) glucose. 5mM glucose plus 20mM mannitol was used as an osmotic control (Man).

Two different types of human renal cells were used, transformed tubular cells (HK-2) and primary cultured mesangial cells (HMCs). A simplified overview of the content of this chapter is shown below (Fig.6.2).

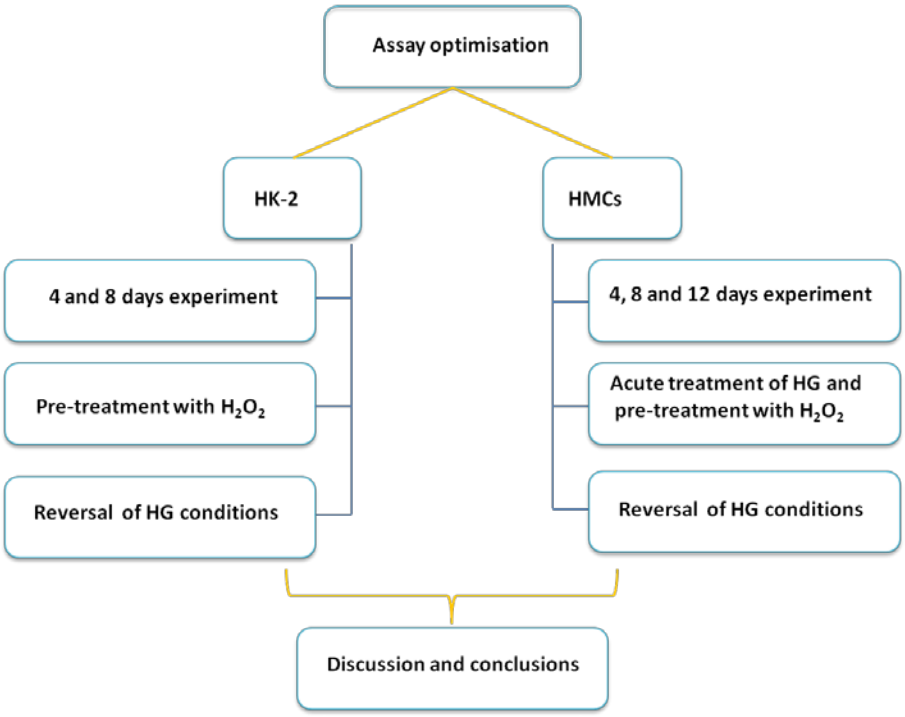

Fig.6.2. Overview of results in chapter 6.

6.4.1 Cell XF mito stress test assay optimization.

In order to define optimal conditions for the use of 'XF cell mito stress test' kit with human primary mesangial and transformed tubular cells, a series of optimization experiments were performed. The parameters which were tested included: a) cell density, b) concentration of ATP-synthase blocker-Oligomycin, c) concentration of mitochondrial uncoupler- FCCP. Rotenone and antimycin A are mitochondrial respiration blockers and usually do not require optimization, in these series of experiments optimal 0.5µM final concentrations were used.

First, a titration experiment with different cell seeding density was performed. Cells were trypsinized and counted using Countess Cell counter. Human primary mesangial cells (HMCs) and human transformed tubular cells (HK-2) were re-suspended at different densities (ranging from 10 000 to 40 000 cells) in 80µl of complete growth media and seeded in assay plates 24 h prior to OCR assessment. On the day of the assessment, media was changed to assay media containing 5mM glucose and 1mM sodium pyruvate, and basal OCR for both cell types were assessed using Seahorse XF^e96 analyzer. Optimal cell density was evaluated based on the OCR values (200-350 pmol/min are considered optimal). As expected there were a significant differences in the OCR values depended on cell density, e.g. 10 000 and 15 000 of cells gave very low reading of basal OCR for both, HMCs (OCR: 55-94 pmol/min) and HK-2 cells (OCR: 50-94 pmol/min) (Fig.6.3). With increasing number of cells an increase in basal OCR was observed. For HMCs optimal cell number based on OCR readings (225-311 pmol/min) was assessed in the range of 25-40 000 cells and 35 000 of cells/ well was chosen (Fig.6.3.A). For HK-2 cells, 20-40 00 cells/ well gave optimal OCR reading (180-270 pmol/min) and 25 000 cells/ well was chosen (Fig.6.3.B). Higher number of cells caused cell detachment during the washing steps, and this occurrence was observed in both HMCs and HK-2 cells.

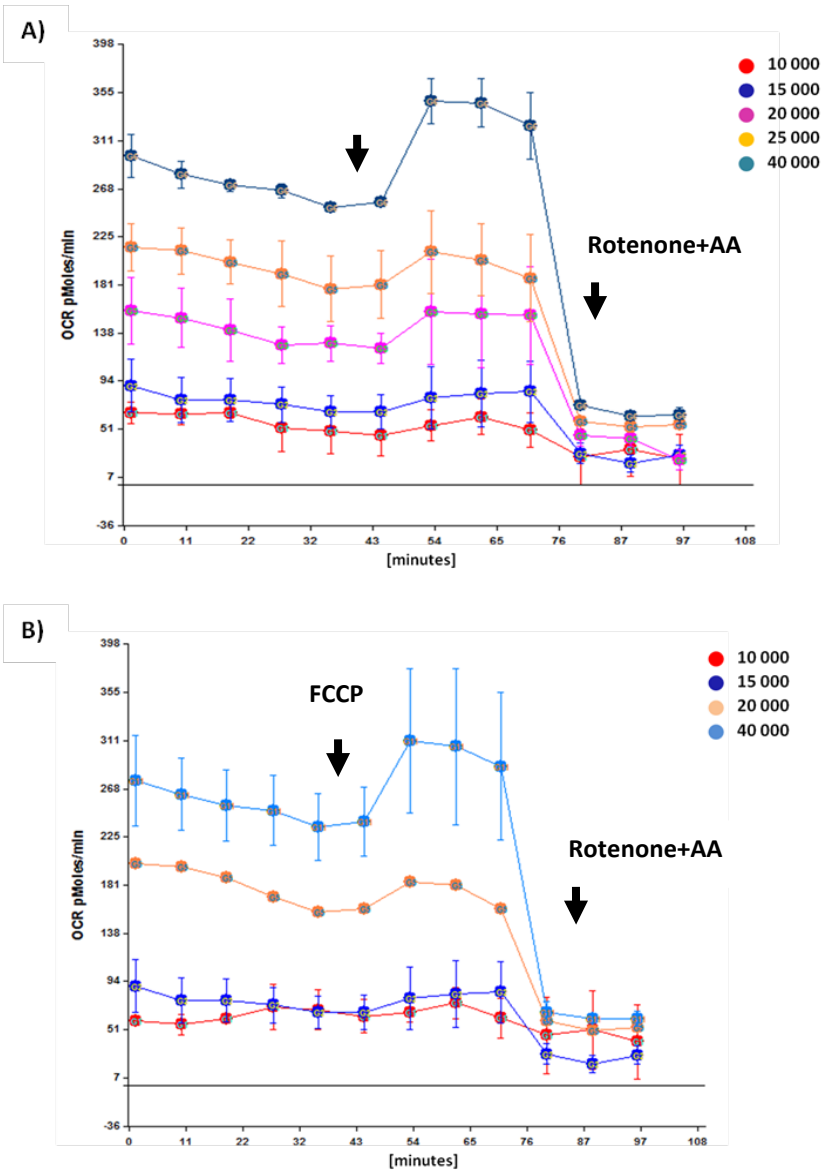

Fig.6.3. Optimization of the cell number. Basal respiration in absolute rates (OCR in pmoles/min) was assessed in: (A) HMCs, harvested from the same culture flask, and seeded at five different densities, (B) HK-2 cells, harvested from the same culture flask, and seeded ad four different densities, as shown on the individual panels on the right. Six measurement of basal respiration were taken, followed by an injection of oligomycin (1µM final). To assess maximal respiration, FCCP was injection at the 0.5µM working concentration. Rotenone and Antimycin A(AA) were injected to completely bloc mitochondrial respiration. OCR show increasing absolute rates with increased cell density. Data shown as a mean ±SD, n=6 observations

Cell seeding density directly impacts not only absolute rates, but also concentration of the injected compounds. Therefore, after estimation of the seeding density, series of the experiments were performed using different

concentration of mitochondrial uncoupler and blockers. Figure 6.4 represents optimization data for oligomycin for HMCs (A) and HK-2 cells (B). HMCs and HK-2 cells were harvested and seeded at same density overnight (35 000 and 25 000 cells/ well respectively). On the day of the experiment growth media was changed to assay media (as described previously) and absolute rate (OCR) were assessed. Oligomycin, ATP synthase blocker, causes drop in respiration trace, which gives an indication of amount of oxygen used for ATP production. Oligomycin was loaded and injected at three different concentrations (n=6 for each concentration), and drop in oxygen consumption was assessed as an indicator of drug concentration efficiency. After injection of 0.3µM and 0.6µM of oligomycin, there was observed a decline in OCR, however the response wasn't rapid for both, HMCs (Figure 6.2 A) and HK-2 cells (Fig.6.4 B). 1µM of oligomycin proved to be sufficient to block ATP-synthase within 3 minutes from injection, giving a nice slope for ATP calculation for both HMCs and HK-2 cells (Fig.6.4 A, B).

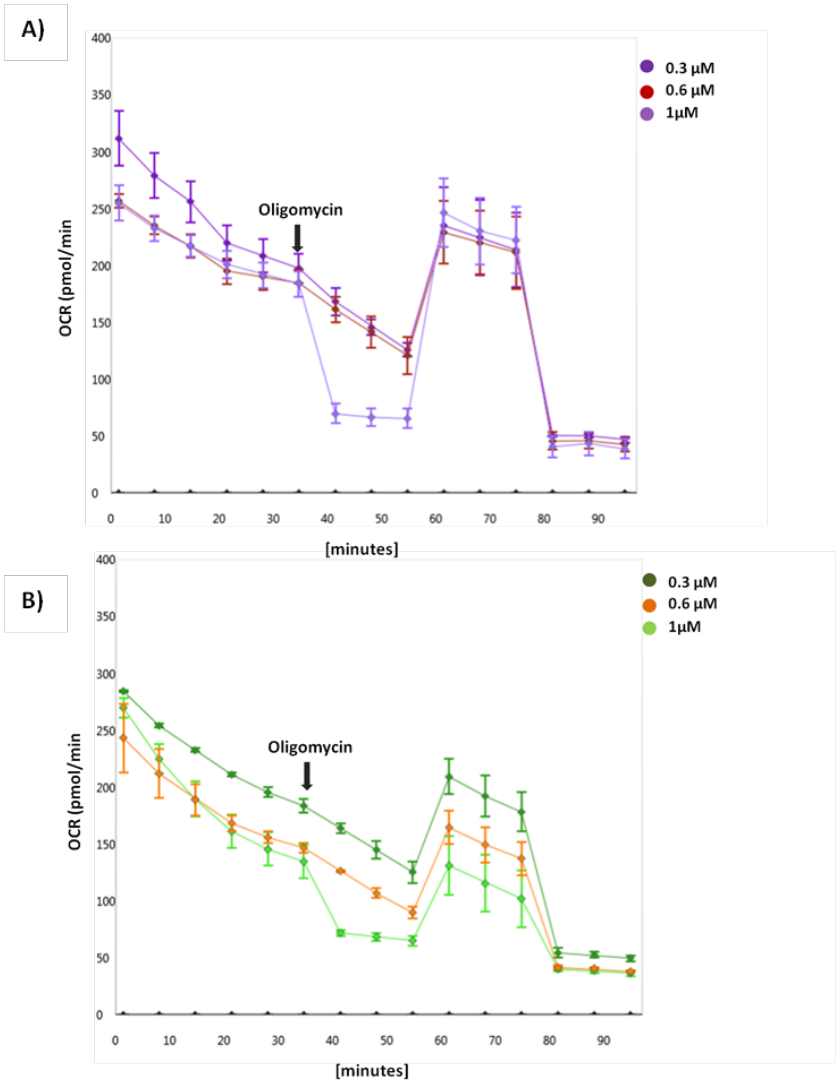

Fig.6.4. Optimization of the oligomycin concentration. Basal respiration in absolute rates (OCR in pmoles/min) was assessed in Seahorse analyzer in: (A) HMCs, (B) HK-2 cells. Cells were seeded at the same density within one plate and six measurement of basal respiration were taken, followed by a three different injections of oligomycin (0.3-1µM final concentration). OCR shows a decline in absolute rates with increased oligomycin concentration. Data presented as a mean ±SD, n=6 observations

In the final set of the optimization experiments, the concentration of the FCCP, which is an ETC accelerator, was estimated. Figures 6.5 and 6.6 represents graphic optimization data for FCCP for HMCs (Fig.6.5A and 6.6A) and HK-2 cells (Fig.6.5B and 6.6.B). Cells harvested from the same flask were seeded at the same density overnight (35 000 and 25 000cells/well respectively). On a day of experiment growth media was changed to assay media (as described above) and absolute rate (OCR) were assessed. When FCCP is injected to the wells, it

disrupts mitochondrial membrane potential by bringing protons ions inside the mitochondria against the proton pump. This causes mitochondrial uncoupling and increase in OCR. FCCP was loaded and injected at six different concentrations (n=6 for each concentration), and maximal respiration (maximal increase in oxygen consumption) was assessed. OCR values rose with increasing low concentrations of FCCP (0.15µM and 0.3µM), but after reaching the peak, it declined with higher concentrations of the FCCP, in both HMCs and HK-2 cells (Fig. 6.5A, B).

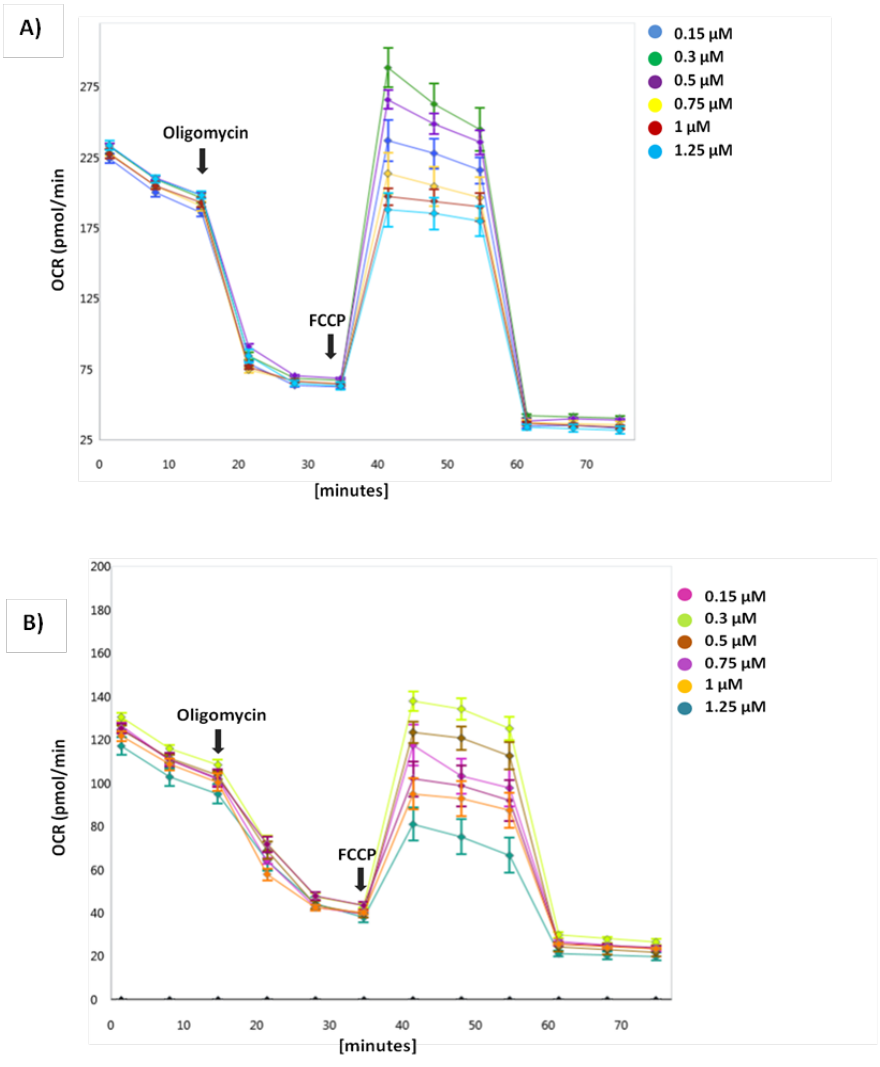

Fig.6.5. Optimization of FCCP concentration. Basal respiration in absolute rates (OCR in pmoles/min) was assessed in: (A) HMCs, (B) HK-2 cells. Cells were seeded at the same density within one plate and OCR was assessed in Seahorse analyzer. Three measurement of basal respiration were taken, followed by an injection of oligomycin (1uM final). To assess optimal concentration of FCCP, cells were next injected with six different concentration of FCCP, ranging from 0.15 -1.25µM (colours corresponding to different concentrations of FCCP shown on the legend on the right upper corner). Data shown as a mean ±SD, n=6 observations

As ETC accelerator is the most sensitive compound in the kit to concentration changes, and high concentration proved to be toxic to the cells, it is really important to assess correct concentration peak. Therefore, maximal respiration rates obtained in the experiment shown in the figure 6.5.A and 6.5.B were calculated as a % maximal OCR and plotted against different concentration of FCCP in µM. 0.3µM final concentration of FCCP caused 40% increase in OCR in both HMCs (Fig.6.6 A) and HK-2 cells (Fig.6.6 B). Additional increase in FCCP concentration did not result in increase but conversely in a decline of OCR.

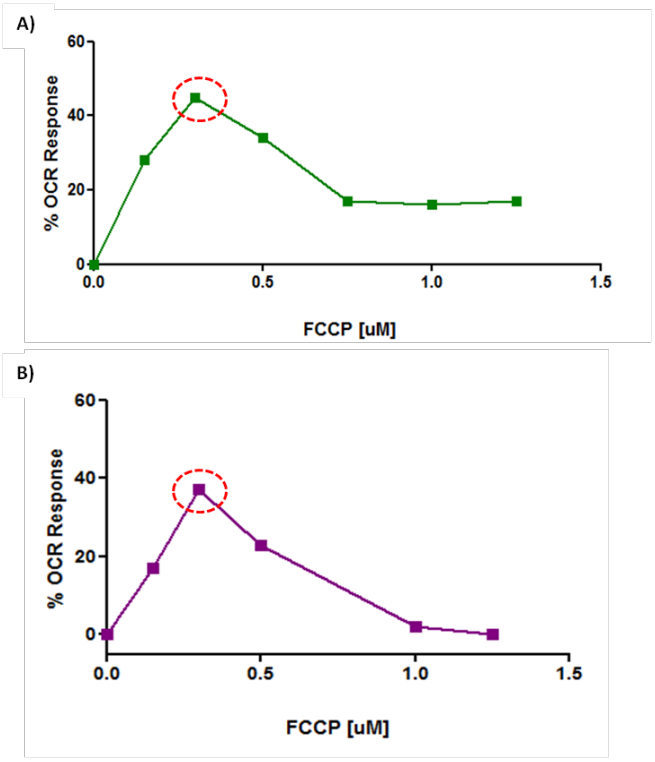

Fig.6.6. FCCP dose response. Cells were seeded at the same density within one plate and maximal OCR dependent on FCCP concentration was assessed in Seahorse analyzer, in HMCs (A) and HK-2 cells (B). OCR values rose with increasing low concentrations of FCCP, peak optimal concentration is highlighted by dotted red circle. Data were plotted as % of basal respiration, n=6

6.4.2 Bioenergetic profile of human primary mesangial cells in normal and high glucose

HMCs were grown in 5mM (NG), 25mM (HG) and 5mM glucose [plus 20mM mannitol (NGM) for 4, 8 and 12 days and determination of OCR and ECAR in real-time was measured by using XF flux analyzer (Seahorse bioscience). Cell seeding

density and mitochondrial inhibitors concentration had been determined in a series of optimization experiments (as shown above). Oligomycin, FCCP, rotenone and antimycin A were injected sequentially through ports in the XF Assay cartridges to final concentrations of 1µM, 0.3µM, 0.5µM and 0.5µM respectively. Upon completion of the experimental run, assay media was removed and cells were treated with 20µl of lysis buffer (content of the buffer is shown in the methods section 2.13) for normalization purposes, therefore all values are presented as pmoles O_2/ min/µg protein.

- *Bioenergetic profile of human mesangial cells cultured in high glucose for 4 days*

After 4 days of culture in NG, HG and NGM, there was no difference in any of the assessed parameters (Fig.6.7 and 6.13). Basal respiration of HMCs cultured in NG and HG was around 250 pmoles/min/µg protein (Fig.6.7). Following the injection of oligomycin there was a 60% decline in OCR in all conditions and it did not differ significantly between treatments (Fig. 6.7 and 6.13.B). Maximal respiration measured after the injection of FCCP resulted in approximately 40% increase in respiration (from 250 to ~ 360 pmoles/min µg/protein) in cells grown in NG, HG and NGM (Fig.6.7 and 6.13C). No significant difference in reserve capacity was observed (Fig.6.7 and 6.13D). There was no difference in proton leak (Fig.6.13E); and although non-mitochondrial respiration was reduced in cells cultured in HG (56 ± 19) when compared to control (39.6 ± 8), it was not statistically significant ($P>0.05$, Fig.6.13F).

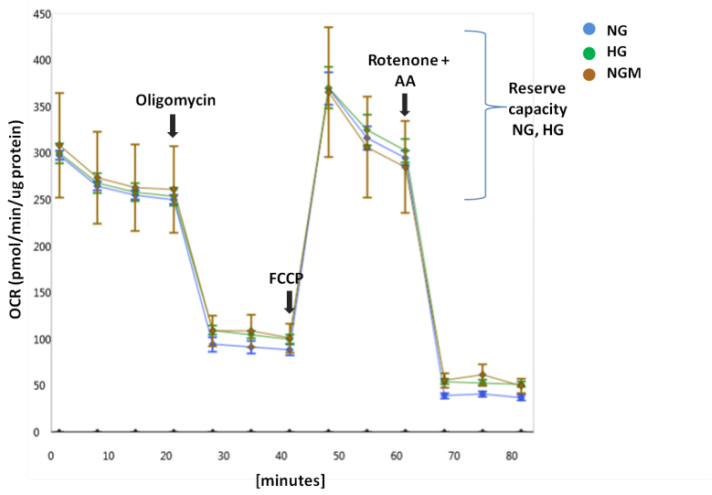

Fig.6.7. Bioenergetic profile of human mesnagial cells cultured in different conditions for 4 days. HMCs were grown in DMEM containing 5mM (NG), 25mM (HG) and 5mM glucose plus 20mM mannitol (NGM) for 3 days. Day before the assessment, cells were trypsinized, counted and seeded at density of 35 000 cells/well in different media. Following media change, OCR was assessed in seahorse analyzer. Four measurement of basal respiration were taken, followed by an injection of oligomycin (1µM final). To assess maximal respiration, FCCP was injection at the 0.3µM working concentration. Reserve capacity, measured as a difference between maximal and basal respiration, is presented via brackets. Data shown as a mean ±SD, n=6-7 observations

No difference in glycolysis (ECAR) based on the measurement of the concentration of protons released into media was observed (Fig.6.8 and Fig.6.14A). The osmotic control- NGM showed a similar bioenergetic profile to that observed for NG and HG.

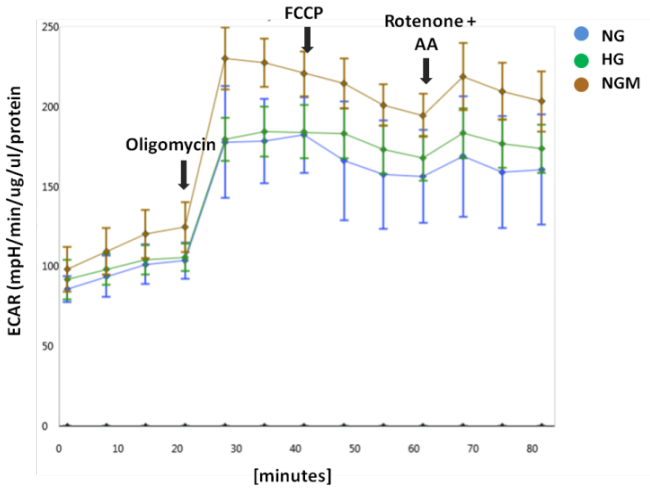

Fig.6.8. Glycolytic profile of human mesangial cells cultured in different conditions for 4 days. HMCs were grown in 5mM (NG), 25mM (HG) and 5mM glucose plus 20mM mannitol (NGM) for 3 days. Day before the assessment, cells were trypsinized, counted and seeded at density of 35 000 cells/well in different media. Following media change, ECAR was assessed in Seahorse XF96e analyzer. Data shown as a mean ±SD, n=6-7.

- *Bioenergetic profile of human mesangial cells cultured in high glucose for 8 days*

In HMCs cultured for 8 days in NG, HG and Man, there was a slight decline in basal respiration in cells cultured under HG when compared to the NG control (260 ± 21 vs. 272 ± 14 respectively), but the difference was not significant (P>0.05, Fig 6.9 and 6.13A). ATP-linked respiration did not differ between treatments and proton leak and non-mitochondrial respiration remain the same in cells cultured in NG, HG or in NGM (P>0.05, Fig. 6.13B and 6.13E-F respectively). Although no changes were observed in basal respiration and respiration used for ATP turnover, cells grown in 25mM glucose had significantly decreased maximal respiration when compared to the controls (375±24 vs. 415±3, respectively, P<0.05, Fig.6.9 and Fig. 6.13C). Reserve capacity, calculated as a maximal minus basal respiration, was also significantly reduced (by 20%) in HMCs after 8 days of culture in HG (P<0.05, Fig. 6.9 and Fig.6.13D).

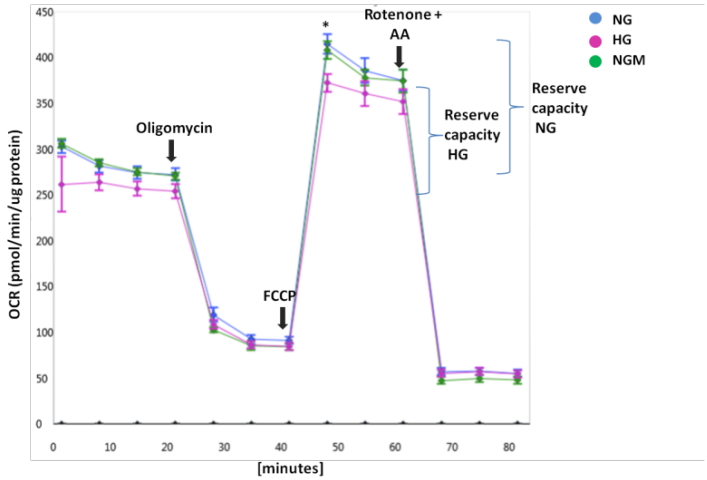

Fig.6.9. Bioenergetic profile of human mesangial cells grown in different conditions for 8 days. HMCs were grown in 5mM (NG), 25mM (HG) and 5mM glucose plus 20mM mannitol (NGM) for 7 days. Day before the assessment, cells were trypsinized, counted and seeded at density of 35 000 cells/well in different media. Following media change, OCR was assessed in Seahorse analyzer. Four measurement of basal respiration were taken, followed by an injection of oligomycin (1µM final). To assess maximal respiration, FCCP was injection at the 0.3µM working concentration. Reserve capacity, measured as a difference between maximal and basal respiration, is presented via brackets. Data shown as a mean ±SD, n=8 observations

No statistically significant difference in ECAR based on measurement of the concentration of protons released into media was observed at basal level or after the injection of oligomycin (Fig.6.10 and 6.14B, P>0.05). Mannitol had no effect on OCR or ECAR (Fig.6.9 and Fig.6.10, P>0.05).

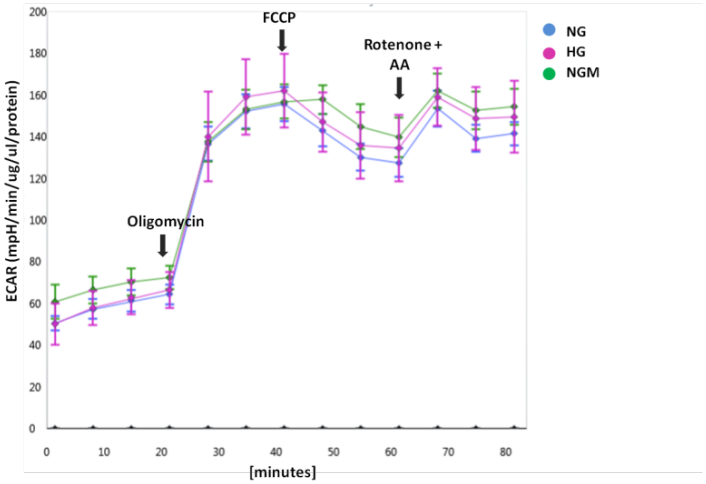

Fig.6.10. Glycolytic profile of human mesangial cells cultured in different conditions for 8 days. HMCs were grown in 5mM (NG), 25mM (HG) and in 5mM glucose plus 20mM mannitol (NGM) for 7 days. Day before the assessment, cells were trypsinized, counted and seeded at density of 35 000 cells/well in different media. Following media change, ECAR (glycolysis) was assessed in Seahorse analyzer. Data shown as a mean ±SD, n=8 observations

- *Bioenergetic profile of human primary mesangial cell cultured in high glucose for 12 days*

Chronic, 12-day exposure to HG glucose decreased basal oxygen consumption in HMCs by more than 50% when compared to control (226±11 vs. 111±4 respectively, P<0.0001 Fig.6.11 and 6.13A). After the injection of oligomycin, cells cultured in HG had their ATP levels reduced by 2.5 fold when compared to cells cultured in NG (151±20 vs. 60±18 respectively, P<0.0001, Fig.6.11 and Fig.6.13B). There was no difference in proton leak and in non-mitochondrial respiration (P>0.05, Fig.6.11 and Fig.6.13E, F). As described previously, maximal respiratory capacity of cells after injection of FCCP, was significantly lower in the cells cultured for 8 days in HG when compared to the controls, and this reduction became highly significant (P<0.0001) after 12 days of culture in HG, with 3 fold

reduction of maximal OCR when compared to the controls (128±29 vs. 365±47 respectively, P<0.0001, Fig.6.11 and Fig.6.13C). There was also a 4 fold reduction in reserve capacity in cells grown in HG after 12 days when compared to cells cultured in NG (47±35 vs. 185±23 respectively, P<0.0001, P<0.001, Fig.6.11 and Fig.6.13D).

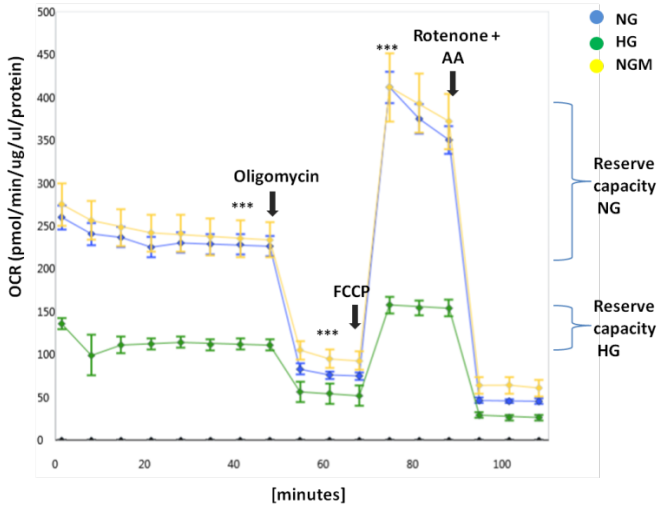

Fig.6.11. High glucose affects bioenergetic profile of human mesangial cells after 12 days of culture. HMCs were grown in 5mM (NG), 25mM (HG) and in 5mM glucose plus 20mM mannitol (NGM) for 11 days. Day before the assessment, cells were trypsinized, counted and seeded at density of 35 000 cells/well in different media. Following media change, OCR was assessed in Seahorse analyzer. Four measurement of basal respiration were taken, followed by an injection of oligomycin (1µM final). To assess maximal respiration, FCCP was injection at the 0.3µM working concentration. Reserve capacity, measured as a difference between maximal and basal respiration, is shown on the right. Data shown as a mean ±SD, n=8 observations

When glycolysis was assessed in these cells, there was a significant reduction in glycolysis at basal level (P<0.05) and also after the addition of oligomycin (which stimulates glycolysis due to inhibition of ATP synthesis) (P<0.01, Fig. 6.12 and Fig. 6.14C).

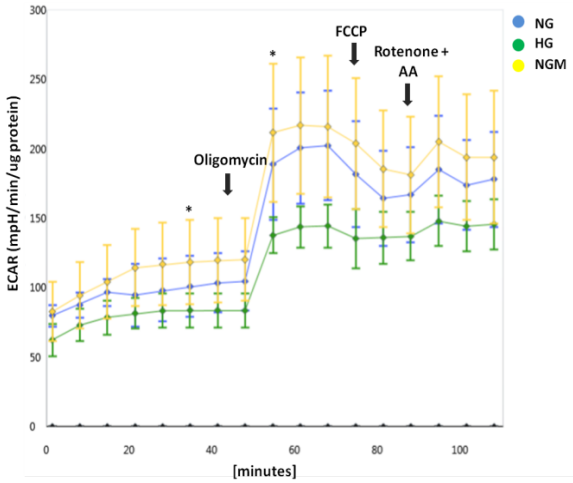

Fig.6.12. Glycolytic profile of human mesangial cells cultured in different conditions for 12 days. ECAR (glycolysis) was assessed in the Seahorse XF^{e}96 analyzer. Data shown as a mean ±SD, n=8 observations

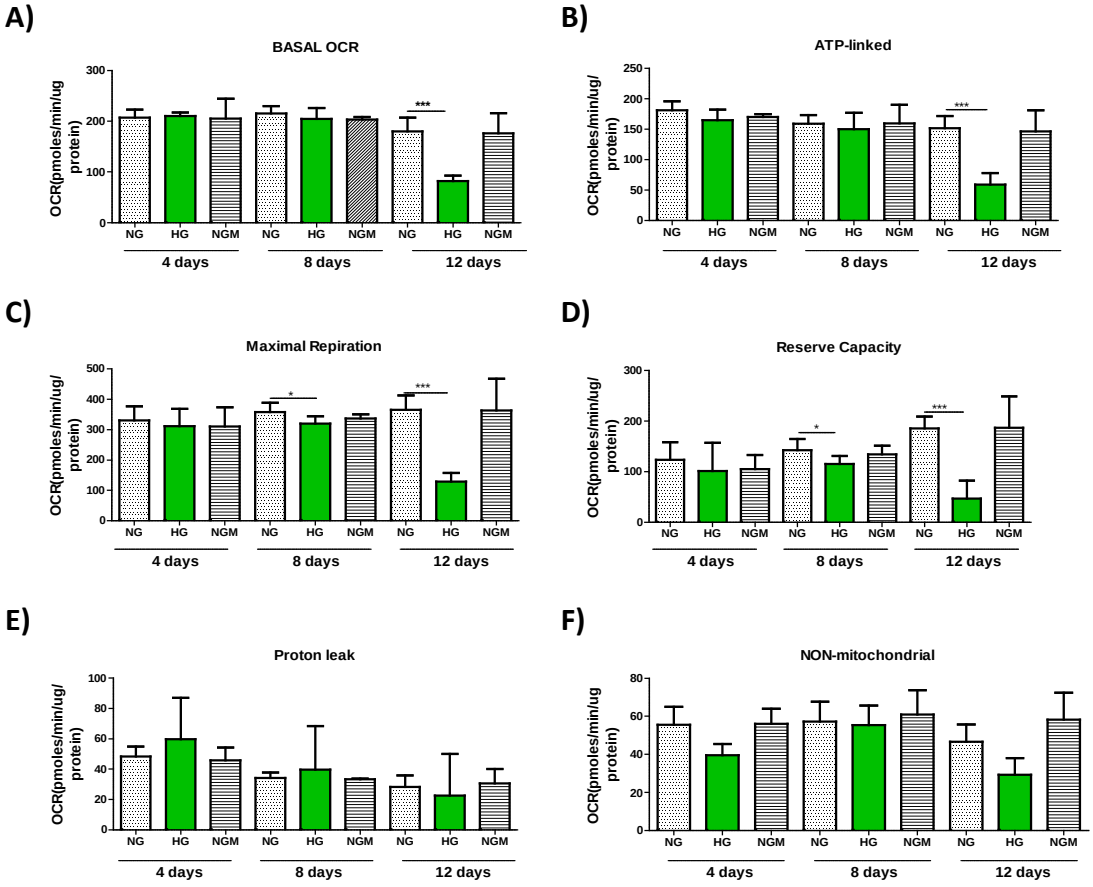

Fig.6.13. High glucose affects metabolic profile of human mesangial cells. Human mesangial cells were grown in 5mM (NG), 25mM (HG) glucose and 5mM glucose plus 20mM mannitol. for 4, 8 and 12 days. OCR was assessed in Seahorse XF^{e}96 analyzer. Basal oxygen consumption rate (OCR) (A). ATP linked respiration (B). proton leak (E). Maximal respiration (C). Reserve capacity, measured as a difference between maximal and basal respiration, is shown on the figure D. All the parameters were calculated by subtracting non-mitochondrial values for each sample (F). Data shown as a mean ±SD, n=8 observations,One way ANOVA with Tukey's post hoc where, *P<0.05, ***P<0.001

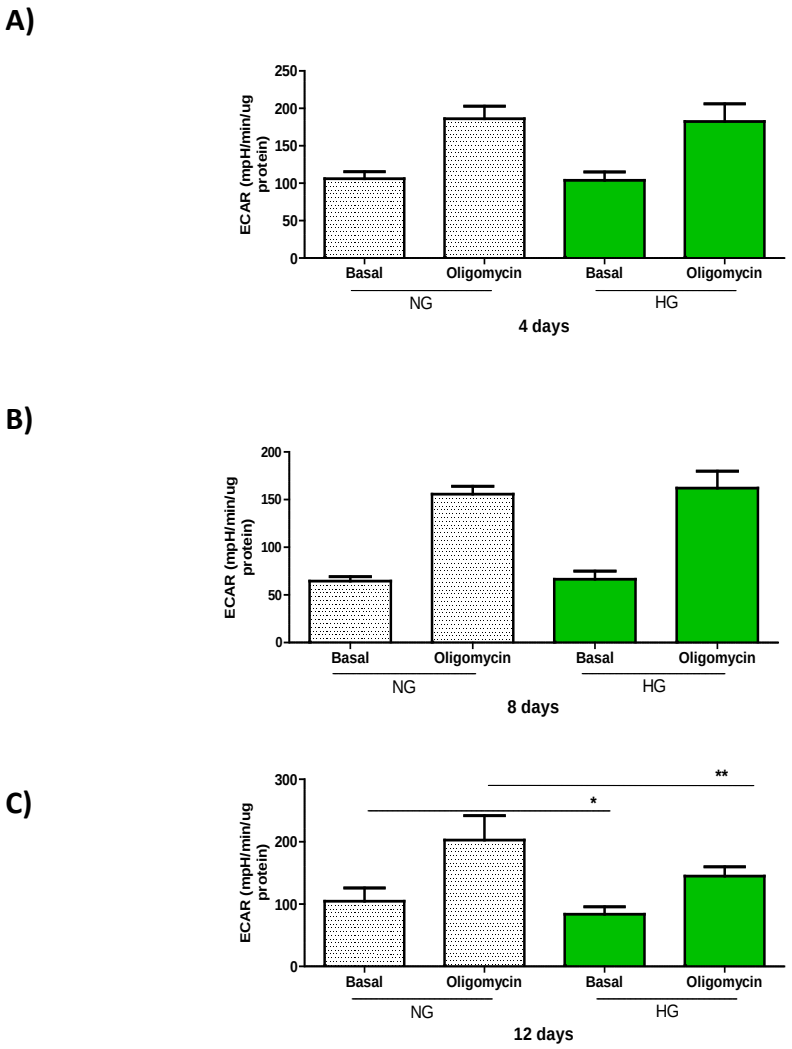

Fig.6.14. Glycolytic profile of human primary mesangial cells cultured in different conditions. Human mesangial cells were grown under 5mM (NG), 25mM (HG) for 4 days (A), 8 days (B) and 12 days (C). Day before the assessment, cells were trypsinized, counted and seeded at density of 35 000 cells/well in different media. Basal ECAR and ECAR after injection of the oligomycin (1µM final) were assessed in XF^{e}96 Seahorse analyzer. Data shown as a mean ±SD, n=6-8 observations, Student's t-test where, *P<0.05, ** P<0.01

In summary, these data show, that 4 days exposure to HG had no effect on any of the measured parameters involved in mitochondrial respiration or glycolysis in HMCs. 8 days exposure of HMCs to HG significantly decreased cells' mitochondrial maximal respiration and reserve capacity but did not affect any other mitochondrial respiration parameters. 12 days exposure of HMCs to HG significantly affected cells' mitochondrial respiration and glycolytic capacity.

Reduction in both glycolysis and OXPHOS function in cells grown in HG may suggest that cells became energetically inactive.

6.4.3 The ratio of glycolysis and oxidative phosphorylation in mesangial cells

Another parameter allowing assessment of the metabolic profile of cultured cells is the ratio of OCR and ECR. Glycolysis and OXPHOS are likely to be integrated during the cellular response to oxidative stress. The OCR and ECAR for a cell is related to the flux through pathways used to generate ATP. The response of both pathways to cellular stress can be assessed by plotting OCR against ECAR at a one time-point, usually at basal level or after injection of the compound of interest as shown in Fig.6.15 A-C which represents metabolic profile of cells grown in 5mM and 25mM glucose for 4, 8 and 12 days respectively. Mean basal ECAR versus OCR ratio didn't change in cells grown under different conditions for 4 and 8 days (Fig.6.15A, B). After 12 days of culture, HMCs cultured in NG and NGM had high ECAR and OCR values (Fig.615 C). Chronic, 12 days exposure of cells to HG, caused a shift in their bioenergetic profile showing that the cells became metabolically less active (Fig. 6.15C).

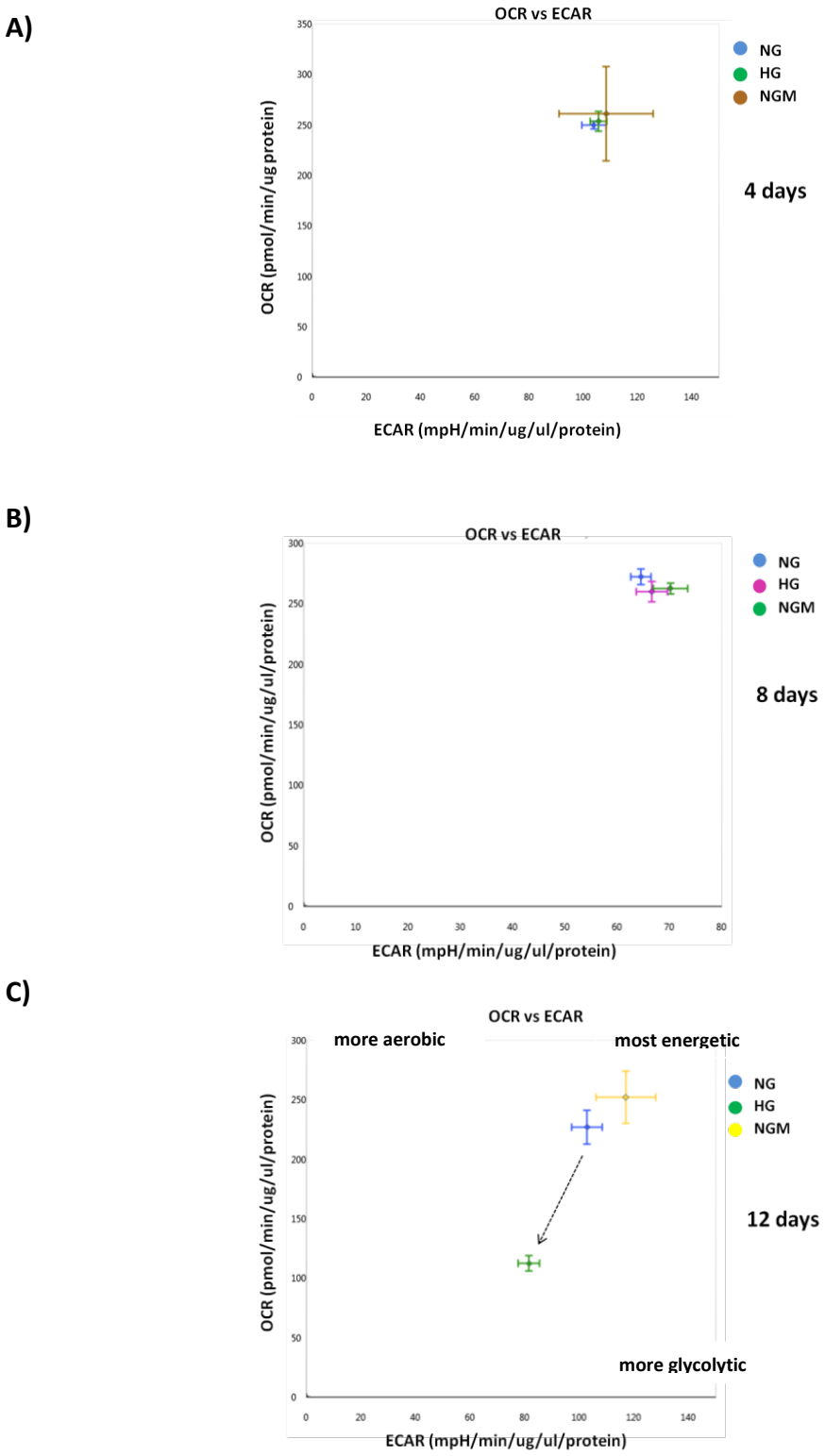

Fig.6.15. The oxygen consumption rate (OCR) and glycolysis (ECAR) of human primary mesangial cells. The mean basal OCR vs. basal ECAR in cells grown in different conditions for 4 days (A), 8 days (B) and 12 days (C). Arrow points a metabolic shift in energy in cells grown in HG. Data shown as a mean ±SEM, n=6-8 observations

6.4.4 The effect of hydrogen peroxide and acute glucose load on the bioenergetic profile of human mesangial cells

HMCs were grown for 12 days in normal glucose (5mM), and exposed for 15 minutes to two different concentrations of H_2O_2. In the second part of this experiment, acute 20mM high glucose was injected into the wells during the Seahorse run. Day before the assessment, mesangial cells were seeded in XF assay plates as described before (35 000 cells/well), and on the day of the experiment were treated with different concentrations either 1µM or 5µM H_2O_2 for 15min in complete growth media with 5mM glucose. Higher than 5µM concentrations of H_2O_2 and longer than 15 minutes treatment proved to be toxic to the cells and caused cell detachment during the media change. HMCs were then washed with XF assay media, and allowed to equilibrate at 37°C for 1 h in a non-CO2 incubator. Mitochondrial function was then assessed as described above using activators and inhibitors of ETC.

- *The effect of H_2O_2 on bioenergetic profile of human mesangial cells*

The aim of these experiments was to assess if oxidative stress have the same effect on mitochondrial function as chronic (12 day) exposure to HG. As shown in Figure 6.16, basal OCR was increased in response to H_2O_2 in HMCs when compared to the control, but this result was not significant (Fig.6.16A). This occurred due to an increase in both, ATP-Linked OCR (10% increase) and proton leak (15% increase), but none of these results were significant ($P>0.05$, Fig. 6.16B and Fig.6.16F). After the addition of FCCP the OCR didn't change and there was no difference in maximal OCR or reserve capacity $P>0.05$, (Fig.6.16C and Fig.6.16D). Interestingly, there was no increase in non-mitochondrial OCR, indicating there is little additional ROS production beyond the H_2O_2 the cells were exposed to initially, however treatment with higher concentrations of H_2O_2 seem to reduce non-mitochondrial respiration which might suggest activation of antioxidant defences ($P=0.09$ when compared to NG).

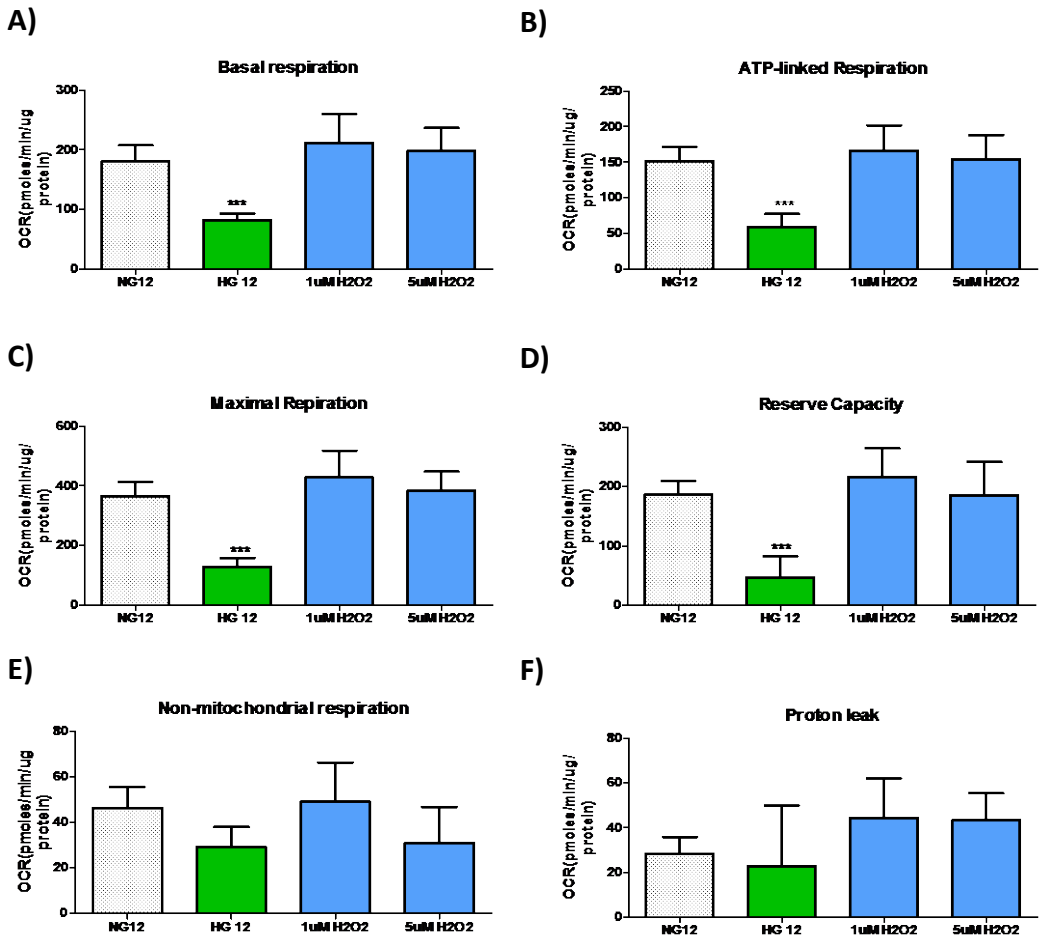

Fig.6.16. Acute oxidative stress does not change bioenergetic profile of human primary mesangial cells. Human mesangial cells were grown in DMEM containing (NG), 25mM (HG) glucose for 12 days. Day before the assessment, cells were trypsinized, counted and seeded at density of 35 000 cells/well in different media. Some of the cells grown in NG were treated with 1µM or 5µM H_2O_2 for 15min before the OCR was assessed in Seahorse analyzer. Four measurement of basal OCR were taken, allowing measuring basal respiration (A). Following the injection of oligomycin (1µM final) assessment of ATP- linked respiration (B) and proton leak (F) were taken. To assess maximal respiration (C), FCCP was injected at the 0.3µM final concentration. Reserve capacity, measured as a difference between maximal and basal respiration, is shown on the figure D. All the parameters were calculated by subtracting non-mitochondrial values for each sample (E). Proton leak is presented on figure F. Data shown as a mean ±SD n=6 for NG and HG and n=3 observations for H_2O_2 treatment,One way Anova with Tukey's post hoc test where, ***P<0.001 vs.NG12

Basal glycolysis rate in cells treated with H_2O_2 was significantly increased by almost 50% when compared to the basal in cell cultured in NG (180±36 vs. 104±21, P<0.01) and this increase was not dose dependent (Fig.6.17). Also after the injection of the oligomycin, glycolytic rate was significantly up-regulated in

cells treated with 1µM H_2O_2 when compared to control (300±75 vs. 202±39, P<0.05, Fig.6.17).

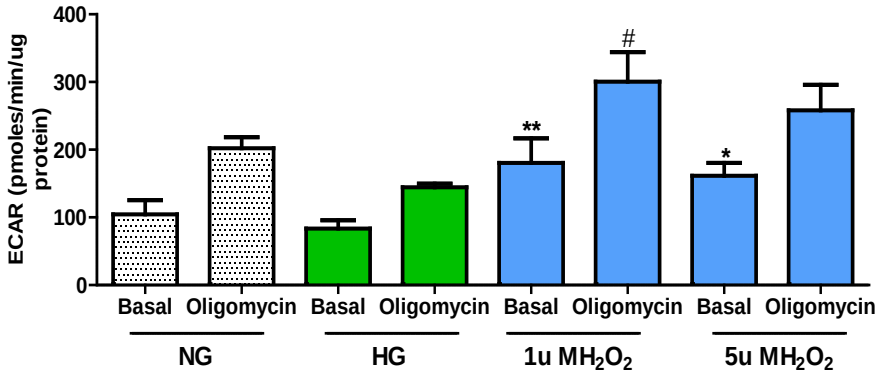

Fig.6.17. Acute oxidative stress affects glycolysis in primary cultured human mesangial cells. Human mesangial cells were grown in DMEM containing 5mM (NG), 25mM (HG) glucose for 12 days. Day before the assessment, cells were trypsinized, counted and seeded at density of 35 000 cells/well in different media. On the day of the experiment of some the cells grown in NG were treated with 1µM or 5µM H_2O_2 for 15min before the basal ECAR was assessed in Seahorse analyzer. Data shown as a mean ±SD, n=6 for NG, HG and n=3 observations for H_2O_2 groups respectively, Kruskal Wallis test with Dunn's post hoc where, *P<0.05, ** P<0.01 vs. NG basal, # P<0.05 vs. NG oligomycin

- *The effect of acute glucose injection on bioenergetic profile of human mesangial cells cultured in 5mM glucose*

The aim of these experiments was to assess if acute oxidative stress have the same effect on mitochondrial function as chronic (12 day) exposure to HG. Basal respiration rate was measured in the cells in which HG was injected into the wells during the Seahorse run, to assess effect of acute treatment with 25mM glucose.

Cells were grown in 5mM glucose for 12 days and day before the assessment seeded in XF assay plates in the complete growth media. On the day of the experiment growth medium was change into assay media which contained 5mM glucose. After 3 measurements of basal OCR, glucose was injected into the well and consecutive measurements of basal OCR were taken followed by a standard

injection of oligomycin, FCCP and rotenone and antimycin A at concentrations described previously.

Basal OCR significantly decreased after HG injection (from 180±27 to 80 ±50 pmol/min), and the reduction was based on decreased ATP-linked OCR (from 140±20 to 43±52) as there was no difference in the proton leak (Fig.6.19 A). Acute HG glucose injection caused slight but not significant increase in maximal respiration and increase in reserve capacity which was close to reach the significance (P=0.051). HG injection significantly increased non-mitochondrial OCR when compared to control (46±9 vs. 71±12 pmol/min respectively) suggesting other cellular processes involved in glucose processing which involve oxygen consumption (Fig.6.18 and Fig.6.19A).

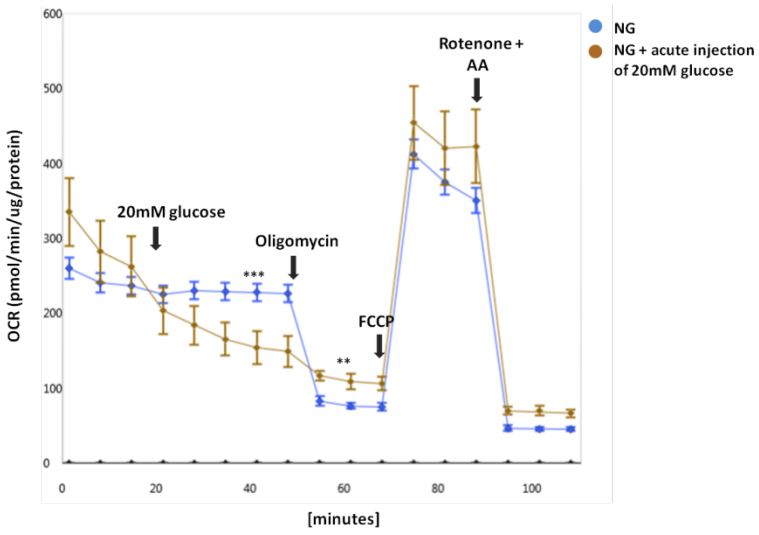

Fig.6.18. Acute injection of high glucose has an effect on the bioenergetic profile of human primary mesangial cells. HMCs were grown in DMEM containing 5mM (NG) glucose for 11 days. Day before the assessment, cells were trypsinized, counted and seeded at density of 35 000 cells/well in different media. Following media change, OCR was assessed in Seahorse analyzer. Three measurements of basal respiration were taken, followed by injection of 20mM glucose and another five consecutive measurements of basal OCR. To measure ATP-linked OCR, oligomycin was injected a 1µM final. To assess maximal respiration, FCCP was injection at the 0.3µM working concentration. Data shown as a mean ±SD, n=4 for acute glucose injection, n= 6 observations for NG, data are representative for one experiment

Measurement of the ECAR (glycolytic rate) was carried out at the same time. Basal ECAR after the injection of acute 20mM glucose and ECAR after the

injection of oligomycin, were measured. As expected, drop in basal OCR described previously caused the switch in metabolism to glycolysis. After the HG injection, basal glycolytic rate significantly increased by more than two fold, when compared to cells injected just with the assay media (248±60 vs. 100±20 mpH/min respectively). After the injection of oligomycin, the fold increase in ECAR rate was not as high as in cells injected with assay media. This data suggest that cells acutely treated with 20mM glucose could reach their maximal glycolytic rate (Fig.6.19B).

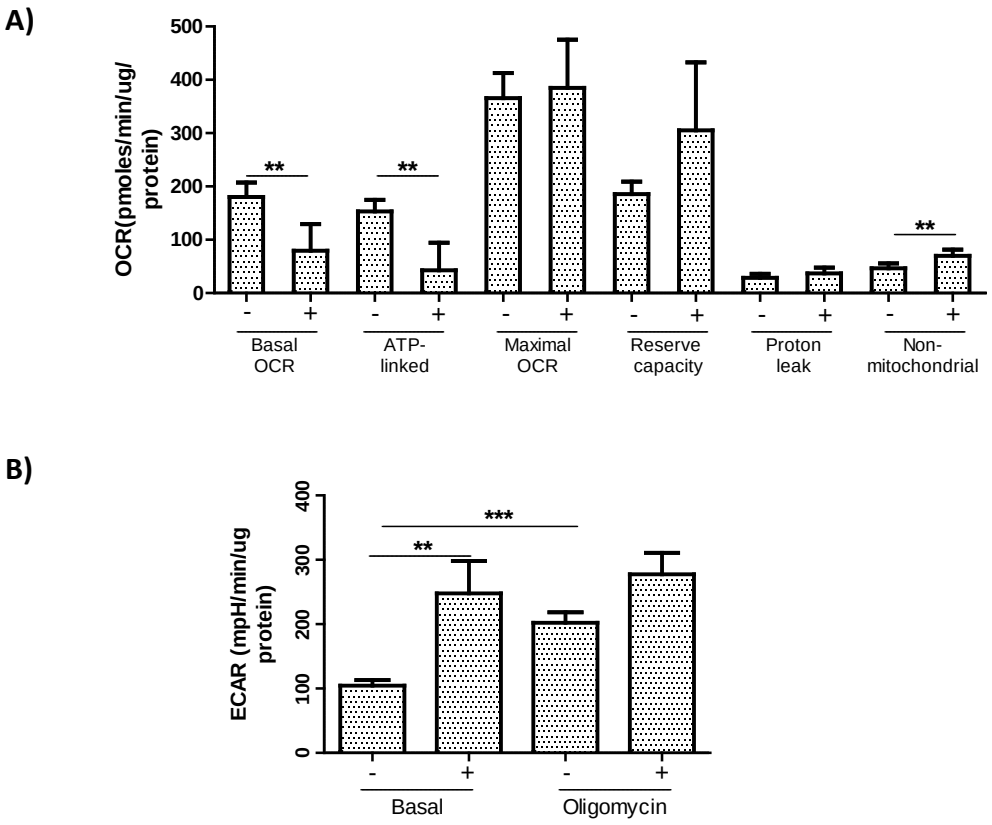

Fig.6.19. Acute injection of high glucose has an effect on the bioenergetic profile of human primary mesangial cells. HMCs were grown in 5mM (NG) for 12 days. Day before the assessment, cells were seeded at density of 35 000 cells/well in different media. Some of the cells grown in the NG were injected with assay media (-) or 20mM glucose (+) during the assessment in Seahorse analyzer. OCR (A) and basal ECAR and ECAR after the injections of oligomycin (B) were assessed in XF96 Seahorse analyzer. Data shown as a Mean ±SD Data shown as a mean ±SD, n=4-8 observations, data are representative for one experiment, Student's t-test where, ** P<0.01, ***P<0.001

- *The effect of acute glucose injection on bioenergetic profile of human mesangial cells cultured in 25mM glucose*

HMCs were cultured for 12 days in 25mM glucose and bioenergetic assessment was carried out in Seahorse XF analyzer as described previously. After 3 measurements of basal OCR, glucose was injected into the well and consecutive measurements of basal OCR were taken followed by a standard injection of pligomycin, FCCP and rotenone and antimycin A (Fig.6.20) at concentrations described previously. As illustrated on Fig.6.21.A cells pre-cultured in high glucose did not reduced their mitochondrial respiration after the 20mM glucose injection as there was no difference in any of the measured parameters of the OCR (P>0.05, Fig.6.21 A).

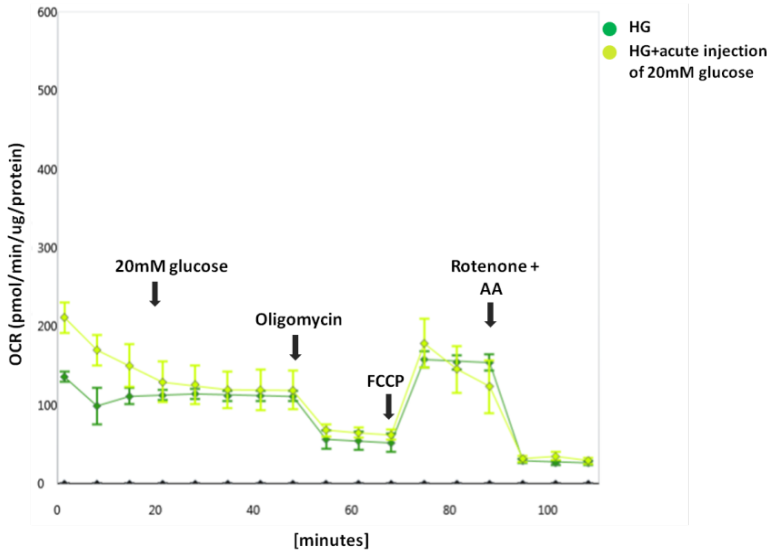

Fig.6.20. Acute injection of high glucose has no effect on the bioenergetic profile of preconditioned human primary mesangial cells. HMCs were grown in DMEM containing 25mM (HG) glucose for 11 days. Day before the assessment, cells were trypsinized, counted and seeded at density of 35 000 cells/well in different media. Following media change, OCR was assessed in Seahorse analyzer. Three measurements of basal respiration were taken, followed by injection of 20mM glucose and another five consecutive measurements of basal OCR. To measure ATP-linked OCR, oligomycin was injected a 1µM final. To assess maximal respiration, FCCP was injection at the 0.3µM working concentration. Data shown as a mean ±SD, n=4 for acute injection, n=8 for HG, data are representative for one experiment.

Basal glycolytic rate did significantly increase after the glucose injection by almost 2 fold when compared to cell injected with assay media only (P<0.01). After the injection of oligomycin, the fold increase in ECAR rate was not statistically significant when compared to the basal level (P<0.05, Fig.6.21B).

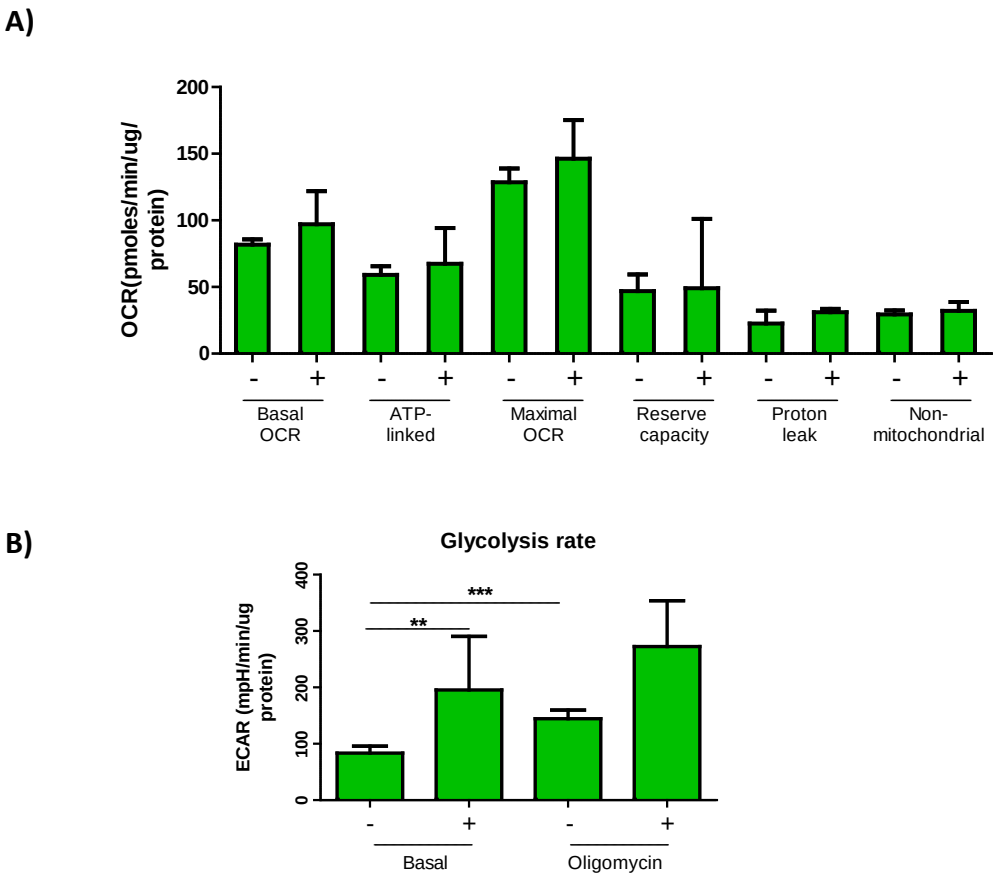

Fig.6.21. Acute injection of high glucose affect only glycolysis in human primary mesangial cells preconditioned in high glucose. Human mesangial cells were grown in DMEM containing 25mM (HG) glucose for 12 days. Day before the assessment, cells were trypsinized, counted and seeded at density of 35 000 cells/well in different media and assessment of OCR (A) and ECAR (B) was performed. Some of the cells grown in the HG for 12 days were injected with assay media (-) or 20mM glucose (+) during the assessment in Seahorse analyzer. To measure ATP-linked OCR and proton leak, oligomycin was injected a 1µM final. To assess maximal respiration, FCCP was injected at the 0.3µM final concentration. Reserve capacity was measured as a difference between maximal and basal respiration. Non-mitochondrial respiration was subtracted from all the values presented in the graph (A). Basal ECAR and ECAR after the injection of 1µM of oligomycin was assessed in HG and in acute HG group (B). Data shown as a mean ±SD, n=4-6 replicates, data are representative for one experiment, Student's t-test where,**P<0.01, ***P<0.001

These data show, that after the acute 20mM glucose injection, HMCs which were cultured in NG, switched their metabolism to glycolysis as basal glycolytic rate significantly increased by more than two fold, and basal and ATP-linked OCR was reduced. HMCs which were exposed to chronic hyperglycaemia lost their flexibility to respond to nutrient load, as they can increase their glycolytic rate but at the same time mitochondrial respiration remains the same which suggest they cannot balance their energy production.

6.4.5 Is inhibiting effect of hyperglycaemia on mitochondria respiration in mesangial cells reversible?

It was shown in the previous paragraph that exposure of HMCs to high glucose for 8 and 12 days significantly affects cells' mitochondrial respiratory function, especially maximal respiration and reserve capacity. To assess if these changes were permanent or possible reversible, study was design to test mitochondrial respiration in cells which were cultured in DMEM with different glucose concentrations (HG media was substituted with low NG one). Two time points were used, cells were grown for 7 days in HG and the media was changed to NG glucose media for 1 day (HG7/NG1) and in the second time point, cells were grown under HG for 8 days and had the media reversed to normal glucose for 4 days (HG8/NG4). In control groups cells were cultured in 5mM glucose for 8 and 12 days. To compare the groups, one-way ANOVA was performed and analysis of variance proved to be significant ($P=0.0005$). Tukey's Multiple Comparison Test show no difference in basal or ATP-linked respiration ($P>0.05$) between HG 8 days, NG 8 days and HG7/NG1 groups (Fig.6.22A and Fig.6.23A). As described previously cell cultured in HG for 4 days had the same OCR profile as control groups, but 8 day culture in HG had significantly decreased maximal respiration and reserve capacity (Fig.6.13). This trend was still observed in cells cultured in HG for 7 days with media change for one day to 5 mM glucose (Fig 6.22A and Fig.6.23A). Maximal respiration didn't get back to normal levels and was still highly significantly lower when compared to NG group ($P<0.001$). Interestingly reserve capacity in HG7/NG1 group was significantly lower than in cells cultured

in HG for 8 days (P<0.05) and highly significantly lower when compared to the controls (P<0.001, Fig.6.23A). However, when cells were cultured for 8 days in HG and then reverted to normoglycaemia for 4 days, there was observed a beneficial effect of reversed conditions. Tukey's Multiple Comparison Test showed no difference in maximal respiration and reserved capacity between NG and HG8/NG4 groups. Also basal, ATP-linked and non-mitochondrial OCR which were significantly down regulated by 12 day treatment of HG returned to control (5mM glucose) levels (Fig.6.22B and Fig.6.23B).

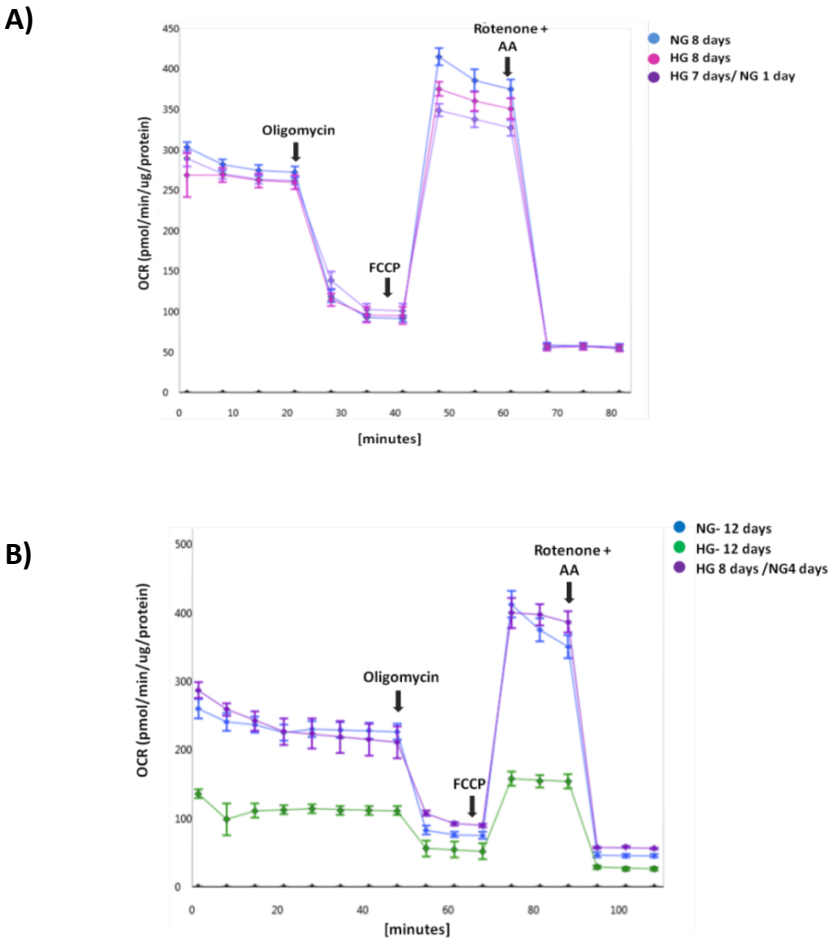

Fig.6.22. Reversing the culture conditions affects bioenergetic profile of human primary mesangial cells. HMCs were grown in DMEM containing 5mM (NG), 25mM (HG) glucose for 11 days and in reversed conditions: HG7/NG1 (A) and HG8/NG4 (B). Day before the assessment, cells were trypsinized, counted and seeded at density of 35 000 cells/well in different media. Following media change, OCR was assessed in Seahorse analyzer. Three measurements of basal respiration were taken, followed by the injection of oligomycin a 1µM final in order to measure ATP-linked OCR. To assess maximal respiration, FCCP was injection at the 0.3µM working concentration. Data shown as a mean ±SD, n=6-8, data are representative for one experiment

A)

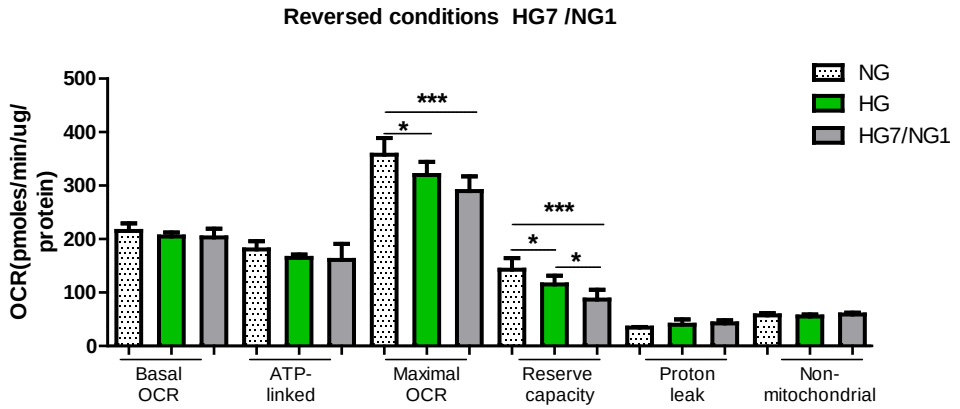

B)

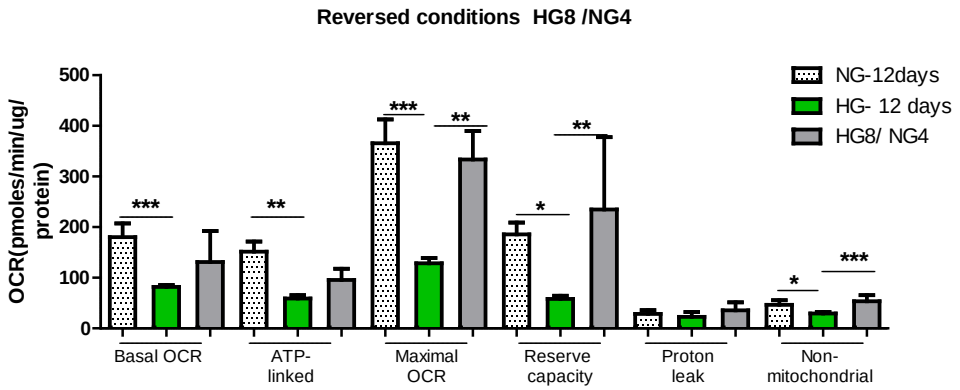

Fig.6.23. Reversing the culture conditions changes metabolic profile of human primary mesangial cells. Mesangial cells were grown either in DMEM containing 5mM (NG), 25mM (HG) for 8 days (A) or in NG and HG for 12 days (B). During the 8 day culture in HG, medium was changed to low glucose after 7 days for 24hr (A). During 12 day culture, after 8 days HG medium was replaced by 5mM one for 4 days (B). Day before the assessment, cells were trypsinized, counted and seeded at density of 25 000 cells/well in different media. OCR was assessed in Seahorse analyzer. Four measurement of basal OCR were taken, allowing measuring basal OCR. Following the injection of oligomycin (1µM final) assessment of ATP- linked respiration and proton leak were taken. To assess maximal respiration, FCCP was injected at the 0.3µM final concentration. All the parameters were calculated by subtracting non-mitochondrial values for each sample. Data shown as a mean ±SD, n=6-8 observations, One way ANOVA with Tukey's post hoc test where, *P<0.05, ***P<0.001

Basal ECAR and ECAR after the injection of oligomycin were also assessed in reversal groups. There was no difference in basal glycolysis and after the induction of oligomycin in HG7/NG1 group when compared to NG and HG groups (Analysis of variance, P>0.05, Fig.6.24A). However when the basal levels and

response to oligomycin was assessed in HG8/NG4 group, Tukey's multiple comparison test showed a significant difference between basal ECAR in cells cultured in HG for 12 days and basal ECAR in HG8/NG4 group, ($P<0.05$). Glycolysis levels in HG8/NG 4 was significantly increased at basal and after the injection of oligomycin, when compared to HG group ($P<0.01$) and seem to return to normal levels when compared to NG group ($P<0.05$, Fig.6.24B).

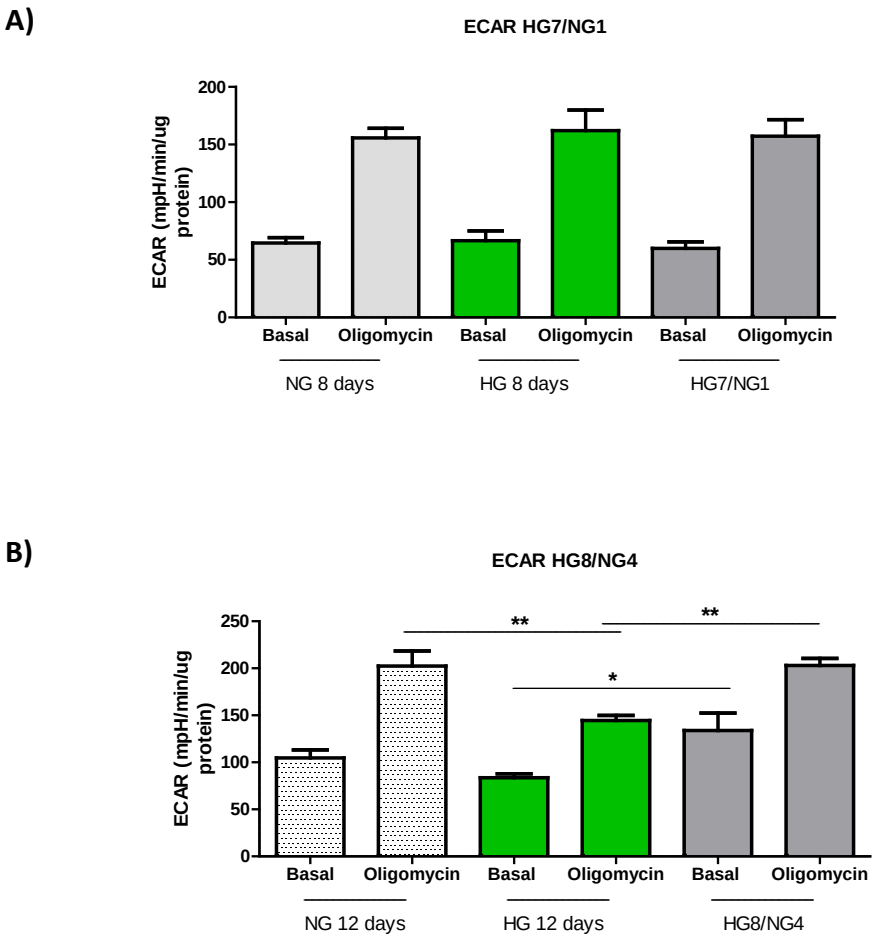

Fig.6.24. Glycolytic profile of human primary mesangial cells cultured in reversed conditions. Human mesangial cells were grown in DMEM containing 5mM (NG), 25mM (HG)glucose and HG/NG conditions for 8 (A) and 12 days (B). Basal ECAR and ECAR after injection of oligomycin were assessed in Seahorse XF96e analyzer. Data shown as a mean ±SD, n=6 for NG, HG and n=8 observations for Hg7/NG1, HG8/NG4 respectively, One way ANOVA with Tukey's post hoc test where, *P<0.05, ** P<0.01

Mean basal ECAR versus OCR ratio didn't change in cells grown under HG7/NG1 (Fig. 6.25A). However prolonged period of normoglycaemia in HG8/NG4 group,

proved to have a beneficial effect of media reversal on OCR/ECAR ratio. After extended NG treatment there was observed a shift in cells bioenergetic profile from less to more metabolically active as highlighted by arrows on Fig.6.25B.

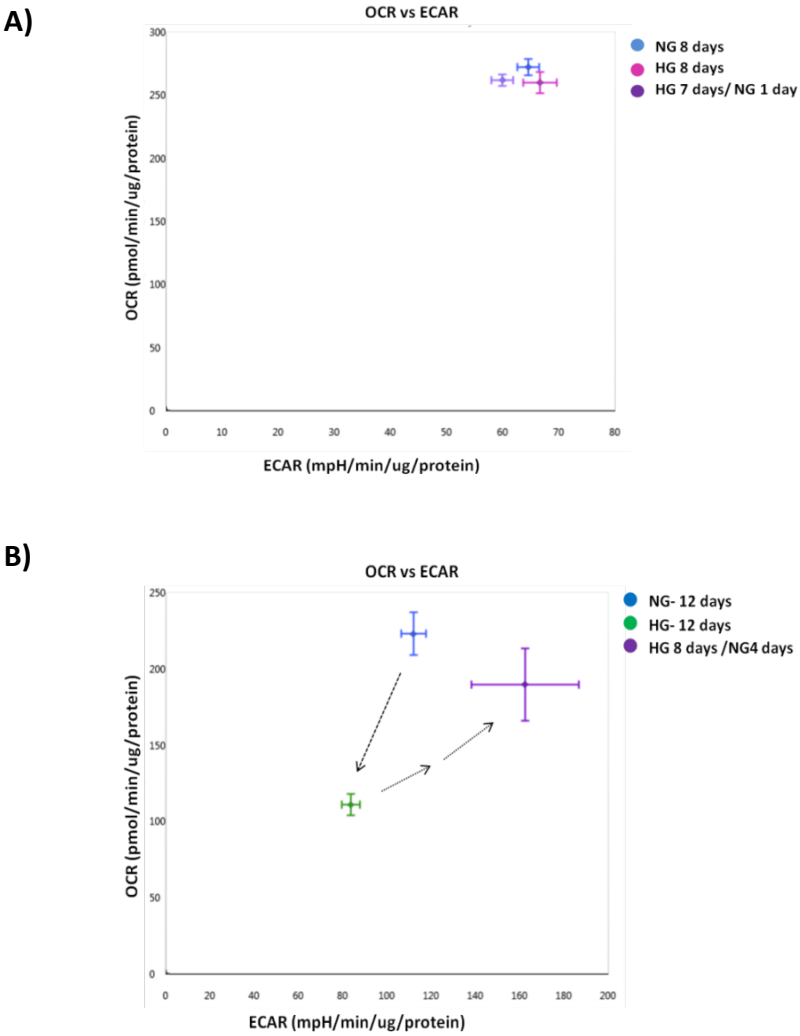

Fig.6.25. The oxygen consumption rate (OCR) and glycolysis (ECAR) of human primary mesangial cells cultured in reversed conditions. The mean basal OCR vs. basal ECAR in cells grown in 25mM glucose (HG) for 7 days (A)and 8 days (B). Cells grown in HG have their media glucose levels reversed to NG for 1 day (A) and for 4 days (B). Arrow points a metabolic shift in energy in cells grown in HG and then when media was reversed to NG. Data shown as a mean ±SEM, n=6-8 observations

6.4.6 Bioenergetic profile of human transformed tubular cells cultured in high glucose

Mesangial cells are central to the development of DN through their role in the development of glomerulosclerosis but tubular cells are the second type of the cells taking part in the development of diabetic nephropathy. During the process of the development of the disease, these cells undergo epithelial to mesenchymal transition. Therefore, the aim of this part of the study was to assess bioenergetic profile of human transformed tubular cells (HK-2) cells grown for 4 and 8 days in 5mM (NG), 25mM (HG) and in osmotic control (NGM, 20mM mannitol + 5mM glucose). Determination of oxygen (OCR) and proton (ECAR) concentration in real-time was measured by using XF analyzer (Seahorse bioscience), as described above. Mitochondrial inhibitors and uncoupler concentrations were set up in a series of optimization experiments (as shown above in section 6.4.1). HK-2 cells were grown under HG for 3 and 7 days in different media, day before the experiment cells were trypsinized, counted using Countless Cells counted and seeding in the density of 25 000cells/ well. Oligomycin, FCCP, rotenone and antimycin A were injected sequentially through ports in the XF Assay cartridges to final concentrations of 1µM, 0.3µM, 0.5µM and 0.5µM respectively. Basal respiration of HK-2 cells cultured in was measured at around 200-250 pmoles/min/µg/protein (Fig.6.26).

- *Bioenergetic profile of human transformed cell cultured in high glucose for 4 days*

Contrary to HMCs cells, in which bioenergetic profile was not affected by HG after 4 days of culture, in HK-2 cells, we observed a significant decrease in most of the assessed parameters (Figure 6.26 and Fig.6.30). Basal OCR was significantly lower in cells cultured in HG (101±22, N=14) when compared to cells grown in NG (130±18, N=17, $P<0.001$, Fig. 6.30A). ATP-linked respiration measured as a drop in OCR, following the injection of oligomycin was also significantly lower by approximately 25% in cells cultured in HG when compared to the controls ($P<0.001$ Fig.6.30B). Independent students t-test and one way ANOVA showed a significant decrease (more than 50%) of maximal respiration

and reserve capacity in HK-2 cells grown in HG for 4 days when compared to NG and osmotic controls (P<0.001, Fig.6.30C-D). There was no difference in proton leak between the treatment group and controls (Fig.6.30F); conversely non-mitochondrial respiration was significantly reduced in cells cultured in HG (29±9) when compared to control (45.6±19), (P<0.05, Fig.6.30E).

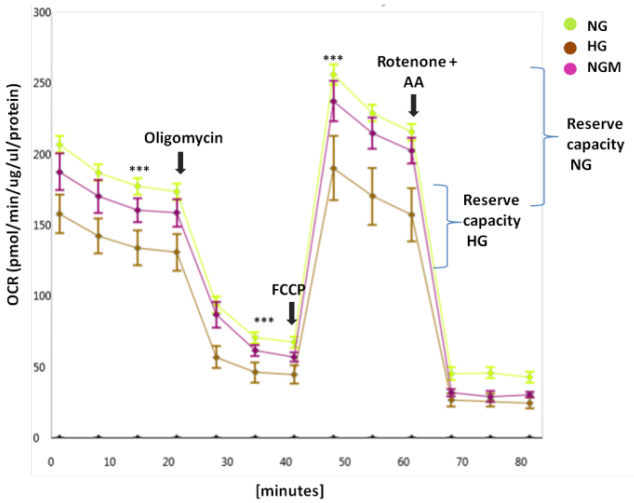

Fig.6.26. Bioenergetic profile of human tubular cells cultured in high glucose for 4 days. HK-2 cells were grown in DMEM containing 5mM (NG), 25mM (HG) glucose and osmotic control for 4 days. Day before the assessment, cells were trypsinized, counted and seeded at density of25 000 cells/well in different media. Following media change, OCR was assessed in Seahorse XF 96e analyzer. Four measurement of basal respiration were taken, followed by an injection of oligomycin (1µM final). To assess maximal respiration, FCCP was injection at the 0.3µM working concentration. Reserve capacity, measured as a difference between maximal and basal respiration, is shown on the right. Data shown as a mean ±SD, n=14 for NG and n=17 observations for HG

As shown in Fig. 6.27 and 6.31A basal ECAR was significantly increased by in HK-2 cells exposed to HG for 4 days when compared to cells cultured in NG (132±11 vs. 94± 9, P<0.05).

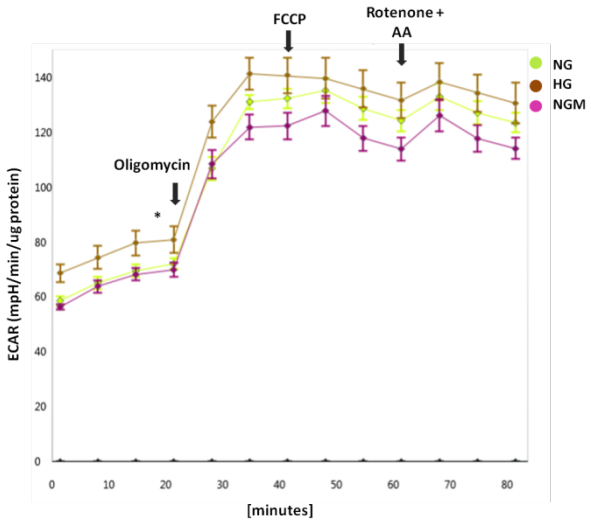

Fig.6.27. Glycolytic profile of human tubular cells cultured in high glucose for 4 days. HK-2 cells were grown in DMEM containing 5mM (NG), 25mM (HG) glucose and osmotic control for 4 days. ECAR (glycolysis) was assessed in Seahorse XF ^{e} 96 analyzer. Data shown as a mean ±SD, n=14 for NG and n=17 observations for HG

- *Bioenergetic profile of human transformed tubular cells cultured in high glucose for 8 days*

4 days of HG treatment caused dramatic changes in mitochondrial respiration parameters in HK-2 cells but there was still reserve capacity left, therefore we extended period of treatment to 8 days. As shown in figure 6.28 extended period of culture in 25mM glucose had more toxic effect on mitochondrial respiration when compared to HK-2 cells grown in different media for only for 4 days. HG significantly reduced basal OCR by approximately 60% ($P<0.01$, Fig.6.30A) and ATP-linked respiration by approximately 70% ($P<0.001$, Fig.6.30B). Similar to 4 days treatment there was no significant difference in the proton leak between groups cultured for 8 days ($P>0.05$, Fig.6.60F) and non-mitochondrial respiration was significantly decreased in HG when compared to the control ($P<0.05$, Fig.6.30E). Interestingly HK-2 cells cultured in HG lost their ability to increase maximal respiration after the injection of FCCP when compared to NG ($P<0.01$, Fig.6.30D).

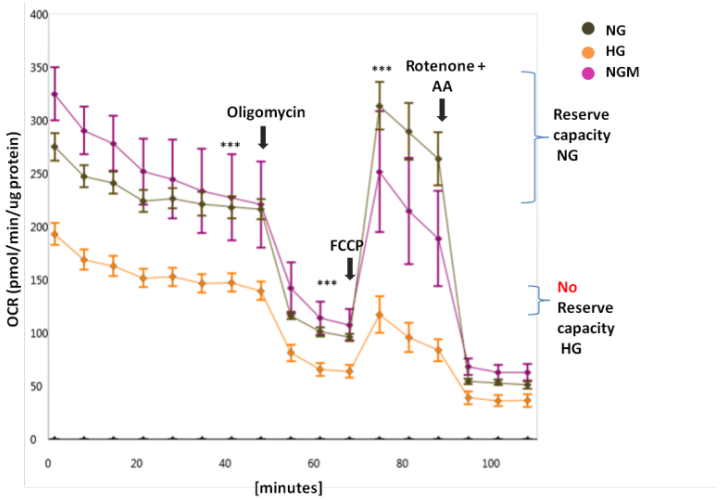

Fig.6.28. Bioenergetic profile of human tubular cells cultured in high glucose for 8 days. HK-2 cells were grown in DMEM containing 5mM (NG), 25mM (HG) glucose and osmotic control for 4 days. Following media change, OCR was assessed in Seahorse analyzer. Four measurement of basal respiration were taken, followed by an injection of oligomycin (1µM final). To assess maximal respiration, FCCP was injection at the 0.3µM working concentration. Reserve capacity, measured as a difference between maximal and basal respiration, is shown on the right. Data shown as a mean ±SD, n=6 observations.

After 8 days of culture basal ECAR was significantly increased in the HG group when compared to control (P<0.05, Fig.6.29 and Fig.6.31B respectively). Moreover in cells grown in NG, there was almost 2 fold increase in basal ECAR between different passages as seen on Fig.6.31.

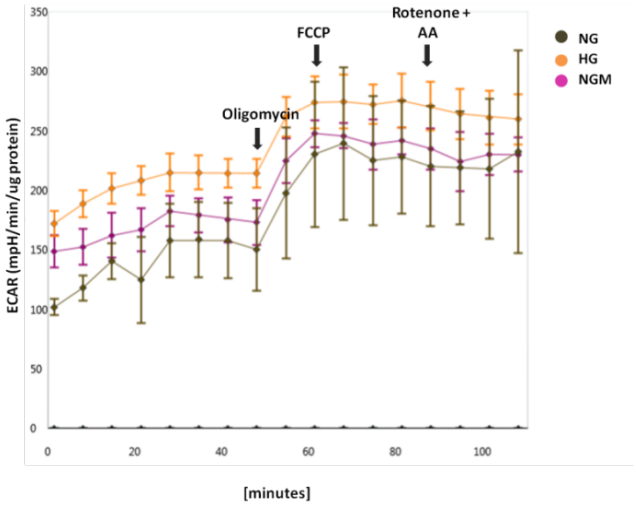

Fig.6.29. Glycolytic profile of human tubular cells cultured in high glucose for 8 days. HMCs were grown in DMEM containing 5mM (NG), 25mM (HG) glucose and osmotic control for 4 days. ECAR (glycolysis) was assessed in Seahorse XF ^{e} 96 analyzer. Data shown as a mean ±SD, n=6 observations

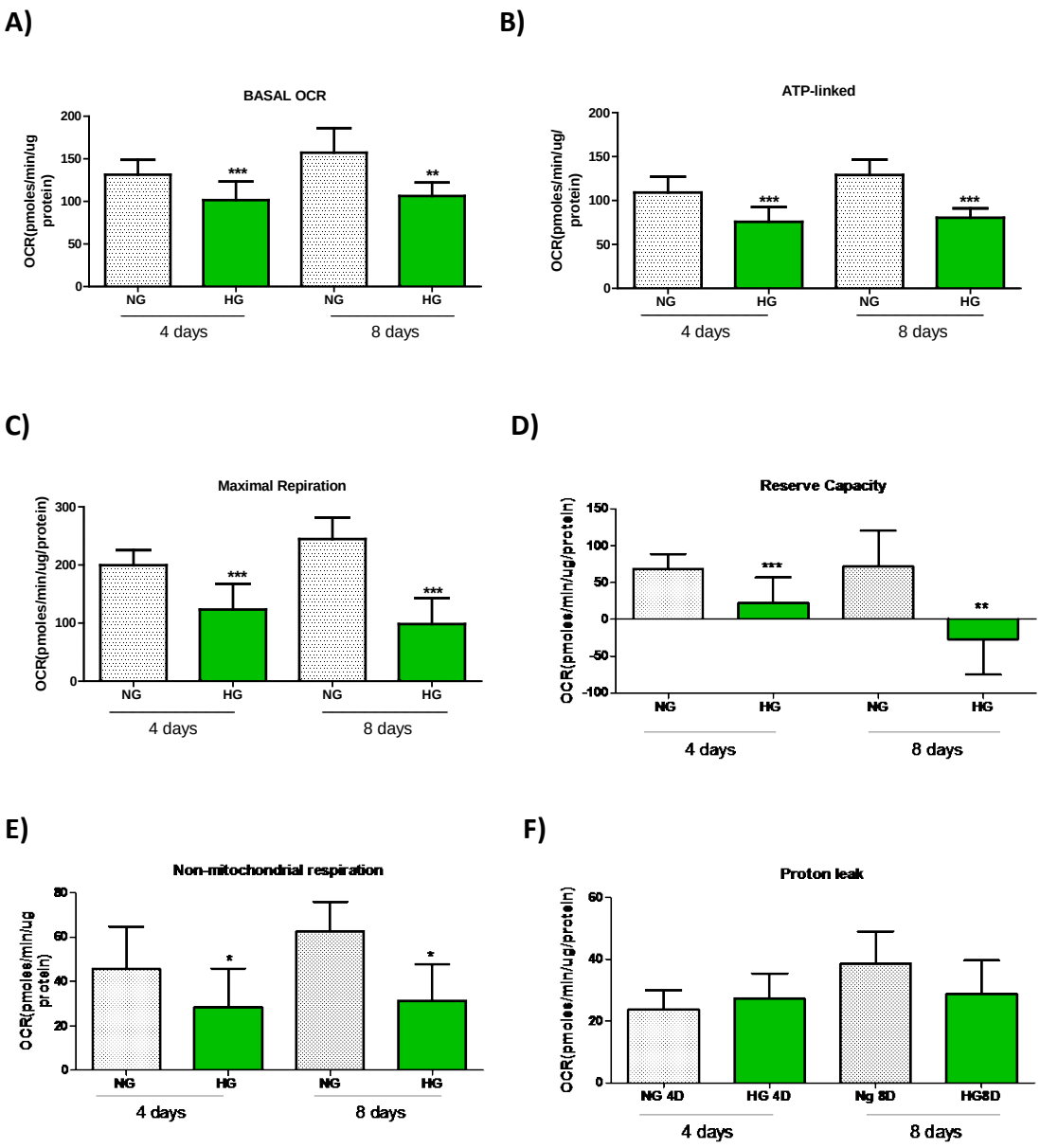

Fig.6.30. High glucose affects metabolic profile of human transformed tubular cells. HK-2 cells were grown in DMEM containing 5mM (NG), 25mM (HG) glucose for 4 and 8 days. Day before the assessment, cells were trypsinized, counted and seeded at density of 25 000 cells/well in different media. OCR was assessed in Seahorse analyzer. Four measurement of basal OCR were taken, allowing measuring basal OCR (A). Following the injection of oligomycin (1µM final) assessment of ATP- linked respiration (B) and proton leak (F) were taken. To assess maximal respiration (C), FCCP was injected at the 0.3µM final concentration. Reserve capacity, measured as a difference between maximal and basal respiration, is shown on the figure D. All the parameters were calculated by subtracting non-mitochondrial values for each sample (E). Data shown as a mean ±SD n=14 replicates from 2 independent experiments for 4 days and n=14-17 replicates from 2 independent experiments for 4 days and n=6 for 8 days, Student's t-test where, *P<0.05, ***P<0.001

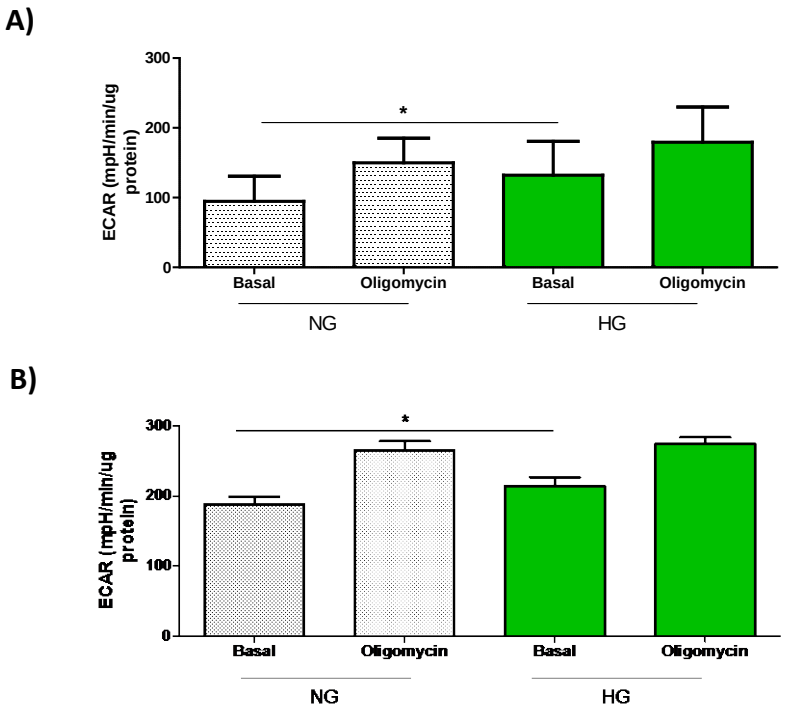

Fig.6.31. Glycolytic profile of human transformed tubular cells cultured in different conditions for 4 and 8 days. Cells were grown in 5mM (NG), 25mM (HG) for 4 days (A), and 8 days (B). Day before the assessment, cells were trypsinized, counted and seeded at density of 35 000 cells/well in different media. Basal ECAR and ECAR after injection of oligomycin (1µM final) were assessed using XF96 Seahorse analyzer. Data shown as a mean ±SD, n=14 and n=17 for NG and HG respectively in 4 days, n=6 for both conditions in 8 days, Studnet's t-test where, *p<0.05,

To assess the ratio between oxidative phosphorylation and glycolysis, ECAR versus OCR was plotted as shown on Fig.6.32. There was a slight shift in metabolic profile in HK-2 cells cultured in HG towards more glycolytic (Fig.6.32A) and less metabolic profile (Fig.6.32B), after 4 and 8 days of the exposure to HG, but the changes were not major.

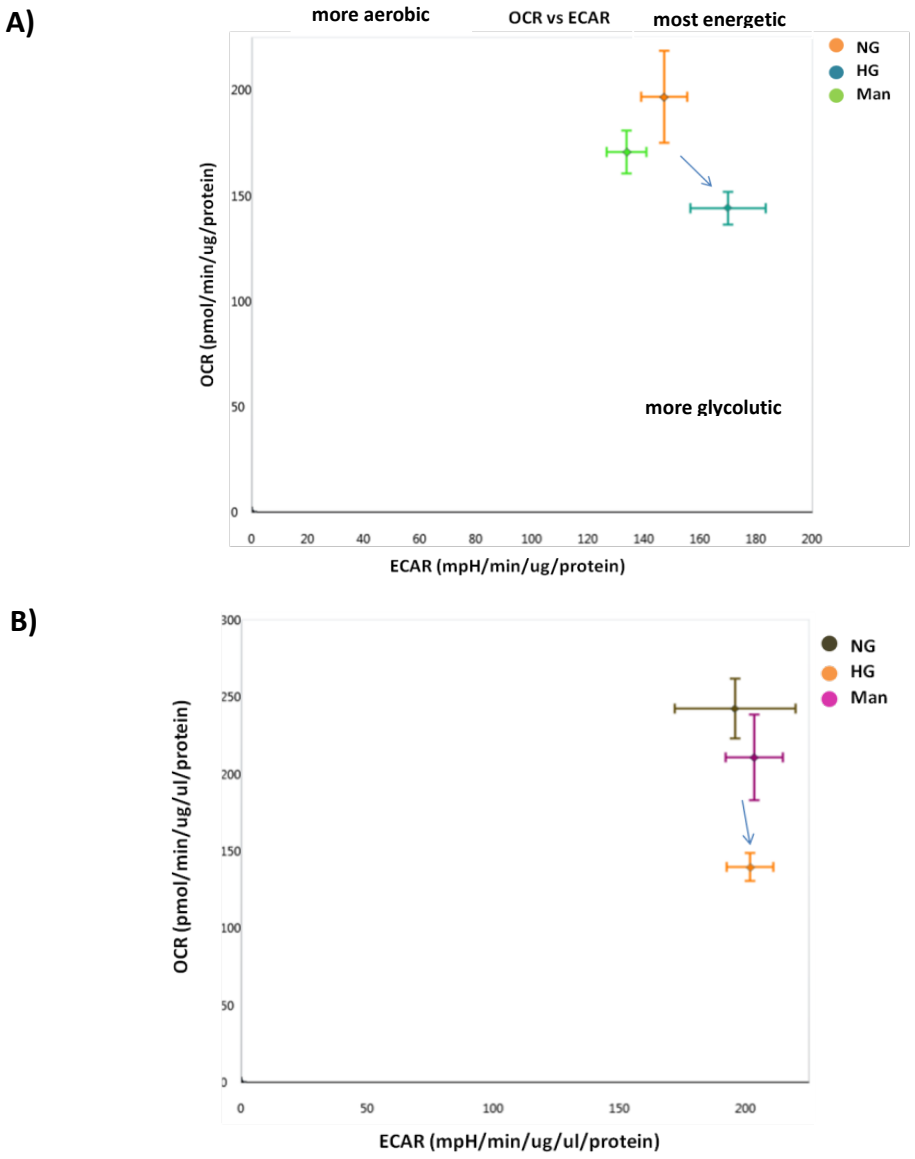

Fig.6.32. The oxygen consumption rate (OCR) and glycolysis (ECAR) of human tubular cells. The mean basal OCR vs. basal ECAR in cells grown in 25mM glucose (HG) for 4 days (A)and 8 days (B). Arrow points a metabolic shift in energy in cells grown in HG and then when media was reversed to NG. Data shown as a mean ±SEM, n=6-17 observations

These data show, that HK-2 cells are more susceptible to HG with decreased mitochondrial respiration basal, maximal and ATP-linked respirations following 4 day of culture. Moreover, 8 days of exposure to hyperglycaemia caused a loss in the reserve capacity. Contrary to the HMCs cells, basal ECAr was increased in HK-2 cells exposed to hyperglycaemia.

6.4.7 The effect of hydrogen peroxide and acute glucose load on the cellular bioenergetics of human tubular cells

It was shown in the previous paragraph that chronic exposure of HK-2 cells to high glucose significantly affects cells' mitochondrial respiratory function. In the next series of experiments, HK-2 cells were grown for 8 days in 5mM glucose and treated with two different concentrations of H_2O_2. The aim of this experiment was to assess, if acute oxidative stress has the same effect on mitochondrial function as chronic exposure to HG. Day before the assessment, tubular cells were seeded in XF assay plates as described before (25 000 cells/well), and on the day of the experiment were treated with different concentrations either 1µM or 5µM H_2O_2 for 15min in complete growth media with 5mM glucose. Higher than 5µM concentrations of H_2O_2 and longer than 15 minutes treatment proved to be toxic to the cells and caused cell detachment during the media change. Mitochondrial function was then assessed as described previously. As shown in Fig.6.33, basal OCR was significantly decreased ($P<0.01$) in response to 1µM H_2O_2 in HK-2 cells when compared to the control (97±47vs. 170±19 pmoles/min respectively, Fig.6.33A). Interestingly, both concentration of H_2O_2 had the same inhibiting effect on ATP synthesis in HK-2 cells as 8 day exposure to HG (Fig.6.33B) but only 1µM H_2O_2 treatment was statistically significant, probably due to the higher number of the repeats ($P<0.01$). H_2O_2 treatment caused also a significant decrease in the maximal respiration ($P<0.05$, Fig.6.33C) and a loss in the reserve capacity ($P>0.05$, Fig.6.33D). Non-mitochondrial OCR was also significantly down regulated in the H_2O_2 treatment groups ($P<0.05$, Fig.6.33E), but no significant difference in the proton leak was observed ($P>0.05$, Fig6.33F).

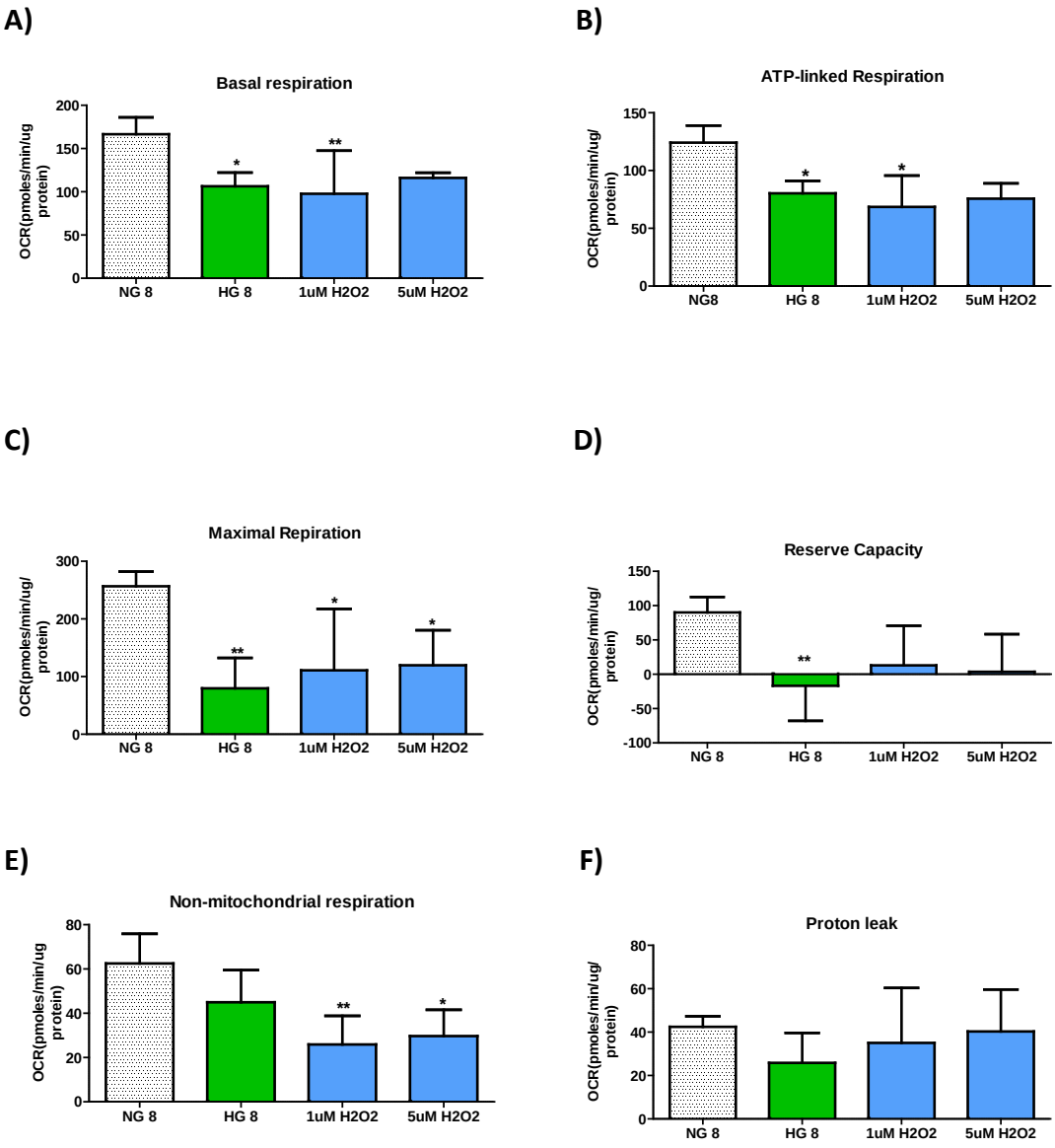

Fig.6.33. Acute oxidative stress affects bioenergetic profile of human transformed tubular cells. Human transformed tubular cells (HK-2) were grown in 5mM (NG) or 25mM (HG) glucose for 8 days. Day before the assessment, cells were trypsinized, counted and seeded at density of 25 000 cells/well in different media. Some of the cells grown under the NG were treated with 1µM or 5µM H_2O_2 for 15min before the OCR was assessed in Seahorse analyzer. Four measurement of basal OCR were taken, allowing measuring basal OCR (A). Following the injection of oligomycin (1µM final) assessment of ATP- linked respiration (B) and proton leak (F) were taken. To assess maximal respiration (C), FCCP was injected at the 0.3µM final concentration. Reserve capacity, measured as a difference between maximal and basal respiration, is shown on the figure D. All the parameters were calculated by subtracting non-mitochondrial values for each sample (E). Proton leak is presented on figure F. Data shown as a mean ±SD, n=6 for NG and HG respectively and n=3-4 for H_2O_2 treatment, One way ANOVA wit Tukey's post hoc where, *P<0.05, **P<0.01,

Basal ECAR in cells treated with H_2O_2 was slightly increased, and close to reach the significance, when compared to NG control (P=0.052), and statistically significant when compared to the basal in HG group (Fig.6.34). Increase in the basal glycolysis was not dose dependent. However, 5µM H_2O_2 caused a significant up-regulation of glycolytic rate after the injection of oligomycin when compared to the basal level (P<0.001, Fig.6.34).

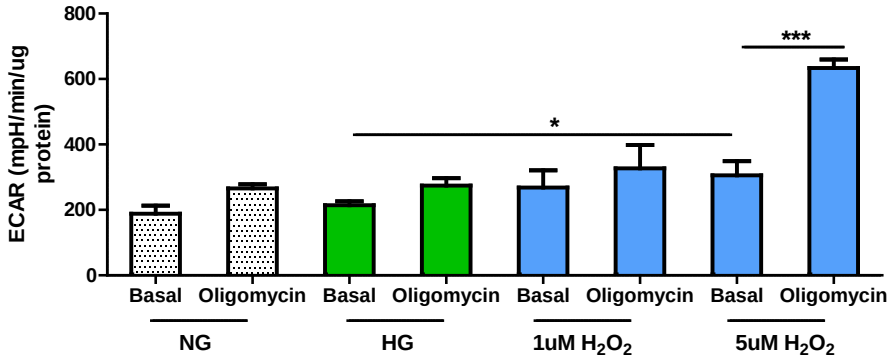

Fig.6.34. Glycolytic profile of human transformed tubular cells cultured in different conditions. Human mesangial cells were grown in 5mM (NG), 25mM (HG) for 8 days. On the day of the experiment of some the cells grown under the NG were treated with 1µM or 5µM H_2O_2 for 15min before the basal ECAR was assessed in Seahorse analyzer. Data shown as a mean ±SD, n=3-8, Mann-Whitney with Bonferroni's correction where *P<0.05, ***P<0.001

In summary, treatment with H_2O_2 had the same down-regulatory effect on basal and ATP-linked respiration in HK-2 cells as culture in HG. Maximal respiration and reserve capacity were also decreased. There was a trend towards the increase in proton leak, and an increase in maximal glycolytic capacity, which may suggest damage in the ETC caused by the exposure to H_2O_2.

6.4.8 Are glucose-induced changes in bioenergetic profile in tubular cells reversible?

It was shown in the previous paragraph that exposure of tubular cells to high glucose for 4 and 8 days significantly affects cells' mitochondrial respiratory function. To assess if these changes were permanent or possible reversible, a

'rescue' study was design, to test mitochondrial respiration in cells which were cultured in reversed media (25mM glucose media was substituted with 5mMglucose one, HG/NG). Two time points were used, cells were grown for 2 days ion HG and the media was changed to low glucose media for 2 days (HG2/NG2) and in the second time point, cells were grown under HG for 4 days and had the media reversed to normal glucose for 4 days (HG4/NG4). In control groups cells were cultured in 5mM glucose for 4 and 8 days respectively. Day before the assessment, cells were seeded in XF assay plates as described before, washed with XF assay media, and allowed to equilibrate at 37°C for 1h in a non-CO2 incubator before assessment.

As described previously cell cultured in HG for 4 days had a drastically reduced all of their bioenergetic parameters and as illustrated on Fig.6.35A, in HG2/NG2 group cell show the same profile as cells cultured in NG. However 2 day culture of the HK-2 cells in HG was not performed therefore it is difficult to assess how quickly these changes occur.

Prolonged culture in NG after HG treatment (HG4/NG4) did not improve mitochondrial respiratory function. As shown on Fig.6.35B, basal and ATP-link respiration was still reduced when compared to NG control ($P<0.001$, $P<0.01$ respectively). Maximal respiration and reserve capacity didn't get back to normal levels and was still highly significantly lower when compared to NG group ($P<0.001$). Interestingly proton leak in HG4/NG4 group was significantly lower than in cells cultured in HG for 8 days ($P<0.05$) (Fig.6.35 B).

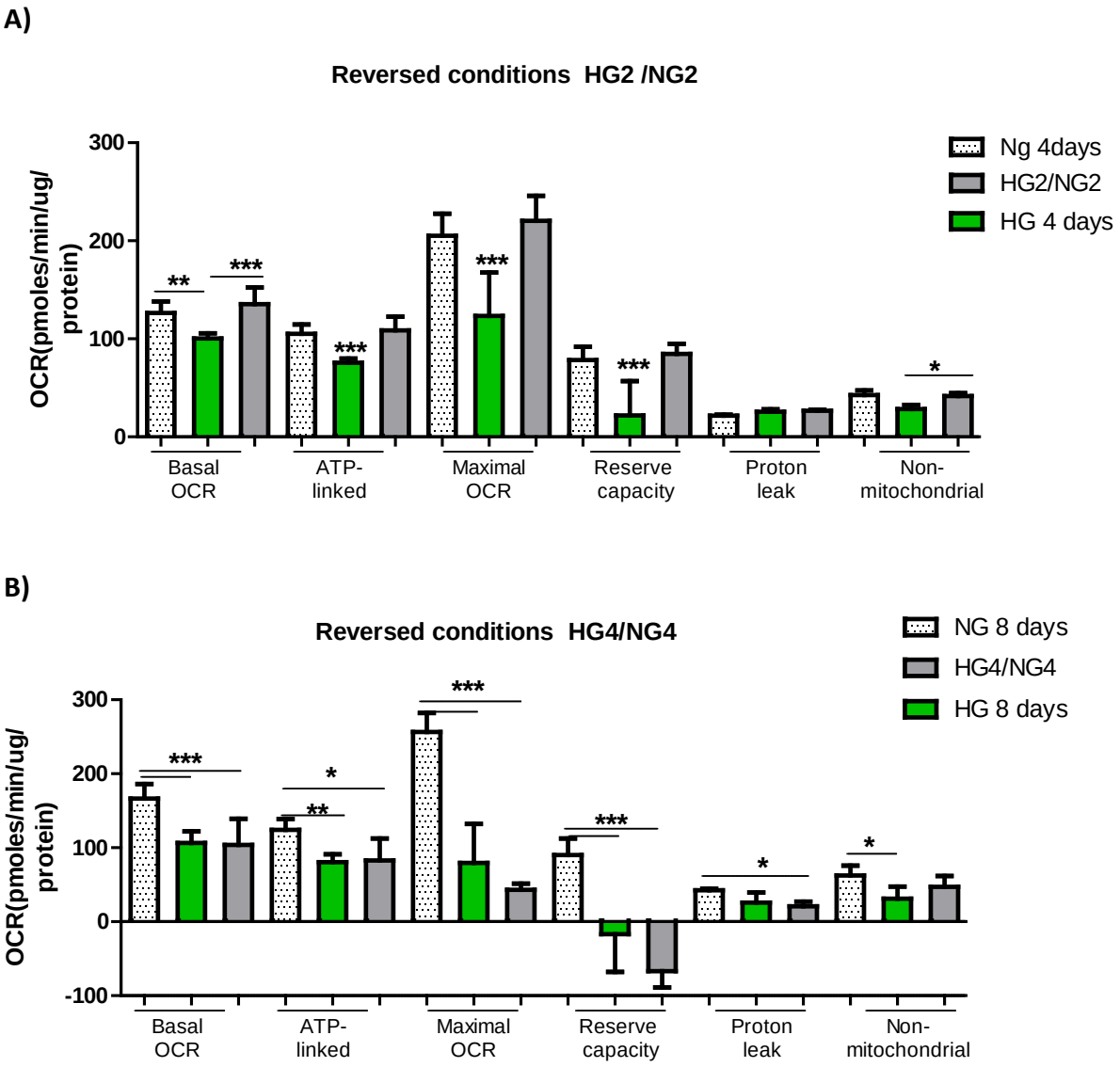

Fig.6.35. Reversing the culture conditions for 4 days had no effect on metabolic profile of human transformed tubular cells. Cells were grown in DMEM containing 5mM (NG), 25mM (HG)glucose for 4 days (A) or in NG and HG for 8 days (B). During the 4 day culture in HG, medium was changed to low glucose after 2 days (A). During 8 day culture, after4 days HG medium was replaced by 5mM one (B). Day before the assessment, cells were seeded at density of 25 000 cells/well in different media. OCR was assessed in Seahorse analyzer. Four measurement of basal OCR were taken, allowing measuring basal OCR. Following the injection of oligomycin (1µM final) assessment of ATP- linked respiration and proton leak were taken. To assess maximal respiration, FCCP was injected at the 0.3µM final concentration. All the parameters were calculated by subtracting non-mitochondrial values for each sample. Data shown as a mean ±SD, n=5-7 observations, One way ANOVA with Tukey's post hoc test where, *P<0.05, **P<0.01, ***P<0.001

Basal ECAR and ECAR after the injection of oligomycin were also assessed in reversal groups. There was no difference in basal ECAR and ECAR after the injection of oligomycin in HG2/NG2 and HG4/NG4 groups when compared to NG and HG groups (Analysis of variance, P>0.05, Fig.6.33A and Fig.6.33B). Injection of oligomycin caused a significant increase in ECAR in all groups (P<0.001, P<0.01, Fig.6.36).

A)

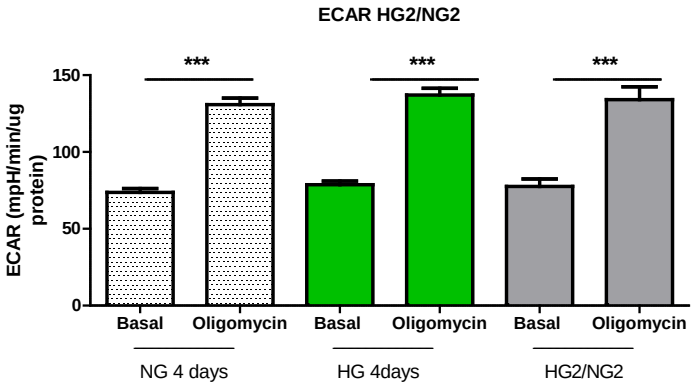

B)

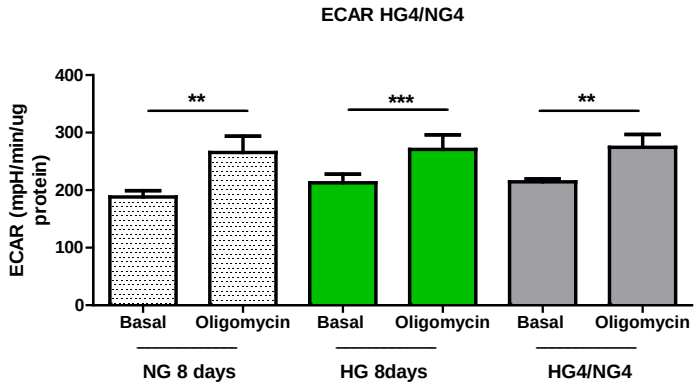

Fig.6.36. Glycolytic profile of human transformed tubular cells cultured in different conditions. HK-2 cells were grown in 5mM (NG), 25mM (HG) and HG/NG conditions for 4 (A) and 8days (B). Basal ECAR and ECAR after injection of oligomycin were assessed in Seahorse XF96^{e} analyzer. Data shown as a mean ±SD, n=5-10 for NG, n=5-6 for HG and n=8-15 observations for HG/NG, Student's t-test where, *P<0.05, ** P<0.01

Mean basal ECAR versus OCR ratio in cells from HG2/NG2 showed slightly improved profile when compared to cells cultured in HG for 4 days (Fig. 6.37A). However in HG4/NG4 group, there was no beneficial effect of media reversal on

OCR/ECAR ratio. Cell in HG4/NG 4 had the same metabolic profile as cells grown in HG for 8 days (Fig.6.37B).

A)

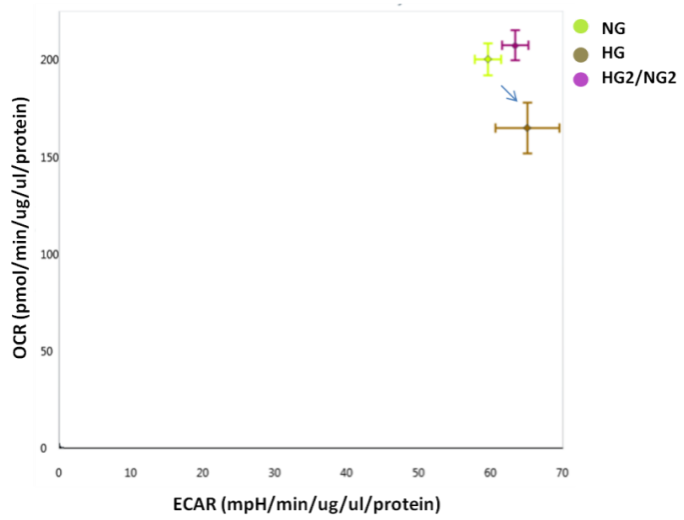

B)

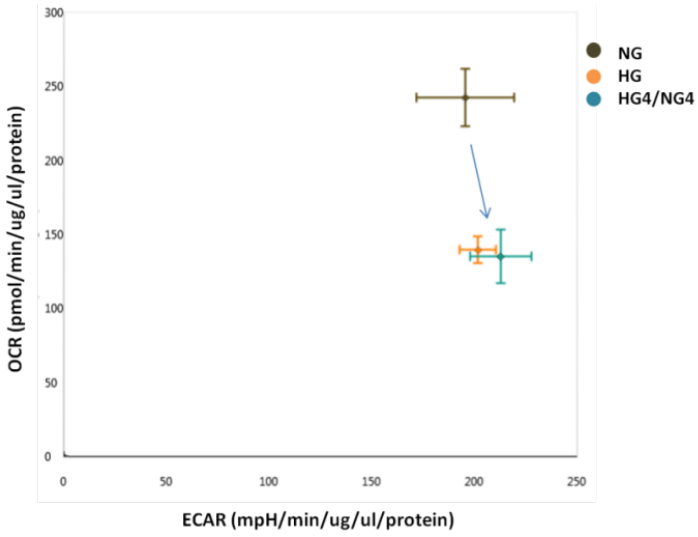

Fig.6.37. The oxygen consumption rate (OCR) and glycolysis (ECAR) of human tubular cells. The mean basal OCR vs. basal ECAR in cells in DMEM containing 5mM (NG), 25mM (HG) glucose and 25/5 mM glucose (HG/NG) for 4 days (A) and 8 days (B). Arrow points a metabolic shift in energy in cells grown in HG and then when media was reversed to NG. Data shown as a mean ±SEM, n=5-15 observations

6.5 Discussion

Since kidney cells are exposed to both, ROS and hyperglycaemia in the course of diabetic kidney disease, I hypothesized that their bioenergetic profile would be affected by the exposure to the high glucose and H_2O_2. By using two different kidney cell types, I have shown a damaging effect of hyperglycaemia on HMCs and HK-2 cells, and the effect of oxidative stress on HK-2 cells mitochondrial respiratory function. To my knowledge, this is the first study assessing bioenergetic profile of primary human mesangial cells (HMCs) and immortalized tubular cells (HK-2) grown in various concentrations of glucose.

Bioenergetic profile of mesangial and tubular cells was negatively affected by the exposure to high glucose. Tubular cells proved to be more susceptible to hyperglycaemia, while mesangial cells showed significant down-regulation of their respiratory function after chronic exposure to high glucose. HMCs data was confirmed by independent experiments using two different Seahorse analyzers, XF^e96 (presented in this chapter) and XF^e24 (data presented in the Appendix III).

Prolonged (8 and 12 days) exposure to the hyperglycaemia had significant down-regulatory effect on mesangial cells' maximal respiration and spare capacity. Moreover after chronic, 12 day exposure to high glucose, basal and ATP-respiration was also affected. There was no difference in the proton leak at any of the investigated time-points, but there was observed a tendency for the increase levels of the proton leak in cells incubated in high glucose. Interestingly, chronic exposure to hyperglycaemia caused also a down-regulation of the ECAR at the basal rate, and in response to the oligomycin injection in HMCs, which might suggest a glycolytic block, possibly through GAPDH inhibition or by increased production of ROS (Brownlee, 2005, Colussi et al., 2000). Second type of the cells used in experiments, tubular cells proved to be highly sensitive to the high glucose treatment with decreased basal, ATP-linked and maximal respiration observed as early as after 4 days of the treatment. More significant effect was found after 8 days of the culture in high glucose, when mitochondria lost completely their reserve capacity. No difference in the proton leak was observed in any of the investigated time point, but tubular cells had also

decreased non-mitochondrial respiration when exposed to high glucose. This result may suggest potential antioxidant defence activation, which was previously observed in human endothelial cells cultured in 20mM glucose (Fiumicino et al., 2000).

To my knowledge this the first report of human kidney cells' mitochondrial dysfunction, assessed by the measurement of cellular bioenergetics in response to the culture in high glucose. The reports in the literature are either in accordance or contrary to our results, but none of the studies was performed in the same experimental design. Chacko et al., (2010) reported down-regulation of the mitochondrial function (including reduced ATP-linked respiration and reserve capacity) in primary mouse mesangial cells cultured for 14 days in high glucose (Chacko et al., 2010a). Trudeau at al., (2010) assessed mitochondrial bioenergetics in rat retinal endothelial cells cultured for 3 and 6 days in 30mM glucose. In their experimental design they observed a reduction in the basal and maximal respiration, but after prolonged, 6 day exposure. They also reported a compensatory increase in ECAR after 6 days of culture which is in accordance to the result observed in tubular cells and contrary to the mesangial cells reported in this study (Trudeau et al., 2010). Faulty bioenergetic profile of cultured neurons derived from STZ- induced rats with decreased maximal respiration and decreased spare capacity was also reported (Chowdhury et al., 2013).

On the other hand, results in the current study are contrary to the findings published by Stieger at al., (2011) who demonstrated an increase in the basal and maximal respiration of immortalized mouse podocytes cultured in high glucose for 10 passages. However, the discrepancy in the results might be caused by the lack of the normalization of the Seahorse data, as the authors suggested there were differences in the plated cell numbers between experimental groups and also reported in parallel a decrease in the complex I and III activities, which is contrary to oxygen consumption rate data (Stieger et al., 2012).

When comparing results from the human studies, increased mitochondrial basal, and maximal respiration rate were found in peripheral blood mononuclear cells (PBMCs) from patients with T2D, when compared to the healthy controls

(Hartman et al., 2014). This report might suggest an adaptive response in mitochondrial respiration in order to cope with nutrient overload.

Not every patient suffering with diabetes will develop diabetic complications and increase in maximal and basal respiration which is still within threshold limit for mitochondria without diminishing spare respiratory capacity may be still tolerable. In contrary, Fink at al., (2012) did not observe any changes in the bovine aortic endothelial cells and human platelets cultured in high glucose for 18 hours and also after acute injection of the high glucose (Fink et al., 2012). Mitochondrial respiration has also been reported to be reduced in the skeletal muscle of T2DM patients (Kelley et al., 2002, Mogensen et al., 2007) and not changed in myocytes from non-diabetic, obese subjects with family history of T2D (Aguer et al., 2013).

I also observed a metabolic shift in cellular bioenergetic of human mesangial cells after prolonged exposure to hyperglycaemia, suggesting that cells become less metabolically active in hyperglycaemia. The shift in the metabolism observed in mesangial cells was not so visible in tubular cells. On the other hand tubular cells had also basal glycolytic rate increased when cultured in high glucose, which in correlation with their falling mitochondria function might suggest and adaptive response to the condition when cells cannot rely on their OXPHOS energy. These results were surprising as tubular cells are known to have low glycolytic capacity (Wirthensohn and Guder, 1986), and it only highlights the differences in the response to the stress conditions between different cell types, even within one organ.

I have also tested an effect of the acute stress conditions on cells respiration, with cells treated with two concentrations of H_20_2 prior the assessment, and also by using acute injection of 20mM glucose during the assessment. Although these experiments were performed only once and require repeating, data which were obtained are very interesting. Treatment with H_20_2 proved to be problematic as both, mesangial and tubular cells demonstrated high sensitivity to even short exposure to the H_20_2, which caused cell detachment. Finally very low concentration was chosen, and exposure time was shorten to 5 minutes. Cells

were allow to recover after the treatment for about 1 h. Short exposure of HMCs to the oxidative stress with pre-treatment of the H_2O_2 had no effect on any of the measured mitochondrial respiration parameters bud it did significantly up-regulated the glycolysis. However data from the tubular cells treated with H_2O_2, suggest that tubular cells are very susceptible to any form of the oxidative stress. Short exposure to H_2O_2 had the same inhibitory effect on tubular cells' mitochondrial respiration as culture in high glucose for 8 days, decreasing basal and ATP-linked respiration. However, there was no difference in the reserve capacity, but glycolysis rate was significantly up-regulated.

These data may suggest a potential damage of H_2O_2 to ETC and compensatory response in the induction of glycolysis. Contrary to my results, Sansbury at al., (2011), reported an increase in the oxygen consumption in mouse and rat cardiomyocytes, but also a decrease in respiration in smooth muscle cells following the cells' exposure to a lipid peroxidation product (Sansbury et al., 2011). However, Dranka et al., (2010) observed a decreased mitochondrial reserve capacity in the adherent bovine aortic endothelial cells in response to NO or another stressor, 2,3-dimethoxy-1,4-napthoquinone (DMNQ) treatment. When compounds were used separately they had no impact on basal mitochondrial respiration and reversible effect on mitochondrial maximal respiration however combination of both caused a permanent damage to mitochondrial which led to cell death (Dranka et al., 2010). In another study the same group observed in primary rat myocytes a dose- and time-dependent increase in OCR and in ECAR in response to the reactive lipid species, but a reduction in the OCR and ECAR after using the same prooxidant agents in mouse mesangial cells (Dranka et al., 2011).

These reports and results from current study highlight the differences in cells' metabolism and may explain different responses to the stressors.

Human primary mesangial cells proved to have a substantial bioenergetic reserve when compared to immortalized tubular cells. In the glucose-challenge experiment, where control and pre-treated cells mesangial cells were challenged with the injection of the 20mM glucose, a different response between the

groups to acute high glucose injection was observed. Acute injection of 20mM glucose to cells, which were cultured in normal glucose media, caused a 'metabolic switch' from OXPHOS respiration to the glycolysis. This was not seen when cells were pre-cultured in 25mM glucose and then injected with 20mM glucose during the assessment. Cells cultured in 5mM glucose showed a metabolic flexibility when injected with high glucose, while cells grown in the high glucose after the injection show no difference in the basal or ATP-linked respiration. These results suggest that cells with compromised bioenergetic profile are vulnerable to any secondary stressor. However, as shown on Fig.6.18, control traces show some difficluties with reaching steady state, which could possibly affect the results, especially ATP-linked and maximal respiration, if cells were 'stressed' prior to the glucose injection.

Data from the current study may suggest that in the conditions of chronic hyperglycaemia, cells which may have defective mitochondria cannot properly response to the changes in the glucose levels and this could lead to the possible disruption in glucose metabolism. The energetic state of the cells is important in cells' respiration and functions in healthy conditions and may be detrimental in hyperglycaemia. It has been shown in the Beta-cells, that proper activation of the mitochondrial respiration and later B-cells' insulin secretion due to the stimuli requires metabolically healthy mitochondria (Ortsater et al., 2002).

In the current study also the effect of a 'rescue experiment' on cells' bioenergetics was investigated. Cells were cultured in 25mM glucose and have their growth media changed to the one containing 5mM glucose. Results obtained from this part of the study in mesangial cells, suggested that toxic effect of hyperglycaemia on OCR and ECAR can be reverted by correcting the glucose levels; however the outcome of was dependent on the time of exposure of the cells to high glucose prior to media change.

In similar manner to the mesangial cells, after reversing the conditions in the tubular cells, there was observe a loss in the recovery which seem to correlate to the toxic effect of glucose after prolonged time of hyperglycaemia. A similar type of experiment was also performed in a rat pancreatic insulinoma cells that had

high glucose media reversed to the low one for 24 hours, where cells recovered they biological bioenergetic function (Spragg et al., 1985). Ruggiero at al., (2011) by using mitochondria isolated from diabetic mice observed an increased levels of mitochondrial superoxide dismutase (MnSOD) and increased mitochondrial ATP-linked respiration in animals kept for 12-weeks, which was not present at later stages, suggesting that there is an adaptive phase to the nutrient overload, but over time, mitochondria became exhausted and their function start to fail (Ruggiero et al., 2011).

Result shown in current study clearly suggest that high glucose had a toxic effect on kidney cell function however the mechanism by which it is caused is still not clear. Reserve capacity which was affected in the current study in cells exposed to high glucose describes bioenergetic mitochondrial reserve, and depends on many factors, like substrate supply, energy demand and integrity of ETC. Possible dysfunction in mitochondrial metabolism can be caused by the direct effect of glucose as described by others (Bickler et al., 1985, Spragg et al., 1985). But it also could be caused by the disruption the synthesis of mitochondrial complexes assembly subunit, caused by the mutations in MtDNA. I have shown in the previous chapters the increase in the rate of the damage in the MtDNA in mesangial cells cultured in high glucose as early as after 4 days, which precedes decline in the mitochondrial respiration.

In conclusion, I have shown that hyperglycaemia alters metabolic profile of both, mesangial and tubular cells and significantly affects their reserve capacity. Also mesangial cells proved to have a substantial bioenergetic reserve when compared to the tubular cells. Proper understanding of bioenergetic responses of different cell types to oxidative stress and nutrient overall, present in diabetes and its complications may give an insight into the development of novel therapies.

This study could be criticized for not using a specific kit in order to properly assess glycolytic function; however I am fully aware of this limitation. Also experiments on tubular cells should be repeated as they were performed only once. Fall in the reserve capacity which was observed in the tubular cells might

be also caused by toxic effect of oligomycin prior to the FCCP injection; therefore another set of experiments with FCCP only should be performed. 'Rescue' experiments with media change, need a further investigation and should be treated as a prelimary results. Future experiments which would involve mitochondrial specific antioxidant require optimization, there was an attempt to use MitoQ in this study however this compound proved to be very toxic to the cells, and cause cells death and detachment and needs further optimization.

Chapter 7
General discussion

7.1 General discussion

The expansion of extracellular matrix through induction of growth factors, increased ROS and chronic inflammation have all been reported in DN (Wada and Makino, 2013, Brownlee, 2001, Giacco and Brownlee, 2010). Is it possible, that dysfunction of this cell organelle, mitochondria is responsible for the activation of of these mechanisms? Between 30-40% of patients with diabetes will eventually develop DN (Singh et al., 2008, Wada and Makino, 2013, Rabol, 2011) and at present, 383 million people in the world are diagnosed with diabetes mellitus (WHO, 2013); it also accounts for more than 100 million people with chronic kidney disease.

Hyperglycaemia has been linked to increased oxidative stress in patients with diabetes and diabetic complications in peripheral blood cells (Lim et al., 2006, Madsen-Bouterse and Kowluru, 2008, Weng et al., 2009b), *in-vitro* cultured cells (Ha and Lee, 2003, Yao and Brownlee, 2010) and animal models of diabetes (Ruggiero et al., 2011, Chowdhury et al., 2010). There is some indirect evidence from human, animal and *in-vitro* studies, suggesting that mitochondria may be involved in the development of diabetic complications, including DN (Sharma et al., 2013, Higgins and Coughlan, 2014, Lee et al., 2014, Lee et al., 2003). Moreover, in several animal and human studies, it has been demonstrated that the increase in both ROS production and inflammation contributes to DN development (Wada and Makino, 2013, Navarro-Gonzalez and Mora-Fernandez, 2008, Catherwood et al., 2002, Ahad et al., 2014).

Based on the preliminary data from our group, the hypothesis was formed that altered MtDNA content may lead to mitochondrial dysfunction, which would contribute to the development of DN.

The studies presented in this thesis have explored the effect of hyperglycaemia on MtDNA biogenesis and mitochondrial function using *in-vitro* and *in-vivo* models of diabetes as an early event, occurring during the development of DN. It has been shown that MtDNA content is elevated in renal mesangial cells cultured in high glucose and also in peripheral blood from diabetic mice, but decreased in

the diabetic mouse kidneys. MtDNA quality, mitochondrial morphology and function were also altered in mesangial cells in response to chronic hyperglycaemia, while no change were observed in mitochondrial transcription and translation. The overall findings are summarised in Fig. 7.1.

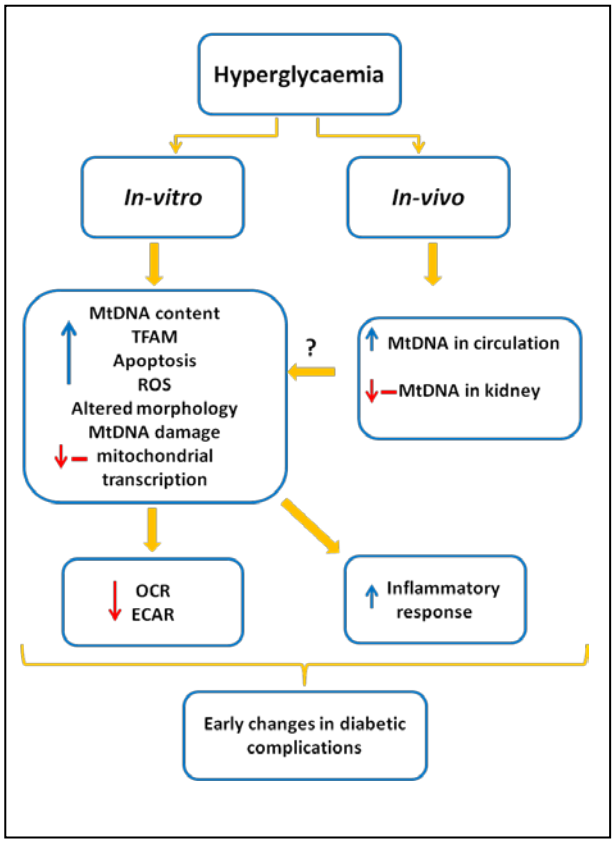

Fig. 7.1. Model arising from findings from this thesis. Hyperglycaemia leads to increased MtDNA content, altered mitochondrial morphology, increased intracellular reactive oxygen species (ROS) MtDNA damage and apoptosis in human mesangial cells. A decrease or no change in the mRNA expression of mitochondrial electron transport chain subunits was also observed. Molecular and physiological alterations lead to inflammation in mesangial cells. These changes precede the reduced respiration (OCR) and glycolysis (ECAR). There was also an increase in MtDNA content in the peripheral blood and decrease/no change in MtDNA copy number in diabetic mouse kidneys, which may be affected by processes observed in the *in-vitro* study. ↑: increase; ↓: decrease; –: no change

Mitochondrial biogenesis

In the current study, it was reported for the first time, increased MtDNA content in human mesangial cells exposed to hyperglycaemia, with the increase in MtDNA copy number observed as early as 24h following incubation in high glucose. To my knowledge, this is also the first report of the measurement of MtDNA content in circulating cells in mouse blood. The MtDNA copy number was significantly up-regulated in the circulation but either no difference or a reduction in mouse kidneys was observed. The decrease of MtDNA in the mouse kidneys may be caused by the increased mitophagy or apoptosis (both induced in diabetes) (Lim et al., 2014b, Osorio, 2014, Liu et al., 2014)) or by release of

mitochondria and MtDNA into the circulation, caused by kidney cell apoptosis or necrosis (Zhang et al., 2010a).

An increase in MtDNA could be beneficial at the early stages and an adaptive response to the nutrient overload or it could be the compensatory effect to the increased oxidative stress. In patients with DN, it was shown that increased MtDNA copy number in peripheral blood was associated with lower prevalence of microalbuminuria (Lee et al., 2009). A study by Ying Sun et al., (2014) reported, that treatment with rotenone (complex I blocker) in mouse model of kidney interstitial fibrosis, improved kidney function and morphology, decreased inflammatory markers and increased MtDNA levels. Data from this study suggest that once mitochondria dysfunction occurs, it activates many pathways and keeps contributing to ROS production and pathology of the disease (Sun et al., 2014).

Oxidative stress and its consequences

Tissue oxidative stress has been proposed to be a major contributor in the development of DN (Brownlee, 2005, Forbes et al., 2008, Coughlan et al., 2009). It has been demonstrated in chapter 5 of this thesis, that increased MtDNA content in mesangial cells correlate with increase ROS and apoptosis. Moreover, when MtDNA integrity was measured, the ratio of mutated MtDNA in cells incubated in high glucose was significantly up-regulated. This result explains why there was no difference in mitochondrial protein levels and also mitochondrial mRNAs were either not changed or down-regulated. These data taken together, suggest that although MtDNA was increased, it was not functional and could not be transcribed and translated into functional OXPHOS subunits.

High glucose has also been shown to cause damage in nDNA and dys-regulation of the expression of nDNA repair system, called base excision repair (BER) genes, which have been shown to be up-regulated in the early stages of hyperglycaemia, but decreased after the chronic exposure (Pang et al., 2012). The BER system has been characterised in MtDNA (Bohr, 2002, Croteau and

Bohr, 1997), but has not been extensively investigated and there are no reports about BER activation in cells exposed to hyperglycaemia.

Mutated MtDNA background can have an effect on susceptibility to the development of diabetes complications. Lazar and colleagues have shown that diabetic rodents with mutated MtDNA were more likely to develop myocardial dysfunction. Moreover, rats with mutated MtDNA had lower ATP production, while this did not exhibit any other physiological changes in their myocardium (Sethumadhavan et al., 2012).

Mitochondrial function

As shown in chapter 6, mitochondrial function was severely affected by hyperglycaemia in both mesangial and tubular cells. This is the first report of the measurement of mitochondrial bioenergetics in human mesangial and tubular cells, and our data are in accordance with the reports in different cell types and models of diabetes including rat retinal cells (Trudeau et al., 2010), mitochondria from rat kidneys (Ruggiero et al., 2011, Chacko et al., 2010b) and muscle mitochondria from patients with T2D (Rabol, 2011) .

OCR is proportional to the rate of transferred electrons and influence of the redox status of the ETC. In conditions of lower mitochondria respiration there is an increased generation of ROS mostly at complex I and III, caused by a reduction of ETC (Wani et al., 2007, Starkov and Fiskum, 2003). Lower *in- vivo* mitochondrial "function" can be the result of several factors, including a reduced mitochondrial density, but also, lower mitochondrial respiratory capacity per mitochondrion. In healthy conditions, the amount of MtDNA is proportionally correlated with mitochondrial function as well as the number of mitochondria and is flexibly regulated due to the energy metabolism demand and redox state of the tissues (Williams, 1986, Hock and Kralli, 2009). However, this does not seem to be the case in disease state. As early as 1979, Simpson and Hecker (1979), proposed that any disturbances in metabolic substrates in acute acidosis (which is associated with DN), would initially lead to flexible changes in mitochondria adapting to new conditions, but eventually would cause a

permanent changes in a substrate shift from the cytoplasm into mitochondria (Simpson and Hecker, 1979). Kidney cells require large amounts of energy in the form of ATP, which is used for active transport of metabolites (Brown and Breton, 1996, Hall et al., 2008).

However, we observed a significant increase in the ratio of mutated MtDNA fragments in mesangial cells, exposed to the high glucose. Energy production in the kidneys, which contain many mitochondria, is largely through respiration, and Warburg demonstrated that the total energy production in quiescent kidney cells was surprisingly similar to that produced in proliferating cancer cells, which indicated how much energy these cells require for proper function (Rocco et al., 1992). The results from my study, clearly suggests that high glucose has a toxic effect on kidney cell function, however the mechanism by which it is caused is still not clear.

It could possibly be caused by the direct effect of glucose, as described by Gohring et al., using rat pancreatic insulinoma, cultured for 48h in either high glucose or high pyruvate, had different responses to the treatment. Cells cultured in high glucose had their bioenergetic profile affected, while there was no difference observed in the mitochondrial respiration when cells were grown in the pyruvate. This suggests a specific toxic effect of glucose on other metabolic pathways within the cells (Gohring et al., 2014).

Glucose is known for causing specific protein modifications (oxidized glycosylations), which can have a detrimental effect on mitochondrial function and life cycle, through modification of mitochondria-localised proteins, involved in the respiratory chain and the TCA cycle (Tan et al., 2014). Gu at al., proposed that one of the O-linked-β-N-acetyl glucosamine (O-GlcNAcylation) modied glucose proteins, O-GlCNAc, can directly modify mitochondrial protein phosphorylation, contributing to mitochondrial dysfunction and insulin resistance (Gu et al., 2011). Increased mitochondrial O-GlcNAcylation in cardiac myocytes, incubated in high glucose also correlated with decreased activity of mitochondrial complexes (Hu et al., 2009).

However, another possible explanation is the activation of the pathways caused by the nutrient overload, when mitochondria might, through an adaptive phase, increase their respiration and contribute to the increased ROS production. Anderson at al., reported increased mitochondrial H_2O_2 production in human and rodent muscles fed with high fat diets, which correlated with a shift in cellular redox balance, without any changes in mitochondrial respiration. The oxidation state of the cells was balanced following treatment of mitochondrial specific antioxidants (Anderson et al., 2009).

The 'Crabtree effect' may also have an inhibitory effect on mitochondrial respiration, when glycolytic enzymes compete with mitochondria for cytoplasmic ADP. Fructose 1,6-biphospate (F16bP) under physiological conditions, induces a decrease in mitochondrial respiration, though blockage of complexes III and IV (Diaz-Ruiz et al., 2008). However, in the current study, as observed by a metabolic shift, cells cultured in the high glucose, also had their glycolysis decreased, which suggests a glycolytic block occurring during prolonged culture in hyperglycaemia, possibly due to the direct effect of ROS (Colussi et al., 2000).

Inflammation

Damaged mitochondria undergo fission and are degraded via mitophagy (Twig and Shirihai, 2011, Ashrafi and Schwarz, 2013), but under oxidative stress, damaged mitochondria and MtDNA can accumulate in the cell (Scherz-Shouval and Elazar, 2007). Accumulation of damaged MtDNA may cause a chronic innate inflammatory response in the cell, through activation of TLR9, the receptor for microbial unmethylated CPG-DNA (Zhang et al., 2010a, Zhang et al., 2010b). In the current study, mRNA expression of NF-κB and MYD88 a TLR-9 signalling molecules were significantly up-regulated in mesangial cells, incubated in high glucose. This, with increased apoptosis in the cells, might suggest a potential inflammatory action of MtDNA. Not only MtDNA alone, but also whole mitochondria and mitochondrial proteins called mitochondrial Danger Associated Molecular Patterns (DAMPs) have the ability to start an inflammatory response. A study by Maeda and Fadell, has reported that mitochondria, which are released from cells, undergo TNF-α-induced necroptosis that eventually

contributes to necrosis. Data from this study suggested that mitochondria released into circulation can still respire and by the constant production of ATP can trigger inflammation (Maeda and Fadeel, 2014). Monocytes isolated from patients with myocardial infarction exhibit high levels of circulating plasma MtDNA, which correlates with increased susceptibility to infections (Fernandez-Ruiz et al., 2014).

Metabolic memory

The DCCT and EDIC studies have shown that intensive glycaemic control prevents the development and progression of diabetic complications in patients with diabetes (DCCT, 1993, de Boer and Group, 2014). Based on the results from these clinical trials a 'metabolic memory' phenomenon has been proposed, which describes the beneficial effects of immediate intensive treatment of hyperglycaemia (Ceriello, 2012, Aschner and Ruiz, 2012).

Reversal and glucose oscillation experiments in the current study have shown, that the glucose concentration and exposure time to hyperglycaemia affects MtDNA content and that this increase cannot be reverted after 4 days of treatment. These results may be caused by the hyperglycaemia-induced oxidative damage, Santos et al., reported that by extending the time of the exposure to oxidative stress, permanent damage in the MtDNA genome occurred, which correlated with loss of mitochondrial function in human fibroblasts (Santos et al., 2003). Glucose fluctuations have been also reported having an adverse effect on endothelial cells in the vascular system in diabetes (Azuma et al., 2006, Brownlee and Hirsch, 2006) and caused increased apoptosis in rat pancreatic Beta-cells (Kim et al., 2010). Rabol at el. (2011), used muscle mitochondria from T2D patients and did not observe a beneficial effect of short-term correction of glucose levels in mitochondrial OXPHOS activity (Rabol, 2011). A different report in a rodent model of diabetic retinopathy, has shown that normalizing glucose levels following 6 months exposure to hyperglycaemia, failed to reverse oxidative damage to MtDNA and mitochondrial function (Madsen-Bouterse et al., 2010). These studies only highlight the importance of the metabolic memory phenomenon in context of mitochondrial dysfunction,

where chronic hyperglycaemia can permanently damage and impair MtDNA and mitochondrial function.

Threshold effect

There is evidence for a heritable genetic susceptibility to DN, but most of the research reports concentrated on nDNA [reviewed in (Herrera and Coffman, 2012)], while the problem may actually lays in the MtDNA and accumulation of the MtDNA mutations. In normal tissues all MtDNA copies are identical (homoplasmy), but with any occurring mutations, a mix of normal and mutated forms of MtDNA present, contributes to heteroplasmy (Dimauro and Davidzon, 2005). Mitochondrial disease may become clinically apparent once the number of affected mitochondria reaches a certain level; this phenomenon is called the "threshold effect". MtDNA is non-Mendelian, maternally inherited, which means there is a possibility of accumulation of mutated MtDNA, which when exceeds the threshold, overcome the wild type MtDNA, potentially leading to disease state (Dimauro and Davidzon, 2005). This may be the reason why healthy lean offspring of T2D patients show signs of MtDNA deletion and mitochondrial dysfunction with MtDNA serving as an indicator for insulin sensitivity (Song et al., 2001, Morino et al., 2005). A minimum amount of the wild-type MtDNA is necessary for proper mitochondrial function (Navis et al., 2013). Therefore, when there is an imbalance between mutated and wild-type MtDNA molecules, with mutated MtDNA crossing the threshold, the overall imbalance in the cell redox status may occur, consequently affecting energy production (Wallace and Fan, 2010, Wallace et al., 2010). This could have a detrimental effect on disease progression, especially in highly energetic organs, like kidneys. A study using cybrids with common tRNA-3243G mutation (associated diabetes and autism, when 10-30% of mutation present) also demonstrated that MtDNA heteroplasmy can affect transcriptional reprogramming, but the effect is dependent on the ratio of the mutated to wild type MtDNA molecules (Picard et al., 2014). These data suggest that a small increase in mutant MtDNAs can contribute to relatively modest defects in oxidative capacity, but results in significant transitions in

cellular phenotype and gene expression, causing changes to mitochondrial function, structure and cell size (Picard et al., 2014).

Accumulation of MtDNA mutations can be tolerated for many years before reaching damaging levels (Chinnery et al., 2002), and a similar mechanism could possibly explain how diabetic complications develop over several years.

Interestingly, it has been also shown that MtDNA haplogroups are also important and may contribute to the susceptibility to certain diabetic complications, such as DN (Achilli et al., 2011), further implicating MtDNA involvement in the development of DN.

Application of the current findings to the clinical setting

Keeping mitochondria healthy in diabetes, in order to keep the balance and the control of the disease, require overcoming several problems including: keeping reliable and uncoupled energy supply and control ROS emissions from mitochondria. One of the solutions is the use of antioxidants, especially the ones that specifically target ROS produced by mitochondria. However, so far none of candidate antioxidant therapies tested in clinical trials have resulted in satisfactory improvement of the mitochondrial dysfunction (Kerr, 2013). This only highlights the importance of diagnosing mitochondrial dysfunction at the early stages.

Data from the current study suggest that the observed increase in MtDNA occurs earlier, before the mutations in MtDNA are present and much earlier than the observed fall in the mitochondria function, therefore the measurement of MtDNA in a clinical setting may be a reliable alternative to currently used markers to assess metabolic changes in patients with diabetes. Currently, it is impossible to distinguish patients with diabetes that subsequently develop DN from those that don't. Also, it is impossible to recognise DN at early stages; patients are diagnosed based on the serum AC ratio and presence of the protein in the urine, which are signs of the already failing kidney function.

A full and proper understanding of the bioenergetic responses of different cell types to oxidative stress and nutrients overall, present in diabetes and its complications may give and insight into novel therapies.

Future directions

Future studies may explore the protective role of the antioxidant system especially mitochondria targeted antioxidants like MitoQ, in order to see if hyperglycaemia-induced changes in MtDNA and mitochondria function can be avoided. Results from current studies suggest, that an increase in MtDNA content precede decreased mitochondrial function. A MtDNA assay may be an alternative technique to monitor patients with diabetes for risk of DN development, as currently no available markers allow diagnosis of the early stages of DN. However, a longitudinal study is needed in order to establish a correlation between MtDNA and failing kidney function in diabetic patients. Measurement of the MtDNA content can be combined with the measurement of mitochondria function, using patients' white blood cells and Seahorse analyzer. Data from our group has shown that patients with diabetes have increased maximal respiration (Czajka, Ajaz et al., submitted), which may be within their threshold limit, therefore monitoring ones mitochondrial health might help pick up pathological changes at an early stage of development. A Bioenergetic Health Index (BHI) formula has been introduced recently, which combines all OCR parameters and translates them into one value, which allow to measure how susceptible a person with diabetes can be used to developing metabolic stress (Chacko et al., 2014). MtDNA content combined with BHI may be a key into personalised medicine, which would be used as a diagnostic tool and help to optimise personalised treatment.

Conclusion

The importance of mitochondrial ROS in oxidative stress and the kidney is well established; mitochondrial targeted antioxidants ameliorate certain markers of renal damage (Chacko et al., 2010b). In the current report, it was demonstrated that hyperglycaemia-induced ROS led to the up-regulation of the MtDNA content

and mRNA expression of the genes involved in the TLR9 pathway, NF-KB and Myd88, suggesting increased inflammation. Cells started to display altered morphology within a few hours of exposure to high glucose, with mitochondrial fragmentation, which may be an attempt at the initiation of an adaptive biogenesis program, leading to increased MtDNA content. Chronic hyperglycaemia can 'overpower' antioxidant defences and lead to mutations in MtDNA, damage to mitochondria and cause mitochondrial dysfunction. Accumulation of damage MtDNA can trigger an inflammatory response, through the activation of TLR9 receptors and further contribute to tissue damage. These changes may result in damaged mitochondria, blocked mitochondrial transcription and translation and an energy deficit.

Data derived from primary mesangial cells and diabetic mouse models supports the hypothesis that glucose can lead to alterations in MtDNA and mitochondrial function. These data are representative of an early stage in diabetes.

The data obtained from my studies further highlights the enigma which is DN; it illustrates the importance of mitochondrial function in the development of diabetic complications. If decreasing mitochondrial function and MtDNA content is confirmed in longitudinal studies in patients with diabetes and DN and continues to be linked with the progression of the DN, then this could be used as potential predictors for the development of DN and help in the development of personalized treatment.

References

2011. Diagnosis and classification of diabetes mellitus. *Diabetes Care,* **34 Suppl 1,** S62-9.

Achilli, A., Olivieri, A., Pala, M., Hooshiar Kashani, B., Carossa, V., Perego, U. A., Gandini, F., Santoro, A., Battaglia, V., Grugni, V., Lancioni, H., Sirolla, C., Bonfigli, A. R., Cormio, A., Boemi, M., Testa, I.*, et al.* 2011. Mitochondrial DNA backgrounds might modulate diabetes complications rather than T2DM as a whole. *PLoS One,* **6,** e21029.

Affourtit, C. & Brand, M. D. 2008. Uncoupling protein-2 contributes significantly to high mitochondrial proton leak in INS-1E insulinoma cells and attenuates glucose-stimulated insulin secretion. *Biochem J,* **409,** 199-204.

Aguer, C., Pasqua, M., Thrush, A. B., Moffat, C., McBurney, M., Jardine, K., Zhang, R., Beauchamp, B., Dent, R., McPherson, R. & Harper, M. E. 2013. Increased proton leak and SOD2 expression in myotubes from obese non-diabetic subjects with a family history of type 2 diabetes. *Biochimica et biophysica acta,* **1832,** 1624-33.

Ahad, A., Ganai, A. A., Mujeeb, M. & Siddiqui, W. A. 2014. Ellagic acid, an NF-kappaB inhibitor, ameliorates renal function in experimental diabetic nephropathy. *Chem Biol Interact,* **219C,** 64-75.

Al-Kafaji, G. & Malik, A. N. 2010. Hyperglycemia induces elevated expression of thyroid hormone binding protein in vivo in kidney and heart and in vitro in mesangial cells. *Biochem Biophys Res Commun,* **391,** 1585-91.

Alberts, B., Johnson, A., Lewis, J., Raff, M., Roberts, K. & Walter, P. 2002. The mitochondrion. *Molecular Biology of the Cell. 4th edition, New York Garland Science*.

Alcolado, J. C., Laji, K. & Gill-Randall, R. 2002. Maternal transmission of diabetes. *Diabet Med,* **19,** 89-98.

Amaral, A., Ramalho-Santos, J. & St John, J. C. 2007. The expression of polymerase gamma and mitochondrial transcription factor A and the regulation of mitochondrial DNA content in mature human sperm. *Hum Reprod,* **22,** 1585-96.

American Diabetes Association 2014. Diagnosis and classification of diabetes mellitus. *Diabetes Care,* **37 Suppl 1,** S81-90.

Anderson, E. J., Lustig, M. E., Boyle, K. E., Woodlief, T. L., Kane, D. A., Lin, C. T., Price, J. W., 3rd, Kang, L., Rabinovitch, P. S., Szeto, H. H., Houmard, J. A., Cortright, R. N., Wasserman, D. H. & Neufer, P. D. 2009. Mitochondrial H2O2 emission and cellular redox state link excess fat intake to insulin resistance in both rodents and humans. *J Clin Invest,* **119,** 573-81.

Armitage, J. A., Poston, L. & Taylor, P. D. 2008. Developmental origins of obesity and the metabolic syndrome: the role of maternal obesity. *Front Horm Res,* **36,** 73-84.

Artal-Sanz, M. & Tavernarakis, N. 2009. Prohibitin and mitochondrial biology. *Trends Endocrinol Metab,* **20,** 394-401.

Asaba, K., Tojo, A., Onozato, M. L., Goto, A., Quinn, M. T., Fujita, T. & Wilcox, C. S. 2005. Effects of NADPH oxidase inhibitor in diabetic nephropathy. *Kidney Int,* **67,** 1890-8.

Aschner, P. J. & Ruiz, A. J. 2012. Metabolic memory for vascular disease in diabetes. *Diabetes technology & therapeutics,* **14 Suppl 1,** S68-74.

Ashrafi, G. & Schwarz, T. L. 2013. The pathways of mitophagy for quality control and clearance of mitochondria. *Cell Death Differ,* **20,** 31-42.

Asmann, Y. W., Stump, C. S., Short, K. R., Coenen-Schimke, J. M., Guo, Z., Bigelow, M. L. & Nair, K. S. 2006. Skeletal muscle mitochondrial functions, mitochondrial DNA copy numbers, and gene transcript profiles in type 2 diabetic and nondiabetic subjects at equal levels of low or high insulin and euglycemia. *Diabetes,* **55,** 3309-19.

Azuma, K., Kawamori, R., Toyofuku, Y., Kitahara, Y., Sato, F., Shimizu, T., Miura, K., Mine, T., Tanaka, Y., Mitsumata, M. & Watada, H. 2006. Repetitive fluctuations in blood glucose enhance monocyte adhesion to the endothelium of rat thoracic aorta. *Arterioscler Thromb Vasc Biol,* **26,** 2275-80.

Bai, R. K., Chang, J., Yeh, K. T., Lou, M. A., Lu, J. F., Tan, D. J., Liu, H. & Wong, L. J. 2011. Mitochondrial DNA content varies with pathological characteristics of breast cancer. *J Oncol,* **2011,** 496189.

Ballinger, S. W., Patterson, C., Yan, C. N., Doan, R., Burow, D. L., Young, C. G., Yakes, F. M., Van Houten, B., Ballinger, C. A., Freeman, B. A. & Runge, M. S. 2000. Hydrogen peroxide- and peroxynitrite-induced mitochondrial DNA damage and dysfunction in vascular endothelial and smooth muscle cells. *Circ Res,* **86,** 960-6.

Barbalat, R., Ewald, S. E., Mouchess, M. L. & Barton, G. M. 2011. Nucleic acid recognition by the innate immune system. *Annu Rev Immunol,* **29,** 185-214.

Barrientos, A., Casademont, J., Cardellach, F., Estivill, X., Urbano-Marquez, A. & Nunes, V. 1997. Reduced steady-state levels of mitochondrial RNA and increased mitochondrial DNA amount in human brain with aging. *Brain Res Mol Brain Res,* **52,** 284-9.

Bashan, N., Kovsan, J., Kachko, I., Ovadia, H. & Rudich, A. 2009. Positive and negative regulation of insulin signaling by reactive oxygen and nitrogen species. *Physiol Rev,* **89,** 27-71.

Bellance, N., Lestienne, P. & Rossignol, R. 2009. Mitochondria: from bioenergetics to the metabolic regulation of carcinogenesis. *Front Biosci (Landmark Ed),* **14,** 4015-34.

Berg, J. M., Tymoczko, J. L. & Stryer, L. 2002. Each Organ Has a Unique Metabolic Profile, in W.H. Freeman (ed). *Biochemistry, 5th edition,* **New York**.

Bickler, P. E., Spragg, R. G., Hartman, M. T. & White, F. N. 1985. Distribution of ventilation in American alligator Alligator mississippiensis. *Am J Physiol,* **249,** R477-81.

Bjerke, M., Franco, M., Johansson, M., Balzarini, J. & Karlsson, A. 2008. Increased mitochondrial DNA copy-number in CEM cells resistant to delayed toxicity of 2',3'-dideoxycytidine. *Biochem Pharmacol,* **75,** 1313-21.

Blake, R. & Trounce, I. A. 2014. Mitochondrial dysfunction and complications associated with diabetes. *Biochim Biophys Acta,* **1840,** 1404-12.

Blokhin, A., Vyshkina, T., Komoly, S. & Kalman, B. 2008. Variations in mitochondrial DNA copy numbers in MS brains. *J Mol Neurosci,* **35,** 283-7.

Bogacka, I., Xie, H., Bray, G. A. & Smith, S. R. 2005. Pioglitazone induces mitochondrial biogenesis in human subcutaneous adipose tissue in vivo. *Diabetes,* **54,** 1392-9.

Bogenhagen, D., Gillum, A. M., Martens, P. A. & Clayton, D. A. 1979. Replication of mouse L-cell mitochondrial DNA. *Cold Spring Harb Symp Quant Biol,* **43 Pt 1,** 253-62.

Bohle, A., Wehrmann, M., Bogenschutz, O., Batz, C., Muller, C. A. & Muller, G. A. 1991. The pathogenesis of chronic renal failure in diabetic nephropathy. Investigation of 488 cases of diabetic glomerulosclerosis. *Pathol Res Pract,* **187,** 251-9.

Bohr, V. A. 2002. Repair of oxidative DNA damage in nuclear and mitochondrial DNA, and some changes with aging in mammalian cells. *Free Radic Biol Med,* **32,** 804-12.

Bonnard, C., Durand, A., Peyrol, S., Chanseaume, E., Chauvin, M. A., Morio, B., Vidal, H. & Rieusset, J. 2008. Mitochondrial dysfunction results from oxidative stress in the skeletal muscle of diet-induced insulin-resistant mice. *J Clin Invest,* **118,** 789-800.

Boyle, J. P., Honeycutt, A. A., Narayan, K. M., Hoerger, T. J., Geiss, L. S., Chen, H. & Thompson, T. J. 2001. Projection of diabetes burden through 2050: impact of

changing demography and disease prevalence in the U.S. *Diabetes Care,* **24,** 1936-40.

Brand, M. D. & Nicholls, D. G. 2011. Assessing mitochondrial dysfunction in cells. *Biochem J,* **435,** 297-312.

Brooks, C., Wei, Q., Cho, S. G. & Dong, Z. 2009. Regulation of mitochondrial dynamics in acute kidney injury in cell culture and rodent models. *J Clin Invest,* **119,** 1275-85.

Brosius, F. C., 3rd, Alpers, C. E., Bottinger, E. P., Breyer, M. D., Coffman, T. M., Gurley, S. B., Harris, R. C., Kakoki, M., Kretzler, M., Leiter, E. H., Levi, M., McIndoe, R. A., Sharma, K., Smithies, O., Susztak, K., Takahashi, N*., et al.* 2009. Mouse models of diabetic nephropathy. *J Am Soc Nephrol,* **20,** 2503-12.

Brosius, F. C., Khoury, C. C., Buller, C. L. & Chen, S. 2010. Abnormalities in signaling pathways in diabetic nephropathy. *Expert Rev Endocrinol Metab,* **5,** 51-64.

Brown, D. & Breton, S. 1996. Mitochondria-rich, proton-secreting epithelial cells. *J Exp Biol,* **199,** 2345-58.

Brownlee, M. 2001. Biochemistry and molecular cell biology of diabetic complications. *Nature,* **414,** 813-20.

Brownlee, M. 2005. The pathobiology of diabetic complications: a unifying mechanism. *Diabetes,* **54,** 1615-25.

Brownlee, M. & Hirsch, I. B. 2006. Glycemic variability: a hemoglobin A1c-independent risk factor for diabetic complications. *JAMA,* **295,** 1707-8.

Caimari, A., Oliver, P., Keijer, J. & Palou, A. 2010. Peripheral blood mononuclear cells as a model to study the response of energy homeostasis-related genes to acute changes in feeding conditions. *OMICS,* **14,** 129-41.

Carugno, M., Pesatori, A. C., Dioni, L., Hoxha, M., Bollati, V., Albetti, B., Byun, H. M., Bonzini, M., Fustinoni, S., Cocco, P., Satta, G., Zucca, M., Merlo, D. F., Cipolla, M., Bertazzi, P. A. & Baccarelli, A. 2012. Increased mitochondrial DNA copy number in occupations associated with low-dose benzene exposure. *Environ Health Perspect,* **120,** 210-5.

Catherwood, M. A., Powell, L. A., Anderson, P., McMaster, D., Sharpe, P. C. & Trimble, E. R. 2002. Glucose-induced oxidative stress in mesangial cells. *Kidney Int,* **61,** 599-608.

Ceriello, A. 2009. Hypothesis: the "metabolic memory", the new challenge of diabetes. *Diabetes research and clinical practice,* **86 Suppl 1,** S2-6.

Ceriello, A. 2012. The emerging challenge in diabetes: The "metabolic memory". *Vascular pharmacology*.

Chacko, B. K., Kramer, P. A., Ravi, S., Benavides, G. A., Mitchell, T., Dranka, B. P., Ferrick, D., Singal, A. K., Ballinger, S. W., Bailey, S. M., Hardy, R. W., Zhang, J., Zhi, D. & Darley-Usmar, V. M. 2014. The Bioenergetic Health Index: a new concept in mitochondrial translational research. *Clinical science,* **127,** 367-73.

Chacko, B. K., Kramer, P. A., Ravi, S., Johnson, M. S., Hardy, R. W., Ballinger, S. W. & Darley-Usmar, V. M. 2013. Methods for defining distinct bioenergetic profiles in platelets, lymphocytes, monocytes, and neutrophils, and the oxidative burst from human blood. *Lab Invest,* **93,** 690-700.

Chacko, B. K., Reily, C., Benavides, C. A., Johnson, M. S. & Darley-Usmar, V. M. 2010a. Chronic hyperglycemia-induced attenuation of mitochondrial reserve capacity mediates mesangial cell dysfunction in diabetes. *UAB, Retrived from http://www.seahorsebio.com/resources/posters/2010-11-17_chacko_chronic_hyperclycemia-induced.pdf*.

Chacko, B. K., Reily, C., Srivastava, A., Johnson, M. S., Ye, Y., Ulasova, E., Agarwal, A., Zinn, K. R., Murphy, M. P., Kalyanaraman, B. & Darley-Usmar, V. 2010b. Prevention of diabetic nephropathy in Ins2(+/)(-)(AkitaJ) mice by the mitochondria-targeted therapy MitoQ. *Biochem J,* **432,** 9-19.

Chan, D. C. 2006. Mitochondria: dynamic organelles in disease, aging, and development. *Cell,* **125,** 1241-52.

Chang-Liu, C. M. & Woloschak, G. E. 1997. Effect of passage number on cellular response to DNA-damaging agents: cell survival and gene expression. *Cancer Lett,* **113,** 77-86.

Chen, H. & Chan, D. C. 2009. Mitochondrial dynamics--fusion, fission, movement, and mitophagy--in neurodegenerative diseases. *Hum Mol Genet,* **18,** R169-76.

Chen, J. B., Lin, T. K., Liou, C. W., Liao, S. C., Lee, L. C., Wang, P. W. & Tiao, M. M. 2008. Correlation of oxidative stress biomarkers and peritoneal urea clearance with mitochondrial DNA copy number in continuous ambulatory peritoneal dialysis patients. *Am J Nephrol,* **28,** 853-9.

Chen, N., Leng, Y. P., Xu, W. J., Luo, J. D., Chen, M. S. & Xiong, Y. 2011. Contribution of endogenous inhibitor of nitric oxide synthase to hepatic mitochondrial dysfunction in streptozotocin-induced diabetic rats. *Cell Physiol Biochem,* **27,** 341-52.

Chene, G., Amellal, B., Pedrono, G., Gourlain, K., Rancinan, C., Journot, V., Cotte, L., Palmer, P., Castro, N. D., Calvez, V. & Molina, J. M. 2007. Changes in the peripheral blood mtDNA levels in naive patients treated by different nucleoside reverse transcriptase inhibitor combinations and their association with subsequent lipodystrophy. *AIDS Res Hum Retroviruses,* **23,** 54-61.

Chien, M. C., Huang, W. T., Wang, P. W., Liou, C. W., Lin, T. K., Hsieh, C. J. & Weng, S. W. 2012. Role of mitochondrial DNA variants and copy number in diabetic atherogenesis. *Genet Mol Res,* **11,** 3339-48.

Chinnery, P. F., Samuels, D. C., Elson, J. & Turnbull, D. M. 2002. Accumulation of mitochondrial DNA mutations in ageing, cancer, and mitochondrial disease: is there a common mechanism? *Lancet,* **360,** 1323-5.

Choi, Y. S., Kim, S. & Pak, Y. K. 2001. Mitochondrial transcription factor A (mtTFA) and diabetes. *Diabetes Res Clin Pract,* **54 Suppl 2,** S3-9.

Choi, Y. S., Lee, K. U. & Pak, Y. K. 2004. Regulation of mitochondrial transcription factor A expression by high glucose. *Annals of the New York Academy of Sciences,* **1011,** 69-77.

Chowdhury, S. K., Smith, D. R. & Fernyhough, P. 2013. The role of aberrant mitochondrial bioenergetics in diabetic neuropathy. *Neurobiol Dis,* **51,** 56-65.

Chowdhury, S. K., Zherebitskaya, E., Smith, D. R., Akude, E., Chattopadhyay, S., Jolivalt, C. G., Calcutt, N. A. & Fernyhough, P. 2010. Mitochondrial respiratory chain dysfunction in dorsal root ganglia of streptozotocin-induced diabetic rats and its correction by insulin treatment. *Diabetes,* **59,** 1082-91.

Chua, S. C., Jr., Chung, W. K., Wu-Peng, X. S., Zhang, Y., Liu, S. M., Tartaglia, L. & Leibel, R. L. 1996. Phenotypes of mouse diabetes and rat fatty due to mutations in the OB (leptin) receptor. *Science,* **271,** 994-6.

Clark, L. C., Jr., Wolf, R., Granger, D. & Taylor, Z. 1953. Continuous recording of blood oxygen tensions by polarography. *J Appl Physiol,* **6,** 189-93.

Clarkson, M. R., Murphy, M., Gupta, S., Lambe, T., Mackenzie, H. S., Godson, C., Martin, F. & Brady, H. R. 2002. High glucose-altered gene expression in mesangial cells. Actin-regulatory protein gene expression is triggered by oxidative stress and cytoskeletal disassembly. *J Biol Chem,* **277,** 9707-12.

Clayton, D. A. 1982. Replication of animal mitochondrial DNA. *Cell,* **28,** 693-705.

Colleoni, F., Lattuada, D., Garretto, A., Massari, M., Mando, C., Somigliana, E. & Cetin, I. 2010. Maternal blood mitochondrial DNA content during normal and intrauterine growth restricted (IUGR) pregnancy. *Am J Obstet Gynecol,* **203,** 365 e1-6.

Colussi, C., Albertini, M. C., Coppola, S., Rovidati, S., Galli, F. & Ghibelli, L. 2000. H2O2-induced block of glycolysis as an active ADP-ribosylation reaction protecting cells from apoptosis. *FASEB J,* **14,** 2266-76.

Cormio, A., Milella, F., Marra, M., Pala, M., Lezza, A. M., Bonfigli, A. R., Franceschi, C., Cantatore, P. & Gadaleta, M. N. 2009. Variations at the H-strand replication origins of mitochondrial DNA and mitochondrial DNA content in the blood of type 2 diabetes patients. *Biochim Biophys Acta,* **1787,** 547-52.

Coskun, P. E., Wyrembak, J., Derbereva, O., Melkonian, G., Doran, E., Lott, I. T., Head, E., Cotman, C. W. & Wallace, D. C. 2010. Systemic mitochondrial dysfunction and the etiology of Alzheimer's disease and down syndrome dementia. *J Alzheimers Dis,* **20 Suppl 2,** S293-310.

Cossarizza, A., Riva, A., Pinti, M., Ammannato, S., Fedeli, P., Mussini, C., Esposito, R. & Galli, M. 2003. Increased mitochondrial DNA content in peripheral blood lymphocytes from HIV-infected patients with lipodystrophy. *Antivir Ther,* **8,** 315-21.

Coughlan, M. T., Thorburn, D. R., Penfold, S. A., Laskowski, A., Harcourt, B. E., Sourris, K. C., Tan, A. L., Fukami, K., Thallas-Bonke, V., Nawroth, P. P., Brownlee, M., Bierhaus, A., Cooper, M. E. & Forbes, J. M. 2009. RAGE-induced cytosolic ROS promote mitochondrial superoxide generation in diabetes. *J Am Soc Nephrol,* **20,** 742-52.

Cree, L. M., Patel, S. K., Pyle, A., Lynn, S., Turnbull, D. M., Chinnery, P. F. & Walker, M. 2008. Age-related decline in mitochondrial DNA copy number in isolated human pancreatic islets. *Diabetologia,* **51,** 1440-3.

Croteau, D. L. & Bohr, V. A. 1997. Repair of oxidative damage to nuclear and mitochondrial DNA in mammalian cells. *J Biol Chem,* **272,** 25409-12.

Cvetkovic, T., Mitic, B., Lazarevic, G., Vlahovic, P., Antic, S. & Stefanovic, V. 2009. Oxidative stress parameters as possible urine markers in patients with diabetic nephropathy. *J Diabetes Complications,* **23,** 337-42.

Dabla, P. K. 2010. Renal function in diabetic nephropathy. *World J Diabetes,* **1,** 48-56.

Dalakas, M. C., Semino-Mora, C. & Leon-Monzon, M. 2001. Mitochondrial alterations with mitochondrial DNA depletion in the nerves of AIDS patients with peripheral neuropathy induced by 2'3'-dideoxycytidine (ddC). *Lab Invest,* **81,** 1537-44.

Dalla Vestra, M., Saller, A., Bortoloso, E., Mauer, M. & Fioretto, P. 2000. Structural involvement in type 1 and type 2 diabetic nephropathy. *Diabetes Metab,* **26 Suppl 4,** 8-14.

Dasgupta, S., Shao, C., Keane, T. E., Duberow, D. P., Mathies, R. A., Fisher, P. B., Kiemeney, L. A. & Sidransky, D. 2012. Detection of mitochondrial deoxyribonucleic acid alterations in urine from urothelial cell carcinoma patients. *Int J Cancer,* **131,** 158-64.

DCCT 1993. The effect of intensive treatment of diabetes on the development and progression of long-term complications in insulin-dependent diabetes mellitus. The Diabetes Control and Complications Trial Research Group. *The New England journal of medicine,* **329,** 977-86.

de Andrade, P. B., Rubi, B., Frigerio, F., van den Ouweland, J. M., Maassen, J. A. & Maechler, P. 2006. Diabetes-associated mitochondrial DNA mutation A3243G impairs cellular metabolic pathways necessary for beta cell function. *Diabetologia,* **49,** 1816-26.

de Boer, I. H. & Group, D. E. R. 2014. Kidney disease and related findings in the diabetes control and complications trial/epidemiology of diabetes interventions and complications study. *Diabetes Care,* **37,** 24-30.

de Haan, J. B., Stefanovic, N., Nikolic-Paterson, D., Scurr, L. L., Croft, K. D., Mori, T. A., Hertzog, P., Kola, I., Atkins, R. C. & Tesch, G. H. 2005. Kidney expression of

glutathione peroxidase-1 is not protective against streptozotocin-induced diabetic nephropathy. *Am J Physiol Renal Physiol,* **289,** F544-51.

DIABETES UK 2014. Number of people diagnosed with diabetes reaches 3.2 million.) *[ONLINE] http://www.diabetes.org.uk/About_us/News/Number-of-people-diagnosed-with-diabetes-reaches-32-million/.*

Diaz-Ruiz, R., Averet, N., Araiza, D., Pinson, B., Uribe-Carvajal, S., Devin, A. & Rigoulet, M. 2008. Mitochondrial oxidative phosphorylation is regulated by fructose 1,6-bisphosphate. A possible role in Crabtree effect induction? *J Biol Chem,* **283,** 26948-55.

Dimauro, S. & Davidzon, G. 2005. Mitochondrial DNA and disease. *Ann Med,* **37,** 222-32.

Dranka, B. P., Benavides, G. A., Diers, A. R., Giordano, S., Zelickson, B. R., Reily, C., Zou, L., Chatham, J. C., Hill, B. G., Zhang, J., Landar, A. & Darley-Usmar, V. M. 2011. Assessing bioenergetic function in response to oxidative stress by metabolic profiling. *Free radical biology & medicine,* **51,** 1621-35.

Dranka, B. P., Hill, B. G. & Darley-Usmar, V. M. 2010. Mitochondrial reserve capacity in endothelial cells: The impact of nitric oxide and reactive oxygen species. *Free radical biology & medicine,* **48,** 905-14.

Dugan, L. L., You, Y. H., Ali, S. S., Diamond-Stanic, M., Miyamoto, S., DeCleves, A. E., Andreyev, A., Quach, T., Ly, S., Shekhtman, G., Nguyen, W., Chepetan, A., Le, T. P., Wang, L., Xu, M., Paik, K. P*., et al.* 2013. AMPK dysregulation promotes diabetes-related reduction of superoxide and mitochondrial function. *J Clin Invest,* **123,** 4888-99.

Dunn, S. L., Siu, W., Freund, J. & Boutcher, S. H. 2014. The effect of a lifestyle intervention on metabolic health in young women. *Diabetes Metab Syndr Obes,* **7,** 437-44.

Durham, S. E., Bonilla, E., Samuels, D. C., DiMauro, S. & Chinnery, P. F. 2005. Mitochondrial DNA copy number threshold in mtDNA depletion myopathy. *Neurology,* **65,** 453-5.

Eddy, A. A. 2005. Progression in chronic kidney disease. *Adv Chronic Kidney Dis,* **12,** 353-65.

Egan, K., Kusao, I., Troelstrup, D., Agsalda, M. & Shiramizu, B. 2010. Mitochondrial DNA in residual leukemia cells in cerebrospinal fluid in children with acute lymphoblastic leukemia. *J Clin Med Res,* **2,** 225-9.

Eknoyan, G. 2006. A history of diabetes mellitus -- a disease of the kidneys that became a kidney disease. *J Nephrol,* **19 Suppl 10,** S71-4.

El-Osta, A., Brasacchio, D., Yao, D., Pocai, A., Jones, P. L., Roeder, R. G., Cooper, M. E. & Brownlee, M. 2008. Transient high glucose causes persistent epigenetic changes and altered gene expression during subsequent normoglycemia. *J Exp Med,* **205,** 2409-17.

Ellinger, J., Albers, P., Muller, S. C., von Ruecker, A. & Bastian, P. J. 2009. Circulating mitochondrial DNA in the serum of patients with testicular germ cell cancer as a novel noninvasive diagnostic biomarker. *BJU Int,* **104,** 48-52.

Falkenberg, M., Larsson, N. G. & Gustafsson, C. M. 2007. DNA replication and transcription in mammalian mitochondria. *Annu Rev Biochem,* **76,** 679-99.

Fan, A. X., Radpour, R., Haghighi, M. M., Kohler, C., Xia, P., Hahn, S., Holzgreve, W. & Zhong, X. Y. 2009. Mitochondrial DNA content in paired normal and cancerous breast tissue samples from patients with breast cancer. *J Cancer Res Clin Oncol,* **135,** 983-9.

Fassett, R. G., Venuthurupalli, S. K., Gobe, G. C., Coombes, J. S., Cooper, M. A. & Hoy, W. E. 2011. Biomarkers in chronic kidney disease: a review. *Kidney international,* **80,** 806-21.

Fedorova, L. V., Tamirisa, A., Kennedy, D. J., Haller, S. T., Budnyy, G., Shapiro, J. I. & Malhotra, D. 2013. Mitochondrial impairment in the five-sixth nephrectomy model of chronic renal failure: proteomic approach. *BMC Nephrol,* **14,** 209.

Fernandez-Ruiz, I., Arnalich, F., Cubillos-Zapata, C., Hernandez-Jimenez, E., Moreno-Gonzalez, R., Toledano, V., Fernandez-Velasco, M., Vallejo-Cremades, M. T., Esteban-Burgos, L., de Diego, R. P., Llamas-Matias, M. A., Garcia-Arumi, E., Marti, R., Bosca, L., Andreu, A. L., Lopez-Sendon, J. L*., et al.* 2014. Mitochondrial DAMPs induce endotoxin tolerance in human monocytes: an observation in patients with myocardial infarction. *PLoS One,* **9,** e95073.

Fernandez-Silva, P., Enriquez, J. A. & Montoya, J. 2003. Replication and transcription of mammalian mitochondrial DNA. *Exp Physiol,* **88,** 41-56.

Fernandez-Vizarra, E., Enriquez, J. A., Perez-Martos, A., Montoya, J. & Fernandez-Silva, P. 2011. Tissue-specific differences in mitochondrial activity and biogenesis. *Mitochondrion,* **11,** 207-13.

Ferrannini, E. 2010. The stunned beta cell: a brief history. *Cell Metab,* **11,** 349-52.

Ferrick, D. A., Neilson, A. & Beeson, C. 2008. Advances in measuring cellular bioenergetics using extracellular flux. *Drug Discov Today,* **13,** 268-74.

Fink, B. D., Herlein, J. A., O'Malley, Y. & Sivitz, W. I. 2012. Endothelial cell and platelet bioenergetics: effect of glucose and nutrient composition. *PloS one,* **7,** e39430.

Fiumicino, S., Martinelli, S., Colussi, C., Aquilina, G., Leonetti, C., Crescenzi, M. & Bignami, M. 2000. Sensitivity to DNA cross-linking chemotherapeutic agents in mismatch repair-defective cells in vitro and in xenografts. *Int J Cancer,* **85,** 590-6.

Forbes, J. M., Coughlan, M. T. & Cooper, M. E. 2008. Oxidative stress as a major culprit in kidney disease in diabetes. *Diabetes,* **57,** 1446-54.

Furda, A., Santos, J. H., Meyer, J. N. & Van Houten, B. 2014. Quantitative PCR-based measurement of nuclear and mitochondrial DNA damage and repair in mammalian cells. *Methods Mol Biol,* **1105,** 419-37.

Gao, C. L., Zhu, C., Zhao, Y. P., Chen, X. H., Ji, C. B., Zhang, C. M., Zhu, J. G., Xia, Z. K., Tong, M. L. & Guo, X. R. 2010. Mitochondrial dysfunction is induced by high levels of glucose and free fatty acids in 3T3-L1 adipocytes. *Mol Cell Endocrinol,* **320,** 25-33.

Garcia-Ramirez, M., Francisco, G., Garcia-Arumi, E., Hernandez, C., Martinez, R., Andreu, A. L. & Simo, R. 2008. Mitochondrial DNA oxidation and manganese superoxide dismutase activity in peripheral blood mononuclear cells from type 2 diabetic patients. *Diabetes & metabolism,* **34,** 117-24.

Garrabou, G., Moren, C., Lopez, S., Tobias, E., Cardellach, F., Miro, O. & Casademont, J. 2012. The effects of sepsis on mitochondria. *J Infect Dis,* **205,** 392-400.

Giacco, F. & Brownlee, M. 2010. Oxidative stress and diabetic complications. *Circulation research,* **107,** 1058-70.

Gianotti, T. F., Sookoian, S., Dieuzeide, G., Garcia, S. I., Gemma, C., Gonzalez, C. D. & Pirola, C. J. 2008b. A decreased mitochondrial DNA content is related to insulin resistance in adolescents. *Obesity,* **16,** 1591-5.

Gilbert, R. E. & Cooper, M. E. 1999. The tubulointerstitium in progressive diabetic kidney disease: more than an aftermath of glomerular injury? *Kidney Int,* **56,** 1627-37.

Gohring, I., Sharoyko, V. V., Malmgren, S., Andersson, L. E., Spegel, P., Nicholls, D. G. & Mulder, H. 2014. Chronic high glucose and pyruvate levels differentially affect mitochondrial bioenergetics and fuel-stimulated insulin secretion from clonal INS-1 832/13 cells. *J Biol Chem,* **289,** 3786-98.

Goldstein, B. J., Mahadev, K., Wu, X., Zhu, L. & Motoshima, H. 2005. Role of insulin-induced reactive oxygen species in the insulin signaling pathway. *Antioxid Redox Signal,* **7,** 1021-31.

Gray, M. W., Burger, G. & Lang, B. F. 1999. Mitochondrial evolution. *Science,* **283,** 1476-81.

Green, D. R. & Reed, J. C. 1998. Mitochondria and apoptosis. *Science,* **281,** 1309-12.

Grohm, J., Plesnila, N. & Culmsee, C. 2010. Bid mediates fission, membrane permeabilization and peri-nuclear accumulation of mitochondria as a prerequisite for oxidative neuronal cell death. *Brain Behav Immun,* **24,** 831-8.

Gu, Y., Ande, S. R. & Mishra, S. 2011. Altered O-GlcNAc modification and phosphorylation of mitochondrial proteins in myoblast cells exposed to high glucose. *Arch Biochem Biophys,* **505,** 98-104.

Ha, H. & Lee, H. B. 2003. Reactive oxygen species and matrix remodeling in diabetic kidney. *J Am Soc Nephrol,* **14,** S246-9.

Ha, H. & Lee, H. B. 2005. Reactive oxygen species amplify glucose signalling in renal cells cultured under high glucose and in diabetic kidney. *Nephrology (Carlton),* **10 Suppl,** S7-10.

Hall, A. M., Unwin, R. J., Hanna, M. G. & Duchen, M. R. 2008. Renal function and mitochondrial cytopathy (MC): more questions than answers? *QJM,* **101,** 755-66.

Halliwell, B. 2007. Biochemistry of oxidative stress. *Biochemical Society transactions,* **35,** 1147-50.

Halliwell, B. 2011. Free radicals and antioxidants - quo vadis? *Trends Pharmacol Sci,* **32,** 125-30.

Halliwell, B. & Gutteridge, J. M. C. 2007. Free radicals in biology and medicine. *Biociences Oxford,* **IV edition**.

Hammond, E., Nolan, D., James, I., Metcalf, C. & Mallal, S. 2004. Reduction of mitochondrial DNA content and respiratory chain activity occurs in adipocytes within 6-12 months of commencing nucleoside reverse transcriptase inhibitor therapy. *AIDS,* **18,** 815-7.

Harbottle, A. & Birch-Machin, M. A. 2006. Real-time PCR analysis of a 3895 bp mitochondrial DNA deletion in nonmelanoma skin cancer and its use as a quantitative marker for sunlight exposure in human skin. *Br J Cancer,* **94,** 1887-93.

Hartman, M. L., Shirihai, O. S., Holbrook, M., Xu, G., Kocherla, M., Shah, A., Fetterman, J. L., Kluge, M. A., Frame, A. A., Hamburg, N. M. & Vita, J. A. 2014. Relation of mitochondrial oxygen consumption in peripheral blood mononuclear cells to vascular function in type 2 diabetes mellitus. *Vasc Med,* **19,** 67-74.

Hattori, Y., Hattori, S., Sato, N. & Kasai, K. 2000. High-glucose-induced nuclear factor kappaB activation in vascular smooth muscle cells. *Cardiovasc Res,* **46,** 188-97.

Henningsen, C., Zahner, G. & Thaiss, F. 2003. High glucose induces type 1 hexokinase gene expression in isolated glomeruli of diabetic rats and in mesangial cells. *Nephron Physiol,* **93,** p67-75.

Hensley, K., Robinson, K. A., Gabbita, S. P., Salsman, S. & Floyd, R. A. 2000. Reactive oxygen species, cell signaling, and cell injury. *Free Radic Biol Med,* **28,** 1456-62.

Herrera, M. & Coffman, T. M. 2012. The kidney and hypertension: novel insights from transgenic models. *Curr Opin Nephrol Hypertens,* **21,** 171-8.

Higgins, G. C. & Coughlan, M. T. 2014. Mitochondrial dysfunction and mitophagy: the beginning and end to diabetic nephropathy? *Br J Pharmacol,* **171,** 1917-42.

Hock, M. B. & Kralli, A. 2009. Transcriptional control of mitochondrial biogenesis and function. *Annual review of physiology,* **71,** 177-203.

Hollis, R. 2013. http://antisensescienceblog.wordpress.com/2013/12/04/a-cornerstone-of-molecular-biology-the-pcr-reaction/.) Antisense Science.

Hosgood, H. D., 3rd, Liu, C. S., Rothman, N., Weinstein, S. J., Bonner, M. R., Shen, M., Lim, U., Virtamo, J., Cheng, W. L., Albanes, D. & Lan, Q. 2010. Mitochondrial DNA

copy number and lung cancer risk in a prospective cohort study. *Carcinogenesis,* **31,** 847-9.

Hsieh, C. J., Weng, S. W., Liou, C. W., Lin, T. K., Chen, J. B., Tiao, M. M., Hung, Y. T., Chen, I. Y., Huang, W. T. & Wang, P. W. 2011. Tissue-specific differences in mitochondrial DNA content in type 2 diabetes. *Diabetes Res Clin Pract,* **92,** 106-10.

Hsu, C. W., Yin, P. H., Lee, H. C., Chi, C. W. & Tseng, L. M. 2010. Mitochondrial DNA content as a potential marker to predict response to anthracycline in breast cancer patients. *Breast J,* **16,** 264-70.

Hu, Y., Suarez, J., Fricovsky, E., Wang, H., Scott, B. T., Trauger, S. A., Han, W., Hu, Y., Oyeleye, M. O. & Dillmann, W. H. 2009. Increased enzymatic O-GlcNAcylation of mitochondrial proteins impairs mitochondrial function in cardiac myocytes exposed to high glucose. *J Biol Chem,* **284,** 547-55.

Hudson, G., Amati-Bonneau, P., Blakely, E. L., Stewart, J. D., He, L., Schaefer, A. M., Griffiths, P. G., Ahlqvist, K., Suomalainen, A., Reynier, P., McFarland, R., Turnbull, D. M., Chinnery, P. F. & Taylor, R. W. 2008. Mutation of OPA1 causes dominant optic atrophy with external ophthalmoplegia, ataxia, deafness and multiple mitochondrial DNA deletions: a novel disorder of mtDNA maintenance. *Brain,* **131,** 329-37.

Hunter, S. E., Jung, D., Di Giulio, R. T. & Meyer, J. N. 2010. The QPCR assay for analysis of mitochondrial DNA damage, repair, and relative copy number. *Methods,* **51,** 444-51.

IDF 2013. Diabetes Atlas, 6th edition.) *International Diabetes Federetion [ONLINE] http://www.idf.org/sites/default/files/EN_6E_Atlas_Full_0.pdf.*

IDF 2014. International Diabetes Federation diabetes Atlas.) *[ONLINE] Avaiable at http://www.idf.org/sites/default/files/DA6_Regional_factsheets. [Accessed 29 September 14].*

Ihnat, M. A., Thorpe, J. E. & Ceriello, A. 2007. Hypothesis: the 'metabolic memory', the new challenge of diabetes. *Diabetic medicine : a journal of the British Diabetic Association,* **24,** 582-6.

Imoto, K., Kukidome, D., Nishikawa, T., Matsuhisa, T., Sonoda, K., Fujisawa, K., Yano, M., Motoshima, H., Taguchi, T., Tsuruzoe, K., Matsumura, T., Ichijo, H. & Araki, E. 2006. Impact of mitochondrial reactive oxygen species and apoptosis signal-regulating kinase 1 on insulin signaling. *Diabetes,* **55,** 1197-204.

Ingalls, A. M., Dickie, M. M. & Snell, G. D. 1950. Obese, a new mutation in the house mouse. *J Hered,* **41,** 317-8.

Jennings, P. E., Chirico, S., Jones, A. F., Lunec, J. & Barnett, A. H. 1987. Vitamin C metabolites and microangiopathy in diabetes mellitus. *Diabetes Res,* **6,** 151-4.

Jiang, W. W., Masayesva, B., Zahurak, M., Carvalho, A. L., Rosenbaum, E., Mambo, E., Zhou, S., Minhas, K., Benoit, N., Westra, W. H., Alberg, A., Sidransky, D., Koch, W. & Califano, J. 2005. Increased mitochondrial DNA content in saliva associated with head and neck cancer. *Clin Cancer Res,* **11,** 2486-91.

Kaaman, M., Sparks, L. M., van Harmelen, V., Smith, S. R., Sjolin, E., Dahlman, I. & Arner, P. 2007. Strong association between mitochondrial DNA copy number and lipogenesis in human white adipose tissue. *Diabetologia,* **50,** 2526-33.

Kao, S. H., Chao, H. T., Liu, H. W., Liao, T. L. & Wei, Y. H. 2004. Sperm mitochondrial DNA depletion in men with asthenospermia. *Fertil Steril,* **82,** 66-73.

Kelley, D. E., He, J., Menshikova, E. V. & Ritov, V. B. 2002. Dysfunction of mitochondria in human skeletal muscle in type 2 diabetes. *Diabetes,* **51,** 2944-50.

Kerr, D. S. 2013. Review of clinical trials for mitochondrial disorders: 1997-2012. *Neurotherapeutics,* **10,** 307-19.

Khan, S., Raghuram, G. V., Bhargava, A., Pathak, N., Chandra, D. H., Jain, S. K. & Mishra, P. K. 2011. Role and clinical significance of lymphocyte mitochondrial dysfunction in type 2 diabetes mellitus. *Transl Res,* **158,** 344-59.

Kim, J. Y., Hwang, J. M., Ko, H. S., Seong, M. W., Park, B. J. & Park, S. S. 2005. Mitochondrial DNA content is decreased in autosomal dominant optic atrophy. *Neurology,* **64,** 966-72.

Kim, M. K., Jung, H. S., Yoon, C. S., Ko, J. H., Jun, H. J., Kim, T. K., Kwon, M. J., Lee, S. H., Ko, K. S., Rhee, B. D. & Park, J. H. 2010. The Effect of Glucose Fluctuation on Apoptosis and Function of INS-1 Pancreatic Beta Cells. *Korean Diabetes J,* **34,** 47-54.

King, A. J. 2012. The use of animal models in diabetes research. *Br J Pharmacol,* **166,** 877-94.

King, P., Peacock, I. & Donnelly, R. 1999. The UK prospective diabetes study (UKPDS): clinical and therapeutic implications for type 2 diabetes. *Br J Clin Pharmacol,* **48,** 643-8.

Koopman, W. J., Verkaart, S., Visch, H. J., van der Westhuizen, F. H., Murphy, M. P., van den Heuvel, L. W., Smeitink, J. A. & Willems, P. H. 2005. Inhibition of complex I of the electron transport chain causes O2-. -mediated mitochondrial outgrowth. *Am J Physiol Cell Physiol,* **288,** C1440-50.

Kopp, J. B. 2013. Rethinking hypertensive kidney disease: arterionephrosclerosis as a genetic, metabolic, and inflammatory disorder. *Curr Opin Nephrol Hypertens,* **22,** 266-72.

Kruegel, J., Rubel, D. & Gross, O. 2013. Alport syndrome--insights from basic and clinical research. *Nat Rev Nephrol,* **9,** 170-8.

Krugel, K., Wurm, A., Pannicke, T., Hollborn, M., Karl, A., Wiedemann, P., Reichenbach, A., Kohen, L. & Bringmann, A. 2011. Involvement of oxidative stress and mitochondrial dysfunction in the osmotic swelling of retinal glial cells from diabetic rats. *Experimental eye research,* **92,** 87-93.

Kwok, C. S., Quah, T. C., Ariffin, H., Tay, S. K. & Yeoh, A. E. 2011. Mitochondrial D-loop Polymorphisms and Mitochondrial DNA Content in Childhood Acute Lymphoblastic Leukemia. *J Pediatr Hematol Oncol*.

Lai, R. Y., Ljubicic, V., D'Souza, D. & Hood, D. A. 2010. Effect of chronic contractile activity on mRNA stability in skeletal muscle. *Am J Physiol Cell Physiol,* **299,** C155-63.

Lan, Q., Lim, U., Liu, C. S., Weinstein, S. J., Chanock, S., Bonner, M. R., Virtamo, J., Albanes, D. & Rothman, N. 2008. A prospective study of mitochondrial DNA copy number and risk of non-Hodgkin lymphoma. *Blood,* **112,** 4247-9.

Lee, H., Abe, Y., Lee, I., Shrivastav, S., Crusan, A. P., Huttemann, M., Hopfer, U., Felder, R. A., Asico, L. D., Armando, I., Jose, P. A. & Kopp, J. B. 2014. Increased mitochondrial activity in renal proximal tubule cells from young spontaneously hypertensive rats. *Kidney Int,* **85,** 561-9.

Lee, H. B., Yu, M. R., Yang, Y., Jiang, Z. & Ha, H. 2003. Reactive oxygen species-regulated signaling pathways in diabetic nephropathy. *J Am Soc Nephrol,* **14,** S241-5.

Lee, H. C., Yin, P. H., Lin, J. C., Wu, C. C., Chen, C. Y., Wu, C. W., Chi, C. W., Tam, T. N. & Wei, Y. H. 2005. Mitochondrial genome instability and mtDNA depletion in human cancers. *Ann N Y Acad Sci,* **1042,** 109-22.

Lee, H. K., Song, J. H., Shin, C. S., Park, D. J., Park, K. S., Lee, K. U. & Koh, C. S. 1998. Decreased mitochondrial DNA content in peripheral blood precedes the development of non-insulin-dependent diabetes mellitus. *Diabetes Res Clin Pract,* **42,** 161-7.

Lee, J. E., Park, H., Ju, Y. S., Kwak, M., Kim, J. I., Oh, H. Y. & Seo, J. S. 2009. Higher mitochondrial DNA copy number is associated with lower prevalence of microalbuminuria. *Exp Mol Med,* **41,** 253-8.

Lee, J. H., Yang, S. H., Oh, J. M. & Lee, M. G. 2010. Pharmacokinetics of drugs in rats with diabetes mellitus induced by alloxan or streptozocin: comparison with those in patients with type I diabetes mellitus. *J Pharm Pharmacol,* **62,** 1-23.

Lehmann, R. & Schleicher, E. D. 2000. Molecular mechanism of diabetic nephropathy. *Clin Chim Acta,* **297,** 135-44.

Leigh-Brown, S., Enriquez, J. A. & Odom, D. T. 2010. Nuclear transcription factors in mammalian mitochondria. *Genome Biol,* **11,** 215.

Liesa, M. & Shirihai, O. S. 2013. Mitochondrial dynamics in the regulation of nutrient utilization and energy expenditure. *Cell Metab,* **17,** 491-506.

Lim, A. I., Chan, L. Y., Tang, S. C., Lai, K. N. & Leung, J. C. 2014a. Albumin and glycated albumin activate KIM-1 release in tubular epithelial cells through distinct kinetics and mechanisms. *Inflamm Res,* **63,** 831-9.

Lim, S. C., Tan, H. H., Goh, S. K., Subramaniam, T., Sum, C. F., Tan, I. K., Lee, B. L. & Ong, C. N. 2006. Oxidative burden in prediabetic and diabetic individuals: evidence from plasma coenzyme Q(10). *Diabet Med,* **23,** 1344-9.

Lim, Y. M., Lim, H., Hur, K. Y., Quan, W., Lee, H. Y., Cheon, H., Ryu, D., Koo, S. H., Kim, H. L., Kim, J., Komatsu, M. & Lee, M. S. 2014b. Systemic autophagy insufficiency compromises adaptation to metabolic stress and facilitates progression from obesity to diabetes. *Nat Commun,* **5,** 4934.

Lin, M., Yiu, W. H., Wu, H. J., Chan, L. Y., Leung, J. C., Au, W. S., Chan, K. W., Lai, K. N. & Tang, S. C. 2012. Toll-like receptor 4 promotes tubular inflammation in diabetic nephropathy. *J Am Soc Nephrol,* **23,** 86-102.

Lindinger, A., Peterli, R., Peters, T., Kern, B., von Flue, M., Calame, M., Hoch, M., Eberle, A. N. & Lindinger, P. W. 2010. Mitochondrial DNA content in human omental adipose tissue. *Obes Surg,* **20,** 84-92.

Liu, X. F., Yu, J. Q., Dalan, R., Liu, A. Q. & Luo, K. Q. 2014. Biological factors in plasma from diabetes mellitus patients enhance hyperglycaemia and pulsatile shear stress-induced endothelial cell apoptosis. *Integr Biol (Camb),* **6,** 511-22.

Liu, Z. & Butow, R. A. 2006. Mitochondrial retrograde signaling. *Annual review of genetics,* **40,** 159-85.

Lu, H., Koshkin, V., Allister, E. M., Gyulkhandanyan, A. V. & Wheeler, M. B. 2010. Molecular and metabolic evidence for mitochondrial defects associated with beta-cell dysfunction in a mouse model of type 2 diabetes. *Diabetes,* **59,** 448-59.

Ma, T., Zhu, J., Chen, X., Zha, D., Singhal, P. C. & Ding, G. 2013. High glucose induces autophagy in podocytes. *Exp Cell Res,* **319,** 779-89.

Ma, Y. S., Wu, S. B., Lee, W. Y., Cheng, J. S. & Wei, Y. H. 2009. Response to the increase of oxidative stress and mutation of mitochondrial DNA in aging. *Biochim Biophys Acta,* **1790,** 1021-9.

Madsen-Bouterse, S. A. & Kowluru, R. A. 2008. Oxidative stress and diabetic retinopathy: pathophysiological mechanisms and treatment perspectives. *Reviews in endocrine & metabolic disorders,* **9,** 315-27.

Madsen-Bouterse, S. A., Mohammad, G., Kanwar, M. & Kowluru, R. A. 2010. Role of mitochondrial DNA damage in the development of diabetic retinopathy, and the metabolic memory phenomenon associated with its progression. *Antioxidants & redox signaling,* **13,** 797-805.

Maechler, P. & Wollheim, C. B. 2001. Mitochondrial function in normal and diabetic beta-cells. *Nature,* **414,** 807-12.

Maeda, A. & Fadeel, B. 2014. Mitochondria released by cells undergoing TNF-alpha-induced necroptosis act as danger signals. *Cell Death Dis,* **5,** e1312.

Mahadev, K., Wu, X., Zilbering, A., Zhu, L., Lawrence, J. T. & Goldstein, B. J. 2001. Hydrogen peroxide generated during cellular insulin stimulation is integral to

activation of the distal insulin signaling cascade in 3T3-L1 adipocytes. *J Biol Chem,* **276,** 48662-9.

Makazan, Z., Saini, H. K. & Dhalla, N. S. 2007. Role of oxidative stress in alterations of mitochondrial function in ischemic-reperfused hearts. *Am J Physiol Heart Circ Physiol,* **292,** H1986-94.

Makino, A., Scott, B. T. & Dillmann, W. H. 2010. Mitochondrial fragmentation and superoxide anion production in coronary endothelial cells from a mouse model of type 1 diabetes. *Diabetologia,* **53,** 1783-94.

Malik, A. N. & Czajka, A. 2013. Is mitochondrial DNA content a potential biomarker of mitochondrial dysfunction? *Mitochondrion,* **13,** 481-92.

Malik, A. N., Shahni, R. & Iqbal, M. M. 2009. Increased peripheral blood mitochondrial DNA in type 2 diabetic patients with nephropathy. *Diabetes Res Clin Pract,* **86,** e22-4.

Malik, A. N., Shahni, R., Rodriguez-de-Ledesma, A., Laftah, A. & Cunningham, P. 2011. Mitochondrial DNA as a non-invasive biomarker: accurate quantification using real time quantitative PCR without co-amplification of pseudogenes and dilution bias. *Biochemical and biophysical research communications,* **412,** 1-7.

Maniura-Weber, K., Goffart, S., Garstka, H. L., Montoya, J. & Wiesner, R. J. 2004. Transient overexpression of mitochondrial transcription factor A (TFAM) is sufficient to stimulate mitochondrial DNA transcription, but not sufficient to increase mtDNA copy number in cultured cells. *Nucleic Acids Res,* **32,** 6015-27.

Masayesva, B. G., Mambo, E., Taylor, R. J., Goloubeva, O. G., Zhou, S., Cohen, Y., Minhas, K., Koch, W., Sciubba, J., Alberg, A. J., Sidransky, D. & Califano, J. 2006. Mitochondrial DNA content increase in response to cigarette smoking. *Cancer Epidemiol Biomarkers Prev,* **15,** 19-24.

May-Panloup, P., Chretien, M. F., Jacques, C., Vasseur, C., Malthiery, Y. & Reynier, P. 2005. Low oocyte mitochondrial DNA content in ovarian insufficiency. *Hum Reprod,* **20,** 593-7.

Medeiros, D. M. 2008. Assessing mitochondria biogenesis. *Methods,* **46,** 288-94.

Meierhofer, D., Mayr, J. A., Foetschl, U., Berger, A., Fink, K., Schmeller, N., Hacker, G. W., Hauser-Kronberger, C., Kofler, B. & Sperl, W. 2004. Decrease of mitochondrial DNA content and energy metabolism in renal cell carcinoma. *Carcinogenesis,* **25,** 1005-10.

Mercer, T. R., Neph, S., Dinger, M. E., Crawford, J., Smith, M. A., Shearwood, A. M., Haugen, E., Bracken, C. P., Rackham, O., Stamatoyannopoulos, J. A., Filipovska, A. & Mattick, J. S. 2011. The human mitochondrial transcriptome. *Cell,* **146,** 645-58.

Michel, S., Wanet, A., De Pauw, A., Rommelaere, G., Arnould, T. & Renard, P. 2012. Crosstalk between mitochondrial (dys)function and mitochondrial abundance. *Journal of cellular physiology,* **227,** 2297-310.

Milenkovic, D., Matic, S., Kuhl, I., Ruzzenente, B., Freyer, C., Jemt, E., Park, C. B., Falkenberg, M. & Larsson, N. G. 2013. TWINKLE is an essential mitochondrial helicase required for synthesis of nascent D-loop strands and complete mtDNA replication. *Hum Mol Genet,* **22,** 1983-93.

Mistry, H. D., Broughton Pipkin, F., Redman, C. W. & Poston, L. 2012. Selenium in reproductive health. *Am J Obstet Gynecol,* **206,** 21-30.

Mizumachi, T., Muskhelishvili, L., Naito, A., Furusawa, J., Fan, C. Y., Siegel, E. R., Kadlubar, F. F., Kumar, U. & Higuchi, M. 2008. Increased distributional variance of mitochondrial DNA content associated with prostate cancer cells as compared with normal prostate cells. *Prostate,* **68,** 408-17.

Mogensen, C. E. 2003. Microalbuminuria and hypertension with focus on type 1 and type 2 diabetes. *J Intern Med,* **254,** 45-66.

Mogensen, C. E., Christensen, C. K. & Vittinghus, E. 1983. The stages in diabetic renal disease. With emphasis on the stage of incipient diabetic nephropathy. *Diabetes,* **32 Suppl 2,** 64-78.

Mogensen, C. E., Keane, W. F., Bennett, P. H., Jerums, G., Parving, H. H., Passa, P., Steffes, M. W., Striker, G. E. & Viberti, G. C. 1995. Prevention of diabetic renal disease with special reference to microalbuminuria. *Lancet,* **346,** 1080-4.

Mogensen, M., Sahlin, K., Fernstrom, M., Glintborg, D., Vind, B. F., Beck-Nielsen, H. & Hojlund, K. 2007. Mitochondrial respiration is decreased in skeletal muscle of patients with type 2 diabetes. *Diabetes,* **56,** 1592-9.

Molina, A. J., Wikstrom, J. D., Stiles, L., Las, G., Mohamed, H., Elorza, A., Walzer, G., Twig, G., Katz, S., Corkey, B. E. & Shirihai, O. S. 2009. Mitochondrial networking protects beta-cells from nutrient-induced apoptosis. *Diabetes,* **58,** 2303-15.

Morino, K., Petersen, K. F., Dufour, S., Befroy, D., Frattini, J., Shatzkes, N., Neschen, S., White, M. F., Bilz, S., Sono, S., Pypaert, M. & Shulman, G. I. 2005. Reduced mitochondrial density and increased IRS-1 serine phosphorylation in muscle of insulin-resistant offspring of type 2 diabetic parents. *J Clin Invest,* **115,** 3587-93.

Mosquera, J. A. 2010. [Role of the receptor for advanced glycation end products (RAGE) in inflammation]. *Invest Clin,* **51,** 257-68.

Mussini, C., Pinti, M., Bugarini, R., Borghi, V., Nasi, M., Nemes, E., Troiano, L., Guaraldi, G., Bedini, A., Sabin, C., Esposito, R. & Cossarizza, A. 2005. Effect of treatment interruption monitored by CD4 cell count on mitochondrial DNA content in HIV-infected patients: a prospective study. *AIDS,* **19,** 1627-33.

Navarro-Gonzalez, J. F. & Mora-Fernandez, C. 2008. The role of inflammatory cytokines in diabetic nephropathy. *J Am Soc Nephrol,* **19,** 433-42.

Navis, A. C., Niclou, S. P., Fack, F., Stieber, D., van Lith, S., Verrijp, K., Wright, A., Stauber, J., Tops, B., Otte-Holler, I., Wevers, R. A., van Rooij, A., Pusch, S., von Deimling, A., Tigchelaar, W., van Noorden, C. J*., et al.* 2013. Increased mitochondrial activity in a novel IDH1-R132H mutant human oligodendroglioma xenograft model: in situ detection of 2-HG and alpha-KG. *Acta Neuropathol Commun,* **1,** 18.

NIH accessed on 1st Sep, 2014. Mitochondrial DNA http://www.genome.gov/. *National Human Genome Research Insitute*.

Nishikawa, T., Edelstein, D., Du, X. L., Yamagishi, S., Matsumura, T., Kaneda, Y., Yorek, M. A., Beebe, D., Oates, P. J., Hammes, H. P., Giardino, I. & Brownlee, M. 2000. Normalizing mitochondrial superoxide production blocks three pathways of hyperglycaemic damage. *Nature,* **404,** 787-90.

Nishikawa, T., Kukidome, D., Sonoda, K., Fujisawa, K., Matsuhisa, T., Motoshima, H., Matsumura, T. & Araki, E. 2007. Impact of mitochondrial ROS production in the pathogenesis of insulin resistance. *Diabetes Res Clin Pract,* **77 Suppl 1,** S161-4.

Nolan, C. J. 2011. Controversies in gestational diabetes. *Best Pract Res Clin Obstet Gynaecol,* **25,** 37-49.

Nowak, G., Bakajsova, D. & Samarel, A. M. 2011. Protein kinase C-epsilon activation induces mitochondrial dysfunction and fragmentation in renal proximal tubules. *Am J Physiol Renal Physiol,* **301,** F197-208.

Oka, T., Hikoso, S., Yamaguchi, O., Taneike, M., Takeda, T., Tamai, T., Oyabu, J., Murakawa, T., Nakayama, H., Nishida, K., Akira, S., Yamamoto, A., Komuro, I. & Otsu, K. 2012. Mitochondrial DNA that escapes from autophagy causes inflammation and heart failure. *Nature,* **485,** 251-5.

Ortsater, H., Liss, P., Akerman, K. E. & Bergsten, P. 2002. Contribution of glycolytic and mitochondrial pathways in glucose-induced changes in islet respiration and insulin secretion. *Pflugers Arch,* **444,** 506-12.

Osorio, J. 2014. Diabetes: Protective role of autophagy in pancreatic beta cells. *Nat Rev Endocrinol,* **10,** 575.

Page, R., Morris, C., Williams, J., von Ruhland, C. & Malik, A. N. 1997. Isolation of diabetes-associated kidney genes using differential display. *Biochem Biophys Res Commun,* **232,** 49-53.

Paigen, B., Mitchell, D., Holmes, P. A. & Albee, D. 1987. Genetic analysis of strains C57BL/6J and BALB/cJ for Ath-1, a gene determining atherosclerosis susceptibility in mice. *Biochem Genet,* **25,** 881-92.

Pang, J., Xi, C., Dai, Y., Gong, H. & Zhang, T. M. 2012. Altered expression of base excision repair genes in response to high glucose-induced oxidative stress in HepG2 hepatocytes. *Med Sci Monit,* **18,** BR281-5.

Park, S. Y., Shin, M. G., Kim, H. R., Oh, J. Y., Kim, S. H., Shin, J. H., Cho, Y. B., Suh, S. P. & Ryang, D. W. 2009. Alteration of mitochondrial DNA sequence and copy number in nasal polyp tissue. *Mitochondrion,* **9,** 318-25.

Peng, J., Li, X., Zhang, D., Chen, J. K., Su, Y., Smith, S. B. & Dong, Z. 2014. Hyperglycemia, p53, and mitochondrial pathway of apoptosis are involved in the susceptibility of diabetic models to ischemic acute kidney injury. *Kidney Int*.

Perry, C. G., Kane, D. A., Lanza, I. R. & Neufer, P. D. 2013. Methods for assessing mitochondrial function in diabetes. *Diabetes,* **62,** 1041-53.

Perry, R. C., Shankar, R. R., Fineberg, N., McGill, J. & Baron, A. D. 2001. HbA1c measurement improves the detection of type 2 diabetes in high-risk individuals with nondiagnostic levels of fasting plasma glucose: the Early Diabetes Intervention Program (EDIP). *Diabetes Care,* **24,** 465-71.

Picard, M., Zhang, J., Hancock, S., Derbeneva, O., Golhar, R., Golik, P., O'Hearn, S., Levy, S., Potluri, P., Lvova, M., Davila, A., Lin, C. S., Perin, J. C., Rappaport, E. F., Hakonarson, H., Trounce, I. A*., et al.* 2014. Progressive increase in mtDNA 3243A>G heteroplasmy causes abrupt transcriptional reprogramming. *Proc Natl Acad Sci U S A,* **111,** E4033-42.

Piko, L. & Matsumoto, L. 1976. Number of mitochondria and some properties of mitochondrial DNA in the mouse egg. *Dev Biol,* **49,** 1-10.

Plotnikov, E. Y., Kazachenko, A. V., Vyssokikh, M. Y., Vasileva, A. K., Tcvirkun, D. V., Isaev, N. K., Kirpatovsky, V. I. & Zorov, D. B. 2007. The role of mitochondria in oxidative and nitrosative stress during ischemia/reperfusion in the rat kidney. *Kidney Int,* **72,** 1493-502.

Pop-Busui, R., Herman, W. H., Feldman, E. L., Low, P. A., Martin, C. L., Cleary, P. A., Waberski, B. H., Lachin, J. M. & Albers, J. W. 2010. DCCT and EDIC studies in type 1 diabetes: lessons for diabetic neuropathy regarding metabolic memory and natural history. *Current diabetes reports,* **10,** 276-82.

Posada, I. J., Gallardo, M. E., Dominguez, C., Rivera, H., Cabello, A., Arenas, J., Martin, M. A., Garesse, R. & Bornstein, B. 2010. [Mitochondrial DNA depletion and POLG mutations in a patient with sensory ataxia, dysarthria and ophthalmoplegia]. *Med Clin (Barc),* **135,** 452-5.

Pugliese, G. 2014. Updating the natural history of diabetic nephropathy. *Acta Diabetol*.

Pugliese, G., Pricci, F., Pugliese, F., Mene, P., Lenti, L., Andreani, D., Galli, G., Casini, A., Bianchi, S., Rotella, C. M. & et al. 1994. Mechanisms of glucose-enhanced extracellular matrix accumulation in rat glomerular mesangial cells. *Diabetes,* **43,** 478-90.

Pyle, A., Burn, D. J., Gordon, C., Swan, C., Chinnery, P. F. & Baudouin, S. V. 2010. Fall in circulating mononuclear cell mitochondrial DNA content in human sepsis. *Intensive Care Med,* **36,** 956-62.

Qu, Z., Yan, P., Fu, J., Jiang, J., Grusby, M. J., Smithgall, T. E. & Xiao, G. 2010. DNA methylation-dependent repression of PDZ-LIM domain-containing protein 2 in

colon cancer and its role as a potential therapeutic target. *Cancer Res,* **70,** 1766-72.

Rabol, R. 2011. Mitochondrial function in skeletal muscle in type 2 diabetes. *Dan Med Bull,* **58,** B4272.

Rackham, C. L., Jones, P. M. & King, A. J. 2013. Maintenance of islet morphology is beneficial for transplantation outcome in diabetic mice. *PLoS One,* **8,** e57844.

Radpour, R., Fan, A. X., Kohler, C., Holzgreve, W. & Zhong, X. Y. 2009. Current understanding of mitochondrial DNA in breast cancer. *Breast J,* **15,** 505-9.

Ritz, E. 2013. Clinical manifestations and natural history of diabetic kidney disease. *Med Clin North Am,* **97,** 19-29.

Rocco, M. V., Neilson, E. G., Hoyer, J. R. & Ziyadeh, F. N. 1992. Attenuated expression of epithelial cell adhesion molecules in murine polycystic kidney disease. *Am J Physiol,* **262,** F679-86.

Roche 2012. http://lifescience.roche.com/shop/en/be/overviews/brand/universal-probe-library.), Roche Diagnostics.

Rodriguez-Enriquez, S., Kai, Y., Maldonado, E., Currin, R. T. & Lemasters, J. J. 2009. Roles of mitophagy and the mitochondrial permeability transition in remodeling of cultured rat hepatocytes. *Autophagy,* **5,** 1099-106.

Rolo, A. P. & Palmeira, C. M. 2006. Diabetes and mitochondrial function: role of hyperglycemia and oxidative stress. *Toxicol Appl Pharmacol,* **212,** 167-78.

Romeo, G., Liu, W. H., Asnaghi, V., Kern, T. S. & Lorenzi, M. 2002. Activation of nuclear factor-kappaB induced by diabetes and high glucose regulates a proapoptotic program in retinal pericytes. *Diabetes,* **51,** 2241-8.

Ruggiero, C., Ehrenshaft, M., Cleland, E. & Stadler, K. 2011. High-fat diet induces an initial adaptation of mitochondrial bioenergetics in the kidney despite evident oxidative stress and mitochondrial ROS production. *Am J Physiol Endocrinol Metab,* **300,** E1047-58.

Rutz, M., Metzger, J., Gellert, T., Luppa, P., Lipford, G. B., Wagner, H. & Bauer, S. 2004. Toll-like receptor 9 binds single-stranded CpG-DNA in a sequence- and pH-dependent manner. *Eur J Immunol,* **34,** 2541-50.

Sandler, S. & Swenne, I. 1983. Streptozotocin, but not alloxan, induces DNA repair synthesis in mouse pancreatic islets in vitro. *Diabetologia,* **25,** 444-7.

Sansbury, B. E., Jones, S. P., Riggs, D. W., Darley-Usmar, V. M. & Hill, B. G. 2011. Bioenergetic function in cardiovascular cells: the importance of the reserve capacity and its biological regulation. *Chemico-biological interactions,* **191,** 288-95.

Santos, J. H., Hunakova, L., Chen, Y., Bortner, C. & Van Houten, B. 2003. Cell sorting experiments link persistent mitochondrial DNA damage with loss of mitochondrial membrane potential and apoptotic cell death. *The Journal of biological chemistry,* **278,** 1728-34.

Santos, T. A., El Shourbagy, S. & St John, J. C. 2006. Mitochondrial content reflects oocyte variability and fertilization outcome. *Fertil Steril,* **85,** 584-91.

Sazer, S. & Sherwood, S. W. 1990. Mitochondrial growth and DNA synthesis occur in the absence of nuclear DNA replication in fission yeast. *J Cell Sci,* **97 (Pt 3),** 509-16.

Scherz-Shouval, R. & Elazar, Z. 2007. ROS, mitochondria and the regulation of autophagy. *Trends in cell biology,* **17,** 422-7.

Schoolwerth, A. C. & LaNoue, K. F. 1985. Transport of metabolic substrates in renal mitochondria. *Annu Rev Physiol,* **47,** 143-71.

Schraufstatter, I. U., Hinshaw, D. B., Hyslop, P. A., Spragg, R. G. & Cochrane, C. G. 1985. Glutathione cycle activity and pyridine nucleotide levels in oxidant-induced injury of cells. *J Clin Invest,* **76,** 1131-9.

Schrepper, A., Schwarzer, M., Schope, M., Amorim, P. A. & Doenst, T. 2012. Biphasic response of skeletal muscle mitochondria to chronic cardiac pressure overload - role of respiratory chain complex activity. *J Mol Cell Cardiol,* **52,** 125-35.

SeahorseBioscience 2014. http://www.seahorsebio.com/.) http://www.seahorsebio.com/.

Selak, M. A., Lyver, E., Micklow, E., Deutsch, E. C., Onder, O., Selamoglu, N., Yager, C., Knight, S., Carroll, M., Daldal, F., Dancis, A., Lynch, D. R. & Sarry, J. E. 2011. Blood cells from Friedreich ataxia patients harbor frataxin deficiency without a loss of mitochondrial function. *Mitochondrion,* **11,** 342-50.

Sethi, G., Ahn, K. S. & Aggarwal, B. B. 2008. Targeting nuclear factor-kappa B activation pathway by thymoquinone: role in suppression of antiapoptotic gene products and enhancement of apoptosis. *Mol Cancer Res,* **6,** 1059-70.

Sethumadhavan, S., Vasquez-Vivar, J., Migrino, R. Q., Harmann, L., Jacob, H. J. & Lazar, J. 2012. Mitochondrial DNA variant for complex I reveals a role in diabetic cardiac remodeling. *J Biol Chem,* **287,** 22174-82.

Seyfried, T. N. & Shelton, L. M. 2010. Cancer as a metabolic disease. *Nutr Metab (Lond),* **7,** 7.

Shadel, G. S. 2005. Mitochondrial DNA, aconitase 'wraps' it up. *Trends Biochem Sci,* **30,** 294-6.

Shadel, G. S. & Clayton, D. A. 1997. Mitochondrial DNA maintenance in vertebrates. *Annu Rev Biochem,* **66,** 409-35.

Sharma, K., Karl, B., Mathew, A. V., Gangoiti, J. A., Wassel, C. L., Saito, R., Pu, M., Sharma, S., You, Y. H., Wang, L., Diamond-Stanic, M., Lindenmeyer, M. T., Forsblom, C., Wu, W., Ix, J. H., Ideker, T*., et al.* 2013. Metabolomics reveals signature of mitochondrial dysfunction in diabetic kidney disease. *J Am Soc Nephrol,* **24,** 1901-12.

Shen, J., Platek, M., Mahasneh, A., Ambrosone, C. B. & Zhao, H. 2010. Mitochondrial copy number and risk of breast cancer: a pilot study. *Mitochondrion,* **10,** 62-8.

Sheng, B., Wang, X., Su, B., Lee, H. G., Casadesus, G., Perry, G. & Zhu, X. 2012. Impaired mitochondrial biogenesis contributes to mitochondrial dysfunction in Alzheimer's disease. *J Neurochem,* **120,** 419-29.

Shikuma, C. M., Gerschenson, M., Chow, D., Libutti, D. E., Willis, J. H., Murray, J., Capaldi, R. A. & Marusich, M. 2008. Mitochondrial oxidative phosphorylation protein levels in peripheral blood mononuclear cells correlate with levels in subcutaneous adipose tissue within samples differing by HIV and lipoatrophy status. *AIDS Res Hum Retroviruses,* **24,** 1255-62.

Silva, A. M. & Oliveira, P. J. 2012. Evaluation of respiration with clark type electrode in isolated mitochondria and permeabilized animal cells. *Methods Mol Biol,* **810,** 7-24.

Simpson, D. P. & Hecker, J. 1979. Effect of arsenite on renal tissue slice metabolism in chronic metabolic acidosis and alkalosis. *Am J Physiol,* **237,** F93-9.

Singh, D. K., Winocour, P. & Farrington, K. 2008. Mechanisms of disease: the hypoxic tubular hypothesis of diabetic nephropathy. *Nat Clin Pract Nephrol,* **4,** 216-26.

Singh, R., Hattersley, A. T. & Harries, L. W. 2007. Reduced peripheral blood mitochondrial DNA content is not a risk factor for Type 2 diabetes. *Diabet Med,* **24,** 784-7.

Sivitz, W. I. & Yorek, M. A. 2010. Mitochondrial dysfunction in diabetes: from molecular mechanisms to functional significance and therapeutic opportunities. *Antioxid Redox Signal,* **12,** 537-77.

Soler, M. J., Riera, M. & Batlle, D. 2012. New experimental models of diabetic nephropathy in mice models of type 2 diabetes: efforts to replicate human nephropathy. *Exp Diabetes Res,* **2012,** 616313.

Son, C., Hosoda, K., Ishihara, K., Bevilacqua, L., Masuzaki, H., Fushiki, T., Harper, M. E. & Nakao, K. 2004. Reduction of diet-induced obesity in transgenic mice overexpressing uncoupling protein 3 in skeletal muscle. *Diabetologia,* **47,** 47-54.

Song, J., Oh, J. Y., Sung, Y. A., Pak, Y. K., Park, K. S. & Lee, H. K. 2001. Peripheral blood mitochondrial DNA content is related to insulin sensitivity in offspring of type 2 diabetic patients. *Diabetes Care,* **24,** 865-9.

Sparwasser, T., Miethke, T., Lipford, G., Erdmann, A., Hacker, H., Heeg, K. & Wagner, H. 1997. Macrophages sense pathogens via DNA motifs: induction of tumor necrosis factor-alpha-mediated shock. *Eur J Immunol,* **27,** 1671-9.

Spragg, R. G., Hinshaw, D. B., Hyslop, P. A., Schraufstatter, I. U. & Cochrane, C. G. 1985. Alterations in adenosine triphosphate and energy charge in cultured endothelial and P388D1 cells after oxidant injury. *J Clin Invest,* **76,** 1471-6.

Stanton, R. C. 2011. Oxidative Stress and Diabetic Kidney Disease. *Curr Diab Rep*.

Starkov, A. A. & Fiskum, G. 2003. Regulation of brain mitochondrial H2O2 production by membrane potential and NAD(P)H redox state. *J Neurochem,* **86,** 1101-7.

Stieger, N., Worthmann, K., Teng, B., Engeli, S., Das, A. M., Haller, H. & Schiffer, M. 2012. Impact of high glucose and transforming growth factor-beta on bioenergetic profiles in podocytes. *Metabolism: clinical and experimental,* **61,** 1073-86.

Suematsu, N., Tsutsui, H., Wen, J., Kang, D., Ikeuchi, M., Ide, T., Hayashidani, S., Shiomi, T., Kubota, T., Hamasaki, N. & Takeshita, A. 2003. Oxidative stress mediates tumor necrosis factor-alpha-induced mitochondrial DNA damage and dysfunction in cardiac myocytes. *Circulation,* **107,** 1418-23.

Sugiyama, F., Yagami, K. & Paigen, B. 2001. Mouse models of blood pressure regulation and hypertension. *Curr Hypertens Rep,* **3,** 41-8.

Sun, Y., Zhang, Y., Zhao, D., Ding, G., Huang, S., Zhang, A. & Jia, Z. 2014. Rotenone remarkably attenuates oxidative stress, inflammation, and fibrosis in chronic obstructive uropathy. *Mediators Inflamm,* **2014,** 670106.

Supale, S., Thorel, F., Merkwirth, C., Gjinovci, A., Herrera, P. L., Scorrano, L., Meda, P., Langer, T. & Maechler, P. 2013. Loss of prohibitin induces mitochondrial damages altering beta-cell function and survival and is responsible for gradual diabetes development. *Diabetes,* **62,** 3488-99.

Szabadkai, G. & Duchen, M. R. 2009. Mitochondria mediated cell death in diabetes. *Apoptosis,* **14,** 1405-23.

Szkudelski, T. 2001. The mechanism of alloxan and streptozotocin action in B cells of the rat pancreas. *Physiol Res,* **50,** 537-46.

Tan, E. P., Villar, M. T., E, L., Lu, J., Selfridge, J. E., Artigues, A., Swerdlow, R. H. & Slawson, C. 2014. Altering O-linked beta-N-acetylglucosamine cycling disrupts mitochondrial function. *J Biol Chem,* **289,** 14719-30.

Tervaert, T. W., Mooyaart, A. L., Amann, K., Cohen, A. H., Cook, H. T., Drachenberg, C. B., Ferrario, F., Fogo, A. B., Haas, M., de Heer, E., Joh, K., Noel, L. H., Radhakrishnan, J., Seshan, S. V., Bajema, I. M. & Bruijn, J. A. 2010. Pathologic classification of diabetic nephropathy. *J Am Soc Nephrol,* **21,** 556-63.

Tesch, G. H. & Allen, T. J. 2007. Rodent models of streptozotocin-induced diabetic nephropathy. *Nephrology (Carlton),* **12,** 261-6.

Tiao, M. M., Lin, T. K., Kuo, F. Y., Huang, C. C., Du, Y. Y., Chen, C. L. & Chuang, J. H. 2007. Early stage of biliary atresia is associated with significant changes in 8-hydroxydeoxyguanosine and mitochondrial copy number. *J Pediatr Gastroenterol Nutr,* **45,** 329-34.

Tonelli, M., Muntner, P., Lloyd, A., Manns, B. J., James, M. T., Klarenbach, S., Quinn, R. R., Wiebe, N., Hemmelgarn, B. R. & Alberta Kidney Disease, N. 2011. Using proteinuria and estimated glomerular filtration rate to classify risk in patients with chronic kidney disease: a cohort study. *Ann Intern Med,* **154,** 12-21.

Trudeau, K., Molina, A. J., Guo, W. & Roy, S. 2010. High glucose disrupts mitochondrial morphology in retinal endothelial cells: implications for diabetic retinopathy. *The American journal of pathology,* **177,** 447-55.

Tsutsui, H. 2006. Mitochondrial oxidative stress and heart failure. *Intern Med,* **45,** 809-13.

Tuppen, H. A., Blakely, E. L., Turnbull, D. M. & Taylor, R. W. 2010. Mitochondrial DNA mutations and human disease. *Biochim Biophys Acta,* **1797,** 113-28.

Tutorvista 2014.).

Twig, G. & Shirihai, O. S. 2011. The interplay between mitochondrial dynamics and mitophagy. *Antioxid Redox Signal,* **14,** 1939-51.

Uranova, N. A., Orlovskaia, D. D., Vikhreva, O. V., Zimina, I. S. & Rakhmanova, V. I. 2001. [Morphometric study of ultrastructural changes in oligodendroglial cells in the postmortem brain in endogenous psychoses]. *Vestn Ross Akad Med Nauk***,** 42-8.

Vallon, V. 2011. The proximal tubule in the pathophysiology of the diabetic kidney. *Am J Physiol Regul Integr Comp Physiol,* **300,** R1009-22.

Vandesompele, J., De Preter, K., Pattyn, F., Poppe, B., Van Roy, N., De Paepe, A. & Speleman, F. 2002. Accurate normalization of real-time quantitative RT-PCR data by geometric averaging of multiple internal control genes. *Genome Biol,* **3,** RESEARCH0034.

Veltri, K. L., Espiritu, M. & Singh, G. 1990. Distinct genomic copy number in mitochondria of different mammalian organs. *J Cell Physiol,* **143,** 160-4.

Vlassara, H. & Striker, G. E. 2011. AGE restriction in diabetes mellitus: a paradigm shift. *Nat Rev Endocrinol*.

Wada, J. & Makino, H. 2013. Inflammation and the pathogenesis of diabetic nephropathy. *Clinical science,* **124,** 139-52.

Wada, T., Miyata, T., Inagi, R., Nangaku, M., Wagatsuma, M., Suzuki, D., Wadzinski, B. E., Okubo, K. & Kurokawa, K. 2001. Cloning and characterization of a novel subunit of protein serine/threonine phosphatase 4 from mesangial cells. *J Am Soc Nephrol,* **12,** 2601-8.

Wallace, D. C. & Fan, W. 2010. Energetics, epigenetics, mitochondrial genetics. *Mitochondrion,* **10,** 12-31.

Wallace, D. C., Fan, W. & Procaccio, V. 2010. Mitochondrial energetics and therapeutics. *Annu Rev Pathol,* **5,** 297-348.

Wang, Y., Liu, V. W., Xue, W. C., Cheung, A. N. & Ngan, H. Y. 2006. Association of decreased mitochondrial DNA content with ovarian cancer progression. *Br J Cancer,* **95,** 1087-91.

Wang, Y., Liu, V. W., Xue, W. C., Tsang, P. C., Cheung, A. N. & Ngan, H. Y. 2005. The increase of mitochondrial DNA content in endometrial adenocarcinoma cells: a quantitative study using laser-captured microdissected tissues. *Gynecol Oncol,* **98,** 104-10.

Wang, Y. C., Lee, W. C., Liao, S. C., Lee, L. C., Su, Y. J., Lee, C. T. & Chen, J. B. 2011. Mitochondrial DNA copy number correlates with oxidative stress and predicts mortality in nondiabetic hemodialysis patients. *J Nephrol,* **24,** 351-8.

Wani, J., Carl, M., Henger, A., Nelson, P. J. & Rupprecht, H. 2007. Nitric oxide modulates expression of extracellular matrix genes linked to fibrosis in kidney mesangial cells. *Biol Chem,* **388,** 497-506.

Wei, Y. H., Lee, C. F., Lee, H. C., Ma, Y. S., Wang, C. W., Lu, C. Y. & Pang, C. Y. 2001. Increases of mitochondrial mass and mitochondrial genome in association with enhanced oxidative stress in human cells harboring 4,977 BP-deleted mitochondrial DNA. *Ann N Y Acad Sci,* **928,** 97-112.

Wei, Y. H. & Lee, H. C. 2002. Oxidative stress, mitochondrial DNA mutation, and impairment of antioxidant enzymes in aging. *Experimental biology and medicine,* **227,** 671-82.

Weng, S. W., Lin, T. K., Liou, C. W., Chen, S. D., Wei, Y. H., Lee, H. C., Chen, I. Y., Hsieh, C. J. & Wang, P. W. 2009b. Peripheral blood mitochondrial DNA content and dysregulation of glucose metabolism. *Diabetes research and clinical practice,* **83,** 94-9.

Whiting, D. R., Guariguata, L., Weil, C. & Shaw, J. 2011. IDF diabetes atlas: global estimates of the prevalence of diabetes for 2011 and 2030. *Diabetes Res Clin Pract,* **94,** 311-21.

WHO 2013. http://www.who.int/mediacentre/factsheets/fs312/en/)*Fact sheet.*

Wild, S., Roglic, G., Green, A., Sicree, R. & King, H. 2004. Global prevalence of diabetes: estimates for the year 2000 and projections for 2030. *Diabetes Care,* **27,** 1047-53.

Williams, G. & Pickup, J. C. 1988. The natural history of brittle diabetes. *Diabetes Res,* **7,** 13-8.

Williams, P. J. & Mistry, H. D. 2013. *Antioxidant micronutrients in pregnancy and early childhood,* London, Quay Books.

Williams, R., Van Gaal, L., Lucioni, C. & Board, C.-A. 2002. Assessing the impact of complications on the costs of Type II diabetes. *Diabetologia,* **45,** S13-7.

Williams, R. S. 1986. Mitochondrial gene expression in mammalian striated muscle. Evidence that variation in gene dosage is the major regulatory event. *The Journal of biological chemistry,* **261,** 12390-4.

Winter, W. E. 2000. Molecular and biochemical analysis of the MODY syndromes. *Pediatr Diabetes,* **1,** 88-117.

Wirthensohn, G. & Guder, W. G. 1986. Renal substrate metabolism. *Physiol Rev,* **66,** 469-97.

Wolf, G. 2004. New insights into the pathophysiology of diabetic nephropathy: from haemodynamics to molecular pathology. *Eur J Clin Invest,* **34,** 785-96.

Wolf, G., Sharma, K., Chen, Y., Ericksen, M. & Ziyadeh, F. N. 1992. High glucose-induced proliferation in mesangial cells is reversed by autocrine TGF-beta. *Kidney Int,* **42,** 647-56.

Wong, J., McLennan, S. V., Molyneaux, L., Min, D., Twigg, S. M. & Yue, D. K. 2009. Mitochondrial DNA content in peripheral blood monocytes: relationship with age of diabetes onsetand diabetic complications. *Diabetologia,* **52,** 1953-61.

Xia, P., An, H. X., Dang, C. X., Radpour, R., Kohler, C., Fokas, E., Engenhart-Cabillic, R., Holzgreve, W. & Zhong, X. Y. 2009. Decreased mitochondrial DNA content in blood samples of patients with stage I breast cancer. *BMC Cancer,* **9,** 454.

Xie, L., Zhu, X., Hu, Y., Li, T., Gao, Y., Shi, Y. & Tang, S. 2008. Mitochondrial DNA oxidative damage triggering mitochondrial dysfunction and apoptosis in high glucose-induced HRECs. *Invest Ophthalmol Vis Sci,* **49,** 4203-9.

Xu, F. X., Zhou, X., Shen, F., Pang, R. & Liu, S. M. 2011. Decreased peripheral blood mitochondrial DNA content is related to HbA(1c), fasting plasma glucose level and age of onset in Type 2 diabetes mellitus. *Diabet Med,* **29,** 47-54.

Xu, S., Zhou, Z., Zhang, L., Yu, Z., Zhang, W., Wang, Y., Wang, X., Li, M., Chen, Y., Chen, C., He, M., Zhang, G. & Zhong, M. 2010. Exposure to 1800 MHz radiofrequency radiation induces oxidative damage to mitochondrial DNA in primary cultured neurons. *Brain Res,* **1311,** 189-96.

Yamada, S., Nomoto, S., Fujii, T., Kaneko, T., Takeda, S., Inoue, S., Kanazumi, N. & Nakao, A. 2006. Correlation between copy number of mitochondrial DNA and clinico-pathologic parameters of hepatocellular carcinoma. *Eur J Surg Oncol,* **32,** 303-7.

Yao, D. & Brownlee, M. 2010. Hyperglycemia-induced reactive oxygen species increase expression of the receptor for advanced glycation end products (RAGE) and RAGE ligands. *Diabetes,* **59,** 249-55.

Yu, M., Zhou, Y., Shi, Y., Ning, L., Yang, Y., Wei, X., Zhang, N., Hao, X. & Niu, R. 2007. Reduced mitochondrial DNA copy number is correlated with tumor progression and prognosis in Chinese breast cancer patients. *IUBMB Life,* **59,** 450-7.

Yuzefovych, L. V., Musiyenko, S. I., Wilson, G. L. & Rachek, L. I. 2013. Mitochondrial DNA damage and dysfunction, and oxidative stress are associated with endoplasmic reticulum stress, protein degradation and apoptosis in high fat diet-induced insulin resistance mice. *PLoS One,* **8,** e54059.

Zeng, H. T., Yeung, W. S., Cheung, M. P., Ho, P. C., Lee, C. K., Zhuang, G. L., Liang, X. Y. & O, W. S. 2009. In vitro-matured rat oocytes have low mitochondrial deoxyribonucleic acid and adenosine triphosphate contents and have abnormal mitochondrial redistribution. *Fertil Steril,* **91,** 900-7.

Zhai, L., Ballinger, S. W. & Messina, J. L. 2011. Role of reactive oxygen species in injury-induced insulin resistance. *Mol Endocrinol,* **25,** 492-502.

Zhang, H. M., Zhang, Y. & Zhang, B. X. 2011. The role of mitochondrial complex III in melatonin-induced ROS production in cultured mesangial cells. *J Pineal Res,* **50,** 78-82.

Zhang, Q., Raoof, M., Chen, Y., Sumi, Y., Sursal, T., Junger, W., Brohi, K., Itagaki, K. & Hauser, C. J. 2010a. Circulating mitochondrial DAMPs cause inflammatory responses to injury. *Nature,* **464,** 104-7.

Zhang, Y., Lee, A. S., Shameli, A., Geng, X., Finegood, D., Santamaria, P. & Dutz, J. P. 2010b. TLR9 blockade inhibits activation of diabetogenic CD8+ T cells and delays autoimmune diabetes. *Journal of immunology,* **184,** 5645-53.

Zhao, S., Yang, Y., Liu, J., Liu, H., Ge, N., Yang, H., Zhang, H. & Xing, J. 2011. Association of mitochondrial DNA content in peripheral blood leukocyte with hepatitis B virus-related hepatocellular carcinoma in a Chinese Han population. *Cancer Sci,* **102,** 1553-8.

Zimmet, P., Alberti, K. G. & Shaw, J. 2001. Global and societal implications of the diabetes epidemic. *Nature,* **414,** 782-7.

Zmyslowska, A., Borowiec, M., Fichna, P., Iwaniszewska, B., Majkowska, L., Pietrzak, I., Szalecki, M., Szypowska, A. & Mlynarski, W. 2014. Delayed recognition of Wolfram syndrome frequently misdiagnosed as type 1 diabetes with early chronic complications. *Exp Clin Endocrinol Diabetes,* **122,** 35-8.

Appendix I

List of publications arising from this thesis and relevant work

Research Papers

1. Malik AN, Czajka A. Is mitochondrial DNA content a potential biomarker of mitochondrial dysfunction? Mitochondrion 2012

2. Rojeen Shahni, Anna Czajka, Baljinder S. Mankoo, Aleks Kamer Guvenel, Aileen King and Afshan N Malik. Nop-7-associated 2 (NSA2), a candidate gene for diabetic nephropathy, is involved in the TGFβ1 pathway. Int.J.Biochem 2012

3 Saima Ajaz*****, Anna Czajka***** and Afshan Malik. Accurate measurement of circulating mitochondrial DNA content from human blood samples using real time quantitative PCR. MiMB Probing Mitochondrial function 2015

4 Anna Czajka*, Saima Ajaz*, Luigi Gnudi, Chloe Rackham, Chandani Kiran Parsade, Peter Jones, Sachin Supale, Pierre Maechler, Fiona Reid, Afshan Malik. Mitochondrial DNA alterations and mitochondrial bio-energetic dysfunction in diabetic nephropathy. Cell metabolism 2015

*****First and second authors made equal contribution

Abstracts and Posters:

Anna Czajka and A N Malik Hyperglycemia-induced changes in mitochondrial DNA and function in cultured renal cells and mouse models of diabetes. Poster presentation at Euromit 2014, Tampere, Finaland 2014

Anna Czajka and A N Malik. Hyperglycemia induced alterations in mitochondrial DNA content and mitochondrial respiration in human glomerular mesangial cells. Poster presentation at EDNSG meeting 2014, London, UK 2014

Anna Czajka and A N Malik. Mitochondrial dysfunction in diabetic nephropathy. Poster presentation at Diabetes UK 2014, Liverpool, UK 2014

Anna Czajka and A N Malik. Accurate quantification of Mitochondrial DNA, a biomarker of mitochondrial dysfunction and oxidative stress. Oral presentation at ISANH Antioxidants 2013, Paris, France 2013

Anna Czajka and A N Malik . Hyperglycemia induced alterations in mitochondrial DNA content and mitochondrial function in cultured human glomerular mesangial cells. Poster presentation at EDNSG meeting, Casteldefls, Spain 2013

Anna Czajka and A N Malik .Hyperglycemia induced alterations in mitochondrial DNA content in cultured human glomerular mesangial cells. Poster presentation at Diabetes UK, Manchester, UK 2013

Anna Czajka and A N Malik The role of alternations in mitochondrial DNA in circulating blood and renal cells in diabetes and diabetic nephropathy. Presented at Unveiling Mitochondria meeting, Poster and oral presentation, Santiago, Chile 2013

Afshan Malik and A Czajka. Mitochondrial dysfunction in diabetic nephropathy. Heart 2011;97:e8 presented at the Mitochondrial dysfunction meeting at UCL, 2011, London UK 2011

Anna Czajka and A N Malik. Is elevated oxidative stress caused by increased mitochondrial content associated with diabetic nephropathy? Poster presentation at King's College graduate showcase, 2011, London, UK 2011

Anna Czajka and A N Malik. The effect of hyperglycemia-induced oxidative stress on mitochondrial DNA content and function in cultured renal cells. Poster presentation at Free Radicals meeting, Birmingham, UK 2011

Appendix II

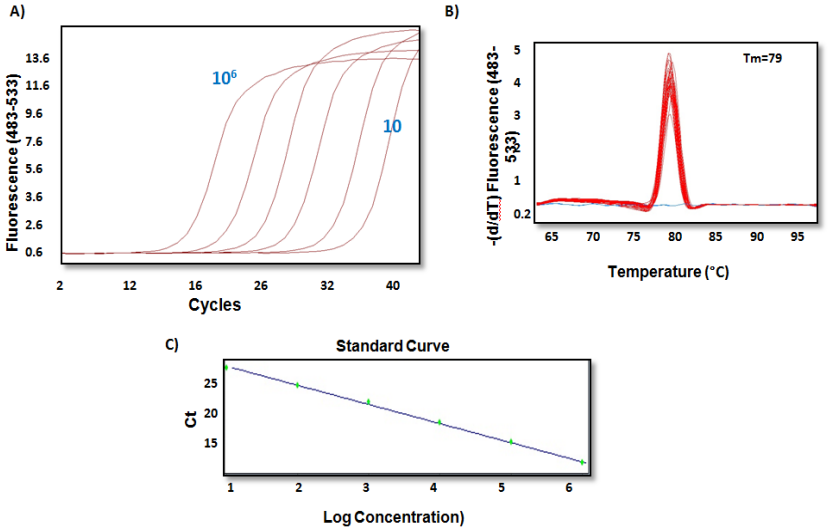

Fig.A2.1. Amplification of mouse β-actin in 10-fold dilutions and standard curve generation. Dilution standards of mouse *β-actin* were prepared and 2ul of each standard was used in qPCR reaction and amplified. Fluorescence data was acquired once per cycle and amplification curve (A) was generated showing dilution series from 10^2 to 10^7 copies of hMito. Melting point analysis (B) represents specificity of multiplied product as one single melt peak is visible at 83.4°C. (C) Standard curve showing the crossing point (Ct) for each of the 10-fold dilutions plotted against a log concentration.

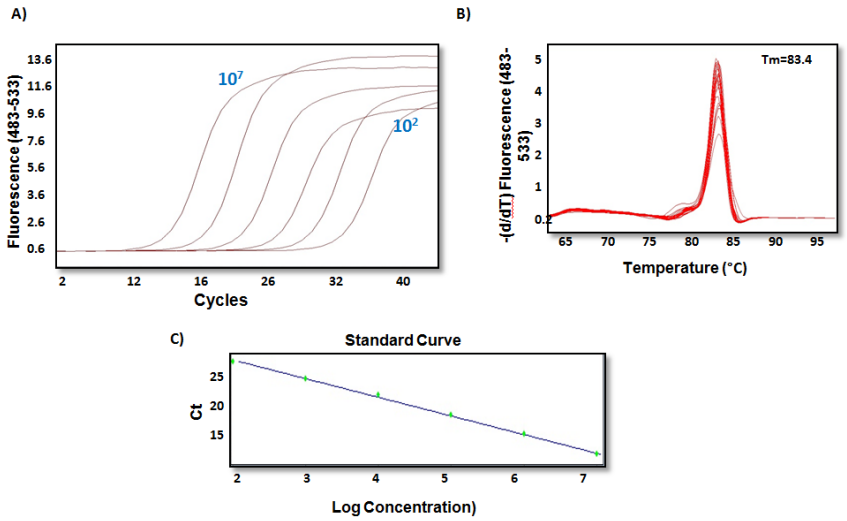

Fig.A2.2. Amplification of mouse TFAM in 10-fold dilutions and standard curve generation. Dilution standards of mouse *TFAM* were prepared and 2ul of each standard was used in qPCR reaction and amplified. Fluorescence data was acquired once per cycle and amplification curve (A) was generated showing dilution series from 10 to 10^6 copies of *TFAM*. Melting point analysis (B) represents specificity of multiplied product as one single melt peak is visible at 79°C. (C) Standard curve showing the crossing point (Ct) for each of the 10-fold dilutions plotted against a log concentration.

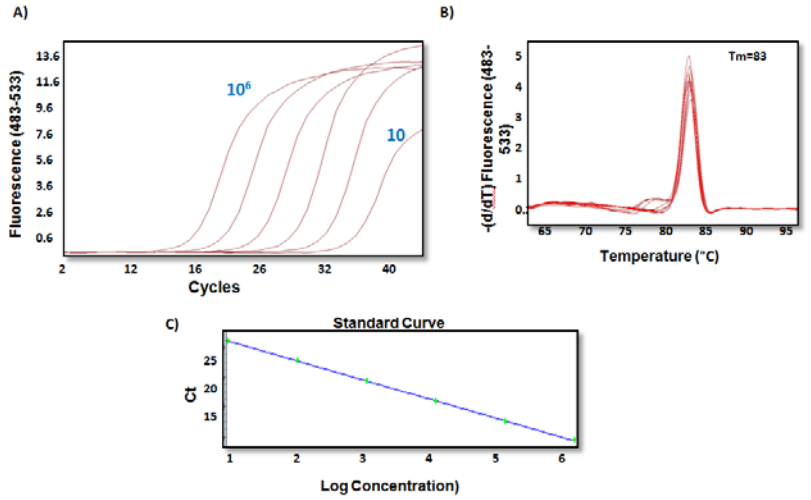

Fig.A2.3. Amplification of mouse PGC1-α in 10-fold dilutions and standard curve generation. Dilution standards of mouse *PGC-1α* were prepared and 2ul of each standard was used in qPCR reaction and amplified. Fluorescence data was acquired once per cycle and amplification curve (A) was generated showing dilution series from 10 to 10^6 copies of *PGC-1α*. Melting point analysis (B) represents specificity of multiplied product as one single melt peak is visible at 83°C. (C) Standard curve showing the crossing point (Ct) for each of the 10-fold dilutions plotted against a log concentration.

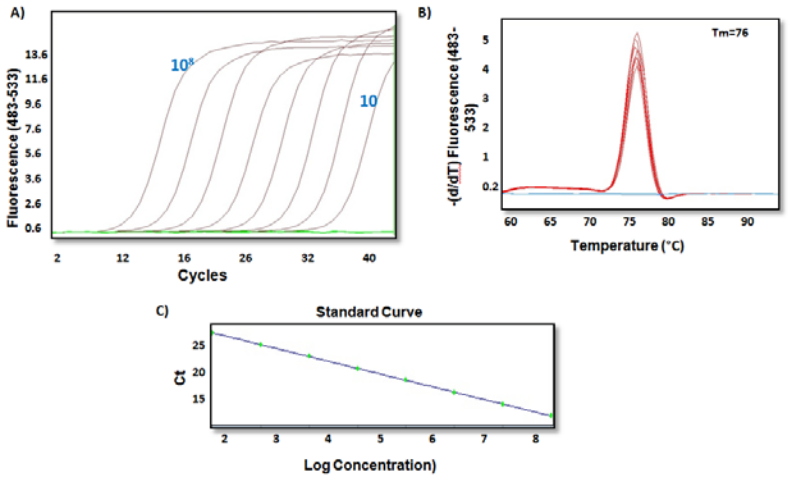

Fig.A2.4. Amplification of human MFN1 in 10-fold dilutions and standard curve generation. Dilution standards of human *MFN1* were prepared and 2ul of each standard was used in qPCR reaction and amplified. Fluorescence data was acquired once per cycle and amplification curve (A) was generated showing dilution series from 10 to 10^6 copies of *MFN1*. Melting point analysis (B) represents specificity of multiplied product as one single melt peak is visible at 76°C. (C) Standard curve showing the crossing point (Ct) for each of the 10-fold dilutions plotted against a log concentration.

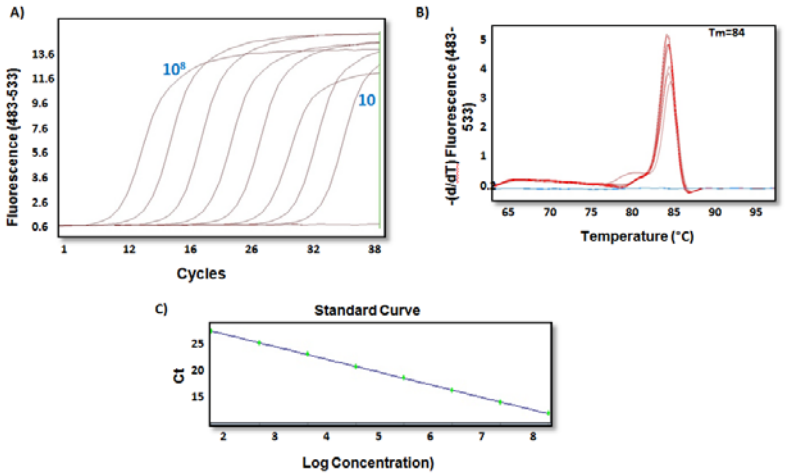

Fig.A2.5. Amplification of human MFN2 in 10-fold dilutions and standard curve generation. Dilution standards of human *MFN2* were prepared and 2ul of each standard was used in qPCR reaction and amplified. Fluorescence data was acquired once per cycle and amplification curve (A) was generated showing dilution series from 10 to 10^8 copies of *MFN2*. Melting point analysis (B) represents specificity of multiplied product as one single melt peak is visible at 84°C. (C) Standard curve showing the crossing point (Ct) for each of the 10-fold dilutions plotted against a log concentration.

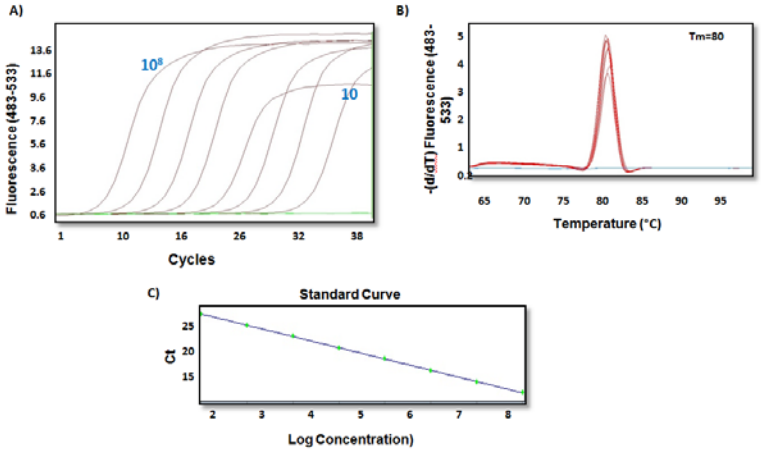

Fig.A2.6. Amplification of human OPA1 in 10-fold dilutions and standard curve generation. Dilution standards of human *OPA1* were prepared and 2ul of each standard was used in qPCR reaction and amplified. Fluorescence data was acquired once per cycle and amplification curve (A) was generated showing dilution series from 10 to 10^6 copies of *OPA1*. Melting point analysis (B) represents specificity of multiplied product as one single melt peak is visible at 80°C. (C) Standard curve showing the crossing point (Ct) for each of the 10-fold dilutions plotted against a log concentration.

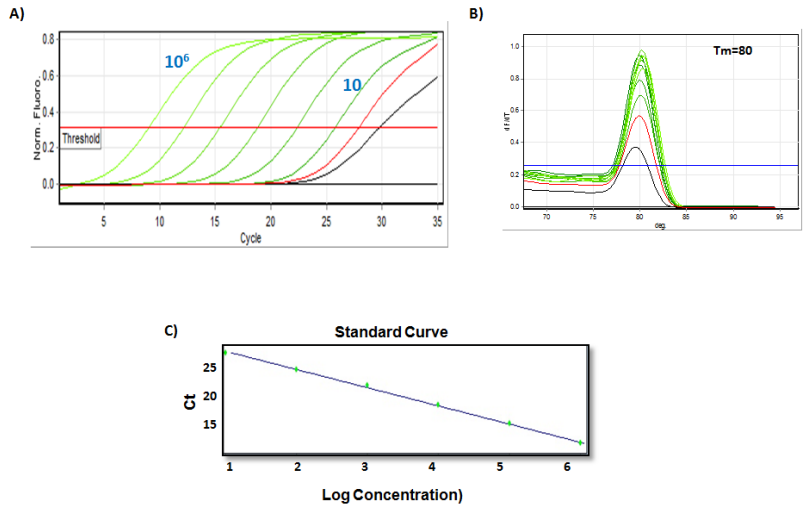

Fig.A2.7. Amplification of human MYD88 in 10-fold dilutions and standard curve generation. Dilution standards of human *MYD88* were prepared and 2ul of each standard was used in qPCR reaction and amplified. Fluorescence data was acquired once per cycle and amplification curve (A) was generated showing dilution series from 10 to 10^6 copies of *MYD88*. Melting point analysis (B) represents specificity of multiplied product as one single melt peak is visible at 80°C. (C) Standard curve showing the crossing point (Ct) for each of the 10-fold dilutions plotted against a log concentration.

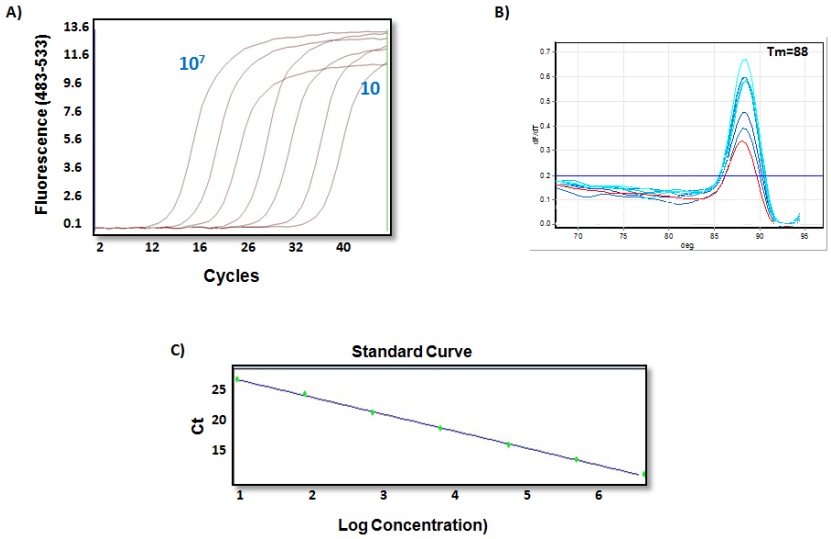

Fig.A2.8. Amplification of human NF-κB in 10-fold dilutions and standard curve generation. Dilution standards of human *NF-κB* were prepared and 2ul of each standard was used in qPCR reaction and amplified. Fluorescence data was acquired once per cycle and amplification curve (A) was generated showing dilution series from 10 to 10^7 copies of *NF-κB*. Melting point analysis (B) represents specificity of multiplied product as one single melt peak is visible at 88°C. (C) Standard curve showing the crossing point (Ct) for each of the 10-fold dilutions plotted against a log concentration.

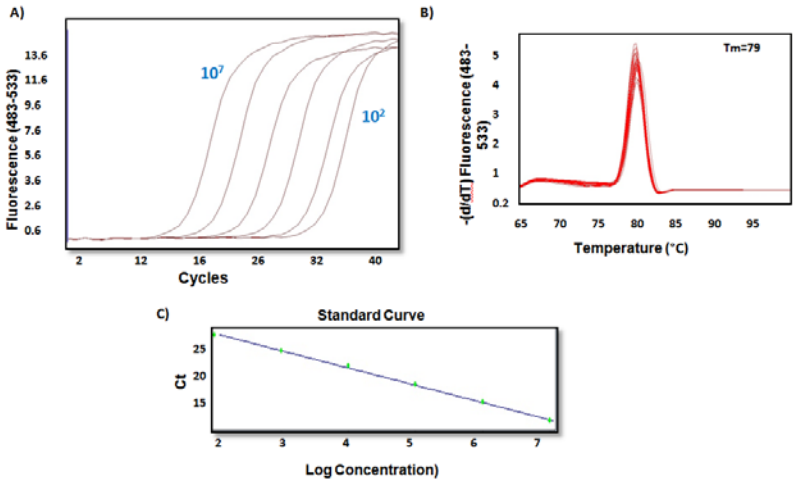

Fig.A2.9. Amplification of human TFAM in 10-fold dilutions and standard curve generation. Dilution standards of human *TFAM* were prepared and 2ul of each standard was used in qPCR reaction and amplified. Fluorescence data was acquired once per cycle and amplification curve (A) was generated showing dilution series from 10^2 to 10^7 copies of *TFAM*. Melting point analysis (B) represents specificity of multiplied product as one single melt peak is visible at 79°C. (C) Standard curve showing the crossing point (Ct) for each of the 10-fold dilutions plotted against a log concentration.

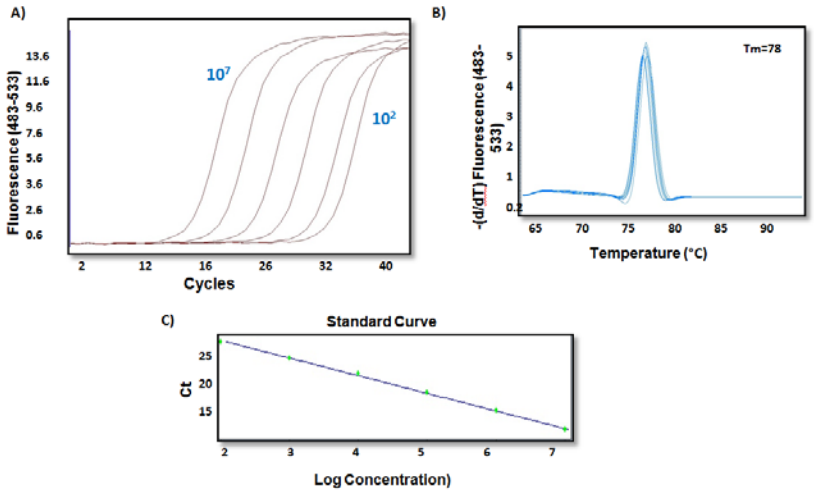

Fig.A2.10. Amplification of human PGC-1α in 10-fold dilutions and standard curve generation. Dilution standards of human *PGC1-α* were prepared and 2ul of each standard was used in qPCR reaction and amplified. Fluorescence data was acquired once per cycle and amplification curve (A) was generated showing dilution series from 10^2 to 10^7 copies of *PGC1-α*. Melting point analysis (B) represents specificity of multiplied product as one single melt peak is visible at 78°C. (C) Standard curve showing the crossing point (Ct) for each of the 10-fold dilutions plotted against a log concentration.

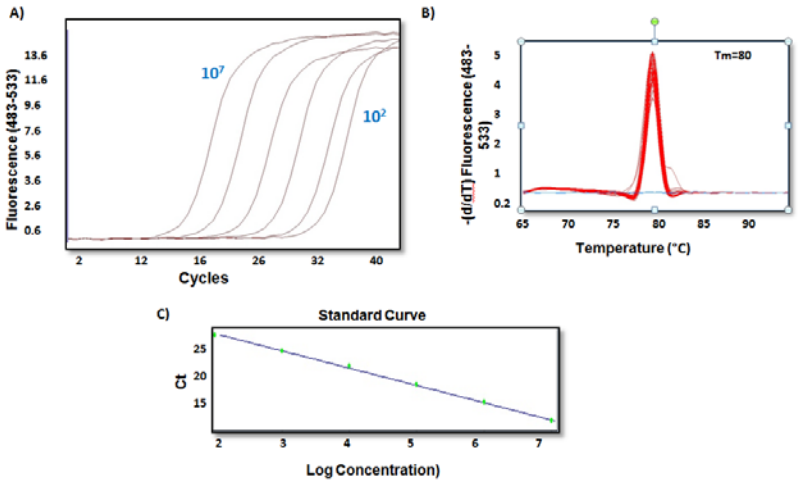

Fig.A2.11. Amplification of human ND1 in 10-fold dilutions and standard curve generation. Dilution standards of human *ND1* were prepared and 2ul of each standard was used in qPCR reaction and amplified. Fluorescence data was acquired once per cycle and amplification curve (A) was generated showing dilution series from 10^2 to 10^7 copies of *ND1*. Melting point analysis (B) represents specificity of multiplied product as one single melt peak is visible at 80°C. (C) Standard curve showing the crossing point (Ct) for each of the 10-fold dilutions plotted against a log concentration.

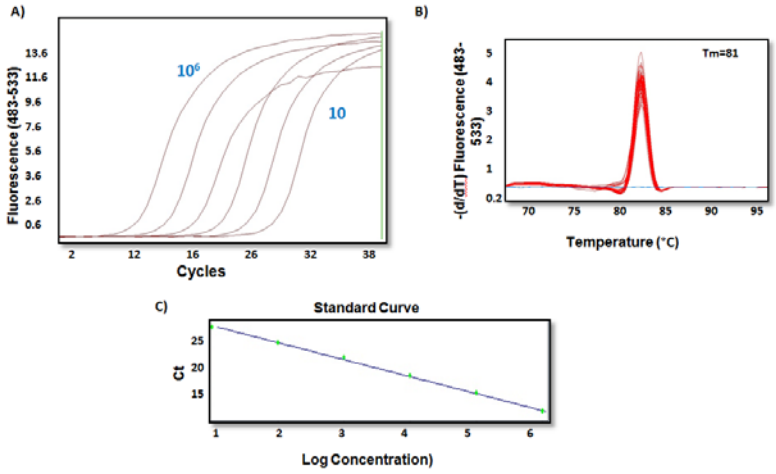

Figure 4. Amplification of hND6dilutions and standard curve generation.

Fig.A2.12. Amplification of human ND6 in 10-fold dilutions and standard curve generation. Dilution standards of human *ND6* were prepared and 2ul of each standard was used in qPCR reaction and amplified. Fluorescence data was acquired once per cycle and amplification curve (A) was generated showing dilution series from 10^0 to 10^6 copies of *ND6*. Melting point analysis (B) represents specificity of multiplied product as one single melt peak is visible at 81°C. (C) Standard curve showing the crossing point (Ct) for each of the 10-fold dilutions plotted against a log concentration

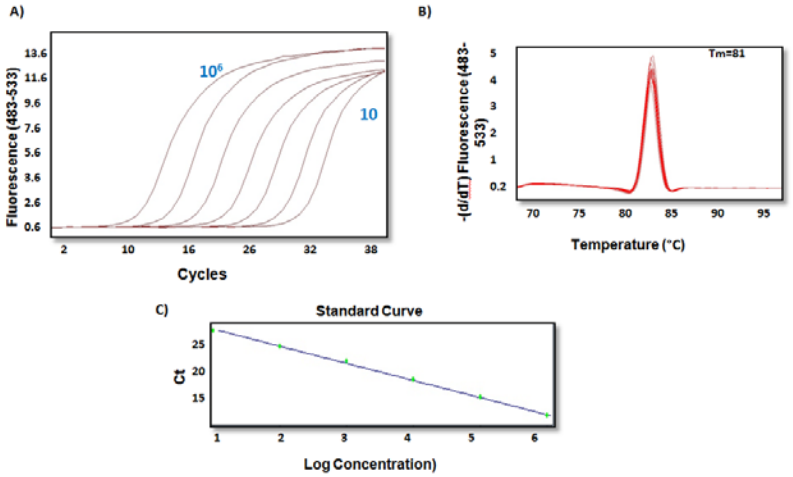

Fig.A2.13. Amplification of human COX3 in 10-fold dilutions and standard curve generation. Dilution standards of human *COX3* were prepared and 2ul of each standard was used in qPCR reaction and amplified. Fluorescence data was acquired once per cycle and amplification curve (A) was generated showing dilution series from 10 to 10^6 copies of *COX3*. Melting point analysis (B) represents specificity of multiplied product as one single melt peak is visible at 81°C. (C) Standard curve showing the crossing point (Ct) for each of the 10-fold dilutions plotted against a log concentration.

Appendix III Cellular bioenergetics

Seahorse XF^{e}24 data

Cells were seeded in a density of 30 000 of cells/ well 4 days prior reading OCR in Seahorse.

A)

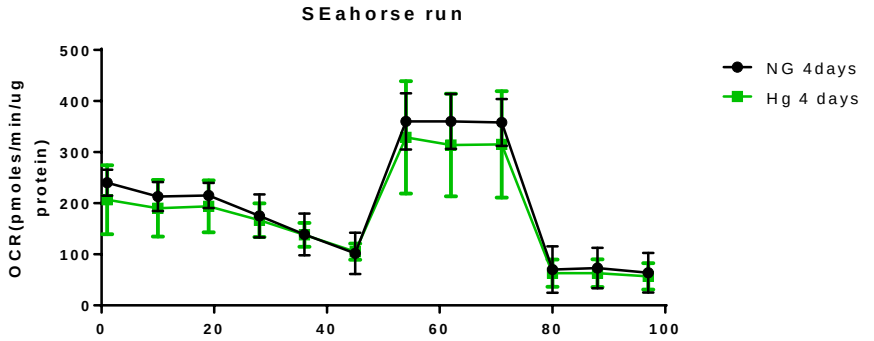

B)

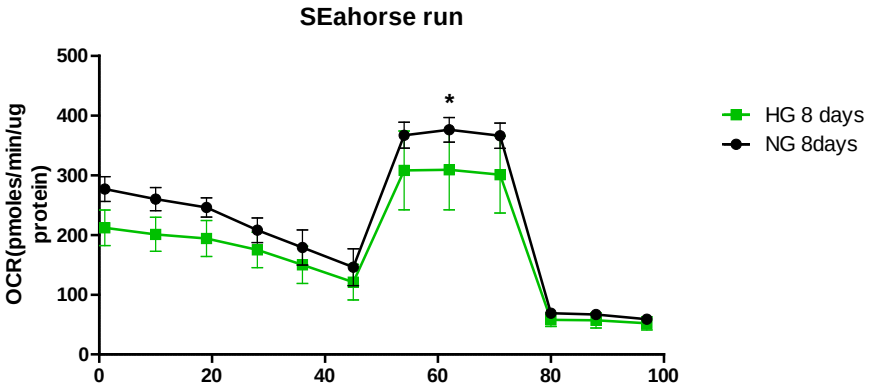

Fig. A6.1. Assessment of cellular bioenergetic in mesangial cells using Seahorse XF^{e}24. Cells were culture in 5mM (NG) and 25mM (HG) glucose for 4 (A) and 8 days (B). Following the exposure to high glucose HMCs were seeded at the density of 30 000 cells/well in 24 XF plates 4 days before the assessment.

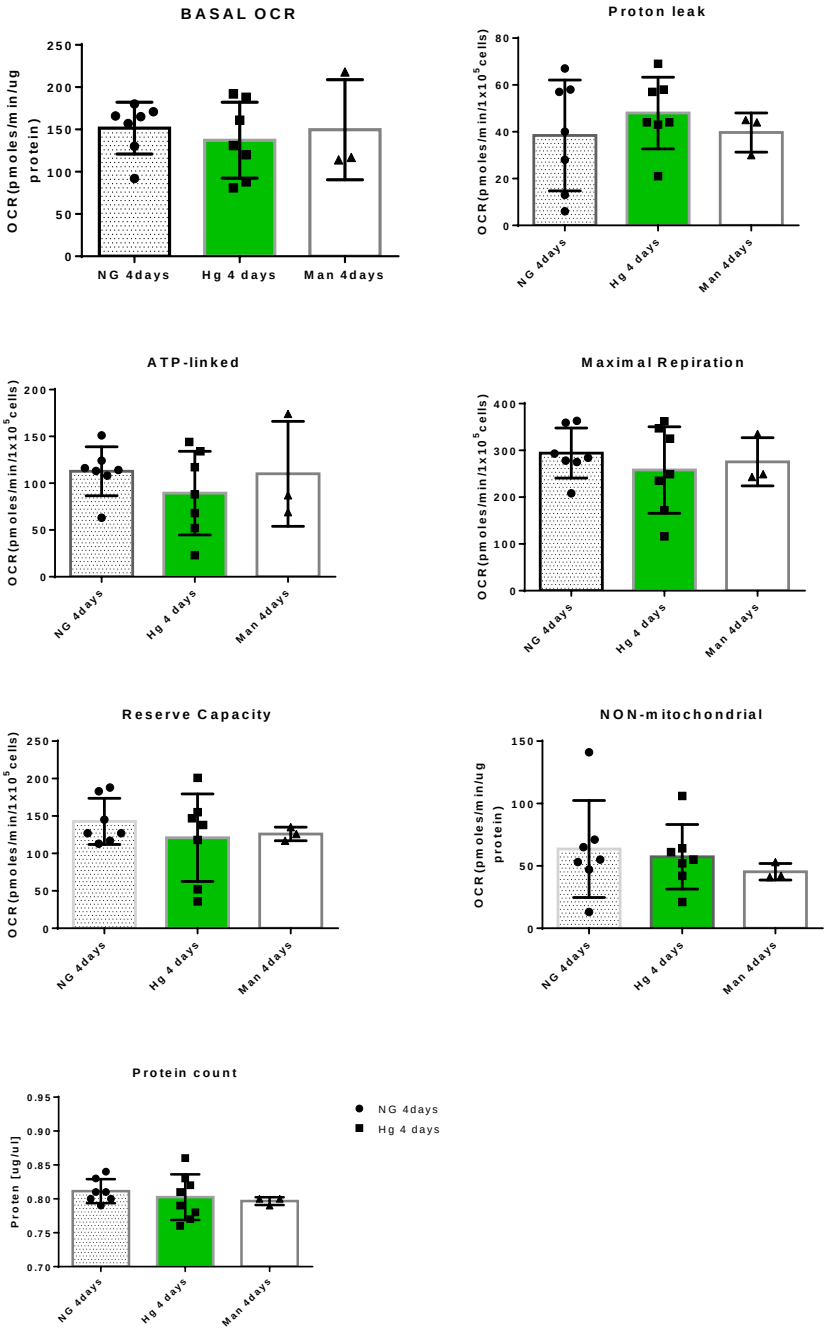

Fig.A6.2. Bioenergetic profile of human mesangial cells is not affected after 4 days of culture in high glucose. HMCs were culture din 5mM (NG) and 25mM (HG) glucose for 4 days and cellular bioenergetic was measured using Seahorse Analyzer. P>0.05

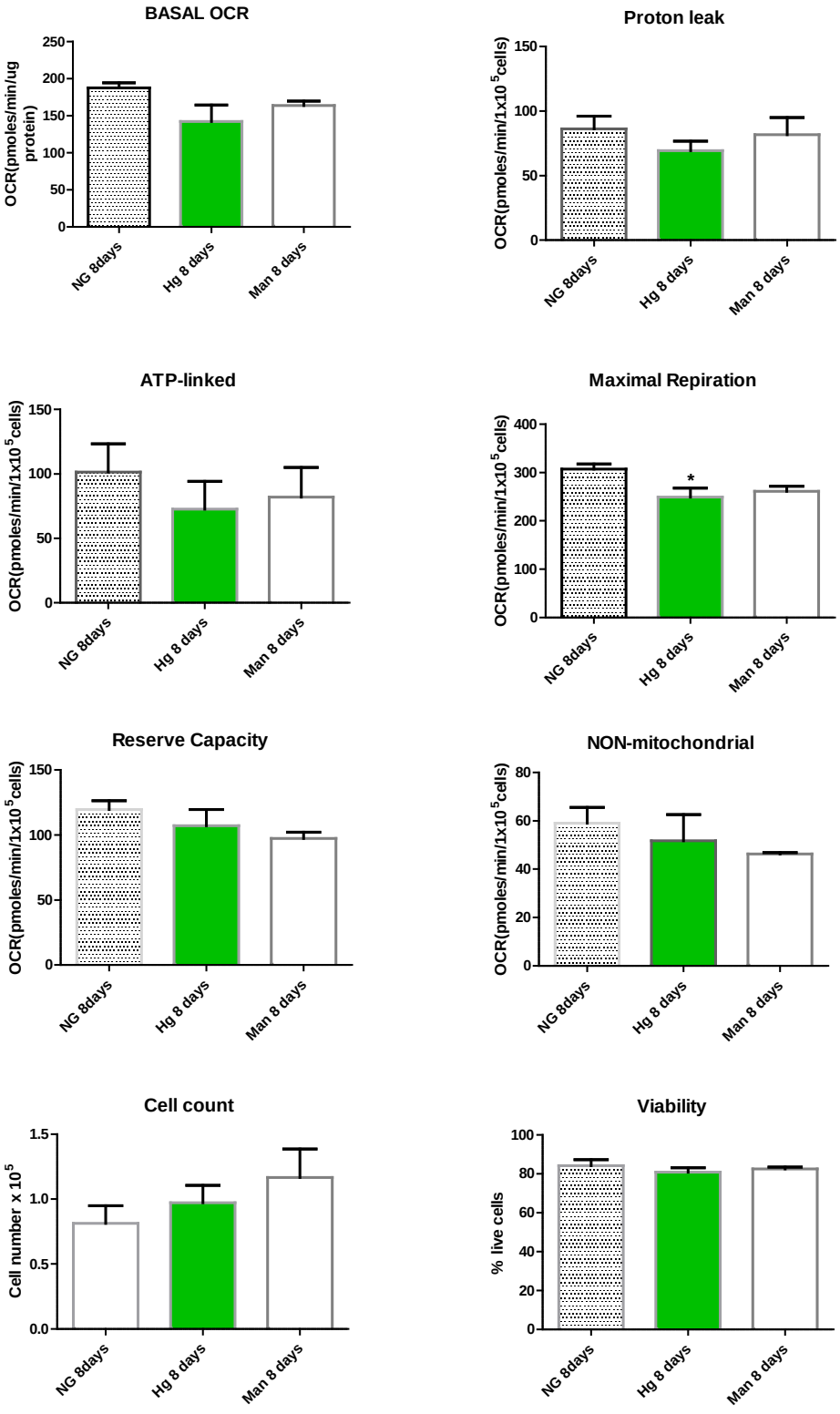

Fig.A6.3. Bioenergetic profile of human mesangial cells is altered after 8 days of culture in high glucose. HMCs were culture din 5mM (NG) and 25mM (HG) glucose for 4 days and cellular bioenergetic was measured using Seahorse Analyzer. Maximal respiration was significantly down regulated in primary cultured mesangial c ells exposed to high glucose for 8 days, *P<0.05